Glucose Transport in the Bovine Ciliary Body/ Epithelium (CBE)

Chu Yan, Chan

School of Optometry and Vision Sciences

Cardiff University

Thesis submitted for the degree of Doctor of Philosophy

April 2005

ProQuest LLC
789 East Eisenhower Parkway
P.O. Box 1346
Ann Arbor, MI 48106-1346

Summary

Diabetic patients are prone to develop cataract, compared to non-diabetic patients (Kyselova *et al.*, 2004). The global prevalence of diabetes is around 150 millions in 2004 (5% of the world population), with 1.8 million people in the United Kingdom affected (Diabetes UK, 2004). In western countries, diabetes accounts for around 12% of the total cataract population (Harding, 1999). It has been proposed that hyperglycemia is the major risk factor in diabetic cataract, and could be the starting point for all of the consequent pathological changes including, glucoxidation, glycation and activation of the polyol pathway, which finally result in diabetic complications (Sensi *et al.*, 1995; Hotta, 1997; Brownlee, 2001).

The present study aimed to characterise the mechanism of glucose transport into the aqueous humour. Using the Ussing-type chamber technique, glucose transport kinetics were characterised for the bovine CBE. The glucose fluxes were sensitive to a number of glucose transporter inhibitors including cytochalasin B (~ 80% inhibition), phloretin (~ 59% inhibition) and phlorizin (~ 21% inhibition), and it also varied with stromal glucose concentration.

In an investigation of mRNA expression using RT-PCR, GLUT1, GLUT3, GLUT4, GLUT5 and SGLT2 were found to be expressed in the bovine CBE. Due to difficulties encountered in the protein expression study, it was not possible to confirm that all of these mRNAs are translated.

Nevertheless, the major glucose transport mechanism across the bovine CBE was determined to be a facilitative and carrier-mediated mode, since the glucose transport was effectively inhibited by the addition of cytochalasin B and phloretin. The transport system is likely to saturate when the plasma glucose concentration reaches 10.6 mM. These results, together with the gene expression data, may provide a new insight into devising a therapeutic strategy in the control of aqueous glucose levels which may eventually prevent the diabetic cataract formation.

Acknowledgements

I would like to thank my supervisor, Dr. Jeremy Guggenheim, for his wisdom, guidance and patience during my study in the Cardiff University. I would also like to thank my co-supervisor, Dr. Chi-ho To, for his advice and support to my research project. I would also like to thank colleagues from the School of Optometry and Vision Sciences of the Cardiff University and the Department of Optometry and Radiography of The Hong Kong Polytechnic University for stimulating collegial experience. It has been my great privilege and pleasure to be able to work with them. I would like to thank Dr. Tony Do, for his expert help and advice on the Ussing-chamber technique.

I also thank my friends especially Monica, Queenie, Fiona, Tim, Toco, Thomas, KK, Dennis, Patrick and Tammy, for they have been my source of endless encouragement and friendship from afar. I must thank Rosalind Creer for being a wonderful friend and team-mate in and out of the laboratory. Special thanks also go to Elsa, Kiet, Brian, Cherry and Becky for their care, support and companionship during my stay in Cardiff.

Finally, my greatest gratitude is to my family and Stannie for their endless love to me and to my life.

Glory to God in the highest!

Table of contents

Chapter 2: Glucose transport kinetics: Ussing-type chamber experiments

Chapter 3: Glucose transport kinetics: Saturation characteristics

Chapter 5: Glucose transporter: Protein expression in the CBE

Chapter 6: General discussion

Chapter 7: Future perspectives

Appendix

List of figures

List of tables

List of abbreviations

AEC	aminoethylcarbazole
AGEs	advanced glycation end-products
AR	aldose reductase
ATP	adenosine triphosphate
BAB	blood-aqueous barrier
BBB	blood-brain barrier
bp	base pair
BPB	blood-placental barrier
BRB	blood-retinal barrier
BVB	blood-vitreous barrier
CAE	cis-acting regulatory element
CB	ciliary body
CBE	ciliary body/ epithelium
cDNA	complementary-DNA
CMDG	corrected 3-O-Methyl-D-glucose
CNS	central nervous system
CO(II)	cobalt chloride (II)
DAB	diaminobenzidine
DAG	diacylglycerol
dNTPs	deoxynucleotide triphosphates
ddNTPs	2', 3'-dideoxynucleotides
DM	diabetes mellitus
DMSO	dimethyl sulfoxide
DNA	deoxyribonucleic acid
dNTPs	deoxynucleotide triphosphates
DR	diabetic retinopathy
DTT	1, 3, Dithio-DL-threitol
E	enzyme
ECL	enhanced chemiluminescence
EGF	endothelial growth factor
ELISA	enzyme-linked immunosorbent assay
ES	substrate complex
EST	expressed sequence tag
ET-1	endothelin-1
FC	flow cytometry
FGF	fibroblast growth factor
GADPH	glyceraldehydes-3-phosphate dehydrogenase
GFAT	glutamine:fructose-6-phosphate amidotransferase
GLUT	facilitative glucose transporter
GLUTs	facilitative glucose transporters
HGF	hepatocyte growth factor
HMIT	proton-dependant-*myo*-inositol cotransporter
HRP	horseradish peroxidase
ICAM-1	intercellular adhesion molecule-1
IDDM	insulin-dependant diabetes mellitus

IFEM	immunofluorescent electron microscopy
IFG-I	insulin growth factor-I
IGEM	immunogold electron microscopy
IGF-1	insulin-like growth factor-1
IHC	immunohistochemistry
I_{sc}	short-circuit current
ISH	*in situ* hybridization
J	unidirectional flux
Jas	glucose flux from aqueous to stromal side
Jsa	glucose flux from stromal to aqueous side
K_d	dissociation constant
K_m	Michaelis constant
LG	L-glucose
MAPK	mitogen-activated protein kinase
MDG	3-O-Methyl-D-glucose
mRNA	messenger RNA
Na^+/H^+ and Cl^-/HCO_3^- antiporter	sodium-proton and chloride-bicarbonate antiporter
$Na^+/K^+/2Cl^-$ cotransporter	sodium-potassium-chloride cotransporter
Na^+, K^+-ATPase	sodium-potassium adenosine triphosphatase
Na^+/H^+ exchanger	sodium-proton exchanger
NAD^+	nicotinamide adenine dinucleotide, oxidized form
NADH	nicotinamide adenine dinucleotide, reduced form
NADPH	nicotinamide adenine dinucleotide phosphate
NIDDM	non-insulin dependant diabetes mellitus
NPE	non-pigmented epithelium
P	product
PCR	polymerase chain reaction
PD	potential difference
PDGF	platelet-derived growth factor
PD_t	transepithelial potential difference
PE	pigmented epithelium
PKC	protein kinase C
PKC-β	protein kinase C-beta
PVDF	polyvinylidene fluoride
R	total resistance
RAGE	receptor of advanced glycation end-product
RCP	retinal capillary pericytes
R_f	fluid resistance
RNA	ribonucleic acid
RNase	ribonuclease
ROS	reactive oxygen species
R_p	paracellular resistance
RPE	retinal pigmented epithelium
rRNA	ribosomal RNA
RT-PCR	reverse transcription-polymerase chain reaction
RVD	regulatory volume decrease
RVE	retinal vascular endothelium
RVI	regulatory volume increase

R_t	transepithelial resistance
R_{tc}	transcellular resistance
S	substrate
[S]	substrate concentration
SDS-PAGE	sodium dodecyl sulfate-polyacrylamide gel electrophoresis
SGLT	sodium-dependant glucose cotransporter
SGLTs	sodium-dependant glucose cotransporters
T_A	annealing temperature
TBS	Tris-buffered saline
TGF-β	transforming growth factor-beta
TGF-β1	transforming growth factor-beta 1
T_m	melting temperature
TTBS	Tween-20 Tris-buffered saline
VEGF	vascular endothelial growth factor
V_{max}	maximum velocity
V_o	initial reaction velocity
WB	Western blotting

Chapter 1

Introduction

1.1 Anatomy and physiology of the ciliary body/ epithelium (CBE)

The ciliary body (CB), together with the iris and choroid, forms the uveal tract. It is triangular in section, with an outer region that attaches to the sclera. It lies in between the retina posteriorly and the scleral spur anteriorly. The ciliary muscle that is located below the sclera within the CB controls the crystalline lens accommodation, thus, governing the accommodative power of the eye (Glasser and Kaufman, 2003).

The CBE is a polarized epithelium that lies along the innermost layer of the CB (Caprioli, 1992). It is the forward continuation of the retina, with a double layer of cells, the outer pigmented epithelium (PE) and the inner non-pigmented epithelium (NPE). These two layers face each other, with their apical membranes adjoining. Together with gap junctions, they form a functional syncytium (Green *et al.*, 1985; Edelman *et al.*, 1994; Oh *et al.*, 1994). These bilayer cells are connected electrically by gap junctions (Raviola, 1977; Raviola and Raviola, 1978; Abdel-Latif, 1997). Functionally, the CBE is widely recognized as the site of aqueous humor production (To and Do, 1998d; Wetzel and Sweadner, 2001).

Electrophysiological studies showed a potential difference (PD) of ~1mV across the CE, with the aqueous side consistently negative (Coca-Prados *et al.*, 1995; Jacob and Civan, 1996). Bicarbonate and chloride ions were believed to be responsible for generating this negative potential in rabbit and in bovine respectively (Coca-Prados *et al.*, 1995; Krupin and Civan, 1995; Do and To, 2000).These ions are, therefore, considered to play a crucial role in driving aqueous humor formation in different species.

The CBE can be divided into two regions, the pars plicata (anterior) and the pars plana (posterior) (Morrison and Freddo, 1996; Abdel-Latif, 1997). The two regions demonstrate different structural and functional features (see section 1.1.4).

1.1.1 Pigmented epithelium (PE)

The PE is the anterior continuation of the retinal pigment epithelium (RPE) and is the outer layer of the CBE (Davson, 1990). It is a 5-6 μm high cell layer with a dark brown appearance due to the presence of melanin granules. The dark colour is further contributed by the unusually compact arrangement of the cytoplasmic organelles and the conspicuous presence of cytoplasmic fibrils (Kozart, 1968). Such an appearance makes it easily distinguishable from the NPE. Compared to the NPE, the PE has a higher anaerobic metabolic rate (Shimizu *et al.*, 1967) and a lesser number of mitochondria (Cole, 1984). It has a large surface area, built by the infoldings of its basal surface, which facilitates solute uptake from the blood stream (Edelman *et al.*, 1994).

1.1.2 Non-pigmented epithelium (NPE)

The NPE is the inner layer of the CBE. It consists of a monolayer cell of 6-8 μm wide and 10-15 μm high (Kozart, 1968). It is the anterior continuation of the neurosensory retina (Morrison and Freddo, 1996; Glasser and Kaufman, 2003), and lies between the PE and the aqueous humor. It possesses numerous basal infoldings and interdigitations, and was originally believed to be the only site responsible for aqueous humor formation (Okisaka and Kuwabara, 1974). In addition, it is the sole layer in the CBE that has intercellular tight junctions that serve the purpose of selective solute transport at the blood aqueous barrier (BAB) (Raviola, 1971). Compared to the PE, the NPE has more mitochondria and rough endoplasmic reticulum, as well as a higher activity of Sodium-Potassium adenosine triphosphatase (Na^+, K^+-ATPase) and adenylate cyclase, enzymes that participate in active fluid secretion (Elena *et al.*, 1984; Riley and Kishida, 1986;

Flugel *et al.*, 1989; Eichhorn *et al.*, 1993a). The NPE expresses enzymes for aerobic metabolism at a very high level (Cole, 1966; Shimizu *et al.*, 1967). All these characteristics indicate its activeness in both secretion and metabolism.

1.1.3 Intercellular junctions

1.1.3.1 Tight junctions

Tight junctions, also known as zonula occludens, are located only at the apical-lateral side of the NPE cells (Raviola and Raviola, 1978). They form a continuous network in which each junction consists of two or more superimposed strands, indicating the co-existence of relatively tight and leaky sites (Noske *et al.*, 1994). They restrict the inter-cellular movement of small water soluble molecules and also membrane protein movement (Bill, 1986). However, these junctions are still regarded as a "leaky" type of tight junction, due to their low fluid permeability (Cunha-Vaz, 1979) and pressure-dependent transport features (Pederson, 1982). Nevertheless, research has suggested that the bilayers' electrical resistance could be high if one considers the total unfolded surface area of the CBE (Krupin *et al.*, 1984). The "tight" epithelial nature has been corroborated in the rabbit iris-ciliary body, which bore the same mannitol permeability as other tight epithelia (Chu and Candia, 1987a). Concerning the transepithelial resistance, anterior ciliary processes were "less leaky" (i.e. possessed a higher resistance) than posterior ciliary processes or pars plana. In the rat, the number of tight junctions appeared to be inconsistent, since the junctional depth and number of superimposed junctional fibrils decreased with age (Arguillere *et al.*, 1986). Despite this, tight junctions of NPE are believed to act as the major "sieve" used for aqueous humor formation. In conjunction

with gap junctions (Bill, 1986), the NPE tight junctions constitute the BAB, with another endothelial component at the level of the iris blood vessels (Cunha-Vaz, 1979) and ciliary muscle capillaries (Schlingemann *et al.*, 1998). This barrier behaves as an isoporous membrane (Dernouchamps and Heremans, 1975) to limit substrate passage (DiMattio and Zadunaisky, 1981; Chu and Candia, 1988) and assure transparency of ocular media by restricting the diffusion of macromolecules into the aqueous chamber (Vegge, 1971; Hirsch *et al.*, 1980). Its barrier function is further validated by the extremely low level of protein in the aqueous humor (Hirsch *et al.*, 1985; Bill, 1986).

1.1.3.2 Gap junctions

Gap junctions (2 nm gap) are highly organized structures composed of "connexon" plasma membrane proteins. They connect the cytoplasm of adjacent cells, as hydrophilic channels (Shin *et al.*, 1996) and act as ion-gated channels for signalling communication between cells (Bazzoni and Dejana, 2004). They allow the passage of small molecules up to molecular size of 1 kDa (Bennett *et al.*, 1991) and 12 Å in diameter (Oh *et al.*, 1994). In the CBE, gap junctions are found in between all cells (i.e. within each epithelial layer and between the bilayers) and are most abundant in between the NPE and PE cells (Raviola and Raviola, 1978; Coca-Prados *et al.*, 1992). No significant difference was found in both the intracellular ion contents (Bowler *et al.*, 1996) and membrane potential (Carre *et al.*, 1992) between these cell bilayers, indicating the presence of free solute or ion exchange. Further evidence of cell-to-cell communication was demonstrated using a micro-iontophoretic dye, which revealed the presence of cell-to-cell substrate coupling. However, such coupling was found to be pH sensitive, and sensitive to high calcium

concentration, as dye coupling ceased under extracellular acidosis or high calcium concentration (Oh *et al.*, 1994). Despite this, gap junctions are an important route of intercellular communication, which ultimately help to build a functional syncytium from the CBE bilayer (Edelman *et al.*, 1994; Oh *et al.*, 1994).

1.1.4 Regional differences in the CBE

The pars plicata is the anterior part of the CBE, which can be further divided into the iridial processes, the ciliary muscle and the ciliary processes (Hara *et al.*, 1977). Its innermost layer folds into finger-like projections, which are believed to be the major site for aqueous humor formation. The pars plana is a smooth, membranous layer of posterior CBE, which has significantly less rough endoplasmic reticulum and mitochondria than pars plicata. It is the region which provides mechanical zonular support to the crystalline lens (Noske *et al.*, 1994), but not a site regarded for active secretion, since Na^+, K^+-ATPase was scarcely observed in it (Flugel *et al.*, 1989). In contrast, different isoforms (alpha 1, alpha 2, alpha 3, beta 1 and beta 2) of Na^+, K^+-ATPase were intensely stained at the pars plicata (Ghosh *et al.*, 1991). In addition, endothelin-1 (ET-1), a chemical messenger which constricts blood vessels to instantly lower intraocular pressure, was mostly observed at the crests of the pars plicata, but not the pars plana (Eichhorn and Lutjen-Drecoll, 1993b). The same was found for carbonic anhydrous staining (Muther and Friedland, 1980). These findings indicate again the active involvement of the pars plicata in aqueous formation.

1.2 Glucose

1.2.1 Structure and function

Glucose is a common form of hexose, which is one of the most important nutrients for mammalian cells (Takata *et al.*, 1993). Living cells require glucose as a starting material for energy production (Mueckler, 1994a). The ability of a plasma membrane to transport glucose is, therefore, a common cellular feature, to maintain this major source of metabolic energy supply (Bell *et al.*, 1990). In general, D-glucose, is the principle isoform of glucose utilized by higher organisms, that exists in three different forms: two hemiacetal structures and one linear structure (Lodish *et al.*, 2003). Under different environment conditions, D-glucose can change its structure to achieve various biological purposes. Figure 1.1 shows the three different structures of D-glucose.

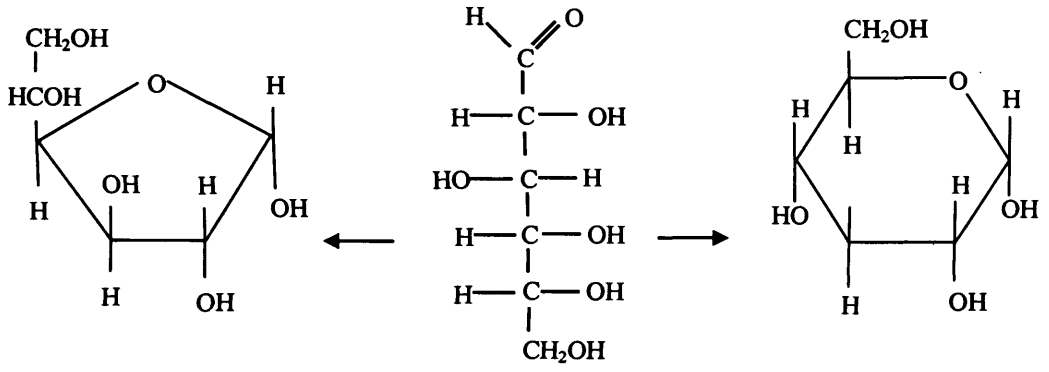

D-Glucofuranose D-glucose D-Glucopyranose

Fig. 1.1 Chemical structures of glucose.

1.2.1.1 Glycolysis

Glucose is a crucial substrate for cell nourishment. It is used to generate adenosine triphosphate (ATP) through glycolysis. Glycolysis is a series of reactions that takes place in the cell cytoplasm, to break down glucose to produce ATP. In each glycolytic cycle, two net ATPs are generated from every glucose molecule. Glycolytic intermediates can further be utilized as substrates to generate more ATP, e.g. pyruvate is consumed in the citric acid cycle of mitochondria, or used for biosynthetic pathways. In the presence of oxygen (i.e. aerobic conditions), nicotinamide adenine dinucleotide (NADH) and pyruvate, two of the glycolytic intermediates, can undergo oxidative phosphorylation for efficient ATP production (~ 30 ATPs per glucose molecule). In anaerobic condition, pyruvate is converted to lactic acid, while NADH is oxidized to NAD^+ that can be reused in glycolysis. The anaerobic metabolism can still generate ATP yet the efficiency is much reduced (i.e. two ATPs per cycle). In the eye, glycolysis is important as it provides the necessary energy to support phototransduction and nicotinamide adenine dinucleotide phosphate (NADPH) for other NADPH-requiring processes such as rhodopsin regeneration in the retina (Hsu and Molday, 1994). In other words, the presence of glucose is vital for the normal functioning of the eyes.

1.2.2 Transepithelial pathways

The plasma membrane consists of a phospholipid bilayer and acts as a selectively permeable barrier. Some molecules such as water and urea can pass through it unaided, while others like amino acids, ions and sugars require integral membrane transporter proteins for their passage. Since glucose is a polar and hydrophilic molecule, an integral

transporter protein is required if it needs to pass across the plasma membrane (Bell *et al.*, 1990). However, glucose can also traverse cells, across tight junctions and along the lateral intercellular spaces without passing through the cells. The former pathway is called the transcellular pathway, whilst the latter is called the paracellular pathway. Figure 1.2 illustrates these two pathways, based on the structure of the CBE. In the transcellular pathway, glucose is taken up by glucose transporters along the basolateral side from the extracellular spaces, into intracellular compartments. From here, they pass through gap junctions and reach the second epithelial layer and are transported out of the cell layer by other transporter proteins along the basolateral membrane.

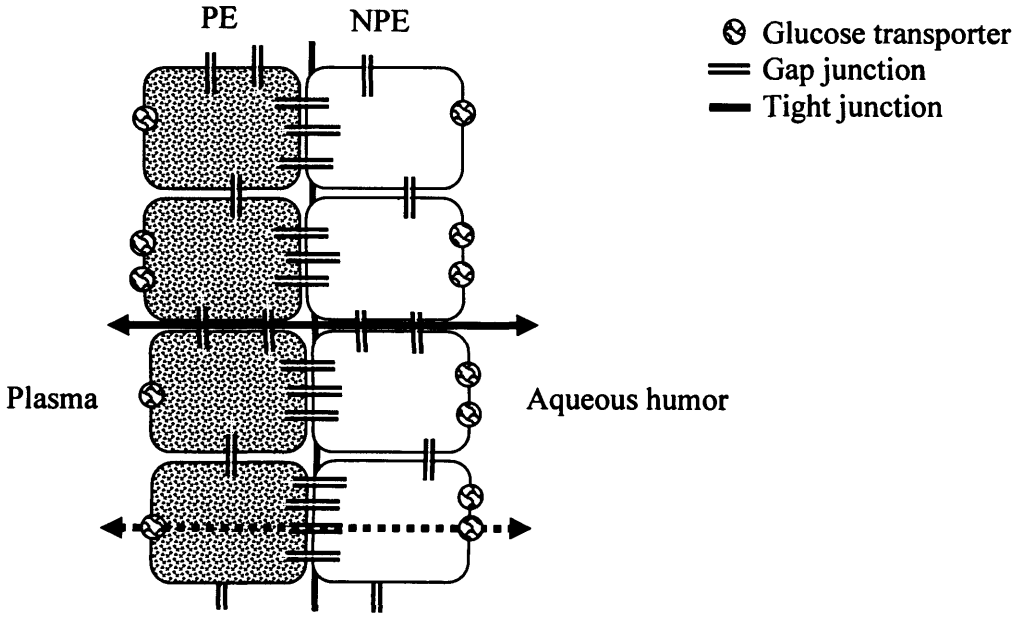

Fig. 1.2 Schematic diagram showing the transepithelial pathways for glucose in the CBE. The solid and dotted arrows indicate the paracellular and transcellular pathways respectively.

1.2.3 Glucose transporter families

The plasma membrane, which isolates the cell body from the extracellular environment, is composed of a phospholipid bilayer that is impermeable to hydrophilic substances such as glucose. Therefore, glucose needs a special transport mechanism in order to diffuse into cells in a rapid and efficient manner. As integral membrane proteins, glucose transporters help to mediate the transport of glucose (or similar substances like fructose) across the cellular membrane (Baly and Horuk, 1988; Carruthers, 1990; Baldwin, 1993) via one of the two different mechanisms. The first mechanism involves passive facilitative transport, and is mediated by members of the facilitative glucose transporter (GLUT) family (gene symbol SLC2). The second mechanism involves active transport by sodium-dependent glucose cotransporters (SGLTs) (Silverman, 1991; Baldwin, 1993; Wright and Turk, 2004).

1.2.3.1 The GLUT family

Classification. Currently, 14 isoforms of the SLC2 family have been identified. This glucose and polyol transporter family comprises members including GLUT1-12, GLUT14 (Wu and Freeze, 2002) and the proton-dependent- *myo*-inositol cotransporter (HMIT) (Uldry and Thorens, 2004) (Table 1.1). GLUTs have been named and distinguished according to their amino sequence, major tissue expression sites, specificity and, affinity and expression response to insulin (Kayano *et al.*, 1990; Gould and Holman, 1993; Mahraoui *et al.*, 1994; Wu and Freeze, 2002; Wood and Trayhurn, 2003). They are responsible for passive hexose transport driven by a glucose concentration gradient, without the consumption of energy (i.e. ATP) (Mueckler, 1994a). They exist in almost all

mammalian cells and are believed to be crucial for basal glucose uptake (Bell *et al.*, 1993). The most common GLUTs in mammals are GLUT1-5, with GLUT1, GLUT2, GLUT3, GLUT4 classified as Class I GLUTs and GLUT5, GLUT7, GLUT9 and GLUT11 as Class II. The remainder are categorized as Class III. This classification system is based on their multiple sequence alignments (Wood and Trayhurn, 2003). At present, no classification has been done for GLUT14, yet there is a high possibility for it to be classified into Class I, as it was found as a duplicon (i.e. an alternate splice form) of GLUT3 specifically present in the testis (Wu and Freeze, 2002).

Structure. In 1985, the 12-helix model for the structure of GLUTs was suggested on the basis of a hydropathy plot (Mueckler *et al.*, 1985), which was later supported by a glycosylation scanning study (Hresko *et al.*, 1994) and by sequence analysis (Sato and Mueckler, 1999). Today, the presence of 12-transmembrane helical domains in GLUT proteins is considered their structural hallmark (Joost and Thorens, 2001). All GLUT proteins have both their amino and carboxy-termini located on the cytoplasmic side of the plasma membrane, together with a N-linked oligosaccharide side-chain located either on the first or fifth extracellular loop (Uldry and Thorens, 2004). The 12-helices, together with intracellularly located carboxyl- and amino-termini, provide the necessary orientation in the plasma membrane and participate in the conformational changes during transport process (Schurmann *et al.*, 1997; Joost and Thorens, 2001). Several charged residues in the cytoplasmic surface were also suggested to mediate the conformational alteration of the protein during translocation process as revealed in mutational analysis (Tamori *et al.*, 1994; Doege *et al.*, 1998). For example, the tryptophan in helix 11, and the

glutamine 161 residue at the amino-terminus of GLUT1, are crucial in mediating the transport activity and substrate binding capacity (Inukai *et al.*, 1994; Mueckler *et al.*, 1994b; Wandel *et al.*, 1996), while serine-294 and threonine-295 are important for normal GLUT4 transport activity (Doege *et al.*, 1998).

GLUT1 or erythrocyte/brain/HepG2-glucose transporter. GLUT1 is a hydrophobic glycoprotein expressed at highest level in the plasma membrane of erythrocytes and in brain tissues (Bell *et al.*, 1993; Wagstaff *et al.*, 1995; Zhang and Ismail-Beigi, 1998). Moderate levels were observed in adipose tissue, muscle and liver (Zeller *et al.*, 1994; Rudich *et al.*, 2003). The differential N-linked glycosylation (Asano *et al.*, 1993) resulted in different GLUT1 glycoforms (with the 45 kDa form the most common) with a core protein of approximately 40 kDa (Morgello *et al.*, 1995; Takahashi *et al.*, 1996; Yu and Ding, 1998). The real function of the glycosylation is unknown, yet it has been suggested to play a role in governing the glucose transport activity that could affect the overall transport capacity (Feugeas *et al.*, 1990) or affinity (Asano *et al.*, 1993).
GLUT1 is considered as the house-keeping transporter responsible for glucose entry into most animal cells (Takata *et al.*, 1990; Takata, 1996) with a relatively high transport capacity (Brown, 2000). Glucose transport by GLUT1 occurs in a bi-directional manner, depending on the concentration gradient across the membrane (Carruthers, 1990). GLUT1-mediated transport can be specifically inhibited by phloretin and cytochalasin B (Bloch, 1973; Drewes *et al.*, 1977; Seyfang and Duszenko, 1991; Fuhrmann *et al.*, 1992). GLUT1 was the first glucose transport protein to be purified, having been confirmed from human erythrocyte ghosts as a zone 4.5 protein (Kasahara and Hinkle, 1977). It is

recognized as the most widely distributed protein among the GLUT family in mammalian cells, being especially concentrated in areas with occluding or barrier functions that constitute the blood-tissue barriers (Harik *et al.*, 1990; Takata *et al.*, 1990; Takata *et al.*, 1992). GLUT1, on the other hand, is also believed to function as a water-channel that facilitates the passage of water across the plasma membrane (Fischbarg *et al.*, 1990). Deficiency of GLUT1 has been widely reported (De Vivo *et al.*, 1991; Klepper *et al.*, 1999). Seizures, acquired microcephaly and developmental delay are found at infancy (Klepper *et al.*, 1998) with GLUT1 deficiency. Other manifestation such as neurobehavioural disturbance has also been noted (Klepper *et al.*, 1999). In patients with Alzheimer disease, a glycoform of GLUT1 was significantly reduced compared to controls, although the underlying mechanisms are not known (Simpson *et al.*, 1994).

GLUT2 or liver glucose transporter. GLUT2 is a low affinity, high capacity glucose transporter (Thorens, 1992), most abundantly expressed in liver, intestine, kidney and pancreatic beta-cells (Ohneda *et al.*, 1993; Zhao *et al.*, 1993; Mahraoui *et al.*, 1994). It is a crucial transporter in cells which play an important role in systemic glucose regulation (Thorens *et al.*, 1988) and is known to have a significant regulatory function in systemic glucose homeostasis (Thorens, 1992). It is recognized as part of the sensing system for blood glucose coupling with secretion of insulin in the pancreatic beta-cells under hormonal control (Unger, 1991). Further evidences of GLUT2 being involved actively in glucose homeostasis has been found in intestinal glucose uptake (Shepherd *et al.*, 2004), glucose reabsorption in the kidney (Cramer *et al.*, 1992), and glucose uptake and release by the liver (Postic *et al.*, 1993). Apart from glucose, GLUT2 is known as a galactose

(Tsang *et al.*, 1994) and fructose transporter (Wright *et al.*, 2003). GLUT2 has been suggested to be an important isoform as regards impaired insulin secretory responses and it showed a reduced expression level in both ageing and diabetic tissues (Novelli *et al.*, 2000). In a study of transgenic mice, the expression of a GLUT2 antisense gene in pancreatic cells led to an 80% reduction in GLUT2 expression and consequently, diabetes (Valera *et al.*, 1994).

The first report of the presence of GLUT2 in the central nervous system (CNS) was the observation of GLUT2 mRNA and protein in retinal Müller cells at the apical membrane (Watanabe *et al.*, 1994). This finding is in line with findings in other tissues such as pancreatic cells, where GLUT2 has been found to be located preferentially on microvilli facing adjacent beta-cells (Orci *et al.*, 1989). As with the apical surface of the Müller cells, this site is very active with respect to nutrient transport (Reichenbach, 1989). The presence of GLUT2 in Müller cells suggests a role in ocular nutrient transport, distributing glucose within the retina (Watanabe *et al.*, 1994). During hyperglycemia, GLUT2 expression is increased, whilst in hyperinsulinaemia the reverse effect is found (Postic *et al.*, 1993). Furthermore, genetic defects of GLUT2 can cause Fanconi-Nickle syndrome, a rare autosomal recessive disorder, which happens at infancy, causing rickets, retarded growth and enlargement of liver and kidney resulting from glycogen accumulation (Santer *et al.*, 1997; Matsuura *et al.*, 2002).

GLUT3 or brain glucose transporter. GLUT3 is a high affinity glucose transporter, which works efficiently at a lower substrate concentration than the other isoforms (Mueckler, 1994a). It exists mainly in high glucose demanding tissues, such as brain

(Kayano *et al.*, 1990; Nagamatsu *et al.*, 1992; Brown, 2000). However, GLUT3 mRNA and protein have been observed in other human tissues such as placenta, liver, fat and muscles (Bell *et al.*, 1990; Gould *et al.*, 1992). GLUT3 and GLUT1 work together to deliver glucose to the brain, with GLUT1 mediating the transport through endothelial cells, whilst GLUT3 completes the glucose transport to the neurons to support sufficient energy metabolism (Brown, 2000). After hypoxic injury, GLUT3 content decreases in the brain, due to death of neural cells (Vannucci *et al.*, 1998a). Similar to GLUT1, the concentration of GLUT3 is reduced in Alzheimer disease, presumably due to neuronal damage (Simpson *et al.*, 1994).

A recent study has revealed the conformational transitions of GLUTs by examining GLUT3 (Dwyer, 2001). It was suggested that GLUT3 mediates glucose transport through an accordion-like movement of the helices with respect to the membrane. This movement modulates the opening of the protein pore and makes the transmembrane segment more flexible for glucose carriage.

GLUT4 or muscle-fat glucose transporter. GLUT4 is an insulin-responsive GLUT isoform, which is found mainly in insulin-sensitive tissues like muscles, fat/adipose tissue and cardiac tissue (James *et al.*, 1989; Birnbaum, 1992). Insulin stimulates glucose uptake in these tissues by upregulating the rate of GLUT4 exocytosis, coupled with a slower rate in endocytosis (Liu *et al.*, 2004). When GLUT4 was released from intracellular GLUT4-containing vesicles onto the plasma membrane surface, it resulted in 10 to 20 fold higher glucose transport rate (Shepherd and Kahn, 1999; Bryant *et al.*, 2002). This insulin-stimulated process is rapid, yet reversible (Mueckler, 1994a). It has

also been suggested that the transport activity of GLUT4 is increased in response to insulin stimulation, independently of its increased translocation to the plasma membrane (Michelle Furtado *et al.*, 2003). This change in transport activity might be related to the degree of phosphorylation (Reusch *et al.*, 1993), yet a solid conclusion has yet to be made.

In fasting conditions, rats show a decrease in GLUT4 expression in adipose tissues, but an increase in muscle cells (Charron and Kahn, 1990). Likewise, during sustained exercise, an increase of GLUT4 expression was observed in muscles (Ebeling *et al.*, 1993). A high-fat diet, however, resulted in a reduction of GLUT4 transcriptional level in both skeletal muscles and adipose tissues, which was associated with decreased glucose utilization (Pedersen *et al.*, 1991; Kim *et al.*, 1994). When comparing the response rate, changes in GLUT4 translocation happened in a much faster manner in response to insulin stimulation, than in response to altered metabolic conditions (Brown, 2000).

Studies have been carried out in a wide range diabetic and non-diabetic model systems, with the aim of drawing a link between GLUT4 expression and insulin resistance. However, the results have not been conclusive. In different GLUT4 knock-out mouse models, various degrees of diabetic complications were exhibited (Zisman *et al.*, 2000; Abel *et al.*, 2001). Therefore, downregulation of GLUT4 protein in diabetic model has been proposed as one of the causes of elevated extracellular glycemic level (Berger *et al.*, 1989; Garvey *et al.*, 1989; Sivitz *et al.*, 1989). However, these diabetic animal models demonstrated a reduction of GLUT4 expression only in adipose tissues, not in muscles (Shepherd and Kahn, 1999; Astrup and Finer, 2000), which argues against the idea that GLUT4 is the main causative factor in insulin resistance (Shepherd and Kahn, 1999).

Researchers currently think that the reduction of GLUT4 expression might more likely be one of the outcomes of diabetes (Brown, 2000).

GLUT5 or intestine glucose transporter. GLUT5 is the GLUT isoform heading the Class II category of the family: it possesses weak homology when compared to the Class I isoforms (Kayano *et al.*, 1990). It is more of a fructose transporter than a glucose transporter, and transports fructose preferentially in the furanose ring form (Kane *et al.*, 1997). It expressed at highest level in the small intestine, where it is generally believed to be crucial for nutritional daily fructose uptake (Davidson *et al.*, 1992; Kane *et al.*, 1997). In the intestine, it is expressed predominantly at the luminal surface of the absorptive epithelial cells, where together with GLUT2 it mediates glucose transport across the intestinal linings (Davidson *et al.*, 1992). It was also reported to exist at a high level in human spermatozoa, and mediates the consumption of fructose by sperm cells from seminal fluid (Burant *et al.*, 1992). Furthermore, it can be found in brain endothelium, kidney, muscle and fat cells, yet at a comparatively lower level (Hundal *et al.*, 1992; Shepherd *et al.*, 1992; Wood and Trayhurn, 2003). It is a high affinity hexose transporter (Miyamoto *et al.*, 1994) and possesses consistent fructose transport across a wide range of pH (i.e. pH 4.5-7.5) (Kane *et al.*, 1997). However, the role of GLUT5 in the brain endothelial cells is unclear, since fructose is not the prime metabolic substrate in the brain (Mantych *et al.*, 1993a).

Examination of GLUT5 transport activity in intestine and spermatozoa has shown that GLUT5 is insensitive to insulin and cytochalasin B, a competitive GLUT inhibitor (Burant *et al.*, 1992; Shepherd *et al.*, 1992). This contradicts a previous study, in which

GLUT5 was observed as a cytochalasin B sensitive transporter in *Xenopus laevis* oocytes (Kayano *et al.*, 1990). In addition, a recent study showed that chronic insulin incubation with a muscle cell line, caused a dose-dependent increase in GLUT5 expression and transport activity. This increase in abundance and functional activity of GLUT5 in skeletal muscle cells was suggested to be mediated via activation of the GLUT5 promoter (Hajduch *et al.*, 2003). The discrepancy in results might be due to different tissues used in the experiment, yet little has been done to clarify the inconsistency.

GLUT6. The name GLUT6 was originally assigned to a pseudogene derived from the GLUT3 gene (Kayano *et al.*, 1990). However, the GLUT6 designation has now been transferred to a gene originally designated GLUT9 (Joost *et al.*, 2002). Human GLUT6 mRNA is expressed predominantly in spleen, peripheral leucocytes and brain, but protein expression has never been observed (Doege *et al.*, 2000b). When constituted in primary adipocytes, GLUT6 was retained in the intracellular compartment, and no stimulus has been shown to cause its translocation (Lisinski *et al.*, 2001).

GLUT7. GLUT7 was recently characterised as a transporter possessing 68% similarity and 53% identity to GLUT5 (Li *et al.*, 2004). It was identified in a genome homology search (Joost and Thorens, 2001) and is known to be expressed in small intestine, colon, testis and prostate as a high affinity glucose and fructose transporter (Li *et al.*, 2004). It contains a six-amino acid chain at its carboxyl terminus, which is similar to a consensus motif in GLUT2 for retention of the protein in the endoplasmic reticulum (Mueckler, 1994a; Joost and Thorens, 2001).

GLUT8. Similar to GLUT6, GLUT8 (formerly GLUT11) was found to be entirely retained intracellularly. It is believed to be involved in mediating glucose homeostasis (Piroli *et al.*, 2002). In addition, GLUT8 revealed a relatively high affinity for glucose transport (Ibberson *et al.*, 2000), with the transport process being both fructose and galactose competitive (Wright and Turk, 2004). Insulin successfully induced translocation of GLUT8 to the plasma membrane in blastocytes (Carayannopoulos *et al.*, 2000), but failed in fat cells (Lisinski *et al.*, 2001). Its mRNA was abundantly found in testis and brain, and at lower level in adipose tissues, heart and skeletal muscles (Ibberson *et al.*, 2000; Sankar *et al.*, 2002). Recently, it has been observed in liver, and suggested to be related to diabetic pathogenesis, as a reduction of GLUT8 mRNA level was found in mouse diabetic models (Doege *et al.*, 2000a). It was suggested that, like GLUT2 and GLUT4, GLUT8 is another GLUT isoform closely involved in glucose homeostasis (Gorovits *et al.*, 2003)

GLUT9. The GLUT9 isoform has the highest degree of similarity with GLUT5 (Joost and Thorens, 2001), which suggested a fructose transport property might exist. A recent study in which GLUT9 was expressed in *Xenopus laevis* oocytes, found that GLUT9 transport activity was cytochalasin B-insensitive and had low transport affinity (Augustin *et al.*, 2004). GLUT9 is mostly found in kidney and liver (Phay *et al.*, 2000; Joost and Thorens, 2001). Low mRNA levels were detected in lung, small intestine, leukocytes, placenta (Phay *et al.*, 2000) and human chondrocytes (Mobasheri *et al.*, 2002).

GLUT10. GLUT10 is a Class III GLUT with highest similarity to GLUT8 (Wood and Trayhurn, 2003). It is expressed in liver and pancreas, with lower mRNA levels found in heart, kidney, placenta and skeletal muscles (McVie-Wylie *et al.*, 2001). The chromosome localization of GLUT10 lies in the same region as a type-2 diabetes susceptibility locus. Therefore, GLUT10 has been suggested as a candidate gene involved in this metabolic disorder (Dawson *et al.*, 2001).

GLUT11. Currently, three different alternative splice isoforms have been derived for GLUT11, due to the presence of three different first exons, that code for three corresponding N-termini (Sasaki *et al.*, 2001). It presents as a functional isoform with low transport affinity, and cytochalasin B-sensitivity (Doege *et al.*, 2001). It is expressed in different tissues, including heart and skeletal muscles (Wu *et al.*, 2002), and at intermediates level in tissues such as brain and small intestine (Wu *et al.*, 2002). A crucial role of GLUT11 has been suggested in muscle glucose homeostasis, due to its specific expression pattern in this tissue (Uldry and Thorens, 2004).

GLUT12. GLUT12 cDNA was cloned from a human embryonic cDNA library and found to be mainly expressed in heart, prostate and moderate levels at skeletal muscles, brown adipose tissues, muscle, small intestine and mammary gland (Rogers *et al.*, 2002; Macheda *et al.*, 2003). Strong expression has been found in breast tumours, which indicates a possible role of GLUT12 in hexose supply under oncogenic conditions (Rogers *et al.*, 2003b). In addition, GLUT12 has shown selective affinity to D-glucose, followed by D-deoxyglucose, D-galactose and D-fructose (Rogers *et al.*, 2003a).

HMIT. No hexose transport activity has been found for HMIT, but it was determined as a specific transporter for *myo*-inositol (Joost and Thorens, 2001). Its transport activity is high and could be activated by lowering the pH, with a maximal transport capacity at pH 5.0 (Uldry *et al.*, 2001; Eladari *et al.*, 2002). The transport affinity of HMIT is sensitive to several inhibitors such as phloretin, phlorizin and cytochalasin B (Hager *et al.*, 1995). In the rat brain, it exists as a 75-90 kDa glycoprotein, but can be converted to a 67 kDa form upon enzymatic deglycosylation . HMIT is expressed in neurons and glial cells, located both intracellularly and on the membrane surface. It is the transporter isoform which is believed to be responsible for *myo*-inositol metabolism and signal transmission process in the brain (Uldry *et al.*, 2001).

GLUT14. The most recently cloned GLUT isoform that was reported two years ago. GLUT14 has remarkable identity to GLUT3, and is assumed to be a pseudogene that arose through duplication of GLUT3. It exists exclusively in the testis, and is present in two different splice forms. The long form (GLUT14-L) differs from the short form (GLUT14-S) by an additional exon coding for a novel N-terminus. In the testis, its mRNA level is three times higher than that of GLUT3 (Wu and Freeze, 2002). However, further details on its functional role have not been investigated.

1.2.3.2 Sodium glucose cotransporters (SGLTs)/symporters

The sodium cotransporters belong to the SLC5 superfamily, which consists of 220 or more members in animal and bacterial cells (Wright and Turk, 2004). Among all, seven SGLT isoforms have been suggested to mediate glucose transport, but only four of them are functionally characterised (Wright, 2001; Wright and Turk, 2004). In the SGLT system, glucose is transported against its own concentration gradient, but down the sodium gradient across the plasma membrane (Wood and Trayhurn, 2003) (Table 1.2). Since sodium in cells is constantly being pumped out by the Na^+, K^+-ATPase, glucose transport via the SGLTs is recognised as an active transport process (Wright, 2001; Wood and Trayhurn, 2003). Thus, SGLTs are secondary active transporters, driven by a pre-established sodium gradient. Glucose transport is coupled such that a single glucose molecule is translocated across the plasma membrane with one or more sodium at one time (Horibe *et al.*, 1997). The SGLTs are believed to play a major role in dietary glucose uptake, particularly at the small intestine (Ferraris, 2001; Stumpel *et al.*, 2001).

Structure. Similar to GLUTs, all cotransporter family members have a 12 transmembrane alpha helical structure, accompanied by clear helical packing in the carboxy-terminus. Their secondary structure suggests the presence of 14 helices, with both the amino- and carboxy-termini on the extracellular side of the membrane (Turk and Wright, 1997; Jung, 2002). Only four amino acids are known to be essential for functional activity, since researchers are encountering difficulties in studying expression constructs (Lostao *et al.*, 1995; Martin *et al.*, 1996). In general, all the transporters in this group seem to work by the same mechanism, in which the rate or direction of transport depends purely on the

number of ligands on each side of the plasma membrane and the membrane potential (Parent *et al.*, 1992; Hirayama *et al.*, 1997; Meinild *et al.*, 2002). They transport substrate in an "alternative access" manner (Loo *et al.*, 1998), with a maximal turnover rate of 1-100 per second at room temperature (Wright and Turk, 2004).

SGLT1. Rabbit SGLT1 was the first isoform to be cloned. It is responsible for high affinity, low capacity glucose cotransport in the rabbit intestine (Hediger *et al.*, 1987). Its human homologue was cloned two years later (Hediger *et al.*, 1989), and found to possess a nucleotide similarity of 71% (Wood and Trayhurn, 2003). It expressed predominantly in the absorptive epithelial cells of the small intestine, where it mediates D-glucose and D-galactose absorption from the gut lumen (Takata, 1996; Ferraris, 2001; Wright *et al.*, 2003). In addition, it also performs glucose reabsorption in the late proximal tubules to prevent glucose loss (Cramer *et al.*, 1992; Lee *et al.*, 1994; Takata, 1996) and is known to bear a 2:1 stoichiometry between sodium and glucose (Panayotova-Heiermann *et al.*, 1995; Mackenzie *et al.*, 1998). Although no obvious selectivity has been revealed for SGLT1 in transporting different hexoses, differences in selectivity do exist between species (Hirayama *et al.*, 1996). In the absence of glucose, SGLT1 also acts as a uniporter of sodium ions, water pump (Loo *et al.*, 1996; Meinild *et al.*, 1998), urea channel or cotransporter for both water and urea (Leung *et al.*, 2000b).

Freeze-fracture electron microscopy has confirmed that SGLT1 functions as a 14-helical monomer in the plasma membrane (Turk *et al.*, 2000). Further studies also suggest that helices 10-13 of GLUT1 form the sugar permeation pathway (Panayotova-Heiermann *et al.*, 1997), while channels for small molecules such as urea have also been observed for

rabbit SGLT1 when expressed in oocytes (Panayotova-Heiermann and Wright, 2001). Malabsorption of glucose and galactose was reported to be related to mutations of human SGLT1 (Turk *et al.*, 1991). The disease was caused by improper trafficking of the mutated SGLT1 to the plasma membrane, which impaired transport activity and decreased transport affinity (Martin *et al.*, 1996). Fortunately, the disorder could be corrected by substituting dietary glucose with fructose (Wood and Trayhurn, 2003).

SGLT2. SGLT2 is a low-affinity glucose cotransporter predominantly expressed in the kidney (Oulianova and Berteloot, 1996). Controversy has surrounded whether SGLT2 is the major SGLT isoform in the kidney, rather than SGLT1 (Wright, 2001; van den Heuvel *et al.*, 2002). SGLT2 is expressed in the convoluted proximal tubules (Kanai *et al.*, 1994) where it is believed to play an important role in bulk glucose transport from the glomerular filtrate back to the blood stream (Oulianova and Berteloot, 1996). It is a low affinity, but high capacity transporter with a stoichiometry between sodium and glucose of 1:1 (Diez-Sampedro *et al.*, 2001). However, unlike SGLT1, it functions as a more selective transporter that prefers D-glucose to D-galactose as a substrate (Mackenzie *et al.*, 1994). In addition, its transport affinity is much lower (~10 fold) than that of SGLT1 (Wright, 2001).

SGLT3. SGLT3, formerly named as pig-SGLT2, is a SGLT isoform that demonstrates the same stoichiometry and affinity as SGLT1 (2:1), but has a specificity similar to that of SGLT2 (Mackenzie *et al.*, 1996). It shares 70% amino acid identity with human SGLT1, and is expressed in small intestine and skeletal muscles (Diez-Sampedro *et al.*,

2003). Its transport process is phlorizin-sensitive, which is a common feature demonstrated in SGLT1 and SGLT2 (Oulianova and Berteloot, 1996; Loo *et al.*, 1998; Diez-Sampedro *et al.*, 2003). However, the functional role of SGLT3 is suggested to be one of glucose sensing, rather than glucose transport (Diez-Sampedro *et al.*, 2003).

SGLT4, SGLT5 and SGLT6. SGLT4 is widely expressed in the body, while SGLT5 is expressed exclusively in the kidney. Further functional characteristics are not yet available for these two isoforms (Wright and Turk, 2004). SGLT6 is a high affinity cotransporter for *myo*-inositol, but with a lower affinity for D-glucose, as demonstrated in the rabbit (Nagata *et al.*, 1999; Coady *et al.*, 2002). SGLT6 is widely expressed in human tissues (Roll *et al.*, 2002; Wright and Turk, 2004).

Sodium-dependent myo-inositol transport (SMIT). This is the last member in the superfamily thought to possess glucose transport function. It is widely expressed (Kwon *et al.*, 1992) and suggested to play a crucial role in the pathogenesis of Down syndrome (Berry *et al.*, 1995). It demonstrated a relatively high affinity in transporting *myo*-inositol, but also different sugars, including D-glucose at a lower affinity (Hager *et al.*, 1995).

Isoform	Gene name	Amino acid residues	Class	Main tissue expression	Major biological roles	Transport Properties*	Primary references
GLUT1	SLC2A1	492	I	Erythrocytes, brain, ubiquitous in different tissues	General basal glucose transport, blood-tissue barriers glucose transport	K_m glucose ~ 20mM K_d ~ 0.08-0.19mM	(Mueckler *et al.*, 1985; Harik *et al.*, 1990; Takata *et al.*, 1990; Gould *et al.*, 1991; Hellwig and Joost, 1991)
GLUT2	SLC2A2	523	I	Pancreas, liver, small intestine, kidney	Pancreatic and hepatic glucose homeostasis, intestinal hexose (including glucose, fructose and galactose) transport and renal reabsorption	K_m glucose ~ 40mM K_d ~ 1.7-1.8mM	(Thorens *et al.*, 1988; Fukumoto *et al.*, 1988b; Gould *et al.*, 1991; Wandel *et al.*, 1996)
GLUT3	SLC2A3	496	I	Brain (neurons)	Glucose transport in the brain neurons	K_m glucose ~ 10mM	(Kayano *et al.*, 1988; Gould *et al.*, 1991; Nagamatsu *et al.*, 1992)
GLUT4	SLC2A4	510	I	Adipose tissue, cardiac muscle, skeletal muscle,	Insulin-dependant glucose transport	K_m glucose ~ 3mM K_d ~ 210±60nM	(Birnbaum, 1989; Fukumoto *et al.*, 1989; James *et al.*, 1989; Wandel *et al.*, 1996)
GLUT5	SLC2A5	501	II	Intestine, kidney, testis	Fructose absorption, low affinity hexose transport	K_m fructose ~ 11.6mM	(Kayano *et al.*, 1990; Burant *et al.*, 1992; Davidson *et al.*, 1992; Shepherd *et al.*, 1992)
GLUT6	SLC2A6	507	III	Brain, leukocytes, spleen	Low affinity glucose transport	K_d ~ 210±30nM	(Doege *et al.*, 2000b; Lisinski *et al.*, 2001)
GLUT7	SLC2A7	524	II	Small intestine, colon, testis, and prostate	Glucose and fructose transport	K_m glucose ~ 0.3mM K_m fructose ~ 0.06mM	(Li *et al.*, 2004)
GLUT8	SLC2A8	477	III	Testes, brain, insulin-sensitive cells	Glucose homeostasis, insulin-stimulated glucose transport	K_m 2-deoxy-D-glucose ~2.4mM K_d ~ 56.6±18nM	(Ibberson *et al.*, 2000; Doege *et al.*, 2000a)
GLUT9	SLC2A9	540	II	Kidney, liver	Low affinity deoxy-D-glucose transport	K_d ~ 105.2±16nM	(Phay *et al.*, 2000; Augustin *et al.*, 2004)
GLUT10	SLC2A10	541	III	Liver, pancreas	2-deoxy-D-glucose, D-glucose, D-galactose transport	K_m 2-deoxy-D-glucose ~ 0.3mM	(Dawson *et al.*, 2001; McVie-Wylie *et al.*, 2001)
GLUT11	SLC2A11	503/ 499/496	II	Cardiac muscle, Skeletal muscle	Fructose transport, low affinity to glucose	K_d ~ 196.6±29.7nM	(Doege *et al.*, 2001; Sasaki *et al.*, 2001; Wu *et al.*, 2002)
GLUT12	SLC2A12	617	III	Heart, prostate	D-glucose transport	---	(Rogers *et al.*, 2002; Rogers *et al.*, 2003b)
HMIT	SLC2A13	629	III	Brain	*myo*-inositol transport	K_m *myo*-inositol ~ 0.1mM	(Joost and Thorens, 2001; Uldry *et al.*, 2001)
GLUT14	SLC2A14	497/520	---	Testis	---	---	(Wu and Freeze, 2002)

Table 1.1 Characteristics of the SLC2 family. Please see remarks on the following page.

Isoform	Gene name	Amino acid residues	Main tissue expression	Major biological roles	Transport properties*	Primary references
SGLT1	SLC5A1	664	Small intestine, kidney, heart	Sodium-dependant intestinal glucose and galactose uptake, renal reabsorption	K_m D-glucose ~ 0.2-0.4mM K_m sodium ions ~ 3mM	(Lee *et al.*, 1994; Hirayama *et al.*, 1996; Oulianova and Berteloot, 1996)
SGLT2	SLC5A2	672	Kidney	Sodium-dependant renal glucose reabsorption	K_m D-glucose ~ 2mM K_m sodium ions ~ 100mM	(Kanai *et al.*, 1994; Oulianova and Berteloot, 1996) }
SMIT	SLC5A3	718	Brain, heart, kidney, lung	Sodium-dependant *myo*-inositol and glucose transport	K_m *myo*-inositol ~ 0.05mM	(Hager *et al.*, 1995)
SGLT3	SLC5A4	660	Small intestine, skeletal muscle	Glucose activated sodium channels	K_m D-glucose ~ 6mM K_m sodium ions ~ 1.5mM	(Mackenzie *et al.*, 1996; Diez-Sampedro *et al.*, 2001)
SGLT4	SLC5A8	659	Brain, liver, lung, kidney, small intestine	---	---	(Li *et al.*, 2003; Wright and Turk, 2004)
SGLT5	SLC5A9	681	Kidney	---	---	(Wright and Turk, 2004)
SGLT6	SGL5A10	673	Brain, heart, liver, lung, small intestine	*myo*-inositol, glucose transport	K_m *myo*-inositol ~ 0.25mM K_m sodium ions ~ 12.5mM	(Nagata *et al.*, 1999; Wright and Turk, 2004)

Table 1.2 Characteristics of the SLC5 family members. *K_m is the Michaelis-Menten constant, which indicates the substrate transport affinity of the transporter; The dissociation constant (K_d) indicates the binding affinity of the transporters to cytochalasin-B. A high K_d indicates high substrate transport capacity, but low substrate affinity.

1.2.4 Glucose transport in blood-tissue barriers

In the body, most substrates can exchange freely between blood vessels and tissue cells. However, specific organs and tissues have developed a barrier which is selectively impermeable to certain substrates. For example, the BAB in the eye is impermeable to proteins, so as to maintain ocular transparency (Bill, 1986). In this section, some tissue barriers which possess a similar functional structure to the BAB are introduced.

1.2.4.1 Blood-brain barrier (BBB)

The brain comprises ~ 2% of body weight but accounts for ~ 20% of total glucose consumption in humans. It has one of the highest metabolic rates of any organ (Sokoloff, 1973). In the BBB, tight junctions are present between endothelial cells, to hinder free substrate exchange (Stewart *et al.*, 1994). Intravenous injection experiments have demonstrated these barrier properties; thus tracers (such as horseradish peroxidase) remain in the lumen of blood vessels, unable to diffuse beyond the vascular endothelium (Reese and Karnovsky, 1967). Since glucose is the primary energy source for the brain, a specific mechanism to ensure continuous glucose supply is clearly necessary.

Glucose transport into brain cells occurs through a series of steps, with a decrease in concentration gradient, but an increase in transporter affinity at each step. From the blood plasma to the extracellular cerebral fluids, the glucose gradient decreased from 6 mM to 4 mM. Further to cerebral cells, the glucose concentration reduced to 0.5 mM. This reduction in glucose concentration was compensated by a general increase in transport affinity against the concentration gradient e.g. the kinetic constant (K_m) of blood capillaries is 8 mM, while at the cellular cells is 5 mM. This increase in transporter

affinity compensates for the falling glucose concentration and helps to maintain an adequate glucose level for cerebral metabolism (Crone, 1965; Bachelard, 1971; Pappenheimer and Setchell, 1973). Currently, GLUT1 is believed to be the predominant form of glucose transporter in the brain. This has been confirmed by immunoblotting (Takata *et al.*, 1990; Pardridge *et al.*, 1990b), northern blotting (Boado and Pardridge, 1990; Kamei *et al.*, 1999) and cytochalasin B-binding assay (Kalaria *et al.*, 1988; Dwyer and Pardridge, 1993). In addition, GLUT3 is also abundantly expressed in brain neurons (Nagamatsu *et al.*, 1992; Nagamatsu *et al.*, 1993; Vannucci *et al.*, 1998a) and GLUT5 in microglia (Maher *et al.*, 1994; Horikoshi *et al.*, 2003). In addition to the facilitated diffusion system, immunohistochemical, immunoblotting (Nishizaki *et al.*, 1995) and tracer studies (Lee *et al.*, 1997; Nishizaki and Matsuoka, 1998) have suggested the presence of SGLT in bovine cortical vessels and BBB respectively. Since the glucose concentration in the brain is only ~20% to that of plasma (Raichle *et al.*, 1975; Gruetter *et al.*, 1992), the presence of SGLTs would seems unnecessary, yet its functional role in the brain has not been investigated.

1.2.4.2 Blood-placental barrier (BPB)

The placenta is an important organ for the exchange of gases, nutrients and metabolites between maternal and fetal blood. Fetal blood is bounded inside a continuous endothelial layer with tight junctions (Heinrich *et al.*, 1976). However, these tight junctions are of the discontinuous type, which indicates the possibility of paracellular transport (Leach and Firth, 1992). The syncytiotrophoblast layer, a continuous single cell layer, is the main BPB component which separates the maternal and fetal circulation (Johnson and Smith,

1985). In order for glucose to reach the fetal circulation, it must pass this syncytial layer. Currently, it is widely accepted that glucose transport across the placenta is by the action of facilitated diffusion transport machinery. Kinetic studies (using the GLUT inhibitors phloretin and cytochalasin B) (Johnson and Smith, 1985), as well as northern blotting, *in situ* hybridization (Kamei *et al.*, 1999; Illsley, 2000), and immunoblotting (Takata *et al.*, 1992; Hahn *et al.*, 1995) studies all suggest the existence of GLUTs, especially GLUT1 and GLUT3 in the placenta. The highest level of GLUT1 expression was found along the syncytiotrophoblast and localized heavily at its microvillous apical membrane (Jansson *et al.*, 1993). In addition, the gap junction protein connexin 26 was found between the double-layered syncytiotrophoblast in rats (Metz *et al.*, 1978; Risek and Gilula, 1991). The protein may act as an intercellular hydrophilic channel for small molecules including glucose (Spray and Bennett, 1985). Similar to CBE, it has been suggested that transplacental glucose transfer begins with glucose entering the cytoplasm of the syncytial layer at the apical side via GLUT1. After passing through the gap junctions and reaching the basal side of the membrane, it also leaves by export through GLUT1 transporters (Takata, 1996). Similar to CBE, GLUT transporters together with gap junctions have been proposed as the major route of BPB glucose transport in human and rat (Takata *et al.*, 1994; Takata, 1996).

1.2.4.3 Ocular barriers

The eyes can be regarded as an extension of the central nervous system (CNS) for they are developed from the neural tube. The blood ocular barrier, including the blood-retinal barrier (BRB) and BAB, is suggested to be comparable to the BBB. The BRB comprises

the retinal microvasculature and the RPE. The former component has the property of the brain barrier (Bill *et al.*, 1980), since tracers such as horseradish peroxidase (Raviola, 1977), or endogenous serum proteins like albumin and immunoglobulin (Pino and Thouron, 1983), fail to cross it. The RPE constitutes the outermost layer of the retina and possesses both tight junctions and gap junctions (Hudspeth and Yee, 1973; Raviola, 1977). This barrier contributes significantly to the provision of nutrition to the outer retina (Ames, 1992), and separates the retina from the choroidal capillaries. Tight junctions in the RPE, make paracellular diffusion of glucose impossible (Ban and Rizzolo, 1997; Rizzolo, 1997). Since retina is one of the highest metabolically active tissues (Sharma and Ehinger, 2002), and derives most of its energy from glycolysis (Krebs, 1972), mechanisms must be present to allow glucose to diffuse across the RPE to the retina.

Transport of glucose in the RPE was found to occur by passive facilitated diffusion, since it was sensitive to inhibitors of facilitative glucose transport (DiMattio and Zadunaisky, 1981; Stramm and Pautler, 1982; To and Hodson, 1998b) and provided rich immunohistochemical staining for GLUT1 (Harik *et al.*, 1990; Mantych *et al.*, 1993b). In the retinal capillaries, GLUT1 was expressed at the barrier site (i.e. the endothelial cells) and also intracellularly and on the cellular membranes (Takata *et al.*, 1990; Kumagai *et al.*, 1996). In general, GLUT1 is believed to be the major barrier glucose transporter present in the retina, whilst intra-retinal glucose distribution is carried out by GLUT 2 (Watanabe *et al.*, 1994) and GLUT3 (Mantych *et al.*, 1993b).

The BAB is the barrier separating the blood plasma and aqueous humor at the anterior part of the eye. The aqueous humor is the major nutrient source (including glucose) for

many avascular ocular tissues such as the cornea and crystalline lens (Chylack and Cheng, 1978; DiMattio, 1984a; Thies and Mandel, 1985). The aqueous glucose concentration is comparable to that of blood (Cole, 1984): approximately 81% of that of plasma (Abdel-Latif, 1997). As illustrated in figure 1.2, glucose transport in the mammalian CE is accomplished by firstly transport from the blood plasma to the stromal layer, then into the PE cells via GLUTs. Then, it diffuses through the gap junctions, which connect the PE and NPE. Finally, it is transported into the aqueous humor by GLUTs (Takata *et al.*, 1997). In this case, GLUT1 acts as a selective gate, whilst the gap junctions act as non-selective channels (Shin *et al.*, 1996). Immunocytochemical studies have revealed heavy staining for GLUT1 in both the PE and NPE cells (Takata *et al.*, 1990; Takata *et al.*, 1991), especially along the basal infoldings in these layers (Takata *et al.*, 1997). These observations support the previous model described for the glucose transport across this part of the BAB.

Endothelial cells of the blood vessels in the iris stroma constitute the other part of the BAB. As the continuation of the CBE (Raviola, 1977), the iridial epithelium shows similar structures or features, such as tight junctions and inter-cellular gap junctions (Freddo, 1984). Heavy labeling was observed for GLUT1 in both the luminal and contraluminal plasma membranes (Takata *et al.*, 1991) and it is possible that glucose uses a similar pathway to enter and leave the iridial layers as it does in the CBE (Takata *et al.*, 1997).

1.3 Diabetes Mellitus (DM)

1.3.1 Prevalence

In the past 20 years, the increasing prevalence of DM and its related systemic complications have drawn the attention of researchers worldwide (Leung and Lam, 2000a). In 1997, an estimated 124 millions people were suffering from DM worldwide, with 97% of them having non-insulin dependent DM (NIDDM). Among all, 46% of diabetes are from the Asia-Pacific region. By the year 2010, this figure is expected to climb to 221 millions (Amos *et al.*, 1997). Since diabetic patients are at risk of various acute (e.g. diabetic ketoacidosis) and chronic complications (e.g. nephropathy), it is regarded, therefore, as a major source of mortality (Gu *et al.*, 1998; Tseng, 2004) and economic burden to the society (American Diabetes Association, 1998; Clarke *et al.*, 2003).

1.3.2 Cause of DM

DM is a disorder of carbohydrate metabolism, which also affects protein and lipid metabolism. It is characterized by excess urine excretion, hyperglycemia and a set of systemic complications that primarily affect the blood vessels of the brain, kidney, eyes and limbs. Two main theories have been proposed to explain the cause of DM. They are the "idiopathic" theory and the "secondary" theory. Idiopathic DM can be further categorized into two types: type 1, also known as insulin dependent DM (IDDM) and type 2, also named NIDDM. Type 1 DM is caused by an autoimmune destruction of the beta-cells in the pancreas, and is manifested at the age of 20 or earlier, so it is also named juvenile onset diabetes. It is a rarer type of DM compared to type 2, yet it more often

develops into ketoacidosis. Type 2 DM is the more common type, which presents with milder hyperglycemia and seldom leads to ketoacidosis. It is mostly in adult onset (thus it is sometimes called adult-onset diabetes). It usually manifests after the age of 40 and has been suggested to be a result of a genetic defect, which causes both insulin resistance and insulin deficiency (Galuk, 1991; Avery, 1998). It can be caused by insufficient number of functional insulin receptors on the surface of plasma membrane, which thus fail to provide adequate glucose uptake under normal conditions (Lonnroth, 1991; Lebovitz, 2001). Hales and co-workers proposed the 'Thrifty Phenotype Hypothesis' for NIDDM in 1992. This is based on the conflict between malnutrition at a certain stage of fetal development and over-nutrition in adulthood (Hales and Barker, 1992). The postnatal over-nutrition conflicts with the early metabolic programming, which finally leads to consequences like NIDDM, ischaemic heart disease and hypertension. This hypothesis has been tested and supported with studies in both humans (e.g. twin studies) (Poulsen *et al.*, 1997; Ravelli *et al.*, 1998) and rats (Snoeck *et al.*, 1990; Hales *et al.*, 1996), both of which indicate the importance of *in utero* conditioning in determining susceptibility to type 2 DM.

There are many disorders that could manifest DM as a secondary illness. These conditions include pancreatic disease, endocrine disease (Yajnik *et al.*, 1990; Watson, 2003), mutations in the insulin or insulin receptor genes (Vaxillaire *et al.*, 1999) and pregnancy (Hornnes, 1985; Godwin *et al.*, 1999). Other genetic syndromes such as Down's syndrome or Walfram syndrome (Robinson and Kessling, 1992; Ristow, 2004) also appear to increase the risk of diabetes or impaired glucose tolerance.

1.3.3 Mechanisms of DM pathogenicity

Various mechanisms have been proposed to explain the pathogenesis of diabetic complications. In general, five major theories have been suggested: the increased rate of polyol metabolism (Gillis and Chylack, 1982; Gaynes and Watkins, 1989), increased protein glycation (Forbes *et al.*, 2004; Zieman and Kass, 2004), activation of protein kinase C (PKC) (Inoguchi *et al.*, 2003; Setter *et al.*, 2003), increased flux in hexosamine metabolism (Kaneto *et al.*, 2001; Bosch *et al.*, 2003) and increased oxidative stress (Dominguez *et al.*, 1998; Ha and Kim, 1999).

1.3.3.1 Polyol pathway

The polyol pathway is a two-step pathway involving the conversion of glucose and galactose into sorbitol and galactitol, respectively, as the first step, and from sorbitol to fructose as the second step. For the first reaction to occur, aldose reductase (AR) must catalyse the NADPH-dependent reduction of the carbonyl compounds (i.e. glucose). In hyperglycemic conditions, AR is activated rapidly, so that glucose is oxidized into sorbitol, which is in turn oxidized to fructose by sorbitol dehydrogenase (Brownlee, 2001; Setter *et al.*, 2003). An excess of glucose increases the rate of the polyol pathway, and accounts for almost one-third of total glucose turnover. Indeed the rate of fructose metabolism is too slow to keep pace, which results in the build-up of sorbitol (Gonzalez *et al.*, 1984). The induced osmotic stress leads to cell swelling and cell disruption (Hotta, 1997; Oates, 2002). The polyol pathway also generates intracellular conditions (high $NADH/NAD^+$ and low NADPH levels) which lead to further hyperglycemic damage to the cells via protein glycation and oxidation (Brownlee, 2001).

1.3.3.2 Protein glycation

Glycation is the process by which non-enzymatic reactions occur between reducing sugars and proteins, leading to the formation of advanced glycation end-products (AGEs) (Stitt, 2001). High concentrations of NADH/NAD^+ resulting from the polyol pathway increase the amount of triose phosphate through inhibition of the glyceraldehyde-3-phosphate dehydrogenase (GAPDH) enzyme (Brownlee, 2001). The elevated triose phosphate stimulates the production of methylglyoxal, a precursor of AGEs (Ahmed *et al.*, 2003). This not only assists the formation of AGEs, but also generates diacylglycerol (DAG), which activates PKC (Xia *et al.*, 1994; Koya and King, 1998). Other potential promoters of AGE formation are glyoxal from glucose degradation (Welten *et al.*, 2003) and 3-deoxyglucosone from the decomposition of the Amadori product (Schalkwijk *et al.*, 1999). These reducing sugars bind to proteins, causing functional alterations and irreversible damage. Studies using inhibitors of AGEs in animal models have shown their preventative role against diabetic complications in kidney (Nakamura *et al.*, 1997) and retina (Hammes *et al.*, 1991). This confirms the critical role of AGEs in hyperglycemic conditions. In general, AGEs interfere with matrix-to-matrix or matrix-to-cell interactions (Haitoglou *et al.*, 1992), which finally lead to altered functions e.g. loss of elasticity in blood vessels due to impairment of Type 1 collagen function (Tanaka *et al.*, 1988; Huijberts *et al.*, 1993). In addition, AGEs can further stimulate cytokine and reactive oxygen species (ROS) production through AGE-specific receptors, and intracellular proteins modifications (Brownlee, 1995), which cause marked diabetic damage.

1.3.3.3 Activation of PKC

Hyperglycemia can increase the level of DAG as it has been revealed in cultured microvascular cells (Xia *et al.*, 1994; Koya and King, 1998). Besides, DAG can also be generated from indirect polyol pathway in hyperglycemic conditions. As a lipid second messenger, DAG can activate nine out of the eleven isoforms of PKC (Brownlee, 2001). Abnormal activation of PKC is known to cause blood-flow abnormalities in kidney (Koya *et al.*, 1997) and decreased production of nitric oxide (Craven *et al.*, 1994). It also inhibits transcription of endothelial nitric oxide synthase (Kuboki *et al.*, 2000) but increases the transcription of vascular endothelial growth factor (VEGF) (Williams *et al.*, 1997), which results in elevated permeability of endothelial cells. Moreover, activated PKC increases microvascular matrix protein accumulation, due to the increased expression of transforming growth factor-beta (TGF-β), fibronectin and type IV collagen (Studer *et al.*, 1993; Phillips *et al.*, 1999). Treatment of diabetic animals using inhibitors for PKC-beta (PKC- β) has greatly reduced the PKC activity and diabetic damage in retina (Nonaka *et al.*, 2000) and renal glomeruli (Koya *et al.*, 2000; Kelly *et al.*, 2003). This shows that activation of the PKC pathway has a crucial role in the pathogenesis of diabetes.

1.3.3.4 Hexosamine pathway

During hyperglycemia, the excess intracellular glucose is shunted to the hexosamine pathway, which causes measurable insulin resistance in diabetic rats (Robinson *et al.*, 1995). It has been suggested that the hexosamine pathway is one of the major mechanisms responsible for insulin resistance in NIDDM (Zraika *et al.*, 2002). However,

it has also been proposed that the activated hexosamine pathway actually causes adverse pancreatic beta-cell function via oxidation (i.e. over-production of hydrogen peroxide) and a reduction in the expression of several beta-cell specific genes (Kaneto *et al.*, 2001). Also, an increase in glutamine:fructose-6-phospate amidotransferase (GFAT), the enzyme that regulates the conversion of glucose to glucosamine in this pathway, has been found to attenuate cellular glucose uptake via activation of the PKC pathway (Bosch *et al.*, 2003). Despite the controversy in the exact underlying mechanism, it is generally believed that activation of the hexosamine pathway could cause various changes in gene expression and protein function, leading to the observed diabetic manifestations, such as diabetic nephropathy (Schleicher and Weigert, 2000; Brownlee, 2001).

1.3.3.5 Oxidative stress

Chronic hyperglycemia induces oxidative stress, which is characterized by an increased level of reactive oxygen species (ROS) and a deficiency in antioxidative defence (Bonnefont-Rousselot *et al.*, 2000). In diabetes, hyperglycemia causes increased ROS levels at the mitochondrial complex II (Nishikawa *et al.*, 2000), where they modulate and affect various biological signal pathways (Suzuki *et al.*, 1997). Excess superoxide production via oxidative phosphorylation in hyperglycemic conditions induces endothelial dysfunction that results in cardiovascular complications (Doi *et al.*, 2001), which is now a leading cause of morbidity and mortality in diabetic patients (Bonnefont-Rousselot *et al.*, 2000). Furthermore, ROS contribute in the formation of atherosclerosis in diabetic patients by activating extracellular matrix metalloproteinases (Uemura *et al.*, 2001). Consumption of NADPH in the polyol pathway causes NADPH depletion and

leads to poor regeneration of glutathione (Brownlee, 2001) which weakens the antioxidative system. Excessive production of AGEs, on the other hand, produces ROS via several complex biochemical mechanisms (Mullarkey *et al.*, 1990) such as reduced signalling through the endothelial receptor of AGE (RAGE) (Heidland *et al.*, 2001). This in turn causes reduced production or activation of transcription factors such as nuclear factor kappa B (Nishio *et al.*, 1998), resulting in vascular abnormalities e.g. inflammatory reactions, smooth muscle cell proliferation, and angiogenesis (De Martin *et al.*, 2000; Collins and Cybulsky, 2001) due to release of pro-inflammatory cytokines or adhesion molecules (Heidland *et al.*, 2001).

Apparently, all of these mechanisms interact with one another. However, recent reports have suggested that the overproduction of superoxide by the mitochondrial electron-transport chain is the common process shared by these pathogenic mechanisms (Nishikawa *et al.*, 2000; Brownlee, 2001; Du *et al.*, 2003). Interruption of the intracellular overproduction of superoxide suppressed cellular damages induced by the activation of polyol pathway, increased AGEs formation, activation of the PKC pathway and hexosamine pathway (Nishikawa *et al.*, 2000; Brownlee, 2001; Hammes, 2003). This demonstrated the crucial role of oxidative stress in diabetic complications and provides a new insight in the treatment of hyperglycaemic-related disorders.

1.3.4 DM induced ocular manifestations

DM can lead to different ocular complications such as diabetic keratopathy (Schultz *et al.*, 1983), iris neovascularization (Fernandez-Vigo *et al.*, 1997; Tolentino and Adamis, 1998), diabetic cataract (Altomare *et al.*, 1995; Duhaiman, 1995; Lee and Chung, 1999; Kyselova *et al.*, 2004) , diabetic vitreopathy (Sebag, 1996; Stitt *et al.*, 1998), diabetic retinopathy (DR) (Ciulla *et al.*, 2003; Khan and Chakrabarti, 2003; Rotimi *et al.*, 2003; Turczynski *et al.*, 2003; Frank, 2004) and diabetic maculopathy (Giovannini *et al.*, 1999; Ikeda, 2000; Misra *et al.*, 2004). Among all, DR and diabetic cataract are the most common visual disabilities and cause the highest visual impairment rates (Seyoum *et al.*, 2001; Rotimi *et al.*, 2003).

1.3.4.1 Diabetic retinopathy (DR)

The deterioration in the retinal blood vessels due to diabetes is known as DR. It is the most common ocular manifestation in diabetic patients (Ciulla *et al.*, 2002; Ciulla *et al.*, 2003) and is the leading cause of blindness in the working age population in the industrialized world (Stanga *et al.*, 1999; Ciulla *et al.*, 2002). DR is characterized by loss of retinal pericytes, retinal capillary closure, ischaemia (Archer, 1999), and neovascularization (Aiello, 1997). Recently, loss of neurons by apoptosis and activation of glial cells were also observed in human DR and in animal models (Barber *et al.*, 1998; Zeng *et al.*, 2000). The prevalence of DR was investigated in diabetic patients, with no significant difference found between type 1 DM and type 2 DM subjects (Seyoum *et al.*, 2001; Hammes *et al.*, 2004). Similar to other diabetic complications, DR is caused by more than single pathogenic mechanism. Increased oxidative stress, promotion of PKC

pathway, increased formation of AGE and more contribute in causing retinal blood vessels abnormalities e.g. blockage, leakage or dilation (Van den Enden *et al.*, 1995; Ono *et al.*, 1998; Chakrabarti *et al.*, 2000; Stitt, 2001). Besides, VEGF is thought to promote retinal leukostasis via induction of intercellular adhesion molecule-1 (ICAM-1) (Lu *et al.*, 1999). This is a process in which leukocytes tend to stick to the vascular endothelium and results in vascular blockage and free radical (i.e. superoxide) generation (Miyamoto *et al.*, 1999).

The loss in vascular permeability has been suggested to be complicated by the down-regulation of membrane barrier transporter GLUT1 (Kumagai *et al.*, 1994; Badr *et al.*, 2000). However, other researchers have found no such changes (Fernandes *et al.*, 2003) or even an increase (Kumagai *et al.*, 1996) in inner GLUT1 level in hyperglycemia. Recent research also suggested another hypothesis, in which the insulin-like growth factor-1 (IGF-1) plays a pathological role. By inhibiting IGF-1, vascular damage and proliferation were diminished (Kuang *et al.*, 2003; Poulaki *et al.*, 2004).

1.3.4.2 Diabetic cataract

Cataractogenesis is one of the most common secondary DM complications (Nielsen and Vinding, 1984; Leske *et al.*, 1991). The explanation for diabetic cataract formation can be traced back as early as in 1959, when the osmotic hypothesis was proposed (van Heyningen, 1959). As mentioned in section 1.3.3.1, a high glucose concentration stimulates AR and promotes an osmotic challenge. Hyperglycemia in the lens causes excess glucose to pass through the polyol pathway, which leads to sorbitol accumulation (Kinoshita *et al.*, 1963). Sorbitol, as an osmotically active substance, causes excessive

water uptake into the lens and results in cell turgidity and fiber cell disruption, thus loss of transparency (Kador *et al.*, 1985; Swamy-Mruthinti *et al.*, 1999). Although this hypothesis has been successfully demonstrated in several animal models (Kuriyama *et al.*, 1983; Richter *et al.*, 2002), researchers who used animal models with a greater similarity to human (i.e. low AR level in the lens) failed to demonstrate a significant level of sorbitol-induced osmotic damage (Varma and Kinoshita, 1974; Garadi and Lou, 1989; Hegde *et al.*, 2003). In mouse lenses, inappropriate addition of GLUT1 in fiber cells was also suggested as the major cause in cataract formation (Gong *et al.*, 2001). Nevertheless, it is still believed that by acting synergistically with other mechanisms, the activation of AR through the polyol pathway could still cause severe damage in DM (Hegde *et al.*, 2003). Other hypotheses, such as those relating to oxidative stress and glycation (Sensi *et al.*, 1995), have also been suggested to be responsible for diabetic cataract formation (Obrosova *et al.*, 1998; Donma *et al.*, 2002; Franke *et al.*, 2003; Pokupec *et al.*, 2003). It is believed that AR can indirectly generate ROS (as revealed by AR inhibition study (Suzen and Buyukbingol, 2003)) and also diminish the antioxidative defence capability by lowering the amount of glutathione (Donma *et al.*, 2002). With high exposure to ultra-violet light, oxidative stress in the crystalline lens may be an important issue, especially in pathological conditions such as DM (Garner *et al.*, 2000). Furthermore, AGEs can induce oxidative stress through chemical and cellular mechanisms e.g. the Fenton reaction (Lin, 1997), which has been found to contribute to cataract formation in both ageing and diabetic lenses (Pokupec *et al.*, 2003). These AGEs can cross-link alpha-crystallins, the basic structural protein in the lens, resulting in loss of chaperone activity and dense protein aggregation (Chellan and Nagaraj, 1999; Derham and Harding, 1999).

A newer proposal has also been suggested by Kistler and others in 1999 for diabetic cataract formation. They believed that the increase in intracellular glucose level induced an elevated anaerobic metabolism, thus leading to an increase in lactate production and reduction in pH. This reduction of pH closed the pH-sensitive gap junctions between cortical cells and hindered cell-to-cell communication. Consequently, normal circulation within lens was blocked and resulted in fluid accumulation and loss of transparency (Kistler *et al.*, 1999).

1.3.5 Glycemic control

Glycemic control is always a major concern in DM patients, as it is regarded to be important in delaying or preventing secondary diabetic complications. Currently, the most effective treatment is subcutaneous insulin delivery, together with a real-time blood glucose measurement using an implanted glucose-oxidase sensor (Renard, 2002). Studies on glycemic control have shown the regain of a good glycemic control, after a period of poor control might not always be helpful in preventing the progress of hyperglycemia-induced complications (The Diabetes Control and Complications Trial Research Group, 1993; Kowluru, 2003a). Earlier diagnosis and treatment is therefore necessary in order to promote a successful healing rate (Stanga *et al.*, 1999). Since good glycemic control is not always easily established, pharmacological studies have been carried out to specifically target certain diabetic complications (Harding, 2001; Kowluru and Koppolu, 2002; Kowluru *et al.*, 2003b). For diabetic cataract, various preventive approaches have been tested and these include glycation inhibitors (Lewis and Harding, 1990; Swamy-Mruthinti *et al.*, 1996), antioxidants (Cao and Phillis, 1995; Evans and Goldfine, 2000)

and AR inhibitors (Beyer-Mears *et al.*, 1996; Suryanarayana *et al.*, 2004). However, they are still at an experimental state, with further development necessary in order for a safe treatment with minimal adverse effects to be found.

1.4 Project objectives and significance

Diabetic patients are more susceptible to cataract development than non-diabetic patients (Kuriyama *et al.*, 1983; Nielsen and Vinding, 1984; Di Benedetto *et al.*, 1999; Kyselova *et al.*, 2004). Therefore, good aqueous glycemic control should help in the prevention of diabetic cataract formation. Since the CBE is responsible for transporting glucose into the aqueous chamber, studies on the glucose transport mechanism across the CBE might help in deriving a strategy to maintain a healthy aqueous glycemic level in DM patients. Furthermore, it might directly contribute to a decreased risk of diabetic cataract formation. Physiologically, it would provide the basic understanding on how glucose transport into the aqueous is achieved and how such transport can be regulated at the transcriptional or translational level.

In this study, an investigation of glucose transport, and its regulation, across the bovine CBE was carried out. This knowledge provides insight into the control of aqueous glycemic level, which may help eventually in the prevention of diabetic cataract formation.

Chapter 2

Glucose transport kinetics: Ussing-type chamber experiments

2.1 Introduction

In the present study, glucose transport across the bovine CBE was characterised using a modified Ussing-type chamber. Glucose fluxes across the tissue were measured under control and inhibited conditions, in both cases with equal glucose concentrations bathing the NPE and PE sides of the preparation. Four inhibitors were used, in order to evaluate the glucose transport mechanism across the bovine CBE, since the inhibitors inhibit different types or aspects of glucose transport. Thus, the aim of this investigation was to reveal the presence of different glucose transport mechanisms in the bovine CBE.

In this study, the use of the modified Ussing chamber eliminates the influence of systemic circulation, hydrostatic pressure and hormonal changes on glucose flux measurements. Therefore, any change in the rate of glucose transport under inhibited condition could be assumed to relate purely to the interaction between the drug and the CBE preparation.

2.1.1 Overview of experimental design

2.1.1.1 Ussing-type chamber

An "Ussing-type chamber" is a simplified term of "Ussing-Zerahn-type chamber", a chamber named after its designers, Ussing and Zerahn (1951), who firstly applied this technique in the measurement of sodium ions across frog skin (Ussing and Zerahn, 1951). All the later modified version of the Ussing-type chambers are named "Modified Ussing-type chamber". Nowadays, this technique has been widely adopted in different ion (e.g. chloride and potassium ions) and solute transport studies (e.g. glucose and ascorbate) (Chu and Candia, 1988; To and Hodson, 1998b; To *et al.*, 2001; Candia *et al.*, 2002).

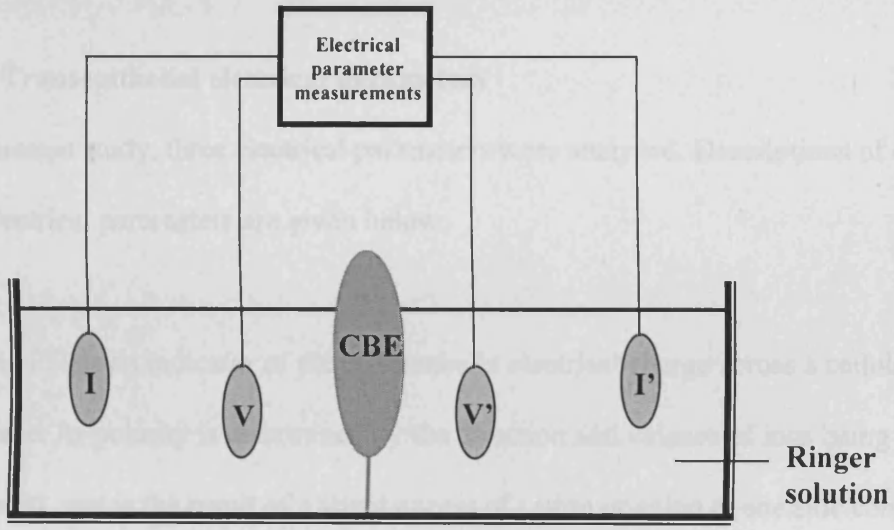

Fig. 2.1 Simplified diagram of an Ussing-Zerahn type chamber.

A simplified diagram is shown to illustrate the schematic configuration of an Ussing-type chamber with a CBE tissue preparation. As seen in figure 2.1, tissue is mounted in-between the chambers, so as to separate the chamber into two halves. The partition allows

the change of solution on one side without affecting the solution on the other side. By changing the chemical content in the Ringer solution, different ionic conditions can easily be established and corresponding effects can be examined. In addition, two sets of electrodes are introduced into the chambers, thus allowing measurements of the electrical parameters across the tissue. The first pair of electrodes (VV'), situated closer to the tissues, measures the transepithelial potential difference (PD_t). The second set of electrodes (II') is for measuring the resistance to current passage. Both electrode sets are connected to voltage monitoring devices for consistent measurement of electrical parameters. Details of the measurement of the electrical parameters will be given in the following sections:

2.1.1.2 Transepithelial electrical parameters

In the present study, three electrical parameters were analyzed. Descriptions of each of these electrical parameters are given below:

PD_t The PD_t is an indicator of the difference in electrical charge across a cellular membrane. Its polarity is determined by the direction and valence of ions being transported, and is the result of a slight excess of cation or anion at one side compared to the other. In CBE, an aqueous-side negative potential is widely accepted, and is believed to relate to a predominance of active anion transport towards the aqueous (Matsui *et al.*, 1996; Crook *et al.*, 2000; To *et al.*, 2001; Wu *et al.*, 2003). In bovine CBE, the negative ion gradient is believed to be generated mainly by active chloride ion transport from

stromal to aqueous (To *et al.*, 1998a; Do and To, 2000). Such a net ion transport has also been observed in rabbit (Crook *et al.*, 2000).

As illustrated in figure 2.1, PD_t can be measured via electrode set VV', which are placed closely aside the tissue to minimise any blank resistance generated by the Ringer solution. In voltage clamp mode, the voltage across the tissue is set to zero. At this point, one can read the current which is necessary to pass through the tissue in order to short-circuit it (Lewis, 1996) (see below).

Transepithelial resistance (R_t). The R_t is a measurement of the resistance across the tissue of interest, and is composed of two major components. These comprise the paracellular resistance (R_p) and the transcellular resistance (R_{tc}). The former indicates the resistance generated by the tight junctions and intercellular spaces, for a solute to pass via the paracellular route. The latter describes the resistance contributed by the cell membranes.

By the use of the Ohm's law, one can easily calculate the R_t across a tissue. It is achieved by passing a known current across the tissue and observing the voltage change. Alternatively, the tissue can be "clamped" to a new voltage and the observed current change can be used to calculate R_t, again using Ohm's law. The first method was used in the present study (a detailed description can be found in section 2.2.7). In general, R_t is directly and inversely related to ionic permeability. Researchers have realised that R_t is useful in categorizing whether an epithelium is of the "tight" or "leaky" types (Diamond, 1974). Epithelia are termed as "leaky", if their R_t is lower than 100 Ωcm^2, while they are termed as "tight" for a R_t higher than 500 Ωcm^2 (Fromter and Diamond, 1972; Diamond,

1974). A stable R_t is regarded as a viability check in the present study, since only a physiologically intact preparation can generate a stable resistance (Hodson and Wigham, 1987).

Short-circuit current (I_{sc}). The I_{sc} is an external current that is passed across the epithelium, so as to reduce the voltage to zero. It is applied to remove any external driving force that is facilitating active transport across a membrane. Any net movement of solute under the short-circuit conditions reveals the active transport activity (Ussing and Zerahn, 1951). I_{sc} is determined by the sum of all the ions that are actively transported across the membrane. It is possible to calculate the I_{sc} if one knows the net ion flux of all ions across the membrane under short-circuit conditions (Koefoed-Johnsen and Ussing, 1958). I_{sc} can then be deduced by the following equation:

$$I_{sc} = \sum_{1}^{i} J_i \cdot z \cdot F$$

Where J_i is the net flux of ion i, z is the valence of ion i (i.e. the number and polarity of an ion), while F is Faraday's constant. Alternatively, I_{sc} can be determined by the use of Ohm's law, since the PD_t and R_t are continuously measured throughout the experiment. Therefore, short-circuit conditions can be used to determine whether there is any active ion or solute transport across the tissue. The I_{sc} is regarded as an index of the net electrogenic ion transfer across the epithelium (Krupin and Civan, 1996). In CBE, a negative I_{sc} was observed along with a consistently negative PD_t across the CBE (To *et al.*, 1998a; Do and To, 2000; To *et al.*, 2001).

2.1.2 Inhibitors

Four inhibitors were chosen for use in this study. They are inhibitors which have been widely accepted to cause inhibition of particular transporter proteins. Phloretin and cytochalasin B are specific inhibitors of the GLUT family, while phlorizin and ouabain target the SGLTs, directly and indirectly, respectively.

2.1.2.1 Phloretin

Phloretin, is a competitive inhibitor of glucose transport via facilitated-diffusion. Its inhibitory effect on glucose transport has been shown in a number of tissues, including red blood cells (Jennings and Solomon, 1976; Krupka, 1985), smooth muscle (Dresel and Knickle, 1987), brain (Halton *et al.*, 1980; Roeder *et al.*, 1985) and small intestine (Alcalde *et al.*, 1986). It is a non-penetrating molecule, which suggests that it exerts its inhibitory effect by binding onto the extracellular side of the transporter proteins (Masterson and Chader, 1981). It was found to exert its action on GLUTs by binding to the phenol site of the transporter and thus the binding of phloretin would be expect to hinder (Alvarado and Crane, 1964; Alvarado, 1978). The phenol site is situated next to the glucose receptor site in the transporter, and thus the binding of phloretin would be expect to hinder glucose binding (Alvarado, 1978). In other words, phloretin lowers glucose transport capacity by slightly altering the transporter configuration (Betz *et al.*, 1975). In the intestinal system, phloretin was not a potent inhibitor (Alvarado and Crane, 1964), since SGLTs but not GLUTs, are the predominant type of glucose transporters for the daily glucose uptake in this organ (Lee *et al.*, 1994; Nagata *et al.*, 1999; Ferraris, 2001; Wright *et al.*, 2003). In other words, phloretin is a potent inhibitor specifically for

GLUTs, as demonstrated in rat lens (Elbrink and Bihler, 1972) and bovine RPE (To and Hodson, 1998b). However, counter-arguments have been made, as an increase of conductance resulted after the addition of phloretin in frog lens (Lucas and Duncan, 1983) and in lipid bilayer membranes (Melnik *et al.*, 1977). It has been also suggested that the inhibitory effect exerted by phloretin might be a secondary effect following the altered intracellular sodium level (Lucas and Duncan, 1983).

2.1.2.2 Cytochalasin B

Cytochalasin B is a potent inhibitor for monosaccharide transport, as demonstrated in tissues such as smooth muscles (Dresel and Knickle, 1987), red blood cells (Lin and Spudich, 1974a), heart (Clow *et al.*, 2004) and brain (Nishizaki and Matsuoka, 1998). It is a fungal metabolite (Bloch, 1973), that is regarded as a highly competitive inhibitor (Lin and Spudich, 1974a), and binds directly to the glucose binding site of the transporter (Lin *et al.*, 1974b; Silverman, 1991). It has emerged as the more potent and specific inhibitor in lowering bi-directional glucose transport across the frog lens, when compared with phloretin (Lucas and Duncan, 1983). However, again, counter arguments have been raised, since cytochalasin B also inhibits various cellular movements by interacting with microfilaments (Wessells *et al.*, 1971), which result in alterations to cell locomotion and cytokinesis (Krishan, 1972). However, even this notion has been challenged by other studies (Bluemink, 1971; Goldman, 1972), which has left the argument unsettled. "Cytochalasin B-binding" activity has been widely used to assess the transport capacity or affinity of a glucose transport system (Wheeler and Hauck, 1985; Hellwig and Joost, 1991; Wandel *et al.*, 1996). Cytochalasin B is a photolabile molecule and can form a

covalent bond with the transporter, and according to the extent of binding, the transport kinetics can be deduced (table 1.1, p.26). In human red blood cells, high and low-affinity binding sites have been revealed for cytochalasin B (Lin and Spudich, 1974a; Lin *et al.*, 1974b). Their binding with cytochalasin B could be inhibited up to 80 to 90 % in the presence of D-glucose, especially at the high-affinity site. This indicates a clear competitiveness of this inhibitor. Furthermore, the inhibitory effect of cytochalasin B in these samples was not affected by pH, in the range 5.0 to 9.0, which agreed with a previous study using D-glucose in the red blood cell membranes (Kahlenberg *et al.*, 1971). However, cytochalasin B binding activity decreases with increasing ionic strength (Brekkan *et al.*, 1996). In addition, the binding of cytochalasin B to GLUT1 was found to occur in two different states, which might exist at equilibrium under normal conditions, but interchange according to surrounding environmental conditions (Gottschalk *et al.*, 2000).

2.1.2.3 Phlorizin

Phlorizin is a natural plant glucoside (Malathi and Crane, 1969). It has long been used as a potent and specific inhibitor for the SGLTs, mainly SGLT1, in kidney (Silverman, 1976; Turner and Moran, 1982a; Miller *et al.*, 1992; Oku *et al.*, 2000) and small intestine (Jervis *et al.*, 1956; Despopoulos, 1966; Tsujihara *et al.*, 1996; Hirsh *et al.*, 1997) to reduce active glucose transport. It is regarded as a competitive inhibitor, as it has been found to directly compete for the glucose binding site with D-glucose (Betz *et al.*, 1975) and even to be transported by the SGLT (Walle and Walle, 2003). More recently, researchers have revealed the mechanism of phlorizin binding (Koepsell *et al.*, 1990;

Veyhl *et al.*, 1993; Oulianova *et al.*, 2001). They suggest that there are two phases in phlorizin binding, composed of a first "fast-binding phase" and a "slower equilibration phase". The heterogeneity observed in previous studies (Turner and Moran, 1982a; Turner and Moran, 1982b), in which high and low-affinity transport pathways were observed in the brush border membrane vesicle, was argued to have been purely due to the presence of these complex transport properties of SGLT1 (Oulianova and Berteloot, 1996). However, whether this is valid argument in other species has yet to be elucidated, since SGLT2 was found widely expressed in kidney in many later studies (Mackenzie *et al.*, 1996; Wright, 2001).

Although generally believed to be an inhibitor of SGLTs, phlorizin also exerts an inhibitory effect on the facilitated-carrier system, as seen in tumour cells (Nelson and Falk, 1993) and cardiac tissues (Clow *et al.*, 2004). This might be explained by the formation of phloretin due to phlorizin hydrolysis (Malathi and Crane, 1969) (Fig. 2.2). Phlorizin also inhibits ascorbate transport across the rabbit CBE, as well as glucose (Chu and Candia, 1988). In recent years, a number of different sodium-dependent vitamin C transporters have been identified (Tsukaguchi *et al.*, 1999; Castro *et al.*, 2001), yet whether phlorizin has direct interaction with all of these transporters remains to be elucidated.

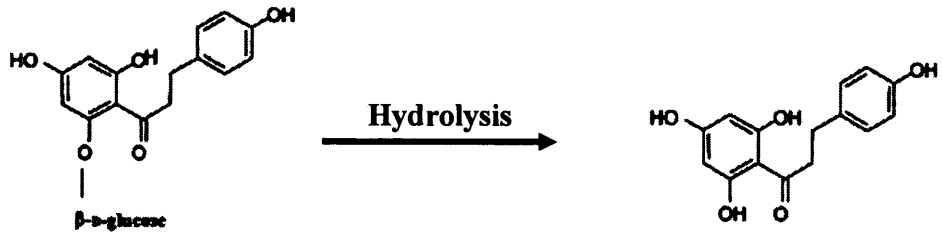

Phlorizin **Phloretin**

Fig. 2.2 Chemical transition between phloretin and phlorizin in hydrolysis.

In the lens, phlorizin demonstrated a reversible but non-specific glucose transport inhibition, with a concurrent influence on the sodium ionic level (Lucas and Duncan, 1983). In addition, it caused a significant reduction in glucose transport of the conjunctiva, when it was added to the mucosal side (Hosoya *et al.*, 1996; Horibe *et al.*, 1997). Although there are many unsettled arguments about the specificity of phlorizin towards SGLTs, it is still a commonly used inhibitor in this type of study.

2.1.2.4 Ouabain

The Na^+, K^+-ATPase, also named the Na^+/K^+-pump, is an integral membrane protein, ubiquitously distributed in cellular epithelia (Lingrel and Kuntzweiler, 1994). It transports two potassium ions from the interstitial fluid into the cytoplasm and three sodium ions in the opposite direction, in every cycle. It, therefore, generates chemical and electrical gradients across cell membranes (Pedemonte and Kaplan, 1990). The driving force for each of the cationic exchange cycles requires the hydrolysis of ATP (i.e. energy consumption) (Ohtsubo *et al.*, 1990). Any transport processes dependent upon the chemical and electrical gradients set up by the Na^+, K^+-ATPase are named energy-driven or simply "active". These include the transport of glucose against a concentration gradient, which make use of the sodium gradient firstly built up by the Na^+, K^+-ATPase (Hirayama *et al.*, 1996; Turk and Wright, 1997).

Ouabain is a cardiac glycoside, which is a specific inhibitor of the Na^+, K^+-ATPase (Lingrel and Kuntzweiler, 1994). It exerts its inhibitory effect by binding to the extracellular surface of the Na^+, K^+-ATPase. The binding strategy was found to be very complex, involving the alpha-subunit as the primary binding site, but the beta-subunit

was reported to be involved too (Hansen, 1984). In addition, different extracellular and transmembrane amino acids, were also found to be important in determining the affinity of the drug towards the sodium-pump (Burns and Price, 1993; Schultheis and Lingrel, 1993). Therefore, ouabain can be used to inhibit active glucose transport indirectly, by dissipating the sodium gradient across a membrane, via the functional abolition of Na^+/K^+ exchange. Without the sodium concentration gradient (Diez-Sampedro *et al.*, 2001), glucose cannot be transported across the membrane against its own concentration gradient. In the eye, ouabain has been used in several studies to help elucidate the corresponding glucose transport mechanism, e.g. in the RPE and lens (Stramm and Pautler, 1982; Lucas and Duncan, 1983; Roeder *et al.*, 1985; To and Hodson, 1998b).

2.1.3 Glucose transport in the eyes

Various ocular tissues have been investigated to find out their mode of glucose transport. The Ussing chamber technique has been a commonly employed method (Hosoya *et al.*, 1996; Horibe *et al.*, 1997; To and Hodson, 1998b; To *et al.*, 1998c), while bolus injection (DiMattio and Zadunaisky, 1981; DiMattio *et al.*, 1984b), and glucose or cytochalasin B-binding assay techniques have also been tested (Stramm and Pautler, 1982; Lucas and Duncan, 1983; Vilchis and Salceda, 1996).

In general, the facilitated-carrier or passive transport mechanism has been found to be the predominant mode of glucose transport in ocular tissues. The tissues which possess a facilitated glucose transport system include bovine RPE (Crosson and Pautler, 1982; To and Hodson, 1998b; To *et al.*, 1998c), rat retina and RPE (Dollery *et al.*, 1971; Stramm and Pautler, 1982; Vilchis and Salceda, 1996), frog RPE (Miller and Steinberg, 1976;

DiMattio and Streitman, 1986), chick RPE (Masterson and Chader, 1981), rat blood-ocular barriers including BAB (DiMattio and Zadunaisky, 1981), rabbit corneal endothelium (Hale and Maurice, 1969) and rat lens (DiMattio, 1984a). Active or sodium-dependent glucose transport has been reported in rabbit conjunctiva (from mucosal side) (Hosoya *et al.*, 1996; Horibe *et al.*, 1997), and sheep RPE, from the retinal to choroidal direction (Pascuzzo *et al.*, 1980). It is interesting to note that the sheep RPE operated using a different mechanism to the other species investigated, since facilitated-carrier transport has been found in all other mammals. This finding might have resulted from a technical difference in experimental design specifically, the mounting of the choroidal layer, which was not done in other studies of RPE.

Studies into the glucose transport of the retina and RPE have been popular (Vinores *et al.*, 1988; Stitt *et al.*, 1994; Badr *et al.*, 2000), possibly since DR is such a common cause of blindness (please refer to section 1.3.4). In contrast, studies on more anterior ocular tissues are scarce. Since, glucose transport across the CBE would directly affect the extent of glucose reaching the aqueous humor, a thorough study of this issue would be meaningful, for some new insights into how best to achieve good ocular glycemic control.

2.2 Methodology

2.2.1 Materials and bathing solution

The composition of the HEPES-buffered Ringer solution was (in mM) 113.0 NaCl, 4.6 KCl, 21.0 $NaHCO_3$, 0.6 $MgSO_4$, 7.5 D-glucose, 1.0 glutathione (reduced form), 1.0 Na_2HPO_4, 10.0 HEPES, and 1.4 $CaCl_2$. The pH of the solution was adjusted to 7.4.

The 3-O-[Methyl-^{14}C]-D-glucose (MDG) was purchased from NEN Life Science Products, Inc. (Boston, MA), while the L-[^{3}H]-glucose (LG), phloretin, phlorizin, cytochalasin B, ouabain, dimethyl sulfoxide (DMSO) and all other chemicals were purchased from Sigma-Aldrich Company (St. Louis, MO).

2.2.2 Tissue preparation and selection

Fresh bovine eyes were taken from a local abattoir, having been enucleated immediately post mortem. They were transported to the laboratory, within an hour, in ice box and kept at 4°C. Eyes were chosen for an experiment if they were externally intact without leakage of aqueous or vitreous caused by external damage and possessed a smooth and clear cornea and lens. They exhibited a regular iridial shape, and the texture of the vitreous was rigid, not dissolved.

2.2.3 Tissue dissection

The bovine CBE was isolated according to the method devised by To and colleagues (To *et al.*, 2001). Connective and extraocular muscles around the globe were removed with a razor blade. Two radial incisions (Fig. 2.3a) were made through the limbus to the equator. The cornea was cut from the incision points to the center and a flap lifted (Fig.

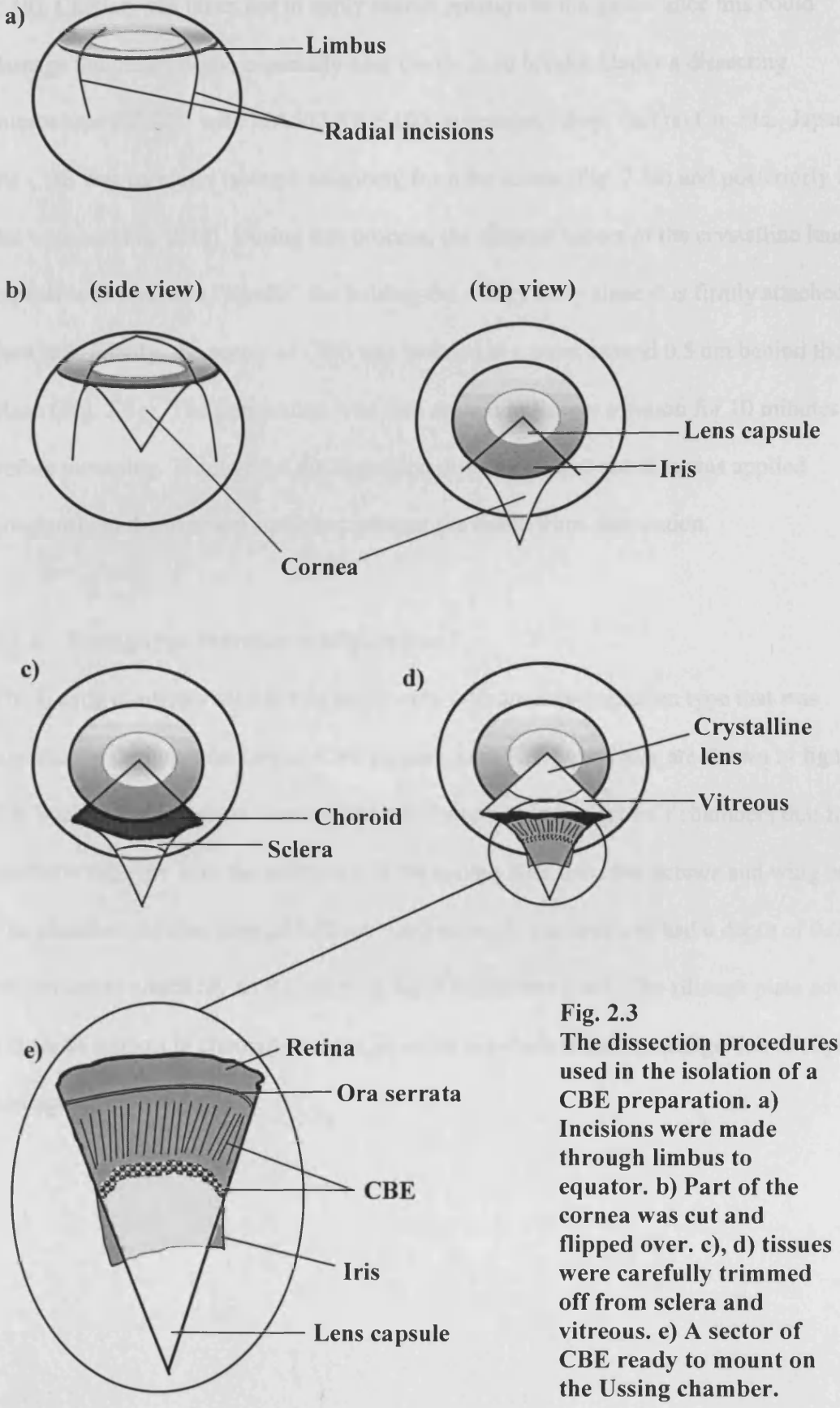

Fig. 2.3
The dissection procedures used in the isolation of a CBE preparation. a) Incisions were made through limbus to equator. b) Part of the cornea was cut and flipped over. c), d) tissues were carefully trimmed off from sclera and vitreous. e) A sector of CBE ready to mount on the Ussing chamber.

2.3b). Caution was taken not to apply excess pressure to the globe since this could damage the ciliary body, especially near the incision breaks. Under a dissecting microscope (EMZ-5 with MA502 SWF 10X eyepieces; Meiji Techno Co. Ltd., Japan), the CBE was carefully isolated anteriorly from the sclera (Fig. 2.3c) and posteriorly from the vitreous (Fig. 2.3d). During this process, the anterior aspect of the crystalline lens capsule was used as a "handle" for holding the ciliary body since it is firmly attached to the CBE. Finally, the sector of CBE was isolated at a point around 0.5 cm behind the pars plana (Fig. 2.3e). The preparation was then soaked in Ringer solution for 10 minutes before mounting. Throughout the dissection process, Ringer solution was applied constantly to the exposed surface to prevent the tissue from desiccation.

2.2.4 Ussing-type chamber configuration

The Ussing chambers used in this study were a continuous-perfusion type that was specifically designed for bovine CBE preparations. Configurations are shown in figure 2.4. Each of the chambers consisted of two Perspex rectangular half chambers that fitted perfectly together with the assistance of the sliding base unit, flat-screws and wing nuts. The chamber cavities were of 0.30 cm^2 in cross-sectional area and had a depth of 0.60 cm, on top of which lay an 0.1 cm thick layer of silicone plate. The silicone plate acted as a cushion support in clamping tissues, in order to reduce solution leakage due to edge damage.

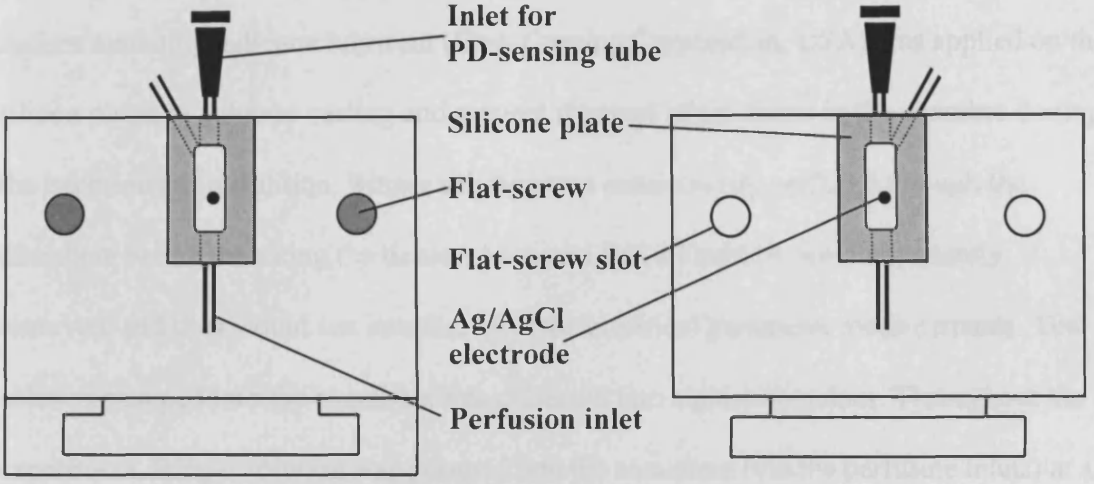

a) Front view of the Ussing-type half-chambers.

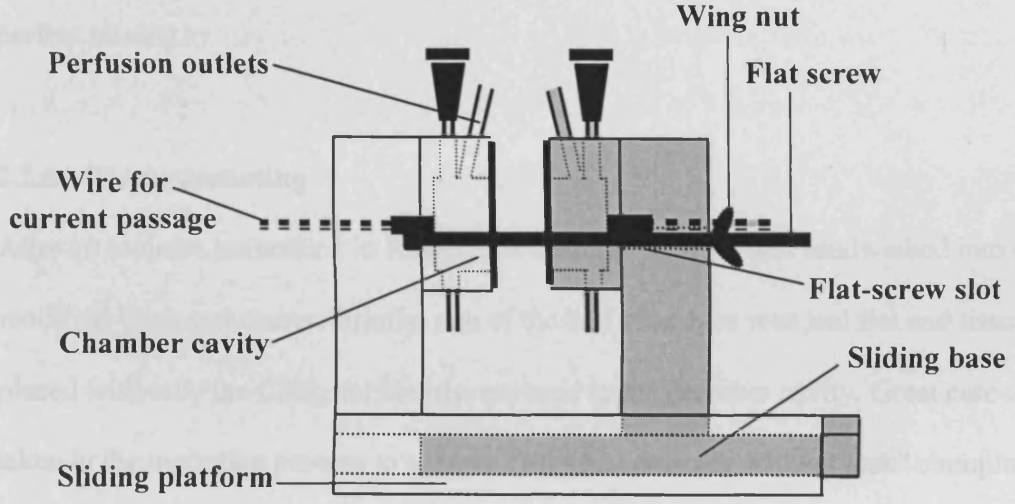

b) Side view of the Ussing chambers. The sliding base and platform, together with the flat-screws are crucial in holding the preparation in place.

Fig. 2.4 Configurations of the continuous-perfusing type Ussing chamber.

Please refer to figure 2.5 for the final setup.

2.2.5 Chamber preparation

Before mounting, silicone lubricant (Dow Corning Corporation, USA) was applied on the silicon plates to enhance sealing and prevent slippage of the tissue in the chamber during the experiment. In addition, Ringer solution was continuously perfused through the chambers before mounting the tissues, to ensure that all bubbles were completely removed, and thus would not interfere with the electrical parameter measurements. The solution pumped into the chambers was collected into a glass container. Throughout the experiment, Ringer solution was pumped into the chambers (via the perfusate inlets) at a rate of 10 ml per hour, under the control of a microprocessor-controlled syringe infusion pump (Cole-Parmer Instrument Ltd., USA). Since the volume of the chamber cavity was 210 μl, the turnover time of the solution in the chamber would be 75.6 seconds, assuming perfect mixing.

2.2.6 Tissue mounting

After 10 minutes immersion in Ringer, the CBE preparation was sandwiched into the modified Ussing chamber. Briefly, one of the half chambers was laid flat and tissue was placed with only the CBE, not the iris, exposed to the chamber cavity. Great care was taken in the mounting process to achieve "minimal pressure without leak" clamping, since excess pressure would cause mechanical damage to the preparation. It was achieved by slowly tightening the chamber screws and nuts until the first point where there was no solution dripping out of the chamber-tissues sandwiches. The temperature of the preparation was maintained at 35-37°C by wrapping pre-calibrated heating cloths around the chambers. Since two CBE tissues were isolated from the same bovine eye in every

experiment, these tissues were mounted into two different chambers to allow measurement of glucose flux in both directions simultaneously.

2.2.7 Electrical parameters measurement

Electrical parameters, the PD_t and R_t, were monitored using the Dual Voltage Clamp-1000 unit (World Precision Instruments, Sarasota, FL, USA). Concurrently, a dual-channel flatbed chart recorder (BD-12E; Kipp & Aonen Inc., Saskatoon, SK, Canada) was used to record the voltage and current output of the preparation (Fig. 2.5).

Just before the experiment, the PD-sensing tubes and by-pass arms were filled with Ringer solution. They were made with polyethylene tubes (PE90; CLAY ADAMS®, Becton, Dickinson, and Company, USA) and were inserted into the PD-sensing inlets of the chambers. Caution was again taken to expel all bubbles trapped inside chamber cavities, PD-sensing tubes and by-pass arms, as this would have resulted in a short circuit, which would generate electrical noise or mask the true potentials. By changing the three-way stopcocks' position, the Ag/AgCl electrodes could either connect to the by-pass arm or the PD-sensing tubes independently. Therefore, the unit allowed a "zero-check" and a voltage measurement of the preparation, respectively. "Zero-check" was done at regular intervals throughout the experiment to correct any drifting of the zero reference and assure that the correct PD was recorded.

During the experiment, a known current was passed across the tissue through the Ag/AgCl electrodes every 5 minutes. This was done by setting the dual-voltage clamp into "timer" mode, at which it was cycled between zero current clamp and current clamp for 5 minutes and 3 seconds respectively. The changes in potential difference were

recorded on the chart recorder and the total resistance (R) was calculated by using Ohm's law:

$$R = \frac{\Delta V}{\Delta I} \cdot A$$

Where ΔV is the change of potential when a known current passed across the preparation; ΔI is the known current used, which was 10 μA in this study and A is the cross sectional area of the exposed tissue, which was 0.30 cm^2.

Since R is composed of both the fluid resistance (R_f) and the R_t, the exact value of R_t can be deduced by the subtraction of R_f from R:

$$R_t = R - R_f$$

R_f could be obtained by measuring the resistance across the chamber with only the fluid perfused through the cavity, without tissue in place.

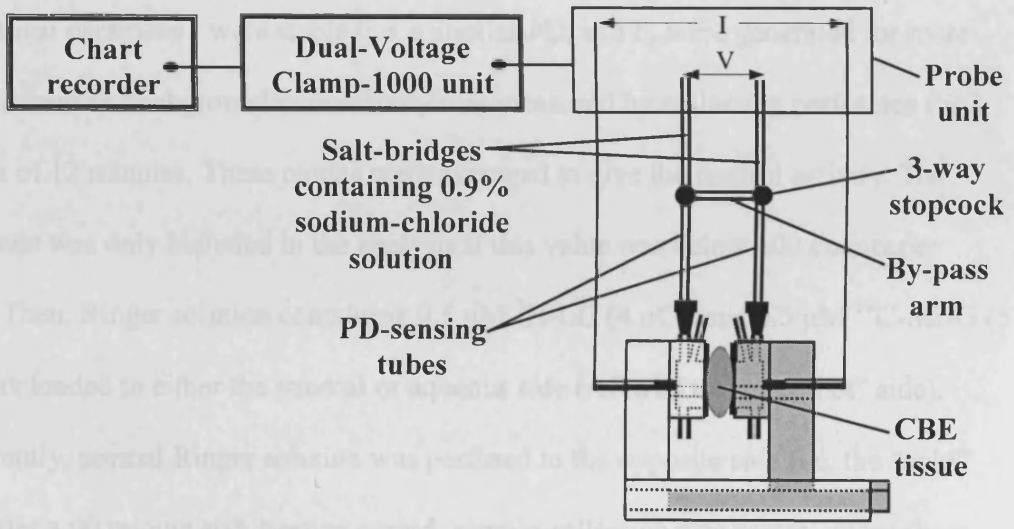

Fig. 2.5 Schematic diagram showing the experimental setup for the electrophysiological study of Ussing chamber. "I" and "V" indicate the unit for applying current clamp and voltage clamp respectively.

2.2.8 Test of viability

The preparations were considered to be viable by three criteria. These include 1) constant PD_t and R_t greater than -0.2 mV and 70 Ωcm^2, respectively before addition of any drug, 2) low diffusional LG flux (i.e. lower than 70 $nmolhr^{-1}cm^2$), and 3) biphasic response to ouabain when it is added to the aqueous side of the preparation as suggested by To *et al.* (1998a). Preparations were rejected if they failed in one of these criteria.

2.2.9 Glucose flux measurement

2.2.9.1 Basal flux measurement

After being sandwiched into the chamber, the tissue was left for 60 minutes for stabilization. The tightness of the chamber clamp sometimes needed adjustment during this period. This was because the thin layer of vitreous on the tissue surface could loosen the clamping, which would then affect the standing potential and result in a leak. When the electrical parameters were stable (i.e. a similar PD_t and R_t were generated for more than 15 minutes), background radioactivity was measured by collecting perfusates for 2 intervals of 12 minutes. These counts were averaged to give the control activity. The experiment was only included in the analysis if this value was below 100 counts per minute. Then, Ringer solution containing 0.5 μM ^{3}H-LG (4 μCi) and 0.5 μM ^{14}C-MDG (5 μCi) were loaded to either the stromal or aqueous side (referred to as the "hot" side). Concurrently, normal Ringer solution was perfused to the opposite side (i.e. the "cold" side). After a 90 minute stabilization period, sample collection was begun, under short-circuited conditions. Perfusates (2 ml) were collected from both sides in clear glass scintillation vials (Wheaton, USA) at a 12-minutes interval, four times. They were mixed

with 15 ml of biodegradable scintillation cocktail (NBCS104; Amersham Radiochemicals, England). Radioactivity of samples was measured with a liquid scintillation counter (Wallac 1414 Winspectral DSA; Wallace, Helsinki, Finland). The counting windows allowed the discrimination of ^{3}H and ^{14}C decays, and the values were determined by averaging consecutive counts for correspondent side samples. The final count data allowed the calculation of bi-directional glucose fluxes from paired preparations, thereby indicating the existence of any active glucose transport in the CBE preparations. The unidirectional flux (J) was calculated using the following equation:

$$J = \frac{C \cdot I \cdot V}{H \cdot A \cdot T}$$

Where C is cold side radioactivity (cpm); I is concentration of the solute-of-interest in the Ringer solution (mM); V is the volume of perfusate collected in each interval (ml); H is the hot side radioactivity (cpm); A is the cross-sectional area of the chamber cavity (cm^2) and T is the collection time for each sample (hour).

The unidirectional fluxes were calculated from the specific activity of the "hot side' and the rate of radioactive tracer appearance on the "cold side" as the experiment progressed. The flux value was expressed in $nmolh^{-1}cm^{-2}$.

2.2.9.2 Effects of inhibitors

Phloretin, cytochalasin B, phlorizin and ouabain are organic chemicals that have poor solubility in water. Hence, they were dissolved in DMSO before use, to give a final concentration of 0.1% in Ringer solution. After the first stabilization period of 60 minutes with normal Ringer solution, Ringer solution with inhibitor (0.1 mM phloretin, 0.01 mM cytochalasin B, 0.1 mM phlorizin or 0.1 mM ouabain) was perfused to both sides of the

preparation for another 60 minutes. Again, background radioactivity counts were done as described earlier. After the completion of background perfusate collection, solution with both radioactive tracers and an inhibitor was perfused to one side of the preparation (i.e. the hot side) and Ringer solution containing only the inhibitor, but not radioisotopes, was perfused to the opposite side (i.e. the cold side). Ninety minutes was allowed for final equilibration before sample collection. Perfusates were collected under short-circuited conditions and then analyzed as described in section 2.2.9.1.

2.2.10 Statistical analysis

All the statistical calculations were performed by using Excel (Miscrosoft) or GraphPad Prism (version 3.02). All data were expressed as mean ± S.E.M. and $p < 0.05$ was considered as statistically significance. The paired Student's t-test was used to analyze the basal flux measurements and the effect of inhibitors, whilst the unpaired Student's t-test and one-way ANOVA with Dunnett's post-hoc test were used to compare the results from different studies and to evaluate variations within a set of tissue samples, respectively.

2.3 Results

2.3.1 Baseline measurement

2.3.1.1 Electrical parameters

Preliminary experiments showed that the preparations were viable for at least five hours with consistent PD_t, I_{sc} and R_t. All of the preparations tested responded to 1 mM ouabain added to aqueous side of the chamber at the end of the experiment (Fig. 2.6). The average PD_t, I_{sc} and R_t of the bovine CBE was -0.47 ± 0.09 mV (with the aqueous side consistently negative), -4.94 ± 0.54 μAcm^2 and 98.50 ± 7.20 Ωcm^{-2} (mean ± S.E.M., n = 9), respectively. After the addition of ouabain, PD_t and I_{sc} increased transiently for a period of 25-30 minutes. This was followed by a depolarization which abolished them to nearly zero after another 120 minutes (Fig. 2.6). The maximum PD_t and I_{sc} attained during ouabain's transient stimulatory phase was 157 ± 12% of the baseline ($p < 0.05$, n = 9) while R_t eventually decreased by 10.8 ± 5.8% after the addition of ouabain ($p > 0.05$, n = 9) for 30 minutes.

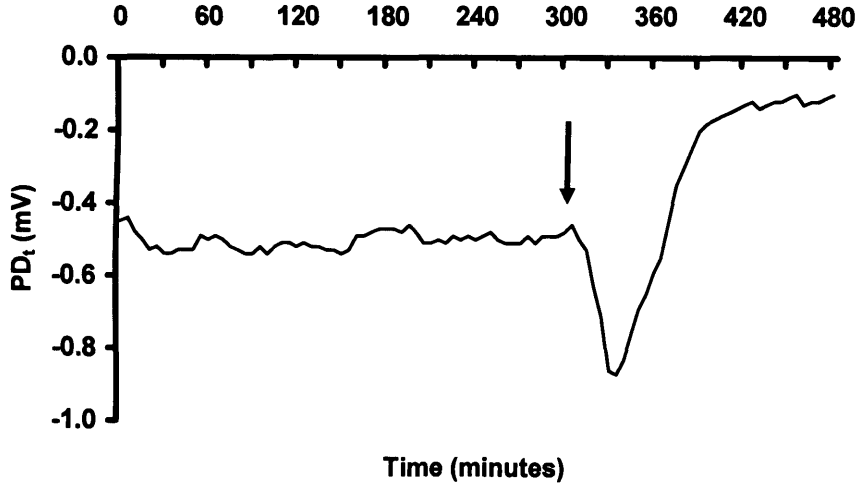

Fig. 2.6 Changes of PD_t over time and in response to the addition of ouabain at the aqueous side (indicated by the arrow) in an control experiment.

For the inhibition study, electrical parameters were significantly affected by the addition of ouabain (Dunnett's post-hoc test, $p < 0.05$), while phloretin, cytochalasin B and phlorizin (Dunnett's post-hoc test, $p > 0.05$) showed no significant influences (Table 2.1). The electrical parameters presented in table 2.1 are the data taken around 150 minutes from the time at which the preparations were mounted. Significant changes were observed in PD_t (ANOVA, $F = 4.55$, $p < 0.05$) and I_{sc} (ANOVA, $F = 11.1$, $p < 0.001$) with *bilateral* ouabain addition (Figs. 2.7 and 2.8). The maximum stimulation was 140 ± 11 % ($p < 0.05$, $n = 16$) and the reduction of R_t was 7.5 ± 6.2 % ($p > 0.05$, $n = 16$).

Condition	PD_t (mV)	R_t (Ωcm^2)	I_{sc} (μAcm^2)	n
Baseline	-0.52 ± 0.08	95.14 ± 6.17	-5.73 ± 1.07	20
Phloretin	-0.42 ± 0.05	91.95 ± 5.77	-4.64 ± 0.48	22
Cytochalasin B	-0.43 ± 0.18	99.70 ± 11.86	-4.37 ± 1.72	18
Phlorizin	-0.46 ± 0.03	104.40 ± 8.45	-4.44 ± 0.27	16
Ouabain	**-0.14 ± 0.03***	88.99 ± 6.13	**-1.63 ± 0.35***	16

Table 2.1 Electrical parameters of baseline measurement and inhibition studies. Data were taken around 150 minutes from the time at which the preparations were mounted. n represents the sample size. * indicates statistical significance level of $p < 0.05$ when compared to the baseline readings. Data are presented as mean ± S.E.M..

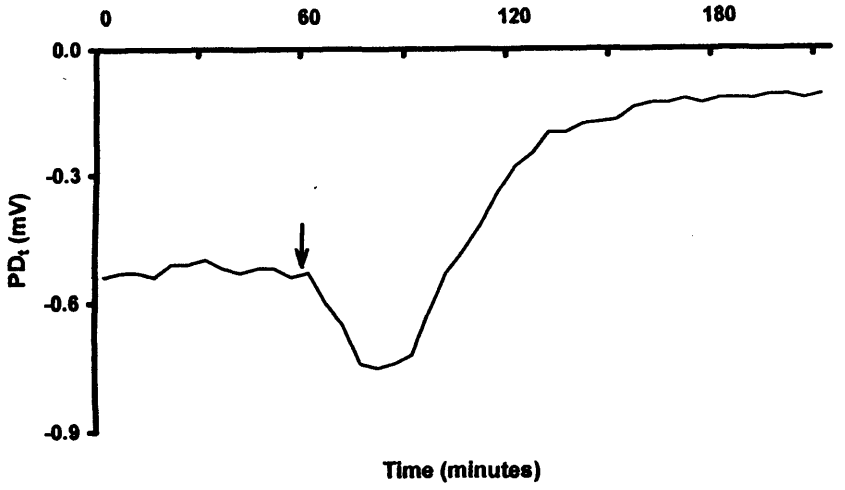

Fig. 2.7 The effect of *bilateral* ouabain addition (indicated by the arrow) on PD_t values of a CBE preparations.

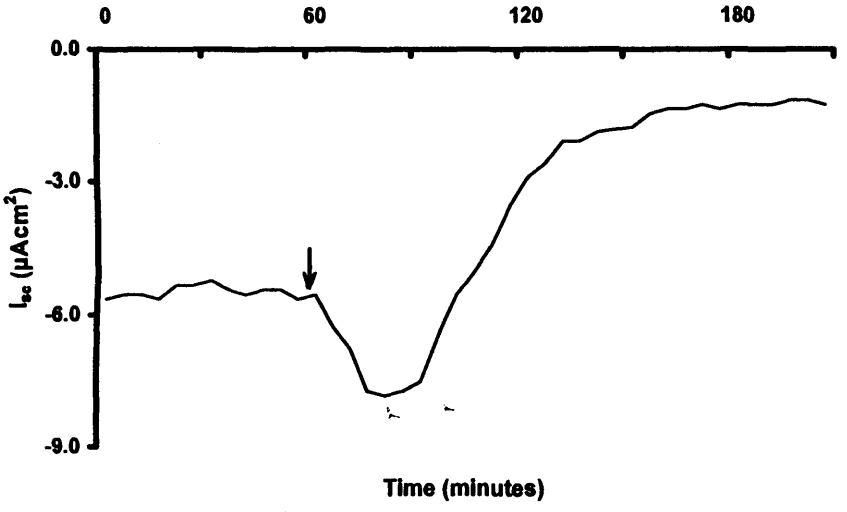

Fig. 2.8 Changes of I_{sc} before and after the *bilateral* addition of ouabain (indicated by the arrow) in both sides of the chambers.

2.3.1.2 Glucose flux measurement

The glucose flux measurements, under normal and inhibited conditions, are summarised in table 2.2. Bovine CBE demonstrated stereospecificity for MDG, with a D-glucose to L-glucose transport ratio of 6.3-6.5 under an equal concentration gradient. No significant net flux was observed for either MDG or LG across the CBE under basal conditions ($p > 0.05$, $n = 10$), or after the addition of phloretin ($p > 0.05$, $n = 11$), cytochalasin B ($p > 0.05$, $n = 9$), phlorizin ($p > 0.05$, $n = 8$) or ouabain ($p > 0.05$, $n = 8$). The corrected MDG (CMDG) flux was deduced by subtraction of the LG flux from the MDG flux to determine the transcellular rate of MDG movement across the bovine CBE. The CMDG flux was drastically decreased with the bilateral addition of cytochalasin B. Comparatively more modest reductions were observed after the addition of phloretin or phlorizin. Ouabain did not cause a significant reduction in the glucose flux. Moreover, LG fluxes were not significantly affected by any of the drugs used (Table 2.2), but decreased steadily as R_t increased, with a correlation factor of 0.71 (Fig. 2.9).

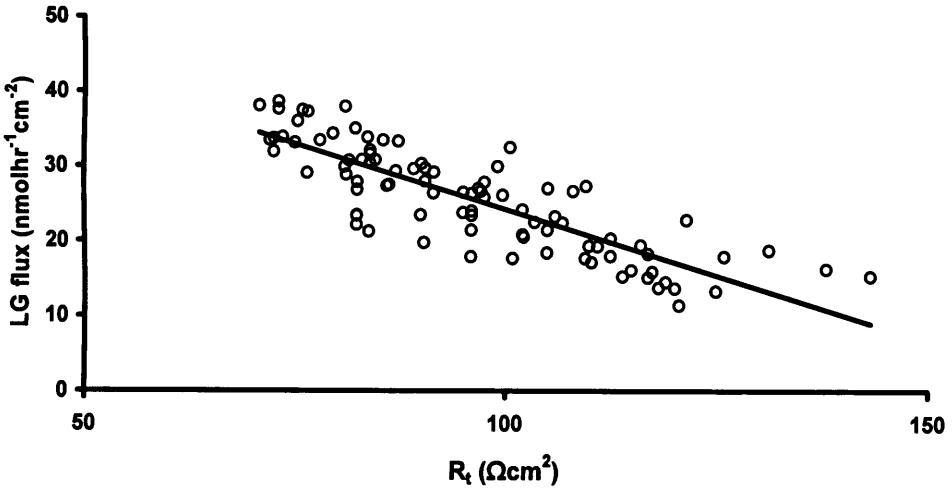

Fig. 2.9 The plot of LG flux against R_t.

Condition	Flux direction	LG	MDG	CMDG	CMGD flux inhibition (%)
Baseline measurement	Jsa (10)	25.8 ± 2.0	189.5 ± 15.1	163.8 ± 14.2	---
	Jas (10)	26.3 ± 2.3	196.1 ± 14.7	169.8 ± 13.2	---
Phloretin	Jsa (11)	24.7 ± 1.9	**91.2 ± 3.5***	**66.5 ± 3.2***	**59.4**
	Jas (11)	24.6 ± 2.1	**93.8 ± 5.3***	**69.2 ± 3.7***	**59.3**
Cytochalasin B	Jsa (9)	27.4 ± 4.5	**60.9 ± 9.0***	**33.5 ± 9.2***	**79.6**
	Jas (9)	26.0 ± 4.6	**58.2 ± 11.8***	**32.1 ± 10.2***	**81.1**
Phlorizin	Jsa (8)	22.0 ± 1.9	**149.4 ± 9.4***	**127.4 ± 7.6***	**22.2**
	Jas (8)	21.3 ± 2.7	**155.7 ± 9.6***	**134.4 ± 8.3***	**20.8**
Ouabain	Jsa (8)	28.4 ± 2.5	169.5 ± 18.5	141.1 ± 16.4	13.9
	Jas (8)	27.5 ± 2.7	173.3 ± 10.6	145.8 ± 9.5	14.1

Table 2.2 Glucose flux measurements under basal and inhibited conditions.

*** indicates statistical significance with $p < 0.05$. Fluxes are presented in $nmolhr^{-1}cm^{-2}$ (mean ± S.E.M). Jsa is the influx, which is the glucose flux measured from stroma to aqueous and vice versa for Jas (i.e. the efflux). Sample size is indicated in parenthesis.**

2.4 Discussion

2.4.1 Bovine CBE in Ussing chamber

Bovine eyes were used in this study for they have much larger CBE area when compared to other animal models such as rabbit (Kishida *et al.*, 1982; Krupin *et al.*, 1984) which facilitates their manipulation. Also, they are readily available in local abattoirs. One could easily distinguish the CBE sector from other ocular tissues in the bovine eye, which made tissue mounting in the Ussing chamber (without iris) highly reliable. This issue is important, as it assures that any electrical parameter and transport rate measurements or changes were purely demonstrated by the CBE, and not adjacent tissue(s). Such assurance is not possible when smaller-sized models are used in this type of study (Iizuka *et al.*, 1984; Krupin *et al.*, 1984; Wiederholt and Zadunaisky, 1987), in which the iris is often exposed to the tissue cavity.

2.4.2 Baseline and control electrical parameters

The consistently negative PD_t across the CBE observed in the present study is consistent with findings from previous studies (To *et al.*, 1998a; Do and To, 2000). A negative PD has been found commonly in iris-ciliary body preparations from a range of different mammalian species, such as monkey (Chu *et al.*, 1987b), cat (Holland and Gipson, 1970), dog (Iizuka *et al.*, 1984) and rabbit (Kishida *et al.*, 1982; Krupin *et al.*, 1984). Such a constant negative potential indicates a predominance of anion transport in the direction from stroma to aqueous, and has been suggested to be the result of the relative transport activities of sodium and chloride ions across the tissue (Wiederholt and Zadunaisky, 1987). Recently, a net chloride flux was revealed in bovine CBE, but not a net sodium

flux (To *et al.*, 1998a). This demonstrates the crucial role of chloride ions in the maintenance of the negative PD across the CBE, and suggests that it might be an important component in driving fluid transport (i.e. aqueous humor production) (Do and To, 2000).

The magnitude of R_t found in the present study is difficult to compare with that in other mammalian species, since R_t varies widely (Holland and Gipson, 1970; Kishida *et al.*, 1982; Iizuka *et al.*, 1984). For example, a study on monkey reported a R_t of 185 Ωcm^2 (Chu *et al.*, 1987b), while 31 Ωcm^2 was reported for shark (Wiederholt and Zadunaisky, 1987). When considering only the bovine studies, a range from 61 to 124 Ωcm^2 has been reported (To *et al.*, 1998a; Do and To, 2000; To *et al.*, 2001). Reassuringly, this included the range we found in the present study.

2.4.3 The biphasic response to ouabain addition

As described in Chapter 1 (section 1.1.2), the NPE and PE possess different densities of Na^+, K^+-ATPase (Riley and Kishida, 1986), with the NPE possessing approximately eight times more Na^+, K^+-ATPase catalytic alpha subunit protein than the PE (Dunn *et al.*, 2001). Since Na^+, K^+-ATPase is located in abundance on the basolateral side of both layers, but working in opposite directions, sodium ions are constantly being pumped out of the CBE in exchange for potassium.

When ouabain was added to the aqueous side, it would inhibit the Na^+, K^+-ATPase located on the basolateral side of the NPE cell layer. The exchange (3 Na^+ for 2 K^+) across the NPE basolateral side would thus be reduced or arrested, leading to a reduction in sodium ions in the aqueous side and producing a hyperpolarization of the PD_t. In

theory, the active chloride ion transport across the CBE would play a role in the change in PD_t after ouabain. The active chloride flow is dependent on the sodium-potassium-chloride cotransporter ($Na^+/K^+/2Cl^-$ cotransporter) located on the basolateral side of PE which moves the chloride into the PE. This uptake process is driven by sodium gradient generated by the Na^+, K^+-ATPase. The subsequent efflux of chloride ions from the bilayers to the aqueous humor is via the chloride channels down its electrochemical gradient (Do and To, 2000). Initially, as the Na^+, K^+-ATPase was inhibited by ouabain, the chloride ion movement into the CBE was not immediately affected as the sodium gradient still remained intact but started to dissipate. Therefore, the chloride transport may not have been contributing to the PD_t changes immediately after ouabain addition. Afterwards, the ouabain either reached the PE from the stromal application or diffused across the bilayer to the stromal side so that the Na^+, K^+-ATPase in the basolateral membrane of PE was subsequently inhibited. This produced the observed depolarization of the PD_t. Finally, all active transport functions were abolished, sodium gradient dissipated and the PD_t decreased slowly towards zero with time. This phenomenon has been widely reported and established in other CBE transport models (Wiederholt and Zadunaisky, 1987; Chu *et al.*, 1987b). The biphasic response observed in the present study is consistent with other studies (Krupin *et al.*, 1984; Wiederholt and Zadunaisky, 1987; Chu *et al.*, 1987b) and has also been used to test tissue viability involving Ussing chamber experiments of the bovine CBE (To *et al.*, 1998a).

In the inhibition study, when ouabain was added bilaterally, the maximal stimulation of PD_t (and I_{sc}) was slightly lower than that when ouabain was added only on the aqueous side. It might be because that in the bilateral application, ouabain reached the PE

basolateral membrane from the bathing solution shortly after it acted on the NPE. The inhibition of the Na^+, K^+-ATPase at the PE side produced depolarization which may have depressed the hyperpolarization peak as observed when ouabain was applied at the aqueous side alone. In both cases, the PD and I_{sc} eventually decreased towards zero and became stable. Measurement of ouabain's effect on glucose transport was started from this point onwards.

2.4.4 L-glucose (LG)

In the present study, LG was used as a diffusional control. This substrate is biologically inactive, and its movement into a tissue is purely dependent on passive paracellular diffusion (DiMattio and Streitman, 1986; To and Hodson, 1998b). This finding has been confirmed by other studies, in which LG was observed to enter into ocular compartments using the same mechanism as urea and sucrose, which also move via passive diffusion (DiMattio and Zadunaisky, 1981). The rate of LG diffusion is a good indicator with which to quantify physical damage of the tissue upon mounting, and to evaluate the physical integrity of the bovine CBE as a measure of its "tightness" as an aqueous barrier. Thus, a low permeability of LG indicates the barrier is tight with low leakiness. Moreover, a low permeability of LG also meant the absence of severe edge damage to tissues, caused by chamber mounting. Since LG passes through cell layers in a paracellular manner or via edge damage during tissue mounting, the subtraction of the LG flux from the MDG flux gives the transcellular glucose flux that is the rate of glucose transport across the membrane by glucose transporters. Figure 2.9 revealed the relationship between LG and R_t: they correlated linearly and inversely.

In the present study, no significant net LG flux was found in any of the experiments. The measured LG fluxes were slightly lower than those reported by others (To *et al.*, 1998a), which indicates that the selected tissue preparations had good integrity and that edge damage was minimal. This discrepancy with previous findings might be due to the modifications that had been made to the chambers, which made the tissue preparation more stable and edge damage less severe. In addition, the lower permeability of CBE towards LG implies that the bovine CBE is generally tight, not leaky.

For the calculation of the glucose flux, the area of the tissue cavity (i.e. 0.30 cm^2) was used as if the tissue surface was flat. However, this would be the maximum estimation of LG flux for the bovine CBE, since the CBE surface is far from flat in reality. The CBE is in fact highly convoluted, yet the actual surface area is hard to estimate. Therefore, the actual LG flux per cm^2 must be smaller than that estimated in the present study, for the convoluted surface area will possess a larger surface area. This issue also applies to the MDG flux calculation.

2.4.5 Passive versus active transport

In this study, MDG was used in an attempt to eliminate the influence of metabolism. MDG is a non-metabolizable sugar, but which is otherwise very similar to D-glucose (DiMattio and Zadunaisky, 1981; DiMattio and Zadunaisky, 1982). MDG would pass through the cell membrane in both a paracellular and a transcellular manner. Thus, the subtraction of the LG flux from the MDG flux gives the transcellular glucose flux. In the present study, no significant net flux (i.e the difference between Jsa and Jas for each eye) was observed for MDG. Therefore, the chance of having active glucose transport in the

bovine CBE seems unlikely. This agrees with previous assumption based on the fact that the concentration of glucose in the aqueous humor is lower than that of the blood stream (DiMattio *et al.*, 1984b; Abdel-Latif, 1997). Hence active transport of glucose across the CBE would be unnecessary, since it could simply move down its concentration gradient.

2.4.6 Stereospecificity

The present study demonstrated that MDG was transported into the aqueous humor more readily than its stereoisomer, LG. This finding is consistent with other studies in which D-glucose also crossed cells more readily (DiMattio and Zadunaisky, 1982; Stramm and Pautler, 1982; DiMattio and Streitman, 1986). This clearly shows that the glucose transport mechanism across the bovine CBE exhibits stereospecificity. However, the D- to L-glucose transport ratio of 6.3-6.5 in the bovine CBE might somewhat underestimate the true value. Although MDG has been widely used to evaluate D-glucose transport in different tissues (Stramm and Pautler, 1982; DiMattio, 1984a), it does possess an additional methyl group not present in D-glucose itself. This modification has been suggested to hinder the transport efficiency of MDG as compared to D-glucose (DiMattio and Zadunaisky, 1981). It has been shown that the transport rate of MDG is slower than that of D-glucose, but faster than urea in ocular epithelia (DiMattio and Zadunaisky, 1981). This result contradicted an early finding in frog RPE, in which MDG was transported at a faster rate than D-glucose (Zadunaisky and Degnan, 1976). Therefore, there may be a slight difference in the transport rate between D-glucose and MDG across the bovine CBE *in vivo*. However, MGD was used in this study because the metabolism

of D-glucose can be variable, relatively complex (DiMattio and Zadunaisky, 1981) and would have been a difficult factor to control in experiments.

The stereospecificity of glucose transport has been demonstrated in aqueous and vitreous barriers of Sprague-Dawley rats (DiMattio and Zadunaisky, 1981). D-glucose was found to transport into the aqueous and vitreous at a higher rate than LG. However, exact stereospecificity between D-glucose and LG was difficult to determine because of the metabolism of D-glucose. Glucose transport stereospecificity has also been investigated for bovine, bullfrog and rat RPE, using D-glucose and also for rat lens by using MDG. The bovine RPE possessed a D- to LG transport ratio of 2.2 (To and Hodson, 1998b) while a ratio of 13.0 was observed in bullfrog RPE (DiMattio and Streitman, 1986). A ratio of 4.6 was found for rat RPE (DiMattio and Zadunaisky, 1983) and of 3.0 in the rat lens (DiMattio, 1984a). Apparently, species and cellular differences are present in glucose transport stereospecificity, and the stereospecificity in bovine CBE is somewhat higher that that measured in bovine RPE (with a ratio of 2.2) (To and Hodson, 1998b). Surprisingly, no stereospecificity of glucose transport was found in the rat cornea (DiMattio, 1984a).

2.4.7 Glucose transport mechanism in the bovine CBE

This study demonstrated that the transport mechanism of glucose across the bovine CBE is primarily via facilitated passive transport. The application of phloretin exhibited a 60% inhibition of the MDG flux and cytochalasin B caused an ~ 80% reduction. These inhibitors are highly specific for GLUTs, which suggested the presence of passive facilitated transport as the major route for glucose transport in the bovine CBE. The

greater potency of cytochalasin B, compared to phloretin, agrees with previous studies in bovine RPE (To and Hodson, 1998b) and frog lens (Lucas and Duncan, 1983). Both phloretin and cytochalasin B did not cause any significant change in LG flux. This suggests that LG diffuses across cell membrane in a paracellular manner, and thus is not affected by these inhibitors.

The significant inhibition by phlorizin (~ 20%) and the mild inhibition by ouabain were unexpected, since facilitative type glucose transport has been presumed to be the only glucose transport mechanism in the CBE, as it is constantly under a stable glucose gradient (Cole, 1984; Abdel-Latif, 1997). Since passive facilitative glucose transport does not require a transmembrane sodium gradient (To and Hodson, 1998b), the dissipation of the sodium gradient with ouabain should not have direct effect on the glucose transport across the bovine CBE.

The binding conditions and inhibitory effects of glucose transport with phlorizin have been widely investigated (Stramm and Pautler, 1982; Lucas and Duncan, 1983; Hosoya *et al.*, 1996; Oulianova and Berteloot, 1996). The significant reduction of glucose flux across CBE by phlorizin might be explained by two possibilities. Firstly, phlorizin could have inhibited a SGLT present in the bovine CBE membrane by binding directly to its glucose binding site. Secondly, phlorizin could have inhibited the GLUTs present in the CBE by transforming (via hydrolysis) into phloretin (Malathi and Crane, 1969). For example, phlorizin caused significant reduction of glucose transport in human tumour cells (Nelson and Falk, 1993), when GLUTs are widely known to be the commonest glucose transporter isoform in the tumour cells (Das, 1999; Kato *et al.*, 2002). In brain tissues, phlorizin's inhibitory effect was significant too (Betz *et al.*, 1975), even though it

is known that GLUT1 and GLUT3 are the predominant isoforms that exist in the brain (Simpson *et al.*, 1994; Vannucci *et al.*, 1997). This evidence of non-specificity of phlorizin towards different glucose transporter families therefore complicates our interpretation in the present study, since it is not possible to determine the extent to which phlorizin was hydrolyzed into phloretin. There were no significant changes in electrical parameters during the bilateral phlorizin addition, which argues against a major contribution by the SGLTs. This is because the inhibition of SGLTs by phlorizin should result in a change in the sodium gradient and potential across the membrane (Hosoya *et al.*, 1996; Horibe *et al.*, 1997). However, we could not rule out the presence of a minor contribution by SGLTs which may produce very small changes in the PD_t or I_{sc} during phlorizin addition. To investigate this issue further, expression studies on transporter genes and proteins were carried out in Chapters 4 and 5.

2.5 Conclusion

This study suggested that the glucose transport across the bovine CBE was via a bi-directional carrier-facilitated transport mechanism. A similar mechanism has been reported in the BRB (Takata *et al.*, 1997; Busik *et al.*, 2002) which shares the same embryological origin as the BAB during development. Active glucose transport, if present, is unlikely to play a major role in the physiological glucose transport across the bovine CBE.

Chapter 3

Glucose transport kinetics: Saturation characteristics

3.1 Introduction

3.1.1 Overview of experiments

In this chapter, the glucose flux (i.e. Jsa) under various glucose concentration gradients was investigated. Five different glucose concentration gradients were established across the bovine CBE, with the stromal side having the higher concentration, and the osmolarity balanced by the addition of sorbitol on the aqueous side. Modifications were made to the modified Ussing-type chambers to reduce tissue damage and improve functional stability.

If glucose transport across the bovine CBE occurs by a carrier-mediated system, it should be saturable – given a sufficiently high plasma glucose concentration. Therefore, there should be a point at which further increases above this saturating plasma glucose concentration would cause no further increase in the glucose flux. To examine this issue, a series of experiments were performed in which the stromal glucose concentration was varied. The change of the glucose transport rate was observed, and the transport kinetic parameters, the Michaelis constant (K_m) and maximum velocity (V_{max}), were estimated by the use of an Eadie-Hofstee plot.

3.1.2 The Michaelis-Menten equation

The enzyme kinetic model is a biochemical scheme, which describes the enzyme-substrate catalytic reaction. It represents an overall reaction composed of two sub-reactions in which enzyme (E) and substrate (S) bind to each other to form an enzyme-substrate complex (ES) and at the same time, the complex is decomposing into product (P) and E:

$$E + S \underset{k_{-1}}{\overset{k_1}{\rightleftharpoons}} ES \xrightarrow{k_2} P + E$$

Where k_1, k_{-1} and k_2 are the rate constants of corresponding reactions. According to this model, the second reaction would become the limiting step of the overall reaction when the substrate concentration ([S]) was high enough to bind all enzymes into ES complex. A further increase in the substrate concentration would have no effect on the overall reaction rate. In other words, it is a model used to explain why, when at low [S], the initial reaction velocity (V_o) is directly proportional to [S], while reaction velocity tends to reach a maximum (V_{max}) that is independent of [S] at high [S]. It is a common concept applied to describe the substrate affinity or transport velocity of a biological system, such as ascorbate transport in the isolated rabbit CE (Chu and Candia, 1988), sugar transport in the dog kidney (Turner and Silverman, 1978) and bovine BBB (Lee *et al.*, 1997). In order to make it useful to use in experimental quantitation, the enzyme-kinetic model can be formulated using the Michaelis-Menten equation:

$$V_o = \frac{V_{max} \cdot [S]}{K_m + [S]}$$

which is a description of the hyperbolic curve of V_o against [S]. The Michaelis constant (K_m) is defined as:

$$K_m = \frac{k_{-1} + k_2}{k_1}$$

and is the sum of the rates of binding and dissociation of substrate and enzyme, compared to the rate of complex formation. Experimentally, it can be determined as the concentration at which a transport system is half-saturated (i.e. $V_{max}/2$). It is also a measure of the affinity of a transporter or enzyme for its substrate. A high K_m indicates weak binding and thus, low affinity of the system. A low K_m indicates strong binding and therefore, high affinity of the system.

In general, two transformations of the Michaelis-Menten equation are commonly used in describing transport kinetics, these include the Lineweaver-Burk plot and the Eadie-Hofstee plot.

3.1.2.1 The Lineweaver-Burke plot

The Lineweaver-Burke plot, also called the "double reciprocal plot" is a graphical representation of enzyme kinetics. It is one of the transformations of the Michaelis-Menten equation, which is commonly used in the analysis of transport kinetics, e.g. in frog RPE (DiMattio and Streitman, 1986), rat retina and RPE (Vilchis and Salceda, 1996), where it was adapted for characterizing the tissues' carrier-mediated glucose transport. The Lineweaver-Burk equation is:

$$\frac{1}{V_o} = \frac{K_m}{V_{max}} \frac{1}{[S]} + \frac{1}{V_{max}}$$

Figure 3.1 illustrates an example double reciprocal plot. The y-intercept represents $1/V_{max}$ and the x-intercept represents $-1/K_m$.

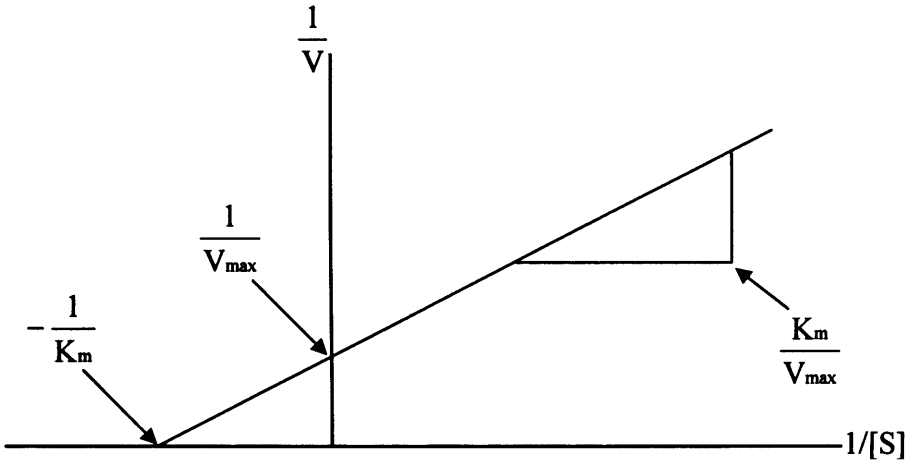

Figure 3.1 An illustration of a Lineweaver-Burk plot.

Despite its useful attributes, the Lineweaver Burk plot is regarded as an inferior method to Eadie-Hofstee plot, since it tends to overweight the contribution of data taken at low substrate concentrations.

3.1.2.2 Eadie-Hofstee plot

The Eadie-Hofstee diagram, also called Woolf-Eadie-Augustinsson-Hofstee or Eadie-Augustinsson plot, is another commonly used linear presentation of the Michaelis-Menten Equation. Similar to the Lineweaver-Burk plot, it is a graphical presentation of enzyme-substrate kinetics, which allows rapid determination of the K_m and V_{max}. The kinetic terms can be deduced by plotting the reaction velocity, which is the transport rate (J_{sa}) in this study, as a function of the velocity-per-unit-substrate concentration. The Eadie-Hofstee equation is:

$$V_o = -K_m \frac{V}{[S]} + V_{max}$$

This transformation has been used in a variety of kinetic analysis studies, such as the glucose transport in chick RPE (Masterson and Chader, 1981) and bovine RPE (To *et al.*, 1998c). It is considered to be superior to the Lineweaver-Burk plot because it gives equal weight to every data point. An illustration of an Eadie-Hofstee plot is given in figure 3.2. Transport kinetics can simply be deduced according to the slope ($-K_m$) and y-intercept (V_{max}).

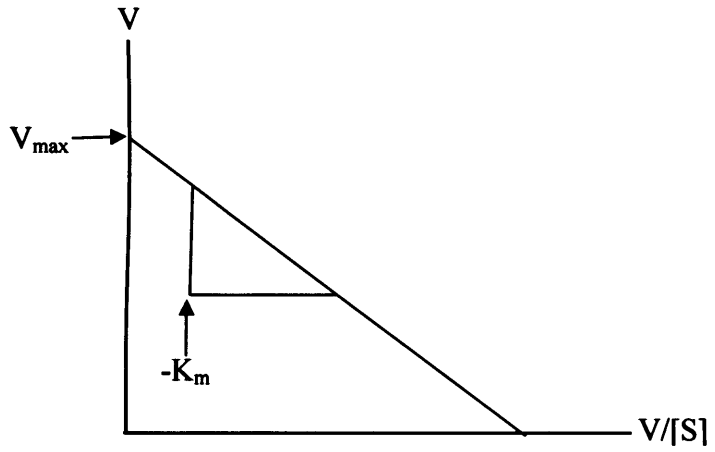

Figure 3.2 An illustration of an Eadie-Hofstee plot.

3.1.3 Saturation studies

Table 3.1 summarises the glucose transport kinetic studies that have been carried out for ocular tissues. Inter-species differences clearly exist. It is noted that only a single study has been carried out in characterizing the glucose transport across the CBE (DiMattio and Zadunaisky, 1981).

Ocular tissues	Species	Substrate	K_m (mM)	V_{max}	Reference
BAB	Rat	D-glucose	6.1	22.5 nmol/min	(DiMattio and Zadunaisky, 1981)
BRB	Rat	D-glucose	0.2 & 7.8	---	(Ennis *et al.*, 1982)
BVB	Rat	D-glucose	4.6	23.8 nmol/min	(DiMattio and Zadunaisky, 1981)
Retina	Rat	2-deoxy-D-glucose	2.0	750 nmol/g/min	(Vilchis and Salceda, 1996)
	Rat (diabetic)	2-deoxy-D-glucose	5.0	1500 nmol/g/min	(Vilchis and Salceda, 1996)
	Frog	2-deoxy-D-glucose	5.1	699 nmol/mg/min	(Witkovsky and Yang, 1982)
RCP	Bovine culture	MDG	1.53	0.50 mmol / (µg DNA)/ min at 37°C	(Li *et al.*, 1985)
RPE	Bovine	D-glucose	27 (C→R) 9.5 (R→C)	2100 nmo/cm^2/hr (C→R) 710 nmol/cm^2/hr (R→C)	(Crosson and Pautler, 1982)
	Bovine	MDG	30.8 (C→R)	2452 nmol/cm^2/hr (C→R)	(To *et al.*, 1998c)
	Chick culture	2-deoxy-D-glucose	2.7	22 nmol/min/mg protein	(Masterson and Chader, 1981)
		MDG	4.5	27.7 nmol/min/ mg protein	(Masterson and Chader, 1981)
	Frog	MDG	19.3 (C→R) 16.2 (R→C)	1050 nmol/cm^2/hr (C→R) 952 nmol/cm^2/hr (R→C)	(DiMattio and Streitman, 1986)
	Human culture	MDG	5.6	0.45 nmol/ mg protein/min	(Busik *et al.*, 2002)
	Rat (Diabetic)	2-deoxy-D-glucose	20.0	750 nmol/g/min	(Vilchis and Salceda, 1996)
	Rat	MDG	1.9 & 640	12.0 nmol/ mg protein/min & 12.2 nmol/ mg protein/min	(Stramm and Pautler, 1982)
RVE	Human culture	MDG	6.3	1.4 nmol/ mg protein/min	(Busik *et al.*, 2002)
	Rat culture	MDG	5.56 ± 0.51	45.3 ± 2.6 nmol/ mg protein/ min	(Hosoya *et al.*, 2001)

Table 3.1 Transport kinetic studies in different ocular tissues. BVB: blood vitreous barrier, RCP: retinal capillary pericytes, RVE: retinal vascular endothelium, (C→R): from choroid to retina direction, (R→C): from retina to choroid direction.

As well as difference between species, e.g. frog retina (Witkovsky and Yang, 1982) was of lower affinity to 2-deoxy-D-glucose than that of rat (Vilchis and Salceda, 1996), studies in the same species also show high variability. These differences vary with the ocular tissues being investigated and the substrates being used. Therefore, a general conclusion cannot be drawn unequivocally due to this variability.

In rat RPE, high- and low-affinity transport systems were found to co-exist (Stramm and Pautler, 1982), and similar transport mechanisms were also observed in the rat BRB (Ennis *et al.*, 1982). This type of high and low-affinity mechanism is not uncommon: different transport affinities have been demonstrated in kidney (Mackenzie *et al.*, 1996; Oulianova and Berteloot, 1996). This was recognised as being the result of the presence of different glucose transporters, which possess their maximum transport capacity at differing glucose concentrations.

In two studies of the bovine RPE, the glucose transport kinetics in the direction choroid-to-retina were comparable, as were the transport capacities (Crosson and Pautler, 1982; To *et al.*, 1998c). MDG was said to be a good substitute for D-glucose in transport kinetic studies, since the results based on MDG alone did not deviate greatly from that of the D-glucose. The bovine RPE revealed a low affinity but high capacity, suggesting that the retina is a highly metabolic tissue (Miceli *et al.*, 1990). Because of its requirements in this regard, a system that does not saturate under physiological conditions is beneficial.

In diabetic models, tissues typically demonstrate a significant decrease in glucose transport affinity (Vilchis and Salceda, 1996). In the rat retina, an increase of 2.5-fold of K_m resulted after exposure to simulated diabetic conditions, and double the amount of glucose could be transported across the cell membrane. This finding agreed with previous

work based on comparisons between normal and diabetic rats (Ennis *et al.*, 1982), and clearly showed that exposure to diabetic conditions can change the normal glucose transport properties of an organ (Ennis *et al.*, 1982; Mandarino *et al.*, 1994).

As shown in table 3.1, previous studies have focused mostly on the retina and RPE, hence little information is available regarding the saturation characteristic in BAB, or the CBE. The present study aimed to investigate these characteristics, and therefore, lead to a better understanding of the mode of glucose transport across the CBE.

3.2 Methodology

3.2.1 Materials and bathing solution

All the materials and the Ringer solution used in this part of the project were the same as in the previous chapter (section 2.2.1), with an additional chemical, sorbitol, which was purchased from Sigma-Aldrich Company (St. Louis, MO). The D-glucose concentration in the Ringer solution was varied, as described below.

3.2.2 Tissue preparation, selection and dissection

Please refer to sections 2.2.2 and 2.2.3 for details.

3.2.3 Ussing-type chamber configuration and modification

Continuous-perfusion-type Ussing chambers, similar to those described in the previous chapter were used, with minor modifications. Figure 3.3 highlights these changes, including newly inserted O-rings surrounding the tissue cavity and also pins introduced between the silicone plates. The modifications provided the advantage of decreased edge damage of tissues upon mounting and therefore decreased leakage. Furthermore, the pins on the silicone plates held the tissues in place in a tighter manner which increased the stability of tissue mounting.

3.2.4 Chamber preparation and tissue mounting

The chamber preparation was similar to that described in section 2.2.5, except that an O-Ring was placed on top of the O-Ring groove after application of silicone lubricant on the silicone plate. After the O-Rings were in place, silicone grease was applied again to seal

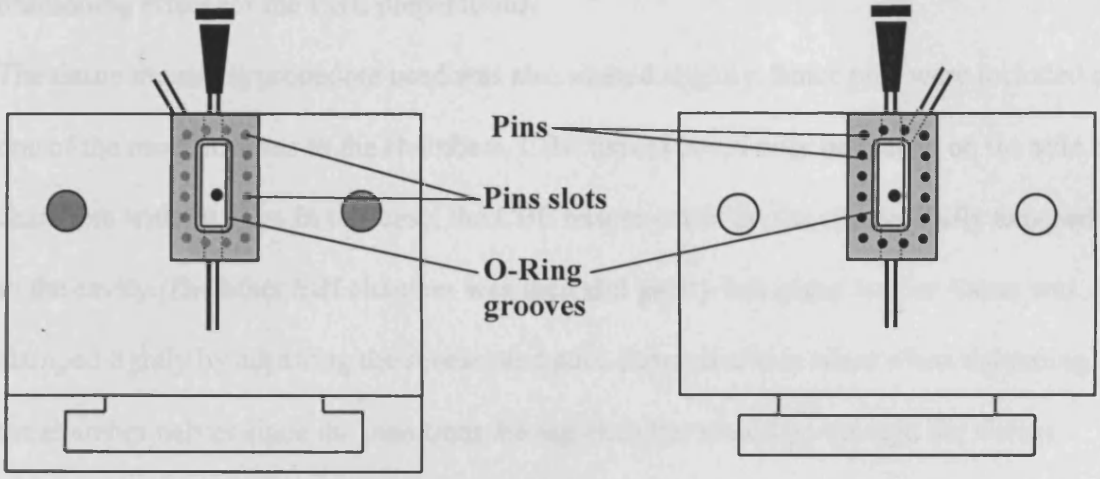

a) Front view of the modified Ussing-type half-chambers.

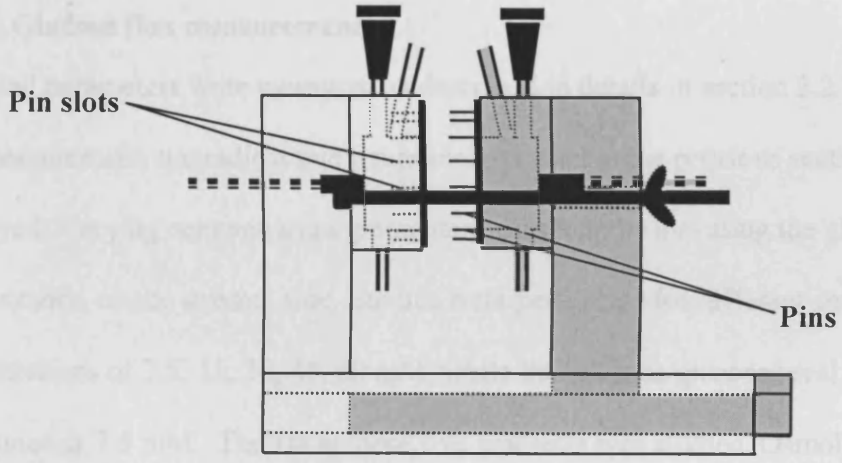

b) Side view of the modified Ussing-type half-chambers.

Fig. 3.3 Configurations of the modified Ussing-type chambers.

the gap between the chambers and the rings. This was to ensure good sealing and a good cushioning effect for the CBE preparations.

The tissue mounting procedure used was also altered slightly. Since pins were included as one of the modifications to the chambers, CBE tissues could only be placed on the side of chambers without pins. In this case, the CBE tissues could lie flat and carefully exposed to the cavity. The other half chamber was then slid gently into place and the tissue was clamped tightly by adjusting the screws and nuts. Extra care was taken when tightening the chamber halves since the pins from the top chamber would go through the tissues which lay outside the tissue cavity area, and then fitted into the pin slots of the lower chamber. The final tightness was adjusted slowly by turning the wing nuts as described in 2.2.6.

3.2.5 Glucose flux measurement

Electrical parameters were measured as described in details in section 2.2.7. For glucose flux measurement, the radioactive tracer method used in the previous section was again employed. Varying concentration gradients were set up by elevating the glucose concentration on the stromal side. Studies were performed for different stromal glucose concentrations of 7.5, 15, 30, 45, 60 mM, while the aqueous glucose level was maintained at 7.5 mM. The Jsa at these five gradients was studied. Osmolarity at the aqueous side was balanced by the addition of sorbitol, a chemical that possesses similar molecular weight to glucose (MW 181.6 versus 181.0), but which is not transported by any of the known glucose transporters. For example, in the experiment involving a 7.5 mM concentration gradient, 15 mM D-glucose Ringer solution was perfused to the stromal side, and 7.5 mM of D-glucose plus 7.5 mM sorbitol Ringer solution to the

aqueous side. Initial stabilization was allowed for 60 minutes and background radioactivity and further radioactive measurement were performed as described in section 2.2.9.1. However, for concentration gradients higher than 15 mM, it was necessary to increase the concentration in a stepwise manner, using 15.0 or 7.5 mM steps, until the desired concentration was reached (Table 3.1). For example, a concentration gradient of 45 mM was started at 15 mM at the stromal side and 7.5 mM D-glucose at the aqueous side. After 30 minutes stabilization, Ringer solution containing 22.5 mM glucose was perfused to the stromal side of the preparation and allowed to equilibrate for another 30 minutes. This resulted in a concentration gradient of 15 mM across the CBE preparation. Then, two more 15 mM changes were performed, with 52.5 mM Ringer perfusing into the stromal side eventually, which produced a 45 mM glucose concentration gradient. After the desired gradient was reached, the preparation was left to stabilise for another 60 minutes and control perfusates were collected. A change of solution to those containing radioactive isotopes was then carried out, and preparations were stabilised for another hour. Finally, radioactive perfusates were collected and analyzed as described earlier.

Change of solutions	**D-glucose concentration (mM)**									
	S	**A**	**S**	**A**	**S**	**A**	**S**	**A**	**S**	**A**
Initial	15	7.5	15	7.5	15	7.5	15	7.5	15	7.5
1st	---	---	22.5	7.5	22.5	7.5	22.5	7.5	22.5	7.5
2nd	---	---	---	---	37.5	7.5	37.5	7.5	37.5	7.5
3rd	---	---	---	---	---	---	52.5	7.5	52.5	7.5
4th	---	---	---	---	---	---	---	---	67.5	7.5
Final concentration gradient	**7.5**		**15**		**30**		**45**		**60**	

Table 3.2 Stepwise build-up of the glucose concentration gradient across the bovine CBE. S is the stromal side, A is the aqueous side.

Glucose flux results were calculated and plotted in an Eadie-Hofstee relationship, to allow the deduction of transport kinetics for CMDG to be determined. The properties, K_m and V_{max}, of the bovine CBE were deduced as described in section 3.1.2.2.

3.2.6 Test of viability

In this part of the study, preparations were considered to be viable if they fulfilled the same criteria as described in Chapter 2 (section 2.2.8): 1) a stable PD_t and R_t greater than -0.2 mV and 70 Ωcm^2 respectively, before the first change of Ringer solution to higher concentration, 2) a low diffusional LG flux (i.e. lower than 70 $nmolhr^{-1}cm^2$), and 3) a biphasic response to ouabain, when added to the aqueous side. Again, preparations were rejected if they failed in any one of these criteria.

3.2.7 Statistical analysis

Statistical calculations were performed by using Excel (Microsoft) or GraphPad Prism (version 3.02). All data were expressed as mean ± S.E.M. and $p < 0.05$ was considered as statistically significance. The unpaired Student's t-test was used to compare the results between different tissue samples. One-way ANOVA with Tukey's multiple comparison test or Dunnett's post-hoc test was performed to evaluate variations within a set of tissue samples.

3.3 Results

3.3.1 Glucose influx across the bovine CBE

Glucose fluxes from stromal to aqueous side were measured and analyzed for five different concentration gradients (Table 3.2). The stereospecificity of CBE in transporting glucose was maintained across a wide range of concentration gradients, with the highest recorded at 30 mM. When compared to 7.5 mM, 30 mM or higher gradients caused a significant increase in both MDG influx and CMDG fluxes (Dunnett's post-hoc test, $p < 0.01$, $n = 6\text{-}8$). The LG influx, on the other hand, increased steadily but slowly with the increase of concentration gradient. When compared to 7.5 mM, 45 mM or higher gradients caused a drastic increase in LG flux (Dunnett's post-hoc test, $p < 0.05$, fig. 3.4).

Concentration gradient (mM)	Jsa ($nmolhr^{-1}cm^{-2}$)			D- to L-glucose ratio
	LG	MDG	CMDG	
7.5 (10)	36.2 ± 8.6	236.6 ± 24.0	200.4 ± 23.6	5.5
15 (6)	39.6 ± 6.1	306.0 ± 28.0	266.4 ± 27.3	6.7
30 (6)	44.2 ± 7.6	353.6 ± 31.2	309.4 ± 27.9	7.0
45 (6)	49.1 ± 3.7	347.1 ± 40.3	298.1 ± 36.4	6.0
60 (8)	62.4 ± 10.1	383.9 ± 40.6	321.4 ± 34.6	5.2

Table 3.3 Glucose fluxes under different concentration gradients. Numbers of completed experiments are in parenthesis. Flux data are all expressed as mean ± S.E.M..

3.3.1.1 Saturation characteristics

An Eadie-Hofstee plot of the CMDG was used to analyze the transport kinetics of glucose across the CBE. The Eadie-Hofstee plot of CMDG showed high linearity, with K_m and V_{max} equal to 5.3 mM and 349.5 $nmolh^{-1}cm^{-2}$ respectively (Fig. 3.5).

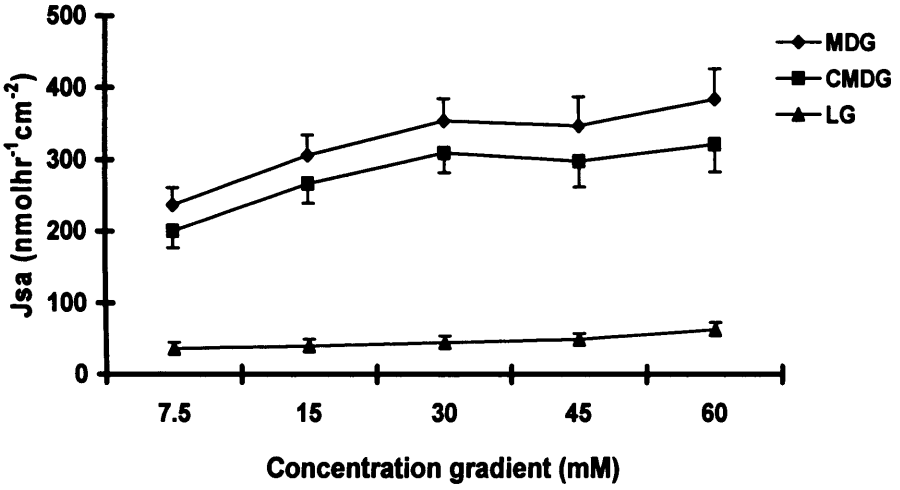

Fig. 3.4 Influx measurements in five glucose concentration gradients.

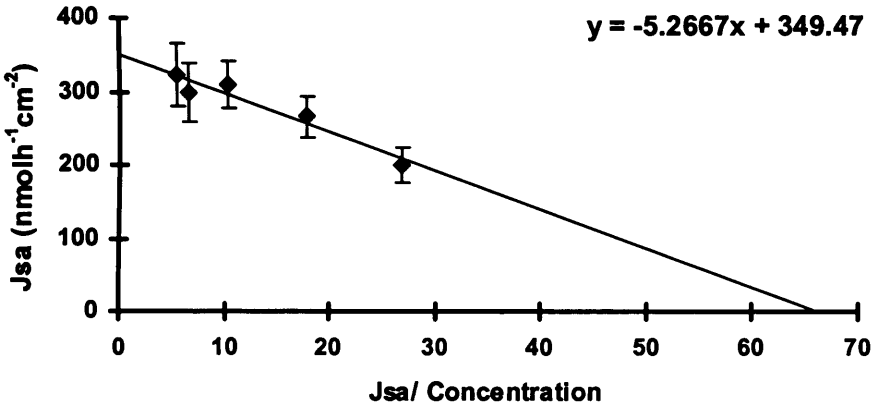

Fig. 3.5 Eadie-Hofstee plot of CMDG (r^2 = 0.93, mean ± S.E.M.).

3.3.2 Electrical parameter measurements

In this study, electrical parameters including PD_t, R_t and I_{sc} were monitored as in the last chapter (Table 3.3). Only a borderline statistically significant influence was observed with different glucose concentration gradients on R_t (Dunnett's post-hoc test, $p > 0.05$, $n = 6$-8). However, significant influences were noted on PD_t and I_{sc} with concentration gradients of 30 mM (Dunnett's post-hoc, $p < 0.001$, $n = 8$), 45 mM (Dunnett's post-hoc test, $p < 0.001$, $n = 8$) and 60 mM (Tukey's post-hoc, $p < 0.001$, $n = 8$), when compared to the 7.5 mM concentration gradient. Representative plots of the changes in PD_t and I_{sc} with concentration gradients and addition of ouabain are given in figures 3.6 and 3.7. A summary of the changes measured at gradients of 30, 45 and 60 (in mM) are shown in figures 3.8-3.10.

Concentration gradient (mM)	PD_t (mV)	R_t (Ωcm^2)	I_{sc} (μAcm^2)	n
7.5	-0.39 ± 0.08	107.7 ± 4.8	-3.54 ± 0.58	10
15	-0.20 ± 0.03	93.8 ± 5.1	-2.12 ± 0.29	6
30	-0.12 ± 0.03	112.0 ± 4.4	-1.01 ± 0.22	6
45	0.16 ± 0.04	102.3 ± 4.3	1.50 ± 0.36	6
60	0.34 ± 0.06	104.6 ± 4.8	3.30 ± 0.63	8

Table 3.3 Electrical parameters of the CBE preparations under different concentration gradients. All the data stated above are data calculated at 60 minutes after the desired concentration gradients were reached. Results are presented as mean ± S.E.M..

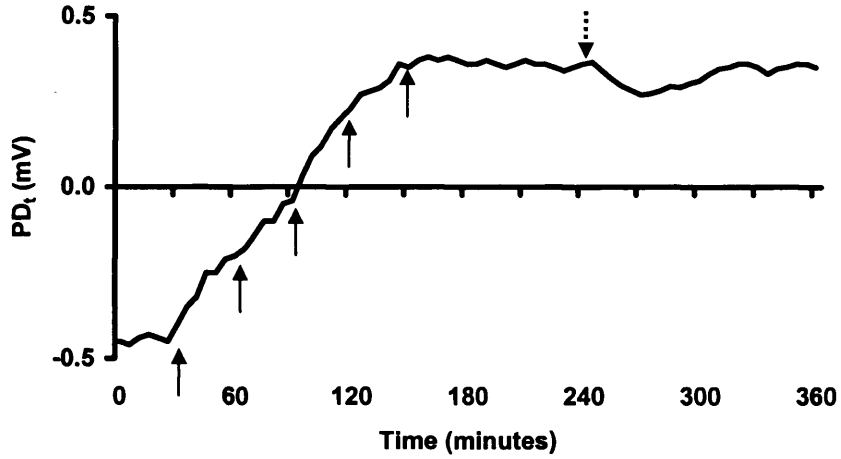

Fig. 3.6 Changes of PD_t with a final glucose concentration of 60 mM. The data indicated the PD_t of the aqueous side with respect to that of stroma across the bovine CBE. Each change in concentration is indicated with an arrow. The broken arrow indicates the addition of ouabain. Please refer to table 3.1 for details.

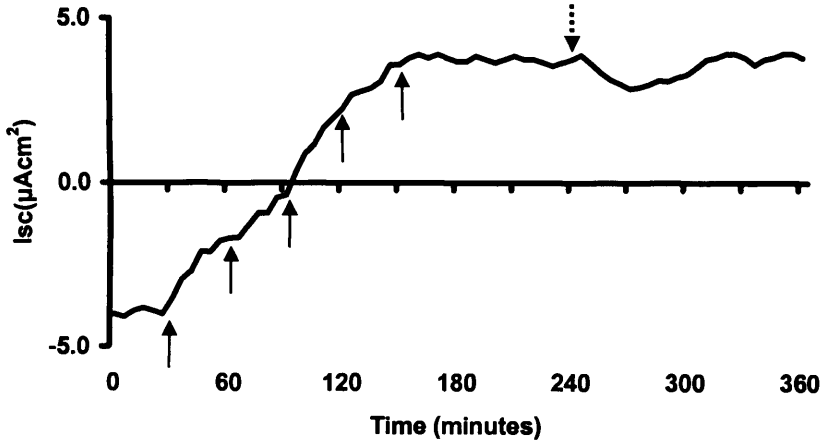

Fig. 3.7 Changes of I_{sc} across CBE with a final glucose concentration gradient of 60 mM. The data indicated the resultant ion transport into the aqueous with reference to the stromal side. Each change is indicated with an arrow. The broken arrow indicates the addition of ouabain.

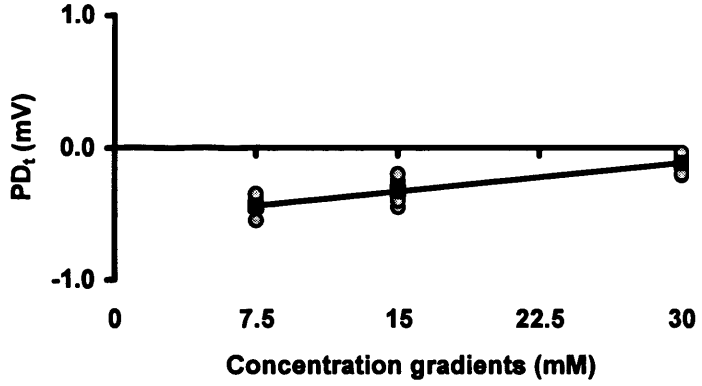

Fig. 3.8 PD_t changes in experiments up to 30 mM concentration gradients ($r^2 = 0.78$).

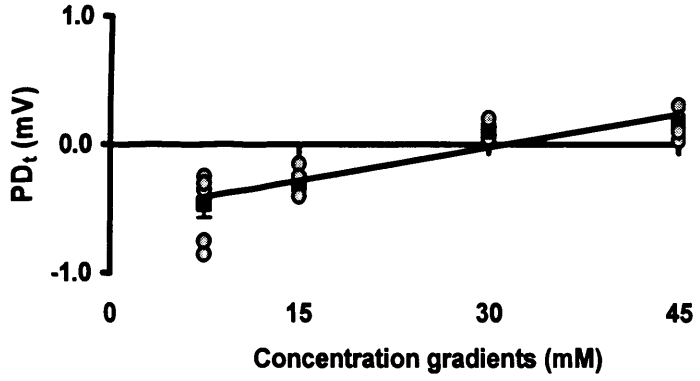

Fig. 3.9 PD_t changes in experiments up to 45 mM concentration gradients ($r^2 = 0.77$).

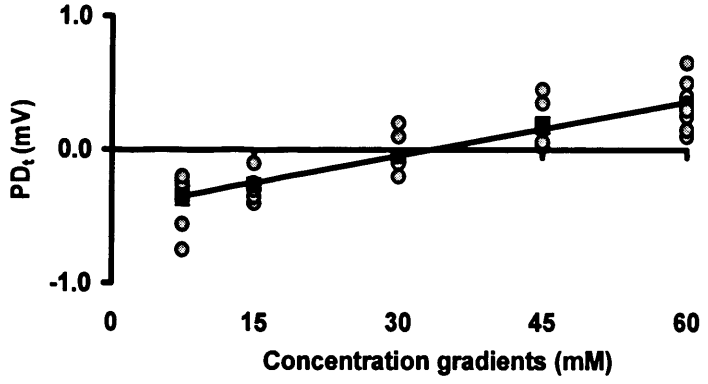

Fig. 3.10 PD_t changes in experiments up to 60 mM concentration gradients ($r^2 = 0.74$).

3.4 Discussion

3.4.1 Glucose saturation characteristics of bovine CBE

The glucose transport kinetics across the bovine CBE were determined by using an Eadie-Hofstee plot. The K_m and V_{max} were 5.3 mM and 349.5 $nmolh^{-1}$ cm^{-2} respectively, and indicated that the glucose transport across the bovine CBE would be likely to saturate at a stromal glucose concentration of $\approx$ 10.6 mM (i.e. double the K_m value) with a maximum glucose transport rate of 349.5 $nmolh^{-1}$ cm^{-2}. Previous studies on bovine RPE demonstrated a lower affinity, but much higher capacity in transporting glucose into the retina (Crosson and Pautler, 1982; To *et al.*, 1998c) than across the CBE. These studies revealed that glucose transport across the RPE is not limiting at normal plasma glucose concentrations. This would be beneficial, since the RPE is crucial in transporting glucose into the retina, in order to ensure an adequate glucose supply to meet the needs of the highly metabolically-active retinal tissues, including the photoreceptors (Adler and Southwick, 1992; To *et al.*, 1998c).

As mentioned above, the experimental work carried out in this chapter suggests that glucose transport across the bovine CBE will saturate at a stromal glucose concentration of $\approx$ 10.6mM. It should be noted that this finding may not necessarily reflect the diabetic condition, since it was an acute rather than a chronic alteration of glucose levels. It is known that tissues which have been exposed to elevated glucose concentrations can become leaky (through an increase in paracellular glucose movement) and that hyperglycemia can affect the glucose transport rate. Similar changes in the transport characteristics of "diabetic exposed" tissues have been reported in rat retina and RPE (Vilchis and Salceda, 1996). These alterations in glucose transport might result from

glucose toxicity (Gaynes and Watkins, 1989; Unger, 1991) and other hyperglycemic complications.

3.4.2 Viability of preparations

3.4.2.1 L-glucose (LG)

LG was again used as the diffusional control. The general LG influx in the present study was low and indicated the new Ussing-type chamber was not leaky. Similar to the last study (Chapter 2), the subtraction of the LG flux from the MDG flux enabled the transcellular glucose flux to be calculated. This (indirectly) caused a reduction of the MDG flux increase at higher glucose concentration gradients. The fact that the LG fluxes were lower than the preset criteria and also smaller than those measured in a previous study (To *et al.*, 1998a), indicated that the preparations were not leaky, and therefore that passive diffusion was not the dominant mode of glucose transport.

3.4.2.2 Ouabain response

At the end of each experiment, ouabain was added to the aqueous side as a final check of viability. Only those preparations (~ 80%) that gave a biphasic response to ouabain were included in the final analysis. Preparations might also be rejected when no stable electrical parameters could be obtained after the first stabilization period (Please refer to Chapter 2 (section 2.4.3) for details).

3.4.2.3 Electrical parameters

All of the results included in the present study were collected from preparations, showing a consistently negative PD_t before the first change of solution. Other electrical parameter changes with the increase of glucose concentration are discussed below.

3.4.3 Electrical parameter changes with glucose concentration

Figures 3.6 and 3.7 illustrate the electrical parameter changes upon increments of plasma-side glucose level. It was noted that a plasma glucose concentration higher than 30 mM caused a polarity change, with the aqueous side becoming positive. In a previous study, significant changes of PD and I_{sc} were also reported at very high glucose concentrations (i.e. 205 mM) in frog RPE and glucose fluxes were affected too with a concentration of 100 mM (DiMattio and Streitman, 1986). However, a glucose concentration as high as 100 mM has been suggested to be detrimental to the RPE (DiMattio and Streitman, 1986; To *et al.*, 1998c). Yet, these concentrations are far higher than those used in the present study, and the preparations studied here were still responsive to ouabain. One could postulate that the tissues were alive, but their electrical characteristics were somehow altered in response to the increase in extracellular osmolarity.

3.4.3.1 Cell volume regulation

Most living cells have the ability to self-regulate their volume, in order to counter balance alterations in extra- or intra-cellular solute content ratio (Rink, 1984). In general, an increase in extracellular osmolarity induces cell volume increase through water absorption, and vice versa. Such compensatory mechanisms, which act to restore proper

cell size and functions, are called regulatory volume increases (RVI) or decreases (RVD) (Civan *et al.*, 1996).

In the bovine CBE, constant ionic and electrochemical gradients are maintained by the actions of various ion transporters and channels (Do and To, 2000). In the present study, the increase in the extracellular solute concentration led to a change in transmembrane polarity. It indicated that there was a net increase either in cation movement in the aqueous direction or anion movement in the stroma direction. Although, the exact ion mechanism for the observed changes in PD_t is unknown, hyperosmotic stress and volume regulation can lead to changes in the potential difference via activations of various ion transporters or channels. Hyperosmotic shrinking has been demonstrated to activate the $Na^+/K^+/2Cl^-$ cotransporter and sodium-proton exchanger (Na^+/H^+ exchanger) to restore the cell volume by water absorption as a secondary effect (Burg, 1995; Lang *et al.*, 1998; Wehner and Tinel, 1998). Activation of chloride and other channels has also been shown in kidney tissues and several cell lines, due to intracellular hypertonicity (Kawahara and Matsuzaki, 1993; Hardy *et al.*, 1995; Kanzaki *et al.*, 1999). In rat muscles, an increase of 20 mM glucose or mannitol activated $Na^+/K^+/2Cl^-$ cotransporter activity, which subsequently induced water absorption into the cells (Gosmanov *et al.*, 2003).

In the ciliary body, potassium channels and chloride channels were found to be activated separately in RVD in human, with or without the help of ion transporters (Yantorno *et al.*, 1989). A study of the NPE demonstrated its ability to induce RVI by activation of four different mechanisms, which mainly stimulated the uptake of sodium and chloride ions from the aqueous humor (Civan *et al.*, 1996).

In the present study, it is possible that the hyperosmolarity altered the transmembrane polarity through complex activation of the $Na^+/K^+/2Cl^-$ cotransporter, sodium-proton and chloride-bicarbonate antiporter (Na^+/H^+ and Cl^-/HCO_3^- antiporter) activities. These may have promoted the accumulation of sodium and chloride ions into NPE and PE cells, whilst effecting volume changes (Strange, 1992; Hardy *et al.*, 1995; Civan *et al.*, 1996). A study into the mechanism of self-regulatory volume in NPE cells also showed that the process of RVD was mediated by separate K^+ and Cl^- conductances. Moreover, the change in the NPE cell volume also induced a change in intracellular calcium (Ca^+) concentration, which facilitated the modulation of cell regulation during RVD (Adorante and Cala, 1995). In cardiac myocytes, high glucose induced a rise in the intracellular Ca^+ concentration (Smogorzewski *et al.*, 1998), which also could be one possible change responsible for the polarity alteration of CBE.

In addition, an increase in the active transport of osmolytes into the epithelial bilayer would be another explanation, since many Na^+-solute transporters including the Na^+/myo-inositol cotransporter (Morimura *et al.*, 1997), Na^+-ascorbate cotransporter (Helbig *et al.*, 1989) and SGLT (details are discussed in Chapter 4) have been found in the CBE. These mechanisms are used in the brain to counter balance any extracellular deviations by actively transporting osmolytes including taurine, glutamate, or myo-inositol (Strange, 1992). Therefore, the changes in the rate of ion, and/or solute transport could have induced an accumulation of sodium in the epithelial bilayers. At higher intracellular sodium ions concentration, the transport rate of the Na^+, K^+-ATPase of the CBE may be increased (such an effect has been demonstrated in Ehrlich ascites tumour cells, in which the sodium efflux increased 2.5 to 3 times in glucose-treated cells (Laris

and Henius, 1982)). This could increase the vectorial transport of sodium into the aqueous and therefore induce a depolarization across the CBE. However, exactly how different ions contributed to the change is yet to be elucidated. In any case, apparently, the Na^+, K^+-ATPases remained unchanged in high-glucose condition, since the biphasic response was still present after the addition of ouabain (Fig. 3.6).

3.5 Conclusion

The present study has demonstrated the glucose transport kinetics across the bovine CBE using a wide range of glucose gradients. The results indicate that glucose transport across the bovine CBE is saturable and it is also consistent with a facilitated and carrier-mediated model of glucose transport mechanism.

Chapter 4

Glucose transporter gene expression in the CBE

4.1 Introduction

In this study, RT-PCR was used to screen the mRNA expression of seven glucose transporters (GLUT1-5 and SGLT1-2) in the bovine CBE. Possible expression differences between the pars plana and pars plicata regions of the CBE were also investigated.

Firstly, bovine glucose transporter mRNA sequences were retrieved from GenBank for primer design. Bovine CBE tissues were isolated and RNA extraction was performed. The RNA samples were reverse-transcripted into cDNA templates and PCR was carried out with the isoform-specific primers. Amplified DNA samples were analyzed by gel electrophoresis and sequencing, for molecular weight determination and identity confirmation, respectively.

The kinetic study (Chapter 2) showed that glucose transport across the bovine CBE is driven mainly by a facilitative mechanism. The present set of experiments was designed to investigate the mRNA expression of the two major transporter families (GLUTs and SGLTs) to elucidate the molecular basis of glucose transport in this tissue.

A previous study suggested that glucose transport across the bovine CBE is likely to be facilitative/passive, as active glucose transport seems unnecessary under the natural glucose concentration gradient (Takata *et al.*, 1991). However, the kinetic study of this project suggested a slightly different point of view, since phlorizin, a specific SGLT inhibitor, reduced the trans-CBE glucose flux significantly. With this molecular study, a clearer picture on the glucose transport across bovine CBE could be drawn.

4.1.1 Gene expression of glucose transporters in the eye

Numerous studies have demonstrated GLUT and SGLT mRNA expression in ocular tissues including the cornea, lens, RPE and retina. Details of gene expression findings on ocular tissues are summarised in table 4.1. However, detailed investigation on their expression in CBE has not been reported previously.

Gene	Ocular tissues	Methods	Gene size (kbp)	Species	Reference
GLUT1	Conjunctiva	Northern blotting	---	Human culture	(Gherzi *et al.*, 1991)
	Corneal epithelium	RT-PCR Northern blotting	2.8	Rat	(Takahashi *et al.*, 1996)
		RT-PCR	---	Rat	(Takahashi *et al.*, 2000)
	Corneal epithelium and endothelium	Nuclease protection assay	---	Bovine	(Bildin *et al.*, 2001)
	Corneal endothelial cells	Northern blotting	2.8	Bovine culture	(Ishida *et al.*, 1995)
	Lens epithelium	RT-PCR Northern blotting *In situ* hybridization	2.9	Rat	(Merriman-Smith *et al.*, 1999)
		Northern blotting Quantitative RT-PCR	2.2	Rat	(Merriman-Smith *et al.*, 2003)
	Retinal capillary endothelial cells and pericytes	Northern blotting	2.8	Bovine culture	(Mandarino *et al.*, 1994)
	Retinal endothelial cells	Northern blotting	2.8	Human culture	(Knott *et al.*, 1996)
	Retinal microvasculature	Northern blotting Quantitative RE-PCR	2.8	Human culture	(Badr *et al.*, 1999)
	BRB, RVE cells and RPE	Northern blotting	2.8	Human culture	(Busik *et al.*, 2002)
	RPE	PCR Southern blotting Northern blotting	2.8	Human culture	(Takagi *et al.*, 1994)
		RT-PCR Northern blotting	3.2	Chick culture	(Ban and Rizzolo, 2000)
GLUT2	Retinal Müller cells	RT-PCR Southern blotting	---	Rat	(Watanabe *et al.*, 1994)
GLUT3	Lens - cortical fiber cells	RT-PCR Northern blotting *In situ* hybridization	4.0	Rat	(Merriman-Smith *et al.*, 1999)
	Lens - epithelial cells	Northern blotting Quantitative RT-PCR	4.0	Rat	(Merriman-Smith *et al.*, 2003)
	Retinal endothelial cells	Northern blotting	4.1, 3.2	Human culture	(Knott *et al.*, 1996)
	Retinal microvasculature	Northern blotting Quantitative RT-PCR	---	Rat	(Badr *et al.*, 1999)
	RPE	PCR Southern blotting	---	Human culture	(Takagi *et al.*, 1994)
		RT-PCR	---	Chick culture	(Ban and Rizzolo, 2000)
GLUT5	RPE	PCR Southern blotting	---	Human culture	(Takagi *et al.*, 1994)

Table 4.1 Gene expression of glucose transporters in ocular tissues.

4.1.2 Regulation of glucose transporter gene expression

Growth factors. Several growth factors have been found to be effective in regulating certain glucose transporter gene expression, including platelet-derived growth factor (PDGF), endothelial growth factor (EGF), and IGF-1. PDGF can stabilise GLUT1 mRNA by increasing its half-life by four-fold (Rollins *et al.*, 1988), while EGF upregulated GLUT1 expression by activating the PKC pathway. However, the effect of certain growth factors has been more controversial. Ishida *et al.* (1995) found that GLUT1 mRNA expression was not affected by IGF-1 in bovine cornea, while Masters et al. (1991) found the cells were IGF-1 responsive in their study. Other growth factors such as transforming growth factor-β1 (TGF-β1) have been found to work synergistically with others (e.g. serum, fibroblast growth factor (FGF), PDGF) to increase glucose uptake and GLUT1 gene expression by increasing the level of transcription (Kitagawa *et al.*, 1991). For human RPE cells, EGF caused a significant increase of GLUT1 mRNA expression, but PDGF, IGF-1, and FGF were ineffective (Takagi *et al.*, 1994). However, FGF was effective in upregulating GLUT1 mRNA in rat fibroblasts (Hiraki *et al.*, 1988), while IGF-1 stimulated GLUT1 expression in brain astrocytes (Masters *et al.*, 1991). Further evidence of species variations have also been demonstrated in a carcinoma study, in which the same signaling pathway that upregulates GLUT1 in rodents (Flier *et al.*, 1987) could only upregulate GLUT3 in chick (Wagstaff *et al.*, 1995; Steane *et al.*, 1998). These studies clearly demonstrated inter-species and tissue differences in gene regulation mechanisms, which might be highly dependent on the relevant intracellular signal transduction pathways or cell surface receptor expression.

Transcriptional factors. Nuclear factors Sp1 and Sp3 were found to be important in GLUT3 mRNA regulation, since the former mediated suppression, while the latter resulted in activation of GLUT3 mRNA transcription in mouse neuroblasts and trophoblasts (Rajakumar *et al.*, 1998). In addition, the transcription factor KLF15 was found to mediate regulation of GLUT4 in cardiac muscle tissues by binding to specific DNA response elements (Gray *et al.*, 2002).

Insulin. Short-term insulin therapy in diabetic rats normalises the GLUT1 mRNA level, yet cannot normalise the GLUT1 protein level (Lutz and Pardridge, 1993). *In vivo*, hyperinsulinaemia caused an inhibitory effect on GLUT2 mRNA expression in rat hepatocytes, but it was partially prevented or dominated by the presence of hyperglycemia (Postic *et al.*, 1993). Furthermore, studies of human subjects suggested that insulin was only useful in upregulating the GLUT4 mRNA level in normal subjects and acute stimulation of GLUT4 mRNA seemed to be altered in diabetic patients (Schalin-Jantti *et al.*, 1994). However, it was found useful to regain the normal level of GLUT4 mRNA in insulin-deficient rats in the adipose tissues (Sivitz *et al.*, 1989). Therefore, effect of insulin on GLUT4 mRNA level remains controversial.

Hypoxia or ischemia. Apart from being regulated by growth factors, certain conditional changes can also change the expression pattern of glucose transporter genes. In a rat liver cell line, GLUT1 mRNA expression was found to be upregulated during inhibition of oxidative phosphorylation, which resulted from an increase in gene transcription and a decrease in mRNA degradation (Shetty *et al.*, 1993). Chronic hypoxic exposure stimulated both GLUT1 and GLUT3 gene expression in both gerbil and rat brain (Lee

and Bondy, 1993; Gerhart *et al.*, 1994) such as in microvessels, which resulted in a 60% increase in capillary density of the cerebrum together with an increase in glucose transport capacity of the brain (Shetty *et al.*, 1993). For GLUT3 and GLUT4, hypoxia also induced an increase of mRNA transcriptional levels in fetal rat brain (Royer *et al.*, 2000), which further indicates responsiveness to hypoxia.

Glucose deprivation. Glucose deprivation was found to increase GLUT1 gene expression in brain capillary endothelial cells, via stabilization of its mRNA (Boado and Pardridge, 1993). Such a mechanism, which was previously postulated to be mediated by PKC, was also found to be related to the participation of a cis-acting regulatory element (CAE). The CAE served to increase the GLUT1 mRNA expression during glucose deprivation, as judged by elevation of a GLUT1-luciferase reporter gene and a decrease in the rate of mRNA decay (Boado and Pardridge, 2002). For GLUT4, glucose deprivation caused a decrease in its mRNA in rat adipose and muscle tissues, while the condition was reversible by glucose intake (Sivitz *et al.*, 1989).

Hyperglycemia or glucose toxicity. Elevated glucose levels or simulated diabetic conditions can alter GLUT2 mRNA expression both *in vitro* and *in vivo*. In an *in vivo* diabetic model, a decrease in GLUT2 expression was seen in pancreatic β-cells, but not in cells of the liver, intestine or kidney (Orci *et al.*, 1990; Ohneda *et al.*, 1993). In *in vitro* cell culture, on the other hand, an increase in GLUT2 mRNA expression was seen in response to high glucose exposure (Waeber *et al.*, 1994). In skeletal muscles, GLUT4 mRNA expression was downregulated in hyperglycemia, and only partly reversible with glycemic correction. In the same study, GLUT1 was upregulated directly with glucose

concentration. This revealed incomplete restoration ability of the insulin responsive system, but not in the basal uptake system (Dimitrakoudis *et al.*, 1992).

Toxic agents. Glucose transporter gene expression changes were found after exposure to agents such as cobalt chloride (II) [Co(II)] and cadmium. After 10-12 days exposed to Co(II), an agent that stimulates hypoxia-responsive genes (Watanabe *et al.*, 1996), GLUT1 and GLUT3 mRNA expression in rat retina were increased by 2.48 fold and 1.5 fold, respectively (Badr *et al.*, 1999). This is consistent with previous studies on GLUT mRNA expression in response to hypoxia. Cadmium, a toxic agent that can cause renal glycosuria, induced different or opposite effects on SGLT expression, with both SGLT1 and SGLT2, expression being reduced. The response, however, was dose-dependent for SGLT1, but not for SGLT2. For SGLT3, expression was increased by five-fold in the kidney as a result of cadmium toxicity (Tabatabai *et al.*, 2001). Not only does this imply that SGLT3 is a stress-response gene, it also indicates response variation within the same transporter family.

4.1.3 RT-PCR and related concepts

GenBank Database. The GenBank database is a repository for known nucleotide and protein sequences, and is hosted by the National Center for Biotechnology Information (NCBI). Newly discovered gene sequence must be submitted to Genbank (or its European or Japanese equivalents) as a normal prerequisite to journal publication. GenBank also contains expressed sequence tag (EST) sequences contributed by numerous authors and sequencing centers (Benson *et al.*, 1999; Stoesser *et al.*, 1999).

Polymerase chain reaction (PCR). PCR was invented by Kary Mullis in 1984 with the first description of this method published in 1985, for its use in amplifying Beta-globin sequences in sickle cell anemia (Saiki *et al.*, 1985). This technique allows *in vitro* amplification of a specific region of DNA, which generates numerous copies of DNA that could be used for further purposes e.g. cloning and sequencing.

In general, a basic PCR reaction involves two oligonucleotide primers that flank the template sequence that is to be amplified. After denaturation of the DNA, the primers hybridise to opposite single-strand DNA. The *Taq* Polymerase then proceeds through the region in between the primers, in the presence of deoxynucleotide triphosphates (dNTPs: dATP, dCTP, dGTP and dTTP), for DNA synthesis. The resulting double-stranded DNA acts as new templates for the next thermal cycle. Amplification of the DNA sequence is achieved by repeat cycles of heat denaturation, primer hybridization and sequence extension. This reaction can generate up to 10^5-10^6 fold amplification of the original target DNA after 20-30 successive cycles (Mueller and Young, 2001).

Primer design. A primer is a short oligonucleotide, which is designed to recognise its complementary sequence on a cDNA template. Two PCR primers are used in a molar excess for each PCR reaction, to provide the specificity of the reaction. After the primers anneal to the heat-denatured DNA template strands, two complete complementary sequences (the region to be amplified) are synthesized. The pair of primers for a target sequence should have: similar GC content, such that they possess a similar melting temperature; minimal secondary structure, to prevent self-complementarity, and low complementarity to each other at their 3'ends. In this study, all primers were designed based on the bovine glucose transporter mRNA sequences present in GenBank. Before

primer design, sequences were aligned with all other mammalian glucose transporter sequences retrieved from GenBank to limit the chances of including sequence errors. After a short oligonucleotide was chosen as primer, it was checked against other glucose transport sequences to avoid non-specific hybridization (cross-reactivity) with non-targeted transporters. In this study, the program Clustal W provided by the EMBL-EBI (European Bioinformatic Institute) was used for sequence alignment, since it allows multiple-sequence alignment so that identities, similarities and differences can be seen.

Melting and annealing temperature. The melting temperature (T_m) of a primer is dependent on its constitution of different bases. The T_m can be determined by using the following equation for 20 or less base pairs primer:

[(number of base (A + T) x 2°C) + (number of base (G + C) x 4°C)]

or by using the nearest-neighbour method (Breslauer *et al.*, 1986). The annealing temperature of the PCR reaction is usually chosen to be 3-5°C lower than the T_m.

RNA extraction. Extraction of RNA involves the removal of protein and DNA from samples using organic solvents (e.g. phenol or chloroform containing 4% isoamyl alcohol) and alcohol. Phenol is an oily chemical that is partly miscible with water. In the presence of 20% water, it forms an aqueous solution that contains phenol micelles surrounded by water molecules. Proteins, which are mainly hydrophobic molecules, can partly dissolve in this organic solvent. When mixing equal volumes of phenol and aqueous protein samples, most of the phenol molecules tend to dissolve in the hydrophobic core of protein. The protein then swells and denatures. Denatured proteins gather more micelles of phenol and dissolve more readily in the phenol phase as a result

of their stronger hydrophobic bonding. The use of both chloroform and phenol helps to unfold proteins and to expose the hydrophobic regions so they can bind more readily to phenol micelles. Thus, proteins can be completely denatured and removed by repeated phenol-chloroform extraction. Since nucleic acids are hydrophilic and highly soluble in water, they stay in the aqueous phase. They can be precipitated with high-salt in the presence of alcohol (i.e. ethanol or isopropanol). In this study, TRI reagent (Sigma-Aldrich Co. Ltd., Dorset) was used for the RNA extraction. It is a mono-phase solution of phenol, guanidine thiocyanate, buffer and solubilizing agents. Guanidine thiocyanate is an effective reagent that inhibits ribonuclease (RNase) activity (Chomczynski and Sacchi, 1987) by denaturing all cellular proteins, including RNase (Chan, 1992).

RNA or DNA quantification. The nucleic acid concentration of a sample can be determined by using spectrophotometry. One unit absorbance at 260 nm corresponds to approximately 50 μg/ml and 44 μg/ml of double-strand DNA and single stranded RNA, respectively. Resonance structures of pyrimidine and purines bases are responsible for the absorbance, while it is also affected by the amount of base ionization and the sample pH (Wilfinger *et al.*, 1997). The absorbance at 260 nm (A_{260}) and 280 nm (A_{280}) can be used as a ratio (A_{260}/A_{280} ratio) for sample purity estimation. In general, pure preparation of DNA and RNA have ratios of 1.8 or 2.0, respectively (Chan, 1992). If ratio is less than the suggested values, it indicates that the samples are contaminated with protein or phenol, which would affect the concentration calculation. Under these circumstances, RNA extraction should be repeated.

RNA integrity. Cellular RNA is mainly comprised of ribosomal (rRNA). Messenger RNA (mRNA) constitutes only a small portion of the total RNA (2-5% of RNA). Through electrophoresis in a 1% formaldehyde agarose gel, good quality RNA should reveal 2 major bands, corresponding to ribosomal units 28S and 18S, or sometimes 3 bands (including the minor 5.8S unit), with the intensity of 28S band double that of 18S. In other words, good quality RNA would show 2 or 3 bright bands against a faint smear of mRNA.

Agarose gel electrophoresis can be used to separate RNA and double-stranded DNA fragments according to their molecular weight. The agarose gel is a complex network of pores, which allows RNA or DNA molecules to travel according to their molecular sizes. Gels can be stained with ethidium bromide after electrophoresis, allowing bands to be visualised. Molecular weight estimation can be done by comparison of a band in a sample lane with a series of molecular weight marker bands.

Reverse Transcription (RT). PCR requires a DNA template for amplification (RNA is a poor substrate). Thus, to facilitate PCR, RNA is reverse-transcribed into complementary-DNA (cDNA), using the enzyme reverse transciptase. This enzyme syntheses a cDNA template by polymerization of dNTPs using the RNA as template. Reverse transcriptase adds nucleotides starting from the 3'end, by making use of a pre-existing primer base paired to the template. As almost all eukaryotic mRNAs possess a string of 50-250 adenine residues at their 3' end, a short string of thymidine (oligo-dT) bases targeted to this poly(A) tail makes a good primer for RT.

HotStar Taq Polymerase. The *Taq* DNA polymerase from the thermophilic bacterium *Thermus aquaticus* was first introduced in 1988 (Saiki *et al.*, 1988). HotStar *Taq* Polymerase, a modified form of the recombinant 94 kDa *Taq* DNA Polymerase, is inactive at ambient temperature, which prevents mis-priming during the initial denaturation step of PCR (Chou *et al.*, 1992). It is activated at 95°C, by means of an extended incubation during this initial denaturation phase.

DNA Sequencing. In general, DNA sequencing employs a "chain termination method", which involves the synthesis of a single-stranded DNA template in the presence of limiting amounts of 2',3'-dideoxynucleotides (ddNTPs). In practice, a primer which is annealed close to the sequence is used to initiate the synthesis in the presence of Klenow fragment of DNA polymerase and the four deoxy-nucleoside 5'-triphosphates (dNTPs). Fluorescent tags are attached to the chain-terminating nucleotides, with each of the four ddNTPs carrying a different fluorophore. When the ddNTP attaches to the chain, the chain can no longer be extended. The resulting DNA fragments can be run on a high-resolution gel, at the bottom of which is a detector, which scans for the fluorescent tags.

4.1.4 Available methods for gene expression study

In situ hybridization, northern blotting and RNase-protection assays are common methods used in RNA expression studies. This section will briefly describe each method and compare their strengths and weaknesses to each other, and to RT-PCR.

In situ hybridization (ISH). It is a technique developed to localise nucleic acid in cells or tissues and was firstly introduced by Paradue and Gall in 1969 (Gall and Pardue, 1969).

A nucleic acid probe is used in the same way as labeled antibodies, to hybridise with the *in situ* nucleic acid of interest and generate a signal. It provides additional information compared to samples extracted using homogenization. The use of ISH in RNA expression studies was firstly introduced by Harrison *et al.* in 1974, who used a DNA probe for RNA detection in liver (Harrison *et al.*, 1974). Later in 1984, Cox *et al.* (Cox *et al.*, 1984) designed an RNA probe for embryonic RNA detection. In general, tissues are gently fixed with the RNA exposed at its original position. The probe and target hybridise and generate a pattern of gene expression in the tissue. This allows insights on differential gene expression in cell compartments that help in explaining functional differences between cells (Alberts *et al.*, 2002).

Northern blotting. A technique named with regard to Southern blotting (which itself was named after its inventor, Edwin Southern), Northern blotting is used to detect and quantify a particular RNA sequence in a complex RNA mixture. Total cellular RNAs are denatured by reagents such as formaldehyde to assure a linear conformation of the RNA molecules by breaking hydrogen bonds between base pairs. The individual RNA molecules are then separated by gel electrophoresis according to their size, and transferred onto nitrocellulose or nylon membranes and exposed to a labeled single stranded-nucleic acid probe. The labeled probe used can be purified RNA, cDNA or a cloned fragment of genomic DNA and acts similarly to antibodies at this point (Darbre, 1999). The size of the targeted RNA molecule can be determined by reference to known RNA standards. With this method, one can get an estimation on the molecular weight as well as comparing the amount (quantity) of the RNA of interest in different samples.

RNase protection Assay. In this method, hybridization is carried out directly in cell lysates, which precludes the need for membrane transfer from gels (Bildin *et al.*, 2001). In general, it involves the hybridization of mRNA with a single stranded RNA or DNA probe in solution. Excess probe and imperfect duplexes are digested by single-strand specific nucleases. The RNA-DNA or RNA-RNA hybrids are finally analyzed by gel electrophoresis (Raval, 1994).

4.1.4.1 Comparison of RT-PCR with other methods

The major advantage of PCR is its sensitivity. In particular, a sample size as small as one single cell can be used as the starting template. It has much higher in sensitivity than Northern blotting and RNase protection assays and can detect copy number in the attomolar (10^{-21}M) range (Miller *et al.*, 1997). In addition, RT of mRNA for RT-PCR can be used to stabilise sample material for long periods. Therefore, RT-PCR is the optimal method in most screening applications, especially in the situation when sample supply is limited.

For questions concerning the level or regulation of mRNA expression, standard RT-PCR alone is inadequate to provide the necessary answers. Quantification of expression can be done by Northern blotting, RNase protection assay or quantitative RT-PCR (Ji *et al.*, 1990; Jindal *et al.*, 1995). Although northern blotting is labour intensive and requires significant amount of starting RNA, it has the advantage that once produced, membrane can be stripped and reprobed many times. The RNase protection assay technique allows multiple transcripts to be screened simultaneously, but the use of high doses of radioactivity is a disadvantage. Among all, only ISH provides resolution at the cellular level, regarding the site of gene expression.

Glucose transporter gene expression in the CBE

Since information about glucose transporter gene expression in CBE is not yet available, a method that can be used for quick screening was desirable. Thus, RT-PCR is very suitable to be used in this study for it provides a rapid way to determine the presence of certain genes, especially in the case of limited sample quantity.

4.2 Methodology

4.2.1 Basic principles

In this study, RNA samples were taken from bovine CBE, and kidney, which were then reverse transcribed into cDNA templates. For each gene whose expression was investigated, a pair of gene-specific primers was designed and tested to ensure successful amplification of mRNA from the "positive control tissue" (kidney). RT-PCR was then carried out on RNA from bovine CBE. PCR products were purified and sent for sequencing for confirmation of amplification specificity.

4.2.2 Tissue preparation

Dissection instruments were baked at 200°C overnight to destroy any contaminating RNase activity. Fresh tissues were obtained from the abattoir and immediately dissected as described in the following sections:

4.2.2.1 Ciliary processes/ pars plicata

Eyes were positioned with the cornea facing upwards (Fig. 4.1a). One corner of the cornea (adjacent to the limbal region) was cut with an RNase-free razor blade. The whole cornea was carefully trimmed off (Fig. 4.1b) with RNase-free scissors started at the cut corner, leaving the underlying structures including the lens (Fig. 4.1c) and ciliary processes exposed (Fig. 4.1d). The ciliary processes' tissues were carefully torn off with RNase-free forceps and submerged in RNA*later* (Ambion European Ltd., Cambridgeshire, UK). This agent is used to preserve RNA quality (Gong *et al.*, 2001). Upon arrival in the laboratory, tissues were immediately frozen in liquid nitrogen and stored at -80°C.

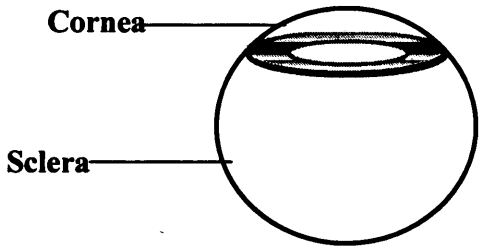

a) Eyes were positioned upwards.

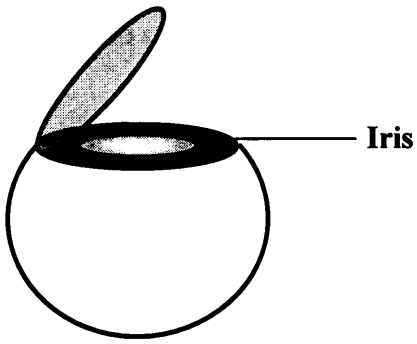

b) The whole cornea was trimmed off.

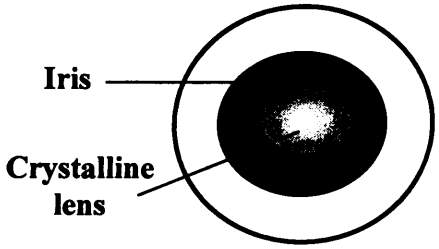

c) The iris was exposed after the removal of cornea (top view).

d) The ciliary processes were exposed after the removal of iris (top view). Forceps can be used to tear off the tissues at this stage.

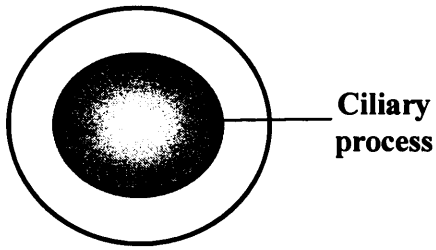

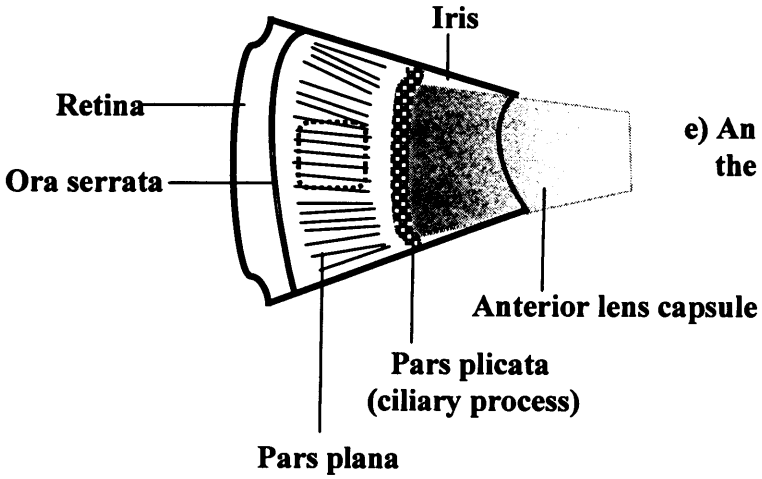

e) An area of pars plana was cut from the whole CBE (back view).

Fig 4.1 Dissection of tissues from bovine eyes.

4.2.2.2 CBE pars plana

The CBE was isolated as described in section 2.2.3. A 0.5cm x 0.5cm area of pars plana tissue was cut from the whole CBE pars plana (Fig. 4.1e) with a sterile scalpel. The tissue was submerged in RNA*later*, frozen immediately in liquid nitrogen and stored at -80°C.

4.2.2.3 Bovine kidney

Two methods were used for the isolation of bovine kidney samples. In the first approach, tissues were dissected in the laboratory, frozen in liquid nitrogen and stored at -80°C. Briefly, a sterile scalpel was used to remove the outer cortex. A new scalpel was then used to cut 0.5cm x 0.5cm pieces of tissue from the inner cortex of kidney. Tissues were frozen in liquid nitrogen and stored at -80°C for later use. For the second method, small pieces of kidney tissues were transferred to RNA*later* at the abattoir, similar to the protocol for ciliary body tissue as described in sections 4.2.2.1 and 4.2.2.2. They were frozen in liquid nitrogen and stored at -80°C on arrival at the laboratory.

4.2.3 RNA extraction

Frozen tissues were powdered at liquid nitrogen temperature using a dismembrator (Mikro-Dismembrator U, B. Braun Biotech International) at 1600 rpm for 2 mins. The isolation of RNA was performed using TRI reagent (Sigma-Aldrich Co. Ltd., Dorset). Dismembrated samples were mixed with 100 µl TRI reagent at 1600 rpm for 2 mins. An 800 µl aliquot of TRI reagent was further mixed with samples at 1600 rpm for 5 mins. Solubilised samples were transferred into a sterile Eppendorf tube. The dismembrator tissue container was finally washed with 100 µl TRI reagent at 1600 rpm for 30 seconds with the washed sample also transferred into the same Eppendorf tube. Lysed samples

were centrifuged at 13,500 x g for 5 mins at room temperature to pellet any insoluble material. Supernatants were transferred to fresh Eppendorf tubes containing an aliquot of silicon grease, and mixed with 200 µl chloroform by vortexing for 1 min. They were left to stand for 10 mins at room temperature before centrifugation at 13,500 x g for 10 mins. After centrifugation, an interface was formed by the silicon grease with a clear upper aqueous phase containing RNA, and a lower phase containing the phenol-chloroform and proteins. The upper aqueous phase was carefully transferred to a fresh Eppendorf tube. It was mixed with 500 µl isopropanol by vortexing and was allowed to stand at -20°C for 15 mins. Centrifugation at 13,500 x g at room temperature was performed again for 10 mins. The supernatant was discarded and the RNA pellet was washed with 1 ml ice-cold 70% ethanol. The mixture was centrifuged at 13,500 x g again for 2 mins and the ethanol was removed. The pellet was partially air-dry by standing at room temperature for 5 mins. To dissolve the pellet, 51 µl sterilised water was added and incubated for 10 mins at 37°C with periodical mixing. DNase treatment was carried out by adding 6 µl 10X DNase reaction buffer, 1 µl RNase OUT, 2 µl DNase I, which was thoroughly mixed with the samples. The DNase reaction mix was incubated at 37°C for one hour. This step was designed to degrade residual DNA that had co-purified with the RNA.

4.2.3.1 Pigment removal from RNA preparations

CBE is enriched with melanin, a pigment which gives the tissues a distinct brownish colour. Melanin, which co-purifies with RNA, is known to inhibit RT as well as PCR reactions (Giambernardi *et al.*, 1998). In this study, the RNAeasy mini kit (Qiagen Ltd., West Sussex, UK) was employed to remove the pigment from the samples (following the manufacturer's instructions). It is kit consisted of filtered-type column which samples can

pass through the sieve-like membrane easily but not the pigment molecules. Kidney samples, as the positive control, were also treated using the same method to ensure experimental consistency. The final RNA sample was eluted in 100 µl RNase-free water. Samples were quantified with a GeneQuant instrument for absorbance at 260 nm, 280 nm and 320 nm. The typical yield of total RNA was ~30 µg for CBE and ~60 µg for kidney tissues.

4.2.3.2 RNA integrity

After extraction, 2 µg of each RNA sample was analyzed by agarose gel electrophoresis. The gel mixture was made by dissolving 1 g agarose in 100 ml 1x MOPS buffer (20 mM MOPS, 8 mM sodium acetate, 2 mM EDTA, pH 7.0). After complete dissolution and de-gasing of the gel mixture, it was allowed to cool to 55°C at room temperature. Formaldehyde was added to a final concentration of 0.7M shortly before the pouring of the mixture into the gel tray.

Before sample loading, 6 µl volume RNA samples were mixed with 14 µl loading buffer (10 µl 20X MOPS; 70 µl 37% Formaldehyde; 200 µl 100% Formamide; 10 µl Ficoll-EDTA). Samples were denatured by heat at 55°C for 15 mins before loading onto the gel. Electrophoresis was carried out at 80 V for 80 mins and the gel was stained with 1X SYBR-GOLD (Molecular Probes, Inc., Eugene, USA) for 20 mins. The gel was examined using a dual-intensity transilluminator (UVP, USA) and photo-documented with a DS34 Direct screen instant camera (Polaroid, UK). Only samples showing high quality rRNA bands were used in the subsequent experiments.

4.2.4 Reverse transcription (RT)

RNA samples were transcribed into cDNA as follows. Initially, samples (5 μg) were mixed with 0.5 μg Oligo $(dT)_{12-18}$, 0.7 mM dNTP mix in water in a final volume of 13 μl, and overlaid with 20 μl of RNase-free mineral oil to prevent evaporation. Samples were then heated at 65°C for 5 mins and cooled to 4°C for 5 mins. Then, 7 μl master mix was added to each sample to give a final concentration of 1X First Strand Buffer; 5 mM DTT; 2U RNase OUT; 10U SuperScript III RT (Invitrogen life technologies, USA). Mixtures were heated at 50°C for another 60 mins. After incubation, mineral oil was removed from all samples and QIAQuick Purification (Qiagen Ltd., West Sussex, UK) was performed. Samples were eluted in 100 μl 10 mM Tris-HCl buffer (pH 8.0). The efficiency of RT is around 30%, which meant the total yield of cDNA samples was expected to be ~1.5μg.

4.2.5 Polymerase chain reaction (PCR)

4.2.5.1 Primer design

In the design of primers, an mRNA sequence search was performed in the GenBank database (http://www.ncbi.nlm.nih.gov). Bovine sequences were the prioritised choices to retrieve (Table 4.2), while other mammalian glucose transporters sequences were also retrieved to ensure the identity of bovine sequences in Clustal alignments. Primers were designed from the bovine mRNA sequences according to the following criteria: i) length of 18-25 base pairs (bp); ii) percentage of GC composition ranged from 50% to 60%; iii) T_m range of 60°C to 75°C, calculated according to Breslauer et al. (1986); iv) beginning with one to two G or C nucleotides and ending with one to three A or T nucleotides; v) avoid stretches of four or more identical bases; vi) prevent self-complementarity, since formation of secondary structure would hinder normal PCR reaction.

Glucose transporter	Sequence used for primer design (GenBank accession number)	Full (F) or partial (P) sequence	Length in base pair (bp)
GLUT1	NM_174602	F	2533
GLUT2	AF308828	P	427
GLUT3	NM_174603	P	1793
GLUT4	D63150	F	2642
GLUT5	AF308830	P	617
SGLT1	AF508807	F	2248
SGLT2	AY208941	F	2275
SGLT2-like bovine EST*	AV605490	---	553

Table 4.2 Bovine mRNA sequences used for primer design.

Clustal alignments (http://www.ebi.ac.uk/clustalw/) were performed for all mammalian glucose transporter mRNA sequences retrieved in order to check for mis-specification. Some sequences for SGLT2 were found to be mis-specified (Appendix I).

* Before the bovine SGLT2 sequence was published in early 2004, a bovine EST sequence was found in GenBank, which aligned well at certain regions with other mammalian SGLT sequences (Appendix II). A pair of primers was designed based on this sequence.

In general, 2 sets of primers were designed for each glucose transporter member with the better performing set chosen depending on the PCR results. The optimised primers used in this study are summarised in Table 4.3.

Glucose Transporter	Primer sequence 5'-3'	GC content (%)	T_m (°C)	T_A* (°C)	Product size (bp)
GLUT1-UP	CACCAGCTAGGCATCGTCGT	60.0	68.7	64	548
GLUT1-DN	GATGGTCATGAGCACTGCACA	52.4	68.8		
GLUT2-UP	CAGCTCTTCACCAATGCCA	52.6	66.4	62	296
GLUT2-DN	CTCAGGAGCACAAGTCCCA	57.9	65.4		
GLUT3-UP	CCAGTTTGGCTACAACACTGGA	50.0	67.1	63	532
GLUT3-DN	GCACTGGATGATGGCTGGT	57.9	67.6		
GLUT4-UP	CCATCTTGATGACTGTGGCT	50.0	63.9	63	621
GLUT4-DN	CCACTGCTAACCACAACACA	50.0	63.4		
GLUT5-UP	GCTTCATCTCCGTGCTGA	55.6	64.1	59	495
GLUT5-DN	CAGTGAAGTTGGAGAGCCAGT	52.4	64.5		
SGLT1-UP	GGTATGGTGCCTTCGTGA	55.6	63.4	59	678
SGLT1-DN	GGTGGTCCCAAGTAACTGGT	55.0	63.7		
SGLT2-UP	CCATCCTGCTCTTCGTCTGCT	57.1	69.1	64	460
SGLT2-DN	ACTGCATTGGACACCCTGAGC	57.1	69.9		
SGLT2-like-UP	GCACTGATGTACACGGACA	52.6	62.0	58	151
SGLT2-like-DN	TGACGGTATCCGAGGATC	55.6	62.2		

Table 4.3 Primers used for PCR in this study. *T_A is the annealing temperature.

4.2.5.2 Positive and negative controls

Bovine kidney was used as the positive control in this study as the literature suggested that kidney expressed all of the GLUT and SGLT transporters examined.

"Mock" RT reactions were performed as negative controls. In mock RT, the enzyme (i.e.Super Script III RT) was substituted by water, while other reagents and experimental procedures remained the same. Under such conditions, cDNA template from the desired mRNA would not be formed. Thus, any positive PCR results from these mock samples would reveal the presence of genomic DNA contamination. This enabled the

identification of false positive PCR reactions by comparison of the PCR results between the normal and mock samples.

Positive controls (i.e. kidney cDNA template) and negative controls (i.e. mock kidney, CE samples) were used along with the CBE cDNA templates in every PCR experiment.

4.2.5.3 Experimental optimization

Optimization of RT-PCR was carried out by using the bovine kidney samples. Unsatisfactory PCR results e.g. faint or no bands, heavy primer dimers or positive results on mock samples were optimised by testing different annealing temperatures, use of Q-solution (HotStar *Taq* DNA Polymerase Kit, QIAGEN Ltd.) and trials of different sample concentrations. Continual failure in optimization necessitated the redesign of primer sets. In this study, the problems encountered were solved by varying the annealing temperature (i.e. GLUT4) or re-design of primers (i.e. GLUT2, GLUT3 and SGLT2).

4.2.5.4 PCR protocol

Two microlitres (~ 0.03 μg) of cDNA templates was mixed with an 18 μl PCR reaction master mix (1X PCR Buffer (QIAGEN Ltd., West Sussex, UK), 0.2 mM dNTPs, 1 μM upstream-primer, 1 μM downstream-primer and 1U of Hotstar *Tag* DNA Polymerase (QIAGEN Ltd., West Sussex, UK)). The mixtures were overlaid with 20 μl mineral oil to prevent evaporation. PCR was performed in a Techne Progene PCR machine. Initially, mixtures were heated at 95°C for 15 mins to activate the polymerase. A profile of 35 cycles, comprising heating at 94°C for 1 min for cDNA denaturation, an annealing phase at a temperature set according to the primer's T_m for 1 min and finally an extension phase

of 72°C heating for 1 min. An additional heating phase (72°C for 5 mins) was performed after the 35 cycles to allow any remaining sequence polymerization to complete.

4.2.6 Gel electrophoresis

PCR products were separated on 2% agarose gels for product size determination. In general, 5 μl of loading buffer (15% Ficoll 400, 10 mM EDTA, 0.13% xylene cyanol FF) was added to 20 μl of PCR product and mixed. Ten microlitres of each sample were loaded onto the gel for electrophoresis (80 V for 80 mins). Gels were stained with ethidium bromide (0.5 mM) for 30 mins and de-stained in distilled water. Some gels were stained with SYBR gold dye (0.1 mM), a more sensitive gel stain to ensure negative findings (see section 4.3.1.). Gels were examined by the transilluminator and photo-documented by using the Polaroid DS34 camera.

4.2.7 Sequencing

4.2.7.1 PCR products preparation

Samples were amplified by PCR as described in the previous section. Five replicate PCR samples were pooled together to give a total volume of 100 μl and purified using the QIAquick kit (Qiagen Ltd.) to remove residual primers and dNTPs. The PCR products were eluted in a volume of 180 μl of 2 mM Tris-HCL (pH 8.0). Two microlitres of glycogen (2 μg /μl) and 20 μl of 3M sodium acetate solution were added to the 180 μl eluant. After mixing and centrifugation, 200 μl of phenol-chloroform was added. The samples were mixed thoroughly for 1 min and centrifuged at 13,000 rpm for 2 mins. The supernatant was transferred into new tube and 400 μl of ethanol was added. The mixture was thoroughly mixed again before it was left to stand at -20°C for 20 mins.

Centrifugation was carried out at 14,000 rpm for 10 mins and the supernatant was discarded. One milliliter of ice-cold 70% ethanol was added to the pellet and the sample was centrifuged again at 14,000 rpm for 2 mins. The supernatant was discarded again and the pellet left to air-dry for 5 mins. The pellet was re-dissolved in 20 µl water. The GeneQuant instrument was used to measure the absorbance at 260 nm (see section 4.2.3.2) and samples were diluted to a final concentration of 25 ng/µl. Ten microliters of each sample was sent to the Cardiff University Sequencing Facility using the ABI Prism 3100 genetic analyzer (Applied Biosystems).

4.2.7.2 Sequencing results verification

All sequences were viewed using the CHROMAS program (Technelysium Pty Ltd, Australia) and exported as a text file. The identity of DNA sequences was examined by BLAST searches against the GenBank non-redundant database (http://www.ncbi.nlm.nih.gov/BLAST/).

4.3 Results

4.3.1 RT-PCR

Polymerase chain reaction products were run on a 2% agarose gel and stained with ethidium bromide (0.5mM). (For GLUT2 and SGLT2, gels were stained with SYBR gold dye in one of the repeated experiment to confirm the presence of positive finding in the positive control only, and rule out the possibility that a very faint band was missed when only using the ethidium bromide). Experimental optimization was done when non-specific bands were visible. Table 4.4 summarises the results using RT-PCR.

Glucose transporter	Kidney	Pars Plicata	Pars Plana
GLUT1	✓	✓	✓
GLUT2	✓	×	×
GLUT3	✓	✓	✓
GLUT4	✓	✓	✓
GLUT5	✓	✓	✓
SGLT1	✓	×	×
SGLT2	✓	✓	✓
SGLT2-like	✓	×	✓

Table 4.4 The RT-PCR results for bovine kidney, pars plicata and pars plana of CBE. ✓: positive RT-PCR result; ×: negative RT-PCR result

4.3.1.1 GLUTs

As seen in fig 4.2a, positive results were found for GLUT1 in both pars plana and pars plicata with an expected size of 548 base pair (bp) (n = 3). For GLUT2, only kidney samples gave a positive control result of 296bp but not pars plicata and pars plana (Fig. 4.2b; n = 4). Figs. 4.2c, 4.2d and 4.2e show the RT-PCR results for GLUT3, GLUT4 and GLUT5, respectively. Their mRNAs were found to be expressed in both pars plicata and pars plana with expected sizes of 532bp (n = 3), 621bp (n = 3) and 495bp (n = 3) respectively.

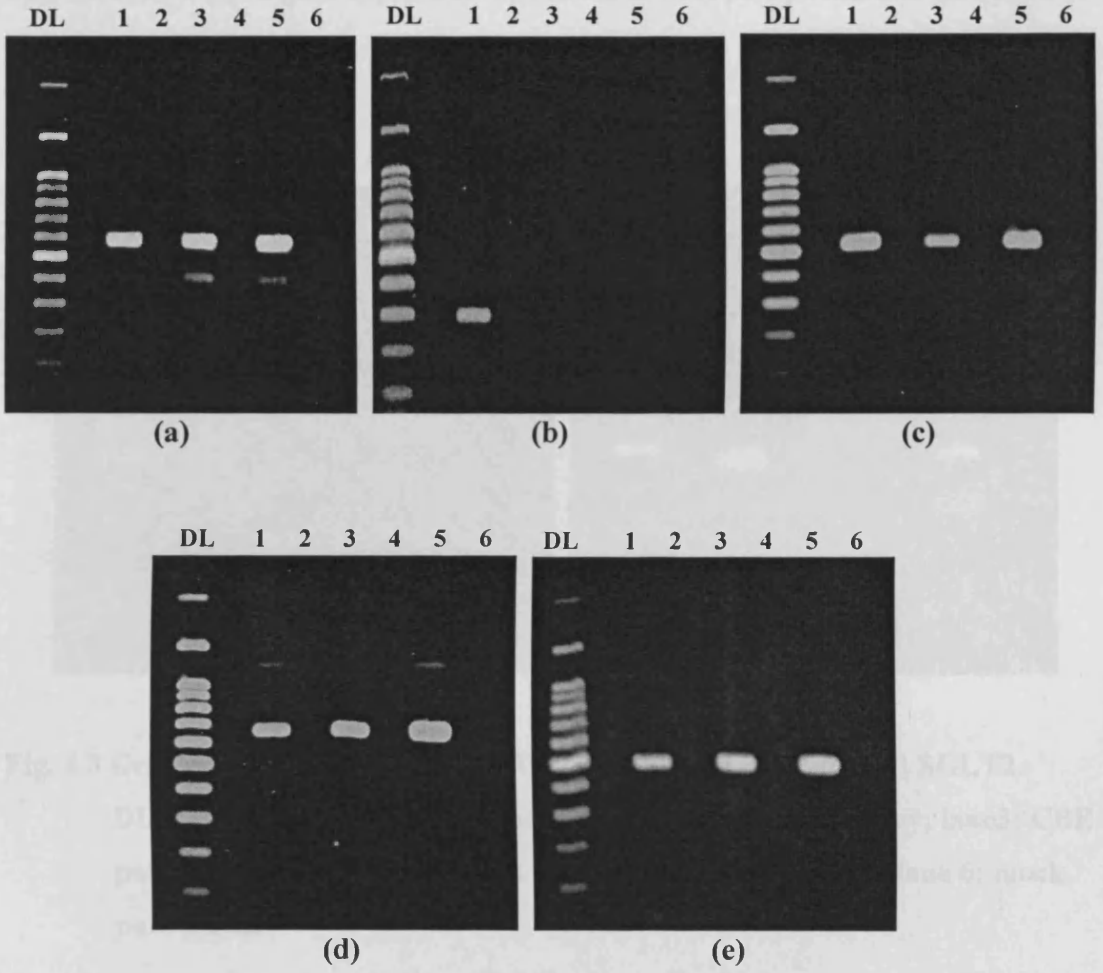

Fig. 4.2 Representative gel electrophoresis results of RT-PCR for (a) GLUT1; (b) GLUT2; (c) GLUT3; (d) GLUT4; (e) GLUT5. DL: DNA ladder; lane 1: bovine kidney; lane 2: mock kidney; lane3: CBE pars plicata; lane 4: mock pars plicata; lane 5: pars plana; lane 6: mock pars plana.

4.3.1.2 SGLTs

There was no SGLT1 mRNA expressed in either pars plicata or pars plana (Fig. 4.3a; n = 3). However, SGLT2 gene expression was found in both pars plicata and pars plana (Fig. 4.3b; n = 4).

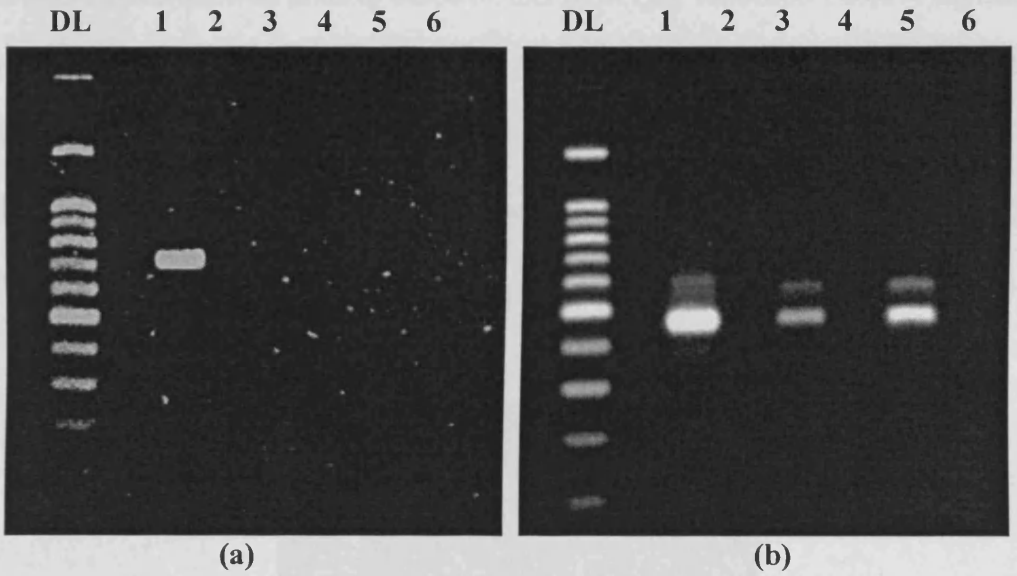

Fig. 4.3 Gel electrophoresis result of RT-PCR for (a) SGLT1 and (b) SGLT2. DL: DNA ladder; lane 1: bovine kidney; lane 2: mock kidney; lane3: CBE pars plicata; lane 4: mock pars plicata; lane 5: pars plana; lane 6: mock pars plana.

4.3.1.3 Presence of SGLT2-like mRNA in the pars plicata

The investigation of glucose transporter mRNA expression was started before the publication of the bovine SGLT2 mRNA sequence in GenBank. A bovine EST sequence was found at this time, which aligned well with other SGLT2 mRNA sequences and RT-PCR was carried out with primers based on this short EST sequence. Positive signals were detected in both kidney and pars plana (Fig 4.4). Its sequencing result produced the highest hit against human SGLT2 sequences (prior to the appearance of the bovine SGLT2 sequence in GenBank –the highest score was against the bovine SGLT2 mRNA sequence once this was available).

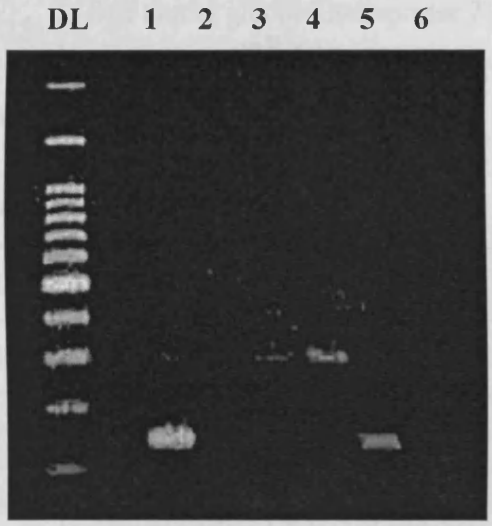

Fig. 4.4 Gel electrophoresis result of the RT-PCR based on the bovine SGLT2-like EST. DL: DNA ladder, lane 1: bovine kidney; lane 2: mock kidney; lane 3: CBE pars plicata; lane 4: mock pars plicata; lane 5: pars plana; lane 6: mock pars plana.

4.3.2 Sequencing

The PCR products for GLUT1-5 and SGLT1-2 were sent for automated sequencing. Sequenced details are attached in Appendix III. Their identities were confirmed by BLAST searches against the GenBank database. Table 4.5 summarises the BLAST search results, with the alignment scores.

PCR sequence	BLAST search alignment results			
	Accession number	Identification	Score*	Nucleotide Identity (%)
GLUT1	NM_174602	Bos taurus solute carrier family 2 (facilitated glucose transporter), member 1 (SLC2A1), mRNA	1019	100
GLUT2	AF308828	Bos taurus glucose transporter 2 mRNA	333	98
GLUT3	NM_174603	Bos taurus solute carrier family 2 (facilitated glucose transporter), member 3 (SLC2A3), mRNA	779	99
GLUT4	D63150	Bos taurus mRNA for glucose transporter type4	872	98
GLUT5	AF308830	Bos taurus fructose transporter Glut5 mRNA	898	99
SGLT1	AF508807	Bos taurus Na+/glucose cotransporter (SGLT1) mRNA	1225	99
SGLT2	AY208941	Bos taurus Na+/glucose cotransporter (SGLT2) mRNA	783	100
SGLT2-like	AY208941	Bos taurus Na+/glucose cotransporter (SGLT2) mRNA	210	100

Table 4.5 BLAST search results for RT-PCR sequences. * The score is calculated by adding all similarities (+1) and differences (-3) between each nucleotide in an alignment.

All BLAST search results demonstrated the best alignment with the respective target mRNA sequence. All the RT-PCR sequences shared 98 to 100% identity to their target sequences. This revealed a highly confident conclusion that all PCR products were derived from the desired mRNA sequences.

4.4 Discussion

4.4.1 Sequence similarity

As mentioned before, all bovine sequences retrieved from GenBank were aligned with all other mammalian glucose transporter mRNA sequences to assess their similarity. In this study, all bovine sequences aligned well with their orthologues in other mammalian groups, which facilitated primer design. However, some sequences previously labeled as SGLT2 or low affinity sodium glucose transporter were found to align better with SGLT3 instead (Appendix I). This might have been due to the period these sequences were submitted (around year 2000), when only the SGLT1 mRNA sequence was well-established for different species. Therefore, all other similar sequences submitted to GenBank were probably named SGLT2.

For the bovine SGLT2-like EST sequence, it was interesting to see how alike it was when clustered against other mammalian SGLT2 sequences (Appendix II). However, when compared with the true bovine SGLT2 mRNA, the similarity score was only 40. These 2 sequences aligned very well at the 3' end of the EST sequence, but poorly at the 5' end (Appendix IV). As shown in appendix IV, the primers designed according to the bovine SGLT2-like EST sequence lay at the 5'end of the true bovine SGLT2 mRNA sequence, where they showed complete identity. This might explain why positive results were only seen on kidney and pars plana samples with the SGLT2-like EST primers. In this study, Oligo (dT) primer was used to synthesize cDNA strands. This method tends to over-represent the 3'end of transcripts, therefore, maximum sensitivity of the cDNA pool will lie with the 3' ends. In this study, primers for the SGLT2-like EST were designed at the 5' end region of the true SGLT2 mRNA sequence. With these primers, gene expression appeared most abundant in kidney, then pars plana and least in the pars plicata. It is

possible that there was incomplete copying of the 5' end of the SGLT2 mRNA in the pars plicata samples, for effective PCR amplification. Later, with primers designed at the 3'end of the complete bovine SGLT2 sequence, the complementary sequences would be much better amplified, since the RT method provides the highest sensitivity at the 3'end. The observation of a stronger intensity band (with SGLT2 primers) for both kidney and pars plana samples might therefore be due to a combination of amplification from both the complete bovine SGLT2 and the SGLT2-like EST mRNA in the samples. Nevertheless, the presence of SGLT2 in all samples is distinctive. Sadly, there was insufficient time to study the SGLT2-like mRNA in further detail.

4.4.1.1 Alternative splicing

In the RT-PCR reaction for SGLT2, a consistent pattern of double bands was seen with the expected band showing the higher intensity. Such a pattern was conserved across a wide range of PCR annealing temperature (63-68°C), which meant the chance of non-specific binding resulting in the formation of the minor band was low. This additional band might be explained by alternative splicing, a process in which different mRNAs are generated by varying the pattern of pre-mRNA splicing. Thus, various mRNAs are produced from the same gene and then the mRNAs are templates for different protein isoforms. Alternative splicing of GLUT14 has been reported in testis (Wu and Freeze, 2002), but other transporter isoforms have no similar report at the present stage. Alternate splicing has been reported to happen in different cell types (Larkin and Park, 1999; Nixon *et al.*, 1999; Omer *et al.*, 2002), yet no direct relationship has been established for particular abnormalities or disease.

To further characterise the splicing pattern for SGLT2 in this study, exon-specific primers could be used to identify the extra amplification products, or direct sequencing for the RT-PCR product (band) purified out from the gel would be another option.

4.4.2 mRNA expression of glucose transporters in the CBE

As revealed in this study, more than one glucose transporter transcript was present in the bovine CBE. The pars plicata and pars plana showed no particular difference in their gene expression profile, but the pars plana seemed to have a higher mRNA expression level overall. This was especially obvious for GLUT3 (Fig 4.2c) and SGLT2 (fig 4.3b). However, as discussed in section 4.1.4.1, RT-PCR is not the best method in assessing gene expression level, since there is a need for stringent standardization (Muller and Kennedy, 1996) throughout the whole procedure (i.e. proper control for RT, amplification and normalization). Thus, simply assessing the staining intensity visually is not sufficient to infer accurate quantitative differences. In the past, researchers have combined RT-PCR with different methods to make quantitative conclusion. These include the use of enzyme-linked immunosorbent assay (ELISA) (Alard *et al.*, 1993; Sabbatini *et al.*, 1993) or Southern blotting (Thompson *et al.*, 1992; Doi *et al.*, 1994). Nowadays, real-time quantitative RT-PCR, Northern blotting and RNase protection assay would be a better choice for accurate mRNA expression quantification. Since the aim of this study was simply to screen for the presence of the different glucose transporters in the bovine CBE, the use of RT-PCR was appropriate to fulfil this goal.

4.4.3 Role of glucose transporters in the CBE

Glucose is crucial for every single cell for metabolism and energy supply. Glucose transporters in the CBE, therefore, are essential for local and also anterior avascular tissue glucose supply. As revealed in this study, the bovine CBE possessed GLUT1, GLUT3, GLUT4, GLUT5 and SGLT2 mRNA. It again shows that one kind of tissue carries more than one glucose transporter isoform. Other examples can be found in bovine skeletal muscle that it has both GLUT3 and GLUT4 mRNA (Zhao *et al.*, 1993); rat placenta, which possessed GLUT1 and GLUT3 mRNA (Boileau *et al.*, 1995); or rat alveolar cells have GLUT1, GLUT4, GLUT5 and SGLT1 mRNA (Mamchaoui *et al.*, 2002).

For GLUT1 and GLUT3 mRNAs, their presence were not surprising since they are present in many blood-tissue barriers, such as the BBB (Boado and Pardridge, 1990; Nagamatsu *et al.*, 1992; Gerhart *et al.*, 1994), BPB (Zhou and Bondy, 1993; Takata *et al.*, 1994) and BRB (Knott *et al.*, 1996). However, GLUT1 is the glucose transporter isoform that is generally recognised to be abundantly expressed in cells with occluding junctions. This protein has been found colocalised with occludin and ZO-1 (i.e. a 210-225 kDa cytoplasmic protein), which are tight junction constituents and absent in non-barrier cells (Tserentsoodol *et al.*, 1998). With its colocalisation with connexin 43, a gap junction protein (Shin *et al.*, 1996), the role of GLUT1 was confirmed as one of the biochemical signatures of "barrier" tissues (Gherzi *et al.*, 1991) as shown in high metabolic-rated tissues like the microvascular endothelium of retina, RPE and CBE (Harik *et al.*, 1990; Mantych *et al.*, 1993b). The presence of GLUT1 mRNA in the CBE is very reasonable, as the CBE is the blood-aqueous barrier, which is responsible for selective substrate transport into the aqueous humor.

GLUT3 is believed to work with GLUT1 for basal cellular glucose uptake, with the 2 proteins expressed ubiquitously in mammalian tissues (Mantych *et al.*, 1993b). However, in rat lens, GLUT1 was found to be expressed mainly in the epithelium, while GLUT3 was expressed in cortical fiber cells. It was suggested that GLUT1 was crucial for external glucose uptake while GLUT3 was crucial for internal glucose exchange (Merriman-Smith *et al.*, 1999; Merriman-Smith *et al.*, 2003). In human retina, GLUT3 was found localised in the plexiform layers and served to take up glucose into neural cells once it had passed the BRB via GLUT1 (Watanabe *et al.*, 1996; Tserentsoodol *et al.*, 1998). Such an expression pattern was also found in the brain (Nagamatsu *et al.*, 1992) and it is therefore not unexpected for the eye to show a similar pattern of expression, since it has the same origin as the brain during development (Sharma and Ehinger, 2002). Furthermore, the CBE is an extension of the neural retina and is regarded as part of the CNS. Thus, the possession of similar glucose transporters as the brain and retina seems logical. Similar to the condition in retina, GLUT1 in CBE might be localised at the tight junctions (to enable barrier glucose transport), while GLUT3 may have some other function. However, such a conclusion cannot be made without further investigation. Studies of GLUT4 in ocular tissues are scarce. Researchers could not find any GLUT4 protein in rabbit iris-ciliary body (Tsukamoto *et al.*, 1995) and retina (Mantych *et al.*, 1993b). GLUT4 is an insulin responsive glucose transporter, which is widely expressed in heart (Abel, 2004), kidney (Marcus *et al.*, 1994), mammary gland (Zhao *et al.*, 1993), skeletal muscle (Hocquette *et al.*, 1995) and adipose tissues (Miura *et al.*, 2003). In the brain, GLUT4 mRNA was found specifically in the cerebellum, while GLUT1 and GLUT3 were found in each brain region including the medulla, midbrain and hypothalamus (Rayner *et al.*, 1994). The presence of GLUT4 was suggested to allow for

insulin-responsive glucose uptake in cerebellum, and suggests that a similar process might operate in the bovine CBE. The presence of GLUT4 mRNA in bovine CBE clearly reveals the presence of an insulin-response glucose transport system, yet how dominant this mechanism is in this tissue has yet to be determined.

GLUT5 is expressed predominantly in small intestine (Burant *et al.*, 1991) and kidney (Davidson *et al.*, 1992), for dietary glucose uptake and glucose reabsorption, respectively. Northern blotting showed its presence in the small intestine and kidney, yet it is also expressed at a very low level in human muscle, adipose tissue (Bell *et al.*, 1990), RPE (Takagi *et al.*, 1994) and brain (Mantych *et al.*, 1993b; Payne *et al.*, 1997). It is known that GLUT5 has a higher transport capacity for fructose than glucose (Shepherd *et al.*, 1992), thus the presence of this transporter in the CBE might indicate the existence of fructose transport along with glucose transport.

The presence of SGLT2 in the bovine CBE was a surprise in this study, since it was assumed that passive transport would be enough to maintain the required glucose flux across CBE. However, the existence SGLT2 is consistent with the energy-dependent glucose transport that was clearly present in this tissue in the electrophysiological study carried out in Chapter 2. Interestingly, similar results have been found in bovine cortical arteries, where GLUT1 is responsible for normal glucose transport, while SGLT1 is used for dealing with stress conditions like hypoglycemia (Nishizaki and Matsuoka, 1998). Therefore, the function of SGLT2 in the CBE might be similar, namely to protect the tissues in conditions of stress by ensuring adequate glucose transport.

In this study, neither GLUT2 nor SGLT1 mRNA was found in the bovine CBE. GLUT2 was not detected in either human (Takagi *et al.*, 1994) or chicken RPE cultures (Ban and Rizzolo, 2000) and rat brain (Rayner *et al.*, 1994). However, it was observed in rat retinal

Müller cells, and is thought to be responsible for intra-retinal glucose homeostasis (Watanabe *et al.*, 1994). GLUT2 mRNA was found to be intensely expressed in bovine liver, but at a lower abundance in kidney and duodenum (Zhao *et al.*, 1993). GLUT2 is not a common GLUT isoform in the CNS, therefore, it is not a surprising result that it is absent from the BAB of the CB.

SGLT1 is the high affinity SGLT, which is largely responsible for galactose and glucose transport in intestine (Wright, 2001). Absence of SGLT1 mRNA in the bovine CBE might indicate that a high affinity glucose transport system is not necessary in the bovine CBE.

4.4.4 Implications of mRNA expression of glucose transporters in the CBE

Different species and different tissues respond to glucose insult in distinct ways. Rat lens cells respond to hyperglycemia by upregulating the transcription of GLUT3, but not GLUT1, by 3.5 fold (Merriman-Smith *et al.*, 2003). Chick RPE increases GLUT1 expression instead of GLUT3 mRNA, under similar circumstances (Ban and Rizzolo, 2000). In bovine retinal endothelial cells, the amount of GLUT3 mRNA increases significantly with increases in glucose levels to physiological concentrations, yet declines in response to adverse glucose insult (i.e. hyperglycemia) (Knott *et al.*, 1993). Such a pattern of regulation is not seen in bovine cultured cells when exposed to various concentrations of galactose, which suggests that GLUT3 mRNA expression is specifically regulated by ambient glucose, yet not galactose. However, such an effect was absent in the same tissue in the study of Rajah *et al.* (2001), in which GLUT1 and GLUT3 expression were stable across a range of glucose concentrations (Rajah *et al.*, 2001). Only brain-derived endothelial cells showed a decrease in GLUT1 expression in

response to hyperglycemic. Again, this result conflicts with another study in rat, in which GLUT1 expression decreased in retinal microvessels, but not brain microvessels (Badr *et al.*, 2000). These differences between studies could be due to species difference, different *in vivo* and *in vitro* experimental conditions, or disparate duration and/or level of glucose exposure. Clearly, dissimilar mechanisms are operating for gene regulation among the various species or tissues.

Even with the findings from the present study, it is difficult to deduce a mechanism for lowering glucose transport across the CBE under elevated glucose conditions. Previous studies have shown that GLUT1 mRNA expression increases under long-standing diabetic conditions in both mouse (Vannucci *et al.*, 1997) and rat (Lutz and Pardridge, 1993) brain, while it decreases in human placental cultures (Hahn *et al.*, 1998). Similarly, overexpression of GLUT3 has been found *in vivo* in pregnant rat placental cells under hyperglycemic conditions (Boileau *et al.*, 1995) while underexpression or unchanged levels have been observed during hyperglycemia in retina (Knott *et al.*, 1996) and human or rat testis. With these contradictory results, it would be difficult to conclude the role of GLUT1 and GLUT3 in CBE under diabetic conditions and thus further *in vivo* studies would be necessary.

The presence of GLUT4, an isoform which is insulin-regulated, in CBE suggests its glucose transport is insulin-sensitive. GLUT4 has mostly been found to decrease in expression (both mRNA and protein) in response to hyperglycaemia, as well as diminish in translocation to the cell surface (Garvey *et al.*, 1991). Furthermore, its reduction in expression has been found in skeletal muscle, a result that was suggested not to be related to either obesity or type 1 or 2 DM (Pedersen *et al.*, 1990; Garvey *et al.*, 1992; Kahn *et al.*, 1992). However, in diabetic rat kidney, both GLUT1 and GLUT4 expression were

significantly increased in acute diabetes, while GLUT2 and GLUT5 expression increased under chronic hyperglycemic condition in rat kidney (Chin *et al.*, 1997). An increased level of GLUT2 and GLUT5 mRNA were also noted in another study, in the intestine of human diabetic subjects. It has been suggested that different GLUTs might respond to various durations or levels of glucose differently, and that even the same GLUT (e.g. GLUT4 mRNA in the brain) could respond differently to similar insults in different tissues (Kobayashi *et al.*, 1996).

There are scarcely any studies on how SGLT2 responds to diabetic conditions. As a low affinity, high capacity, sodium-glucose co-transporter, its presence would seem to be reasonable as a backup or reserve to maintain acceptable glucose transport across CBE under adverse condition e.g. hypoglycemia.

4.5 Conclusion

The published glucose transporter mRNA sequences were used to enable a RT-PCR investigation to determine which glucose transporter isoforms are expressed by CBE. GLUT1, GLUT3-5 and SGLT2 mRNA were present in this tissue. However, which among these transporters is the major candidate responsible for abnormal glucose transport under hyperglycemic condition is yet to be elucidated. Further *in vivo* studies, both electrophysiological and biochemical, in which the effects of hyperglycemia can be monitored, are required, to provide a better understanding of how different transporters respond to hyperglycemia. However, armed with this information, therapeutic intervention aimed at either the transcriptional level or translational level could be attempted.

Chapter 5

Glucose transporter: Protein expression in the CBE

5.1 Introduction

5.1.1 Overview of the experiment

In this part of the study, western blotting was used to examine the expression of glucose transporter proteins in the bovine CBE. Any difference in protein expression between pars plicata and pars plana was also assessed.

Protein samples from the bovine CBE were extracted and separated by gel electrophoresis according to their molecular size. Proteins were then transferred onto a membrane support. Antibodies targeted against different glucose transporters were used to identify protein of interest, and visualised by the use of an enhanced chemiluminescense (ECL) detection system. Light emitted from the membrane was captured on photographic film, thereby providing information as to the molecular weight of the glucose transporter detected.

Western blotting was used in order to confirm the results in the previous chapter. Unfortunately, various difficulties were encountered in optimizing the immunoblotting system, therefore, few conclusive results could be made from these experiments.

5.1.2 Western blotting

5.1.2.1 Basic principle

Western blotting, also named immunoblotting, is used for identifying a particular protein of interest in a complex mixture. It is one of the most powerful methods in detecting specific proteins (Towbin *et al.*, 1979). In general, tissue samples are solubilised with detergent e.g. SDS, and the mixture of proteins is separated by SDS-polyacrylamide gel electrophoresis (SDS-PAGE) according to molecular weight (Laemmli, 1970). The separated proteins are then transferred onto a supporting membrane e.g. polyvinylidene fluoride (PVDF) or nitrocellulose membrane. Antibodies specific for the protein of interest are used to react with the protein on the membrane and then the antibody-antigen complexes are revealed using anti-immunoglobulin "secondary" antibodies. Depending on which system is used, the anti-immunoglobulin might be labeled with a radioisotope, a fluorescent dye or an enzyme. Generally speaking, the sensitivity of western blotting depends on the specificity of the antibodies used and also the sensitivity of the detection system.

5.1.2.2 Antibody-antigen interactions

The vertebrate immune system produces antibodies as a defence response to a foreign substance, or "antigen". The antigen can be a protein, polysaccharide or a nucleic acid. Different antibodies are unique in structure, with different binding sites that recognise their specific antigen. For large, protein antigens, the antibody targets a specific cluster of amino acids called the epitope. Due to their specificity, antibodies are widely used to reveal target protein molecules in cells or tissues in biological studies.

The antibodies that are commonly used in immunological studies can generally be categorised into two types: monoclonal and polyclonal antibodies. The former type of antibody was firstly exploited by Köhler and Milstein (1975), who elegantly showed that monoclonal antibodies can possess exquisite specificity for a single epitope. Polyclonal antibodies are a heterogenous mixture of antibodies, that can recognise many epitopes of a single antigen. They therefore provide a higher chance of target protein detection, yet the reaction might not be as specific as that of monoclonal antibodies (Rosenberg, 1996).

5.1.2.3 Protein detection system

In the present study, a biotin-avidin or a biotin-streptavidin system was chosen because of their high sensitivity (Kurien and Scofield, 2003). In general, membrane-bound proteins were incubated with primary antibodies, and then with secondary antibodies conjugated with biotin. Biotin, also known as vitamin H, has an extraordinary high affinity for avidin, which has led to their application in immunological work. Four molecules of biotin can bind to one avidin molecule, and with more than one biotin molecule conjugated to each antibody molecule, this gives the ability of the target protein to bind more than one avidin molecule, thus providing signal amplification. Avidin, which can be conjugated with an enzyme, or fluorochrome, can then be used for signal detection. However, since avidin is a glycoprotein (Bruch and White, 1982), it tends to give rise to background staining by interacting with other glycoproteins (Bayer *et al.*, 1987). Streptavidin isolated from *Streptomyces acidinii*, therefore, was developed as a substitute for avidin, in order to reduce background by decreasing the non-specific binding, yet retaining the same high sensitivity (Green, 1990; Dunn, 1994).

5.1.2.4 Signal detection schemes

Chemical methods are commonly used to enhance the signal detection from antibodies. Several methods can be adapted to produce the final visual image, the most common of which are described below:

Enzyme-linked antibodies. Enzyme-coupled secondary antibodies are one of the most commonly adapted methods in signal detection. Alkaline phosphate- or horseradish peroxidase (HRP)-coupled antibodies are well-known examples (Knecht and Dimond, 1984). The antibody-enzyme conjugated antibodies, when reacted with substrate, give rise to a coloured reaction product , e.g. an HRP reaction with diaminobenzidine (DAB) yields a brown coloured product (Knecht and Dimond, 1984), while reaction with aminoethylcarbazole (AEC) results in a red product (Imam *et al.*, 1986). However, this method of detection can not account for accurate quantitation, and has limited sensitivity (Rosenberg, 1996).

Chemiluminescent detection. This system makes use of the chemiluminescence of luminol, a substrate that can be oxidised to produce an excited state product that emits light (Leong *et al.*, 1986; Vachereau, 1989). Signal detection is then achieved by the use of X-Ray film. During immunoblotting, enzyme-conjugated antibodies are used (as above). The enzyme then catalyzes the dephosphlorylation of the substrate, e.g. HRP catalyses the oxidation of luminol in the presence of hydrogen peroxide, to result in an excited stated luminol, which emits light as it returns to its ground state. This system is the most sensitive detection method available, and can detect as little as 1 pg of antigen in a sample (Vachereau, 1989). It has the advantages of allowing re-probing of the

membrane with different antibodies. Furthermore, the exposure and reaction times are generally short and the film records can be stored permanently (Leong *et al.*, 1986; Kurien and Scofield, 2003).

Radioactive. In this system, radioactive labels such as iodinated (^{125}I) staphylococcal protein A or streptococcal protein G can be conjugated to secondary antibodies (Dimond and Loomis, 1976; Harper *et al.*, 1990). Subsequent autoradiography can then be performed to enable detection of antigen. These methods allow quantitation of target protein or antigen in the sample and provide good imaging quality (Kurien and Scofield, 2003).

5.1.3 Dot blotting

Dot blotting is a useful technique to screen for optimised concentration of samples, antibodies or other reagents e.g. blocking solutions. It is performed by dotting samples of interest or controls, directly onto a membrane support and then carrying out the immunological procedures. However, dot blotting can only act as a quick reference or starting point since its result might differ from that after proteins have gone through electrophoresis and electrotransfer, before being probed with the antibodies.

5.1.4 Regulation of glucose transporter proteins

Wound healing. GLUT1 protein was upregulated in the corneal wound healing process (Takahashi *et al.*, 1996). This increase was related to an elevated transcriptional level and was believed to be essential for glucose supply during epithelial migration following wound closure. The increased level of GLUT1 was sustained well after two weeks of

wound closure (Takahashi *et al.*, 1996). However, an alternative hypothesis has been proposed to explain the increase of GLUT1 expression after wounding, based on the transporters' role as a water channel (Fischbarg *et al.*, 1990). This activity was thought to be crucial in regulating corneal homeostatic volume following wound healing (McCartney and Cantu-Crouch, 1992). Interestingly, a change in the localization of GLUT1 was also observed during wound healing, and was suggested to be a sign of redistribution of energy demand (Takahashi *et al.*, 1996).

Hyperglycemia. GLUT1 protein expression was down-regulated in the cerebral microvessels of diabetic rats (Harik *et al.*, 1988; Mooradian and Morin, 1991) and BBB of diabetic mice (Cornford *et al.*, 1995). Yet in diabetic human cornea, its expression remained unchanged (Kumagai *et al.*, 1994). In rat lens, an increased level of GLUT3 was found in the major damaged zone induced by hyperglycemia, and this increase occurred before any change in mRNA level. This suggested that GLUT3 protein might insert into the membrane from the cytoplasmic pool, rather than due to the change in mRNA level (Merriman-Smith *et al.*, 2003). However, GLUT3 expression did not show differential expression in rat testis when diabetic and normal groups were compared (Burant and Davidson, 1994).

Moreover, glucose transport function was found to be retarded, due to the downregulation of GLUT4 expression, in the adipose tissues and muscles of diabetic rats (Berger *et al.*, 1989; Garvey *et al.*, 1989). Yet no significant change was observed in the protein expression level of GLUT1 and GLUT4 with various hyperglycemic levels in skeletal muscles (Pedersen *et al.*, 1990). In contrast, GLUT1 protein expression was enhanced in murine fibroblast cells starved of glucose (Haspel *et al.*, 1986).

Growth and transcriptional factors. PDGF and serum induced an increase of GLUT1 protein in the membrane preparation of human RPE cells. This elevation of protein level was not related to a change in mRNA, and therefore, the change might be post-translational (Takagi *et al.*, 1994). Similar changes of GLUT3 protein expression have also been observed in the mouse brain (Choeiri *et al.*, 2002). In rodents, GLUT3 provides a basal level of glucose transport, but GLUT1 is upregulated in response to mitogens or oncogens, which have an instant effect, to increase, mRNA levels (Wagstaff *et al.*, 1995). Chickens, however, differed from rodents by upregulating GLUT3 in response to *v-src* (Wagstaff *et al.*, 1995; Steane *et al.*, 1998). These results highlight a species difference in the basal mechanism of glucose transporter protein expression, and in the response to different stimulants. Also, it is clear that mRNA and protein levels can be regulated independently, e.g. GLUT3 in rat lens (Merriman-Smith *et al.*, 2003). This agrees with a previous study, which also showed an increase in protein level without an increase in mRNA expression (Khayat *et al.*, 1998). This could be due to the regulation occurring at the translational or post-translational level, as demonstrated in the muscle cell study for GLUT3 (Khayat *et al.*, 1998).

Others. Insulin is known to cause an increase in the translocation of GLUT4 from the intracellular cytoplasmic pool to the cellular membranes (Marcus *et al.*, 1994; Kobayashi *et al.*, 1996). However, the process was found to be retarded during both diabetic and fasting stages (Berger *et al.*, 1989). On the other hand, glucose transporter expression also changes with developmental stage, and only the GLUT1, GLUT3, GLUT8 and SGLT1 isoforms were found to be present constantly during bovine embryo growth (Augustin *et al.*, 2001). Moreover, GLUT4 expression decreases with growth in ruminant species,

such as bovine (Abe *et al.*, 2001), but increases in non-ruminant species, such as rodents (Castello *et al.*, 1994).

5.1.5 Previous studies on glucose transporters

There have been many studies on glucose transporter protein expression or localization in different ocular tissues. GLUT1 has been the most commonly studied isoform in ocular tissues including retina and RPE (table 5.1). GLUT2 was found as a 60 kDa band in rat retina and was believed to be used in local glucose homeostatic functions as well as systemic glucose regulation (Watanabe *et al.*, 1994). On the other hand, GLUT3 was noted in the fibers of the inner synaptic layer, which is rich in neuronal connections and plays an important role in meeting the metabolic requirement of synapses (Mantych *et al.*, 1993b). GLUT4, being one of the two isoforms in the GLUT family that are responsive to insulin (Wood and Trayhurn, 2003), has only been found in bovine lens (Jacobs, 1993). There has not been any study to date on the SGLTs protein expression in ocular tissues.

Transporter protein	Ocular Tissues	Method	Protein size (kDa)	Species	Reference
GLUT1	Conjunctival epithelium	FC IHC	---	Human culture	(Gherzi *et al.*, 1991)
	Corneal endothelium	IHC	---	Human	(Kumagai *et al.*, 1994)
	Corneal epithelium	FC	---	Human culture	(Gherzi *et al.*, 1991)
		IHC	---	Human	(Kumagai *et al.*, 1994)
		WB IHC	55 & 60, 40 after glycosidase F digestion	Rat	(Takahashi *et al.*, 1996)
		WB	~ 50	Rat	(Takahashi *et al.*, 2000)
	Canal of Schleme	IHC	---	Human	(Kumagai *et al.*, 1994)
	Ciliary body	WB	---	Rat	(Takata *et al.*, 1990)
		CB-binding assay	---	Rabbit Rat Marmoset Baboon Human	(Kaulen *et al.*, 1991)
		IHC	---	Human	(Mantych *et al.*, 1993b)
	CBE - Pars plana	IHC	---	Human	(Mantych *et al.*, 1993b)
	CBE	IFEM	---	Mice	(Tserentsoodol *et al.*, 1998)
		IHC	---	Rat Human	(Harik *et al.*, 1990)
		IHC	---	Human	(Kumagai *et al.*, 1994)
		IFEM WB	44	Rat	(Shin *et al.*, 1996)
		IHC	---	Rat	(Takata *et al.*, 1991)
	Ciliary muscle capillary	EM IHC	---	Rabbit Human	(Schlingemann *et al.*, 1998)
	Iris-ciliary body	WB	45-50	Rat	(Tsukamoto *et al.*, 1995)
	Iris	WB	---	Rat	(Takata *et al.*, 1990)
	Iris epithelium	Cyto-chalasin B-binding assay	---	Rabbit Rat Marmoset Baboon Human	(Kaulen *et al.*, 1991)
		IHC	---	Rat	(Takata *et al.*, 1991)
		IHC	---	Human	(Mantych *et al.*, 1993b)
	Iridial stroma	IFEM	---	Mouse	(Tserentsoodol *et al.*, 1998)
	Iridial capillaries	IHC	---	Human	(Kumagai *et al.*, 1994)
	Iridial microvessels	IHC	---	Rat Human	(Harik *et al.*, 1990)
	Iridal vasculature	IHC	---	Human	(Mantych *et al.*, 1993b)
	Trabecular meshwork	Cyto-chalasin B-binding assay	---	Rabbit Rat Marmoset Baboon Human	(Kaulen *et al.*, 1991)
	Lens fiber cells	WB	---	Bovine	(Jacobs, 1993)

Transporter protein	Ocular Tissues	Method	Protein size (kDa)	Species	Reference
GLUT1	Lens epithelial cells	IHC WB	45	Rat	(Merriman-Smith *et al.*, 1999)
		IHC	---	Rat	(Merriman-Smith *et al.*, 2003)
	Lens cortex and nucleus	Cyto-chalasin B-binding assay	---	Rabbit Rat Marmoset Baboon Human	(Kaulen *et al.*, 1991)
		WB	---	Mouse	(Gong *et al.*, 2001)
	Optic nerve	IHC	---	Rat Human	(Harik *et al.*, 1990)
	RPE	IHC	---	Rat Human	(Harik *et al.*, 1990)
		IHC	---	Human	(Mantych *et al.*, 1993b)
		IHC	---	Human	(Kumagai *et al.*, 1994)
		WB	40-43	Human culture	(Takagi *et al.*, 1994)
		IFEM IGEM	---	Mouse	(Tserentsoodol *et al.*, 1998)
		IF IG	---	Rat	(Bergersen *et al.*, 1999)
	RPE	WB	---	Chick Culture	(Ban and Rizzolo, 2000)
		WB	45	Rat	(Badr *et al.*, 2000)
	Vitreous hyaloid vessels	IHC	---	8 week gestation human eye	(Mantych *et al.*, 1993b)
	Choroidal plexus	WB	---	Rat	(Takata *et al.*, 1990)
	Retinal capillary pericytes	WB	45-50	Bovine culture	(Mandarino *et al.*, 1994)
	Retinal capillary endothelial cells	WB	45-50	Bovine culture	(Mandarino *et al.*, 1994)
		IHC	---	Human culture	(Knott *et al.*, 1996)
		WB	---	Rat culture	(Antonetti *et al.*, 1998)
		IFEM IGEM	---	Mouse	(Tserentsoodol *et al.*, 1998)
		WB	54	Bovine culture	(Sone *et al.*, 2000)
		WB	55 and 60	Bovine culture	(Rajah *et al.*, 2001)
		WB	---	Bovine Culture	(Zhang *et al.*, 2003)
		WB	55	Rat culture	(Hosoya *et al.*, 2001)
	Retinal capillaries	IHC	---	Human	(Kumagai *et al.*, 1994)
		WB	---	Human	(Tang *et al.*, 2003)
	Retinal microvessels	WB	45	Rat	(Badr *et al.*, 2000)
	Retinal microvasculature	IGEM	---	Human	(Kumagai *et al.*, 1996)
		IGEM	---	Rat	(Fernandes *et al.*, 2003)
		IHC WB	45-55	Rat	(Badr *et al.*, 1999)
	Retina	WB	---	Rat	(Zhang *et al.*, 2003)

Transporter protein	Ocular Tissues	Method	Protein size (kDa)	Species	Reference
GLUT1	Retina	IHC	---	Rat	(Takata *et al.*, 1990)
	Retina – Rod outer receptors	IHC WB	45	Bovine	(Hsu and Molday, 1991)
	Retina – Cone outer segments			Chick	
	Retina – Photoreceptor cells and Müller cells	WB IHC	50	Human	(Mantych *et al.*, 1993b)
	Retina – Photoreceptors Inner and outer plexiform layers Nucleus layers	Cyto-chalasin B-binding assay	---	Rabbit Rat Marmoset Baboon Human	(Kaulen *et al.*, 1991)
	Retina – Nerve fiber layer Ganglion cells Photoreceptor cells Müller cells	IHC	---	Human	(Kumagai *et al.*, 1994)
GLUT2	Retina – Müller cells	EM IHC WB	60	Rat	(Watanabe *et al.*, 1994)
GLUT3	Iris-ciliary body	WB	55	Rat	(Tsukamoto *et al.*, 1995)
	Lens epithelial cells	IHC WB	45	Rat	(Merriman-Smith *et al.*, 1999)
		IHC WB	47	Rat	(Merriman-Smith *et al.*, 2003)
	Lens fiber cells	WB	---	Bovine	(Jacobs, 1993)
		IHC WB	45	Rat	(Merriman-Smith *et al.*, 1999)
		IHC WB	47	Rat	(Merriman-Smith *et al.*, 2003)
	Lens cortex and nucleus	WB	---	Mouse	(Gong *et al.*, 2001)
	Retinal endothelial cells	IHC	---	Human culture	(Knott *et al.*, 1996)
		WB	47	Bovine culture	(Rajah *et al.*, 2001)
	Retinal vasculature	IHC WB	45	Rat	(Badr *et al.*, 1999)
	Retina – inner synaptic layer	IHC WB	50	Human	(Mantych *et al.*, 1993b)
	Retina – Inner and outer plexiform layers Inner nuclear layer	IHC WB	44	Rat	(Watanabe *et al.*, 1996)
GLUT4	Lens fiber cells	WB	---	Bovine	(Jacobs, 1993)

Table 5.1 Summary of glucose transporter protein studies for the ocular tissues. FC: flow cytometry, IHC: Immunohistochemistry, WB: Western blotting, IFEM: Immunoflourescent electron microscopy, IGEM: Immunogold electron microscopy.

5.2 Methodology: Western Blotting

5.2.1 Materials

All of the primary antibodies were purchased from Santa Cruz biotechnology, Inc. (UK). The biotin conjugated affinity purified secondary antibody was purchased from Chemicon international, Inc. (Hampshire, UK). The avidin-HRP and streptavidin-HRP conjugates were purchased from Bio-Rad Laboratories, Inc. (Hertfordshire, UK) and Amersham Biosciences (Bucks, UK) respectively. Kaleidoscope prestained standard and biotinylated SDS-PAGE standard (low range) were purchased from Bio-Rad Laboratories, Inc. (Hertfordshire, UK), while the SuperSignal® West Pico Chemilluminescent Substrate was purchased from Pierce Biotechnology, Inc. (Rockford, IL). Other reagents such as glacial acetic acid were purchased from Fisons Scientific Equipment (Loughborough, UK), acrylamide/Bis-acrylamide stock solution (30%) from Severn Biotech Ltd. (Worcestershire, UK), Ponceau S from Kodak (Eastman Fine Chemicals, New York, US), glycine, methanol and Tris-Base were from Fisher Scientific (Leicestershire, UK) and the rest including bromophenol blue, coomassie blue G-250, DAB, 1,3, Dithio-DL-threitol (DTT), gelatin, glycerol anhydrous, SDS, sodium chloride, temed, polyoxyethylenesorbitan monolaurate (Tween-20) were purchased from Sigma-Aldrich Co. Ltd. (Dorset, UK)

5.2.2 Sample preparation

Bovine kidney and CBE were isolated and stored as described in section 4.2.2, except that the tissues were not immersed in RNA*later*, but directly in liquid nitrogen. For the isolation of retina, the bovine globe was cut open around the equator, and the anterior part

of the eyes (including the vitreous) was carefully removed. The retina could then be peeled off directly from the RPE and choroid, and was immediately immersed in liquid nitrogen. Tissues frozen in liquid nitrogen were homogenised using a dismembrator (Mikro-Dismembrator U, B. Braun Biotech International) at 1600 rpm for 2 mins. They were solubilised in 1 ml of 1x SDS sample buffer (50mM TrisCl (pH6.8), 5mM DTT, 1% SDS, 0.1% bromophenol blue and 7.5% glycerol). The mixture was centrifuged at 12,600 x g for 10 mins and the supernatant transferred to a new Eppendorf tube. Protein concentrations were measured using a BCA protein assay kit (Pierce Biotechnology, Inc., Rockford, IL) according to manufacturer's instructions.

5.2.3 SDS-polyacrylamide gel electrophoresis (SDS-PAGE)

Gel plates were cleaned and assembled in the Protean II cell cassette (Bio-Rad Laboratories, Inc., Hertfordshire, UK). Resolving gel mixtures were prepared in an universal container with a final acrylamide percentage of 10%. Gels were poured in between the glass plates and allowed to stand for 40 mins for polymerization. Butanol (Sigma-Aldrich Co. Ltd., Dorset) was used to overlay the gel surface during polymerization. With the presence of a sharp interface between the polymerised gel and the overlay, the butanol was poured off and gel surface was washed twice with Milli-Q water. A small volume of 5% stacking gel was poured on top of the resolving gel in which a comb was inserted to form the sample wells. The stacking gel was left to stand for another 40 mins for polymerization. After the stacking gel was set, the comb was carefully removed and the sample wells were rinsed with Milli-Q water. Every well was washed twice to ensure removal of the residual stacking gel fragments. For each sample,

40 ug of total protein was loaded. The samples were separated in the SDS-PAGE by applying 100 V for 135 mins. Coomassie blue G-250 solution (2.5 mM, 50% methanol, 10% glacial acetic acid and filtered with Whatman no.1 filters) was used to stain the separated proteins on gels. Any degraded samples (which showed up as smears of proteins without sharp bands) were discarded.

5.2.4 Protein transfer

Preliminary experiments revealed better and more consistent transfer efficiency using a wet blotting rather a semi-dry blotting system. Therefore, protein samples run on gels were transferred to PVDF membrane (Bio-Rad Laboratories, Inc., Hertfordshire, UK) by using the wet blotting method using a Protean II cell blotting kit (Bio-Rad Laboratories, Inc., Hertfordshire, UK) under a voltage of 50 V for 3 hours. The PVDF membranes were stained with 1% Ponceau S solution to ensure good protein transfer efficiency. The membrane was then washed in Tris-buffered saline (TBS) for 15 mins to destain the membrane.

5.2.5 Blocking, antibodies incubation and detection

The PVDF membranes were blocked with a blocking solution of 3% non-fat dry milk (Marvel dried skimmed milk, Lincolnshire, UK) in 0.01% Tween-20 TBS (TTBS) for one hour. Then, they were incubated in primary antibody solution for an hour or more. After two changes of TTBS for 10 mins each, the PVDF membranes were incubated in biotinylated secondary antibodies for a further hour. They were washed again in TTBS for 30 mins with three consecutive changes of solution of 10 mins each. Lastly, they were

incubated with avidin-HRP or strepavidin-HRP, which was diluted in 3 % blocking milk (0.01 % Tween-20) with 1 % gelatin for one hour, and then washed with TBS three times, for five mins each, before signal detection. Chemilumiescent signals were visualised using the SuperSignal® West Pico Chemilluminescent Substrate kit (Pierce Biotechnology, Inc., Rockford, IL) according to the manufacturer's instructions.

5.2.6 Control experiments

Kidney or retina samples were used as the positive controls, and were loaded alongside the CBE samples in every experiment. Negative controls were done by omitting the primary antibody.

5.2.7 Dot blotting protocol

Different concentrations of positive control sample (kidney), negative control samples (bovine serum albumin) and standard (molecular weight marker proteins) were dotted onto PVDF membrane and allowed to dry. Membranes were incubated in different concentrations of primary antibodies and secondary antibodies. Initially, 1:100 or 1:1000 primary antibody dilutions were tested, along with 1:20000 secondary antibody solutions. The optimal concentrations observed in dot blotting experiments were used as a starting point for later western blotting experiments.

5.2.8 ECL versus DAB

Serial dilutions of biotinylated standard protein (1:10, 1:50, 1:100, 1:200, 1:400 and 1:800) were loaded and separated by SDS-PAGE. Proteins were transferred onto PVDF

membrane, and blocked with 3% non-fat dry milk in 0.1% TTBS. Membranes were incubated with avadin-HRP for one hour, before being developed using DAB or ECL reagents.

5.3 Results

5.3.1 SDS-PAGE results

Three sets of kidney and of bovine CBE protein samples were analysed by SDS-PAGE, for any signs of degradation (Fig. 5.1). Samples which showed smears of proteins without sharp bands were not used for further experiments.

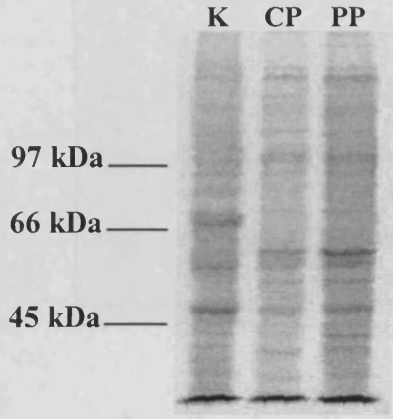

Fig. 5.1 Representative result of bovine samples separated by SDS-PAGE. K: kidney; CP: ciliary processes; PP: pars plana samples.

5.3.2 ECL versus DAB

Serial dilutions of biotinylated standards were transferred onto PVDF membrane, and detected with either ECL or DAB. As shown in figure 5.2, ECL was clearly much more sensitive, and therefore was used for all subsequent experiments.

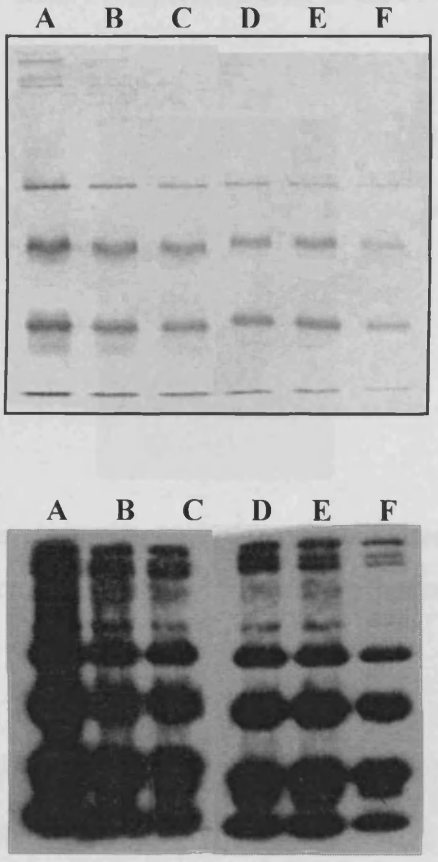

Fig. 5.2 Signal detection using DAB (top) or ECL (below) kit. A: 1:10; B: 1:50; C: 1:100; D: 1:200; E: 1:400; F: 1:800 dilutions of biotinylated-standards.

5.3.3 Strategies to minimise background staining of Western blots

As shown in figure 5.3, preliminary experiments showed a high level of non-specific background staining. Such staining persisted when primary and secondary antibodies were omitted, which indicated that the non-specific binding might be due to particular protein bands (especially in kidney samples) binding to the avidin-HRP conjugates.

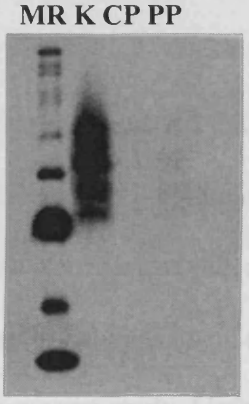

Fig. 5.3 Background staining in preliminary experiment. MR: Biotinylated standard marker; K: kidney; CP: ciliary processes; PP: pars plana samples.

Several strategies were tried to reduce the background problem:

Reduction of the avidin-HRP concentration. This was partially successful, but also resulted in a loss of sensitivity. At a concentration at which the avidin-HRP did not give any background staining, specific staining was also abolished e.g. the biotinylated-molecular weight standard markers were barely detectable. Therefore an increased concentration of the biotinylated marker had to be loaded onto the gel to compensate for the loss in sensitivity.

Alternative blocking agents. The use of teleost gelatin, and alterations in the Tween-20 concentration (0.01-0.05%) provided little or no improvement.

The use of Streptavidin-HRP to substitute for avidin-HRP conjugates. This caused lesser background staining, but at the expense of sensitivity. The concentration which gave no background staining, also abolished staining of the biotinylated-standard markers.

The use of non-avidin biotin detection system. All the primary antibodies were raised from goat. Without commercial anti-goat HRP-conjugated secondary antibodies being available at the time the experiments were carried out, a direct detection system could not be utilised. Recently, a "CruzMarker" system (Santa Cruz Biotechnology Inc, UK) was launched, and this was tested in the present study. Unfortunately, the kit exhibited even lower sensitivity and specificity in comparison to the avidin-biotin system.

Due to the difficulties discussed above, no Western blotting protocol could be devised that was completely free from background staining when using primary antibodies raised in goat.

5.3.4 Western blotting of GLUT and SGLT proteins

Only two glucose transporter proteins were detected using Western blotting, and even for these, the evidence was extremely weak.

Firstly, a band of molecular weight 41 kDa corresponding to GLUT1 was detected in a single experiment (fig. 5.4). An antibody against the human C-terminal (antibody sc-1605) was used. However, this result could not be repeated in three other experiments. Also, no 41 kDa band was present in the kidney sample, which is known to express GLUT1.

In addition, due to the high background staining on kidney samples, retina samples were also adapted to use as positive controls in this experiment, but no positive results could be obtained after optimization of the detection system.

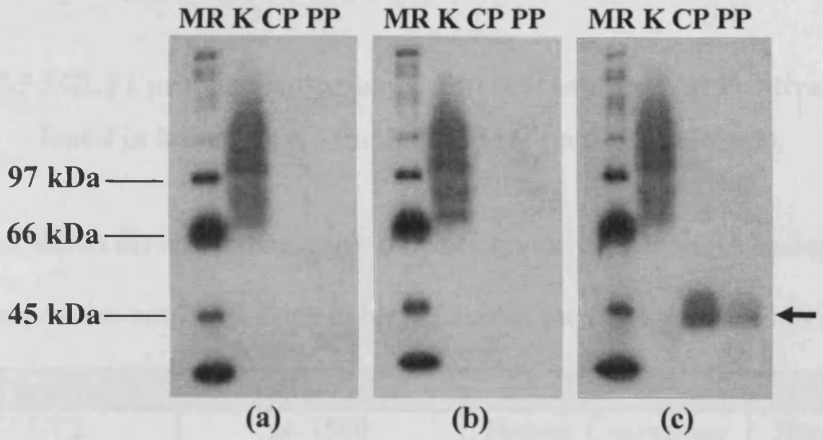

Figure 5.4 GLUT1 protein expressed on the first set of bovine CBE samples. (a) control experiment without primary antibody incubation; (b) control experiment without primary and secondary antibodies incubation; (c) GLUT1 expressed on both the CP and PP samples. Note the non-specific binding background on higher molecular weighted range of kidney samples.

Secondly, SGLT1 was detected as a 75 kDa protein band in kidney samples (n = 4) and also in pars plana in 2 out of these 4 replicate experiments, using tissues from different eyes in each case (Fig. 5.5). This was done by using a primary antibody against the mouse C-terminus of SGLT1 (antibody sc-20582).

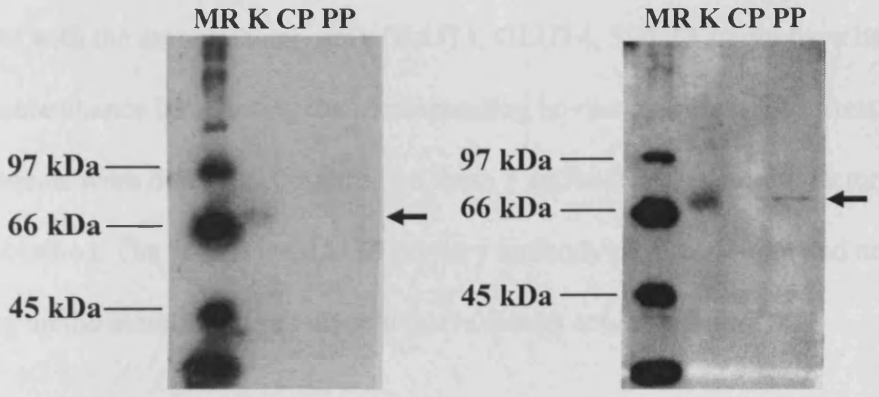

(a) (b)

Fig. 5.5 SGLT1 protein expression in different samples. (a) Positive staining was found in kidney (n = 4) and also in (b) pars plana (n = 2).

Table 5.2 shows the antibodies which did not provide signals above background when tested on positive control (bovine kidney) samples and on samples of bovine CBE:

Target	Product code	Epitope	Cross-reactivity
GLUT2	sc-7580	Human C-terminus	Human, mouse, rat
GLUT3	sc-7582	Mouse C-terminus	Mouse, rat
GLUT4	sc-1608	Human C-terminus	Human, mouse, rat
GLUT5	sc-14844	Rat N-terminus	Mouse, rat

Table 5.2 Antibodies providing no signals during Western blotting experiments. Goat anti-SGLT2 antibodies were not available, they were not tested in this study.

5.4 Discussion

5.4.1 Specificity of antibodies

As there were no commercially available anti-bovine glucose transporter protein antibodies, all of the primary antibodies used in the present study were targeted against human, mouse or rat glucose transporter proteins. When the respective epitopes were checked with the manufacturer, only GLUT1, GLUT4, SGLT1 might have had a reasonable chance in detecting the corresponding bovine glucose transporters. Therefore, experiments were done concentrating on these 3 antibodies, yet no satisfactory results were obtained. The goat anti-GLUT4 primary antibody gave very high and non-specific binding on the membrane, and no conclusive results could be drawn.

5.4.2 Glucose transporter proteins in the bovine CBE

According to the results obtained in chapter four, one would expect the expression of several glucose transporter proteins in the bovine CBE. Unfortunately, due to the technical problems encountered in this study, no conclusive results could be drawn. However, it would not be a surprise to find the presence of GLUT1, since it is the most common form of GLUT transporter, and exists in all mammalian cells studied to date (Gherzi *et al.*, 1991; Takata *et al.*, 1991). However, the presence of SGLT1 in both kidney and pars plana in 50% of the experiments raised the concern whether this antibody was actually working non-specifically. (Unfortunately, the manufacturer could not give any related information to confirm the likelihood of cross-reactivity). No conclusion can be deduced at the present stage. In the RT-PCR experiment, no SGLT1 mRNA was found in the bovine CBE, therefore, the possibility of the anti-SGLT1 antibody binding to SGLT2 or other SGLT1-like proteins in the bovine CBE could not be eliminated. Still, a

more complete story would only be possible if there were more bovine-specific antibodies for glucose transporters available. At present, no concrete evidence can be given for the protein expression profile of different glucose transporters in the bovine CBE.

Chapter 6

General discussion

6.1 Implications of glucose transporters in the CBE

Glucose transporters are important for mammalian cells, as they are crucial to ensure the flow of glucose in living tissues for normal metabolic functions (Kayano *et al.*, 1990; Gould and Holman, 1993). In the CBE, glucose transporters might have other functions than just transporting glucose or other substrates and glucose transporters have been thought to transport water across cell membranes (Fischbarg *et al.*, 1990; Loike *et al.*, 1993; Zampighi *et al.*, 1995; Loo *et al.*, 1996). Since the CBE is known as the primary site for aqueous humour secretion, it is intriguing to suggest that glucose transporters may somehow facilitate aqueous humour formation. However, the exact mechanism by which these transporters might contribute to the aqueous humor formation remains to be elucidated.

In this study, SGLT2 mRNA was expressed in the bovine CBE. The presence of the SGLT isoform was interesting, since a facilitative transport mechanism might have been expected to ensure an adequate glucose flow from blood to aqueous, in order to meet the metabolic needs of the avascular ocular tissues. One possibility, as has been discussed earlier (section 4.4.4), is that the presence of the SGLT isoform is a supplementary mechanism for the glucose transport system, in case adverse conditions occur. Another possibility, derived from recently published study, is that the SGLT2 transporter might act as a "nutrient-sensing device": it was noted that SGLT3, expressed in *Xenopus laevis* oocytes, could mediate glucose-induced depolarization of the membrane potential, and yet the transport itself did not show any glucose transport activity. SGLT3 has also been suggested as a glucose sensor in cholinergic neurons, thereby regulating muscle activity (Diez-Sampedro *et al.*, 2003). In addition, GLUT1 has been thought to act as a glucose-sensor, for glucose activation by mitogen-activated protein kinase (MAPK)

(Bandyopadhyay *et al.*, 2000), while GLUT2 has been suggested to play a similar role in hepatocytes (Guillemain *et al.*, 2000). Furthermore, sugar entry via SGLT1 and SGLT3 was proposed to act as a glucose sensor in the GLUTag cell, a model of intestinal L-cells (Gribble *et al.*, 2003). Therefore, it is possible that the SGLT2 expressed in the bovine CBE is functioning as a glucose-sensing device. However, this idea remains speculative at this stage and awaits further experimentations.

6.2 Glucose transport across the CBE

According to the present study, the major glucose transport mechanism in the bovine CBE is carrier-mediated facilitative transport. The system demonstrates a stereospecificity for MDG over LG, and is likely to saturate when the plasma glucose concentration reaches approximately 10.6 mM. One might expect that, even under poor glycemic control, there would be a limit at which the glucose transport across the CBE would be stabilised, and that further increases in plasma glucose concentration would not potentially cause damage. However, it was found that glucose transporter mRNA level could alter shortly after an hour of hyperglycemic exposure (Knott *et al.*, 1996), and remarkably, the K_m value was increased two-fold after two months of exposure to diabetic conditions (Ennis *et al.*, 1982). Thus, the present study will not be directly comparable to the *in vivo* condition in diabetic patients, since the true increase in plasma glucose concentration would be more subtle and much more sustained. One study has suggested that glucose is more detrimental than sucrose in causing barrier leakage (DiMattio and Streitman, 1986). In addition, the decrease in facilitated glucose transport is accompanied by an increase in passive glucose transport, due to the loss of barrier function under hyperglycemic condition in rats (DiMattio and Zadunaisky, 1983). This

caused an overall change in glucose transporter regulation, damage to barrier function and an increase or decrease in the glucose flux. These alterations could cause anomalous fluctuations of glucose concentrations e.g. varied glucose level across the CBE, as occur in the eyes of diabetic patients. This has been suggested to increase the glucose influx across the CBE, which might accelerate cataract formation (Swamy-Mruthinti *et al.*, 1999). According to an earlier study, it was proposed that there existed a glycemic threshold, beyond which the rate of diabetic cataract formation would increase exponentially (Nagaraj *et al.*, 1996). Beyond this threshold, formation of pentosidine, a product formed through glycoxidation, accelerated, as did the glycation rate. Therefore, one can postulate that if the glycemic threshold is lower than that of the saturation concentration, a cataract would inevitably form, despite the saturation kinetics. Therefore, it would be beneficial if one could downregulate the glucose influx across the CBE and prevent the aqueous humour from reaching abnormal glucose concentration which can precipitate the cataract formation process.

With the presence of GLUT1, GLUT3, GLUT4, GLUT5 and SGLT2 mRNA, one would also expect the presence of corresponding proteins in the tissues. Unfortunately, the protein study in this project could not be completed. Therefore, it is impossible to tell how the mRNA and protein levels are inter-related. Nevertheless, it is reasonable to postulate that the glucose transport across the CBE is insulin-responsive and mainly depends on concentration gradients across the CBE, since the presence of different GLUT isoforms confirmed our electrophysiological results that the transport mechanism was mainly facilitative and passive.

6.3 Aqueous glycemic control and diabetic cataract

The different glucose transporters perform differently under hyperglycemic conditions. Even the same isoform can give varied responses when expressed in different tissues (or in different species). For example, expression of GLUT3, but not GLUT1, increased after hyperglycemic insult, in rats (Merriman-Smith *et al.*, 2003). In addition, diabetes down-regulated GLUT1 expression in the rat retina and retinal microvessels, but not in the cerebral cortex (Badr *et al.*, 2000).

With the present data, it is difficult to conclude which of the glucose transporters present in the CBE is the best candidate to target in order to lower the glucose influx in diabetic patients. However, a member of the GLUT family would probably make a better choice, since there are likely to be at least four of the family members expressed in the CBE. Also, it may be better to target a transporter involved in basal conditions (e.g. SGLT2 may not be functional under normal conditions, or may not be responsible for the bulk of glucose transport). From the electrophysiological study, it was clear that the glucose flux was sensitive to certain drugs. Treatment with such glucose transporter inhibitors might be one possible way to lower the aqueous glucose level, yet how these drugs could be used to specifically target the CBE would require further investigation. Another approach would be gene therapy, in which the selected (targeted) isoform could be down-regulated. Firstly, however, it will be important to determine which glucose transporter isoform(s) are specifically upregulated under diabetic conditions. At this moment, the present study provides information of how glucose is transported across the CBE, and gives some ideas as to how the system could be regulated. It therefore represents a useful starting point from which further therapeutic approaches may be devised in order to lower the glucose concentration in the aqueous humour of diabetic patients.

Chapter 7

Future perspectives

7.1 Future perspectives

Two directions have been proposed to prevent cataract formation (Harding, 1999). The first one is to eliminate the risk factor while the other is to use anti-cataract drugs. The present study aimed to characterise the glucose transport into the eye which defines the glycemic level of the aqueous humour. By keeping the aqueous glycemic level normal, the crystalline lens will no longer be at risk of diabetic cataract and no cataractous and pathological pathways will be triggered. However, the ways by which glucose transporters are targeted so as to reduce the glucose flux across the CBE *in vivo* by drug or gene-therapy will require further investigation. Future experiments are needed to test the tissue specificity of potential pharmaceutical agents that are lower in toxicity, before clinical trials can be considered.

In addition, a more complete picture of the glucose transporter expression profile in the CBE is needed. With appropriate and specific antibodies against the glucose transporters, the protein expression profile will hopefully be characterised in the near future. The relationship between mRNA and protein expression can be deduced and a clearer picture regarding how different glucose transporters contribute to the glucose transport across the CBE will emerge. This basic information will help in extending important *in vivo* studies in which the expression profile of glucose transporters can be investigated under hyperglycemic conditions. With this knowledge, candidate genes or proteins which are differentially expressed in hyperglycemic conditions can be targeted and altered by drugs or even gene therapy. For gene therapy to be successful, a number of technical aspects will have to be addressed. These include a thorough knowledge about the target gene, the accessibility of the target cells or tissues and a suitable vector system with which to

introduce the gene into the target organ. Viral and non-viral methods are used to transport foreign genetic material into cells. In diabetes, studies have suggested that gene therapy may be a highly effective therapeutic treatment. In general, gene therapy has been widely investigated in different diabetic complications such as diabetic nephropathy (Zern and Kresina, 1997; Kitamura, 1999) and diabetic retinopathy (Igarashi *et al.*, 2003). At late-stage neuropathy, hepatocyte growth factor (HGF) gene-therapy has showed promising results in improving the functional abnormalities (Cruzado *et al.*, 2004). Lentivirus-mediated HIV-angiostatin expression reduced the severity in mouse diabetic retinopathy model (Igarashi *et al.*, 2003), while ciliary neurotrophic factor administered by eye drops inhibited retinal degeneration in diabetic rats (Aizu *et al.*, 2003). A recent study has also demonstrated the possibility of using an *ex vivo* HGF gene in facilitating islet transplantation (Rao *et al.*, 2004). Although these studies are at an experimental stage in animal models, the same scheme of treatment may possibly be applicable to the CBE. With careful gene therapy design, for example, a candidate gene responsible for the abnormal upregulation of glucose transport in the CBE could be modulated (i.e. downregulated) at the transcriptional level and consequently the aqueous glucose concentration might remain normal. To date, there have been few studies exploring the possibility of targeting glucose transporters directly, in order to lower their level of expression, to combat diabetic complications. Therefore, to tackle hyperglycemia via such an approach is a new direction for treating diabetic patients. In fact, it can even be used as a preventive measure to delay or prevent any consequent hyperglycemia-induced complications.

7.2 Conclusion

The present study is important in demonstrating that the application of a number of drugs can regulate the glucose transport in the bovine CBE and thereby control the aqueous glycemic level. By characterising the transport kinetics and genetic expression of various glucose transporters, it is now possible to envisage new ways to lower the risk of diabetic cataract.

Appendix

Appendix I

CLUSTAL cladograms for GLUT1-5 and SGLT1-3 mammalian mRNA sequences

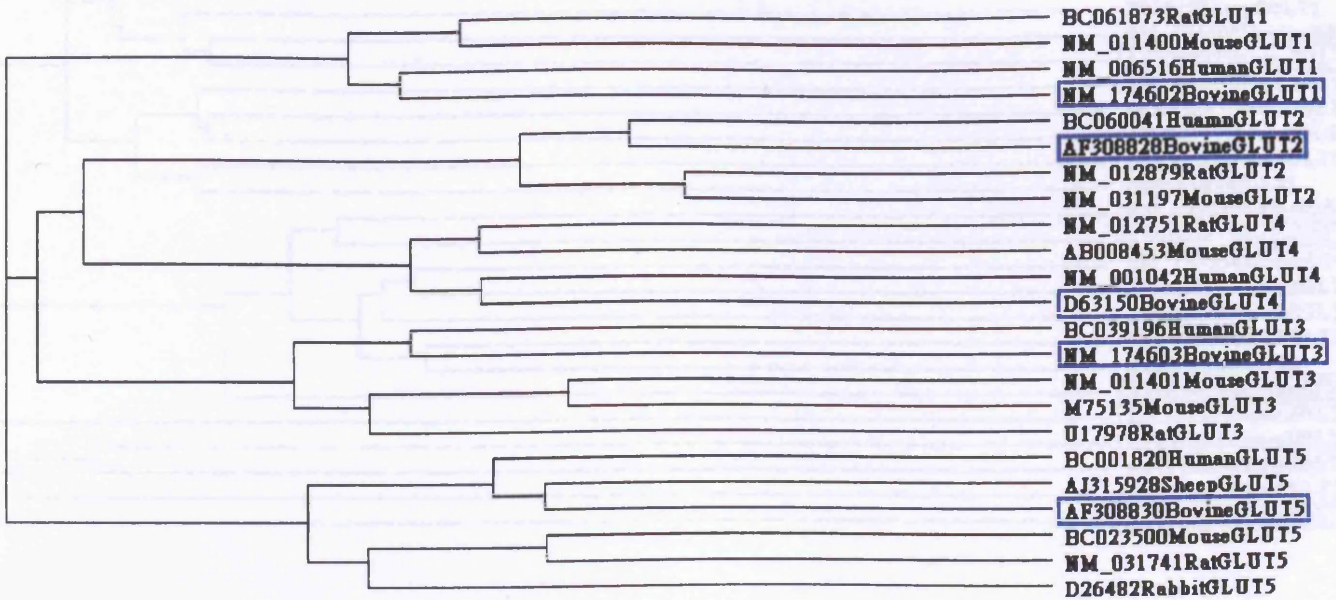

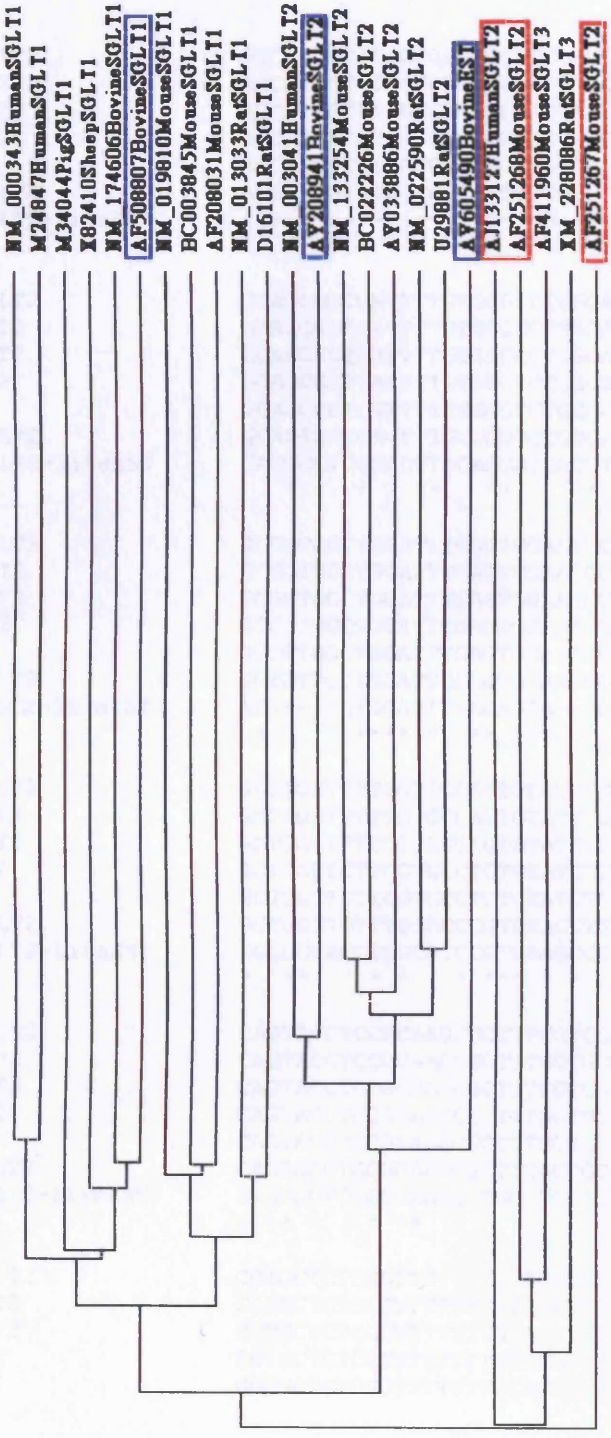

The sequences in blue brackets are the bovine sequences used for primer design in this study.
Red bracketed sequences are sequences with likely mis-assigned labels.

Appendix II

CLUSTAL analysis of mammalian SGLT2 mRNA and the bovine SGLT2-like EST sequences

```
NM_133254MouseSGLT2              AGCATGGTGTGGTGGCCGGTTGGAGCCTCTCTGTTCGCCA-GCAACATCG 223
BC022226MouseSGLT2               AGCATGGTGTGGTGGCCGGTTGGAGCCTCTCTGTTCGCCA-GCAACATCG 223
AY033886MouseSGLT2               AGCATGGTGTGGTGGCCGGTTGGAGCCTCTCTGTTCGCCA-GCAACATCG 233
NM_022590RatSGLT2                AGCATGGTGTGGTGGCCGGTTGGAGCCTCTCTGTTCGCCA-GCAACATCG 228
U29881RatSGLT2                   AGCATGGTGTGGTGGCCGGTTGGAGCCTCTCTGTTCGCCA-GCAACATCG 228
NM_003041HumanSGLT2              AGCATGGTGTGGTGGCCGGTTGGGGCCTCTCTCTTCGCCA-GCAACATCG 249
AV605490BovineSGLT2-likeEST      ------------------------------------CCACGCGTCCGCC 13
                                                                     *** **  *  *

NM_133254MouseSGLT2              GCAGCGGTCATTTTGTGGGCCTGGCAGGGACTGGCGCAGCAAGTGGCTTG 273
BC022226MouseSGLT2               GCAGCGGTCATTTTGTGGGCCTGGCAGGGACTGGCGCAGCAAGTGGCTTG 273
AY033886MouseSGLT2               GCAGCGGTCATTTTGTGGGCCTGGCAGGGACTGGCGCAGCAAGTGGCTTG 283
NM_022590RatSGLT2                GCAGCGGTCATTTTGTGGGCCTGGCGGGGACTGGTGCAGCAAGTGGCTTG 278
U29881RatSGLT2                   GCAGCGGTCATTTTGTGGGCCTGGCGGGGACTGGTGCAGCAAGTGGCTTG 278
NM_003041HumanSGLT2              GCAGTGGCCACTTTGTGGGCCTGGCAGGGACTGGCGCTGCAAGTGGCTTG 299
AV605490BovineSGLT2-likeEST      CACGCGTCCGCCTTACAGGATCACCTCCTTCTGTTACA-CACACGAGAAA 62
                                    * *  *   **   **     *     ***   *  **   *

NM_133254MouseSGLT2              GCGGTGGCTGGATTTGAGTGGAATGCGCTCTTCGTGGTGCTGCTCC-TCG 322
BC022226MouseSGLT2               GCGGTGGCTGGATTTGAGTGGAATGCGCTCTTCGTGGTGCTGCTCC-TCG 322
AY033886MouseSGLT2               GCGGTGGCTGGATTTGAGTGGAATGCGCTCTTCGTGGTGCTGCTCC-TCG 332
NM_022590RatSGLT2                GCCGTGGCTGGATTTGAGTGGAATGCGCTCTTTGTGGTGTTGCTCC-TCG 327
U29881RatSGLT2                   GCCGTGGCTGGATTTGAGTGGAATGCGCTCTTTGTGGTGTTGCTCC-TCG 327
NM_003041HumanSGLT2              GCTGTTGCTGGATTCGAGTGGAATGCGCTCTTCGTGGTGCTGCTAC-TGG 348
AV605490BovineSGLT2-likeEST      AC-----CTGGACTT-AGAGGA--GGGCCTGTAGTGGAGGTCCTACACTG 104
                                  *     ***** *  ** ***  * **   * **** * * ** *   *

NM_133254MouseSGLT2              GATGGCTTTTTGTGCCAGTGTATCTGACCGCTGGTGTGATCACAATGCCT 372
BC022226MouseSGLT2               GATGGCTTTTTGTGCCAGTGTATCTGACCGCTGGTGTGATCACAATGCCT 372
AY033886MouseSGLT2               GATGGCTTTTTGTGCCAGTGTATCTGACCGCTGGTGTGATCACAATGCCT 382
NM_022590RatSGLT2                GCTGGCTCTTCGTGCCTGTGTATCTGACCGCCGGAGTGATTACCATGCCT 377
U29881RatSGLT2                   GCTGGCTCTTCGTGCCTGTGTATCTGACCGCCGGAGTGATTACCATGCCT 377
NM_003041HumanSGLT2              GCTGGCTGTTTGCACCCGTGTACCTGACAGCGGGGGTCATCACGATGCCA 398
AV605490BovineSGLT2-likeEST      GGGGGCACCTGGCATCCGTGAAGCCC----------CAAACTCAGCCCCA 144
                                 *  ***   * *   * *** * *              *   *    **

NM_133254MouseSGLT2              CAGTACCTCCGCAAGCGCTTTGGTGGGCACCGTATTCGCCTCTACCTGTC 422
BC022226MouseSGLT2               CAGTACCTCCGCAAGCGCTTTGGTGGGCACCGTATTCGCCTCTACCTGTC 422
AY033886MouseSGLT2               CAGTACCTCCGCAAGCGCTTTGGTGGGCACCGTATTCGCCTCTACCTGTC 432
NM_022590RatSGLT2                CAGTACCTCCGCAAGCGCTTTGGTGGGCGCCGTATTCGCCTCTACCTGTC 427
U29881RatSGLT2                   CAGTACCTCCGCAAGCGCTTTGGTGGGCGCCGTATTCGCCTCTACCTGTC 427
NM_003041HumanSGLT2              CAGTACCTGCGCAAGCGCTTCGGCGGCCGCCGCATCCGCCTCTACCTGTC 448
AV605490BovineSGLT2-likeEST      CTGTGCTCACCCAGACCTGCCTCCTGACGCCGGAGT-GCAGGAGCTCG-- 191
                                 * ** *   * **  *         * * *** *   **     *  *

NM_133254MouseSGLT2              CGTGCTCTCGCTTTTTTTGTACATTTTCACCAAGATCTCGGTGGATATGT 472
BC022226MouseSGLT2               CGTGCTCTCGCTTTTTTTGTACATTTTCACCAAGATCTCGGTGGATATGT 472
AY033886MouseSGLT2               CGTGCTCTCGCTTTTTTTGTACATTTTCACCAAGATCTCGGTGGATATGT 482
NM_022590RatSGLT2                CGTGCTCTCGCTTTTTTTGTACATTTTCACCAAGATCTCGGTGGATATGT 477
U29881RatSGLT2                   CGTGCTCTCGCTTTTTTTGTACATTTTCACCAAGATCTCGGTGGATATGT 477
```

```
NM_003041HumanSGLT2                TGTGCTCTCCCTTTTCCTGTACATCTTCACCAAGATCTCAGTGGACATGT 498
AV605490BovineSGLT2-likeEST        -GAGAATGGGCCATCATTTTGAAATCT------GCCCTCCAGGAAAATTA 234
                                    * *      *  *   * *  *  *       *  ***   * * **

NM_133254MouseSGLT2                TCTCTGGGGCAGTATTCATTCAACAGGCCCTGGGCTGGAACATTTACGCT 522
BC022226MouseSGLT2                 TCTCTGGGGCAGTATTCATTCAACAGGCCCTGGGCTGGAACATTTACGCT 522
AY033886MouseSGLT2                 TCTCTGGGGCAGTATTCATTCAACAGGCCCTGGGCTGGAACATTTACGCT 532
NM_022590RatSGLT2                  TCTCCGGAGCAGTATTCATTCAACAGGCCCTGGGCTGGAACATTTACGCT 527
U29881RatSGLT2                     TCTCCGGAGCAGTATTCATTCAACAGGCCCTGGGCTGGAACATTTACGCT 527
NM_003041HumanSGLT2                TCTCCGGAGCTGTATTCATCCAGCAGGCTCTGGGCTGGAACATCTATGCC 548
AV605490BovineSGLT2-likeEST        ATTGGAAAGGGGGAATCCTTTTCCAGTTCCCCGCAAAGACAGTCTATGTA 284
                                     *     *  * * ** *    ***   *  *    **   * ** *

NM_133254MouseSGLT2                TCGGTCATCGCTCTCTTGGGCATCACCA--TGATTTATACTG-TGACAGG 569
BC022226MouseSGLT2                 TCGGTCATCGCTCTCTTGGGCATCACCA--TGATTTATACTG-TGACAGG 569
AY033886MouseSGLT2                 TCGGTCATCGCTCTCTTGGGCATCACCA--TGATTTATACTG-TGACAGG 579
NM_022590RatSGLT2                  TCTGTCATCGCACTCTTGGGCATCACCA--TGATTTATACTG-TGACAGG 574
U29881RatSGLT2                     TCTGTCATCGCACTCTTGGGCATCACCA--TGATTTATACTG-TGACAGG 574
NM_003041HumanSGLT2                TCCGTCATCGCGCTTCTGGGCATCACCA--TGATTTACACGG-TGACAGG 595
AV605490BovineSGLT2-likeEST        CTAGAGGCAGCCTGTCTGGGCTGTGCCCCCTGACCCAGGCCGGTTGCAGG 334
                                     *     **     *****    **   ***   *  * * *  ****

NM_133254MouseSGLT2                AGGGCTGGCGGCACTGATGTACACAGACACTGTGCAGACCTTCGTCATTC 619
BC022226MouseSGLT2                 AGGGCTGGCGGCACTGATGTACACAGACACTGTGCAGACCTTCGTCATTC 619
AY033886MouseSGLT2                 AGGGCTGGCGGCACTGATGTACACAGACACTGTGCAGACCTTCGTCATTC 629
NM_022590RatSGLT2                  AGGGCTGGCGGCACTGATGTACACAGACACTGTGCAGACCTTCGTCATTC 624
U29881RatSGLT2                     AGGGCTGGCGGCACTGATGTACACAGACACTGTGCAGACCTTCGTCATTC 624
NM_003041HumanSGLT2                AGGGCTGGCCGCGCTGATGTACACGGACACGGTACAGACCTTCGTCATTC 645
AV605490BovineSGLT2-likeEST        AGGGCTGGCG[GCACTGATGTACACGGACAC]GGTGCAGACCTTCGTCATTC 384
                                   ********* ** *********** ***** ** ****************

NM_133254MouseSGLT2                TTGCCGGGGCCTTCATCCTCACTGGTTATGCTTTCCATGAAGTGGGCGGG 669
BC022226MouseSGLT2                 TTGCCGGGGCCTTCATCCTCACTGGTTATGCTTTCCATGAAGTGGGCGGG 669
AY033886MouseSGLT2                 TTGCCGGGGCCTTCATCCTCACTGGTTATGCTTTCCATGAAGTGGGCGGG 679
NM_022590RatSGLT2                  TTGCCGGGGCCTTCATCCTCACTGGTTATGCTTTCCATGAAGTGGGCGGG 674
U29881RatSGLT2                     TTGCCGGGGCCTTCATCCTCACTGGTTATGCTTTCCATGAAGTGGGCGGG 674
NM_003041HumanSGLT2                TGGGGGGCGCCTGCATCCTCATGGGTTACGCCTTCCACGAGGTGGGCGGG 695
AV605490BovineSGLT2-likeEST        TCGCCGGGGCCTTCGTCCTCATGGGTTACGCCTTCCACGAGGTGGGCGGG 434
                                   * *  ** **** * ******  ***** ** ***** ** **********

NM_133254MouseSGLT2                TACTCGGGTCTCTTCGACAAATACCTGGGAGCAATGACTTCACTGACGGT 719
BC022226MouseSGLT2                 TACTCGGGTCTCTTCGACAAATACCTGGGAGCAATGACTTCACTGACGGT 719
AY033886MouseSGLT2                 TACTCGGGTCTCTTCGACAAATACCTGGGAGCAATGACTTCACTGACGGT 729
NM_022590RatSGLT2                  TACTCAGGTCTCTTCGACAAATACCTGGGAGCAGTGACTTCACTGACGGT 724
U29881RatSGLT2                     TACTCAGGTCTCTTCGACAAATACCTGGGAGCAGTGACTTCACTGACGGT 724
NM_003041HumanSGLT2                TATTCGGGTCTCTTCGACAAATACCTGGGAGCAGCGACTTCGCTGACGGT 745
AV605490BovineSGLT2-likeEST        TATTCGGGGCTTTTCGACAAATACTTGCGGGCAGTGACGTCCC[TGACGGT 484
                                   ** ** ** ** ************ ** * ***  *** ** *********

NM_133254MouseSGLT2                GTCCAAGGATCCATCTGTTGGCAACATCTCCAGCACCTGCTAC-CAGCCG 768
BC022226MouseSGLT2                 GTCCAAGGATCCATCTGTTGGCAACATCTCCAGCACCTGCTAC-CAGCCG 768
AY033886MouseSGLT2                 GTCCAAGGATCCATCTGTTGGCAACATCTCCAGCACCTGCTAC-CAGCCG 778
NM_022590RatSGLT2                  GTCCAAGGATCCAGCTGTTGGCAACATCTCCAGCACCTGCTAT-CAGCCG 773
U29881RatSGLT2                     GTCCAAGGATCCAGCTGTTGGCAACATCTCCAGCACCTGCTAT-CAGCCG 773
NM_003041HumanSGLT2                GTCCGAGGATCCAGCCGTGGGAAACATCTCCAGCTTCTGCTAT-CGACCC 794
AV605490BovineSGLT2-likeEST        [ATCCTAGGATC]CGGCCGTGGGCAACATCTCCAGCTCCTGCTATTCGACCC 534
                                    *** *******  * ** ** ************  ******  *  **

NM_133254MouseSGLT2                AGGCCTGACTCCTATCACCTGCTGCGTGACCCTGTGACAGGAGACCTGCC 818
BC022226MouseSGLT2                 AGGCCTGACTCCTATCACCTGCTGCGTGACCCTGTGACAGGAGACCTGCC 818
```

```
AY033886MouseSGLT2              AGGCCTGACTCCTATCACCTGCTGCGTGACCCTGTGACAGGAGACCTGCC 828
NM_022590RatSGLT2               AGGCCCGACTCCTATCACCTGCTGCGTGACCCTGTGACAGGAGGGCTGCC 823
U29881RatSGLT2                  AGGCCCGACTCCTATCACCTGCTGCGTGACCCTGTGACAGGAGGGCTGCC 823
NM_003041HumanSGLT2             CGGCCCGACTCCTACCACCTGCTCCGGCACCCCGTGACCGGGGATCTGCC 844
AV605490BovineSGLT2-likeEST     CGGCCGGACTCCTACCACT------------------------------- 553
                                **** ******** ***
```

Short sequences highlighted in red were the primers designed based on the bovine SGLT2-like EST.

Appendix III

Sequencing results for GLUT1-5, SGLT1-2 and SGLT-2like EST

GLUT1

CTCCATCATGGGCAACCAGGAACTGTGGCCCCTGCTGCTGAGCGTCATCTTCATCCCAG
CCCTGTTGCAGTGCATCCTGCTGCCCTTCTGCCCCGAGAGCCCCCGCTTCCTGCTCATT
AACCGCAACGAGGAGAACCGGGCCAAGAGCGTGCTGAAGAAGCTGCGTGGGACCGCGGA
CGTGACCCGCGACCTGCAGGAGATGAAGGAGGAGAGCCGGCAGATGATGCGGGAGAAGA
AGGTCACCATCCTGGAGCTGTTCCGCTCAGCCGCCTACCGCCAGCCCATCCTCATTGCC
GTGGTGCTGCAGCTGTCCCAGCAGCTGTCCGGCATCAACGCTGTTTTCTATTACTCCAC
AAGCATCTTCGAGAAGGCGGGGGTGCAGCAGCCCGTGTATGCCACCATCGGCTCTGGCA
TCGTCAACACAGCCTTCACTGTCGTGTCGCTATTTGTGGTGGAACGAGCCGGCCGGCGG
ACCCTGCACCTCATAGGCCTGGCCGGCATGGCAGGCTGTGCA

GLUT2

ACAGCTGGAATCAGCCAACCTGTTTATGCAACCATTGGAGTTGGTGCTGTCAACACAGT
TTTCACTGCTGTCTCTGTGTTCCTTGTGGAGAAGGCAGGGCGACGCTCTCTGTTCCTAA
TTGGAATGAGTGGGATGTTTGTTTGTGCCATCTTCATGTCGGTGGGACTGGTNGCTCCT
GAGA

GLUT3

CCTTGTCTGTGGCCATCTTCTCCGTGGGTGGTATGATTGGCTCCTTCTCCGTCGGACTC
TTTGTCAACCGATTTGGCAGGCGCAATTCAATGCTTATTGTCAACCTGTTGGANATAGC
TGGCGGCTGCCTTATGGGATTCTGCAAAATAGCAGAGTCGGTTGAAATGCTGATCTTGG
GCCGACTGATTATCGGCCTCNTCTGCGGACTCTGCACAGGATTCGTGCCCATGTACATT
GGAGAGATCTCCCCTACTGCCCTGCGGGGCGCCTTTGGCACTCTCAACCAGCTGGGCAT
CGTTATCGGAATTCTGGTGGCCCAGATCTTTGGTCTAAAAGTCATCTTGGGGACTGAAG
ATCTCTGGCCTCTGCTCCTGGGCTTCACCATCTTACCAGCCATCATCCAGTGCAAA

GLUT4

GTGGCTGGGTACGTCCAACTGGACATGCAACTTCATCATCGGCATGGGTTTCCAGTATG
TGGCGGATGCTATGGGTCCCTACGTCTTTCTTCTATTCGCGGTCCTCCTGCTTGGCTTC
TTCATCTTCACCTTCTTAAAAGTGCCTGAAACCCGTGGCAGGACGTTTGACCAGATCTC
AGCCGTTTTCCACCGGACACCTTCTCTTCTGGAGCAGGAAGTGAAACCCAGCACAGAAC
TGGAGTACTTAGGGCCAGATGAGCATGACTGAGGGCCACAGAGGGGTGGGAGAGCCAGT
TCTCTCCACTTGCCCAGAGACCCCCCTCCTTTTCTCTGCAGCACTTTAACCCTCTCTTC
CCCATTACTTCCAGGGCAGAGAANACCCCTGCAGCCTGGTGGGATTGGGAAGCTGGAGG
GAACGGTGGTCTGAGCACCCCCTCATTCCCCTCGTGTGACCTCTTGGATTATTTGTGTT
GTGGGTTAGCAGTGG

GLUT5

CTCCATCATCGTCCTCATGGCGGGCCAGCAGCTCTCCGGAGTGAATGCGATCTACTACT
ACGCAGACCAGATTTACCTGAGTGCTGGAGTGAATGAGGACGATGTCCAATATGTGACG

SGLT1

AAGGCAGAGTGCTACACCCCGAGGGCTGACTCCTTCCACATCTTCCGCGATCCTCTCAA
GGGAGACCTGCCCTGGCCTGGGCTCATCTTTGGGCTGACCATCATCTCCCTGTGGTACT
GGTGCACAGACCAGGTCATTGTGCAGCGCTGCCTCTCNGCCAAAAACATGTCCCACGTG
AAGGCCGGCTGCATCATGTGTGGGTACCTGAAGCTGCTGCCCATGTTCCTCATGGTGAT
GCCAGGGATGATCAGCCGCATCCTGTTCACAGAGAAAGTTGCCTGCACGGTCCCCTCAG
AGTGTGAGAAATACTGCGGCACCAAGGTTGGCTGTACCAACATCGCCTACCCGACCTTG
GTGGTGGAGCTCATGCCCAATGGACTGCGAGGCCTGATGCTGTCGGTCATGCTGGCCTC
GCTCATGAGCTCGCTGACCTCCATCTTCAACAGTGCCAGCACCCTCTTCACCATGGACA
TCTACACCAAGATCCGGAAGAAAGCCTCTGAGAAAGAGCTCATGATCGCAGGACGGTTG
TTCATGCTGGTGCTGATCGGTGTCAGCATCGCCTGGGTGCCCATCGTGCAGTCAGCACA
GAGTGGACAGCTCTTCGACTACATCCAGTCCATCA

SGLT2

CAACCGCCCATTCCGCGCAAGCACCTCTACCGCCTGGTTTTCAGTCTCCGGCACAGCAA
GGAAGAGAGGGAGGACCTGGATGCTGAGGAGCTAGAAGGTCCAACCGCAGCCCCCGTGC
AGAACGGGCGCCCTGAGCACGCAGTGGAGATGGAGGCGCCCCCGCCCCCAAGGCCAGGC
CTGTTGCGGCAGTGCCTGCTCTGGTTCTGTGGCGTGAGCAGGGGTGGGGTGGGCAGCCC
CCAACGCCCTACCCAGGAGGAGACGACTGCTGCAGCCAGGCGGCTGGAGGACATCAGTG
AGGACCCACGCTGGGCCCGCGTGGTCAACCTCAACGCCCTGCTCATGATGGCCGTGGCC
ACATTCCTCTGGGGCTTTTATGCCTGAGGCCCANTGCATTGGAACACCCTGAGCAA

SGLT2-like EST

GGGGCCTTCGTCCTCATGGGTTACGCCTTCCACGAGGTGGGCGGGTATTCGGGGCTTTT
CGACAAATACTTGCGGGCAGTGACGTCCCTGACGGTATCCGAGGATCACNTANGCGGGG
TGGTCCGAGGGAGGGCCTTGTCGCGGGTGCCGGGTCCCCTGACGGCCGTGCCCTCACAG
CCTTCCACGAGGTGGGCGGGTATTCGGGGCTTTTCGACAAATACTTGCGGGCAGTGACG
TCCCTGACGGTATCCGAGGATCA

The next two pages are examples of the sequencing output in ABI format.

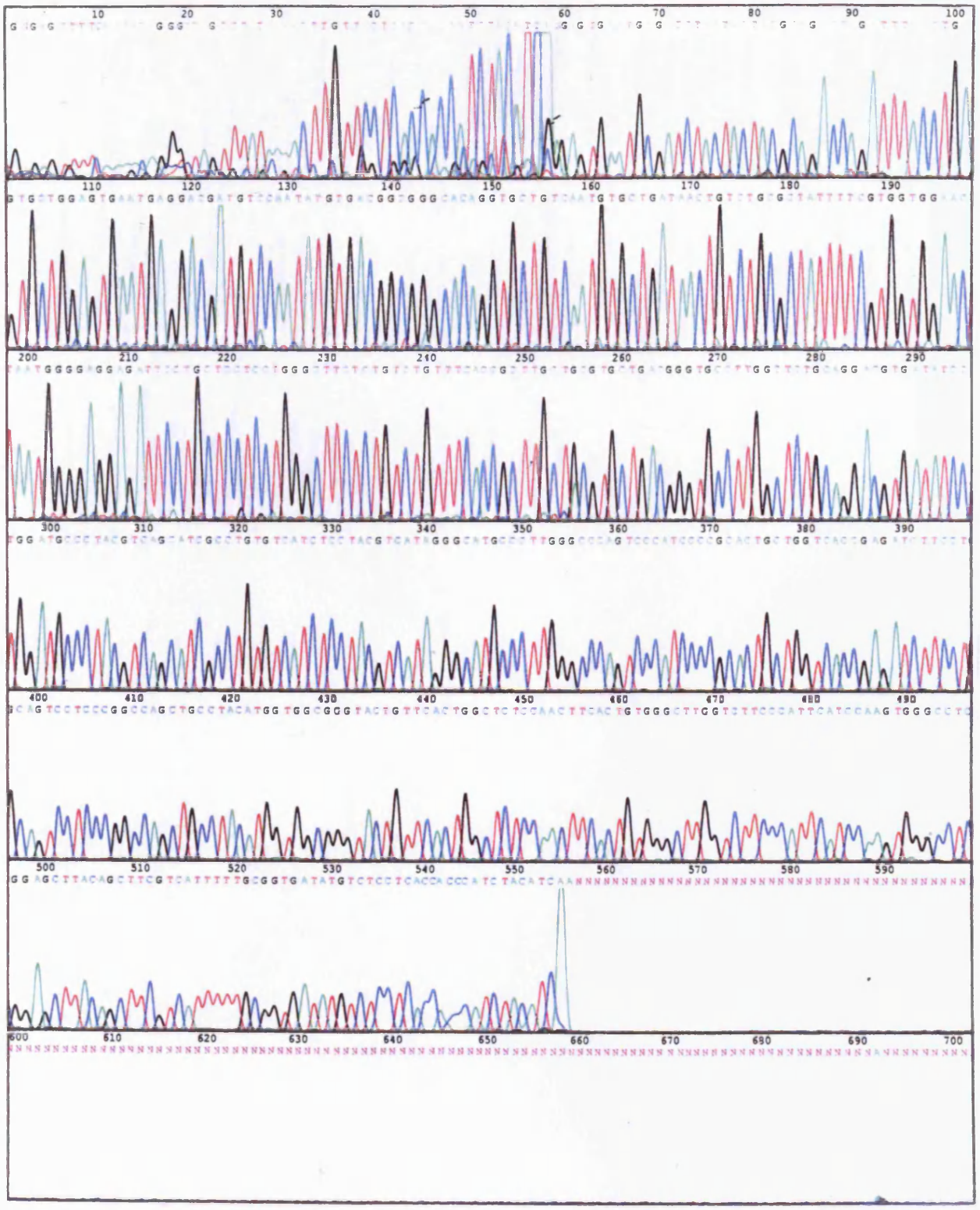

Sequencing output in ABI format of GLUT5 mRNA expressed in kidney sample.

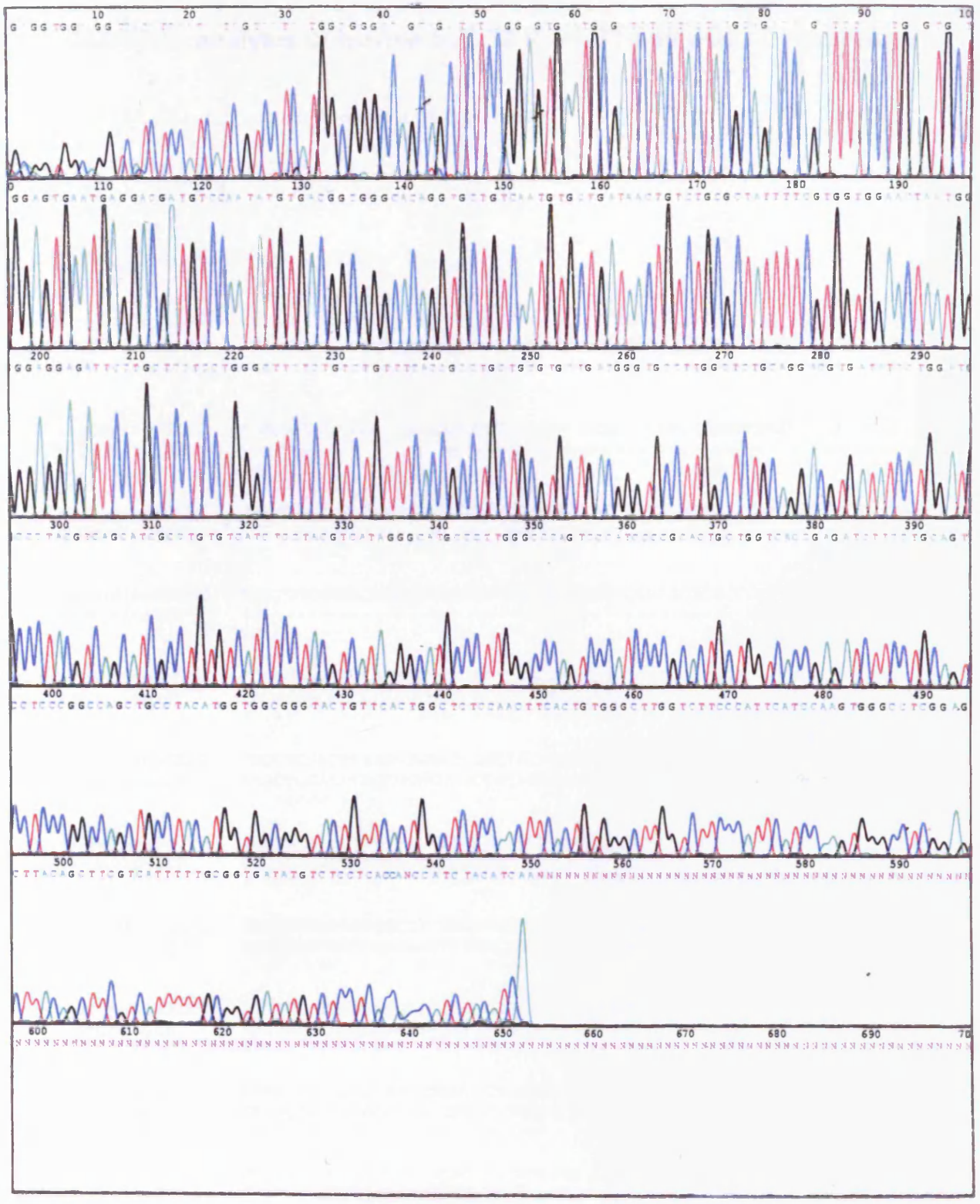

Sequencing output in ABI format of GLUT5 mRNA expressed in the ciliary process.

Appendix IV

CLUSTAL analysis of bovine SGLT2-like EST and SGLT2 sequences

```
CLUSTAL W (1.82) Multiple Sequence Alignments

Sequence format is Pearson
Sequence 1: AV208941BovineSGLT2     2275 bp
Sequence 2: AV605490BovineEST        553 bp

Sequences (1:2) Aligned. Score:  40


AV208941BovineSGLT2   AGATCGTGGGCAGAATGGAGGAGCACACAGAGGCAGGCTCAGCACCAGTGCTGGGGGAAC 60
AV605490BovineEST     ------------------------------------------------------------


AV208941BovineSGLT2   AGAAGGCTCTAATTGACAATCCTGCTGACATCCTAGTCATCGCTGCTTATTTCCTGCTGG 120
AV605490BovineEST     ------------------------------------------------------------


AV208941BovineSGLT2   TCATTGGTGTCGGCTTGTGGTCCATGTGCAGAACCAACAGAGGCACCGTCGGCGGCTACT 180
AV605490BovineEST     ------------------------------------------------------------


AV208941BovineSGLT2   TCCTGGCGGGACGGAACATGGTGTGGTGGCCGGTCGGGGCCTCTCTCTTTGCCAGCAACA 240
AV605490BovineEST     ------------------------------------------------------------C 1


AV208941BovineSGLT2   TCGGCAGTGGCCACTTCGTGGGCCTGGCAGGGAC---CGGTGCGGCGAGCGGCCTGGCGG 297
AV605490BovineEST     CACGCGTCCGCCCACGCGTCCGCCTTACAGGATCACCTCCTTCTGTTACACACACGAGAA 61
                        **    ***    ***  ****  ****  *      * * *  *    *  *


AV208941BovineSGLT2   TGGCTGGATTTGAGTGGAATGCACTGTTCGTGGTCCTGCTACTTGGGTGGCTCTTCGTGC 357
AV605490BovineEST     AACCTGGACTTAGAGGAGGGCCTGTAGTGGAGGTCCTACA--CTGGGGGGCACCTGGCAT 119
                        ***** **    *     *  *  * * ****** *    **** *** * * *


AV208941BovineSGLT2   CAGTGTA-CCTGACTGCCGGCGTCATCACCATGCCGCAGTACCTGCGAAAGCGCTTCGGC 416
AV605490BovineEST     CCGTGAAGCCCCAAACTCAGCCCCACTGTGCTCACCCAG-ACCTGC-------CTCCTGA 171
                      * *** * **  *    * **  **      *  * *** ******       ** * *


AV208941BovineSGLT2   GGCCATCGTATCCGCCTCTACTTGTCCGTGCTCTCGCTTTTTCTGTACATCTTCACCAAG 476
AV605490BovineEST     CGCCGGAGTG-CAGGAGCTCGGAGAATGGGCCATCA-TTTTGAAATCTGCCCTCCAGGAA 229
                       ***   **  * *   **    *   * **  **  ****    *    * **    *


AV208941BovineSGLT2   ATTTCGGTGGACATGTTCTCCGGGGCAGTATTCATTCAACAGGCTCTGGGCTGGAACA-T 535
AV605490BovineEST     AATTAATTGGAAA--------GGGGGAATCCTTTTCCA----GTTCCCCGCAAAGACAGT 277
                      * **   **** *        **** * *  *  * **    * **   **    *** *


AV208941BovineSGLT2   CTATGCCTCCGTCATCGCGCTCCTGGGCATCACCA--TGATCTACACTG-TGACAGGAGG 592
AV605490BovineEST     CTATGTACTAGAGGCAGCCTGTCTGGGCTGTGCCCCCTGACCCAGGCCGGTTGCAGGAGG 337
                      *****     *     **    ******    **   *** * *  * * *  *******


AV208941BovineSGLT2   GCTGGCGGCACTGATGTACACGGACACGGTGCAGACCTTCGTCATTCTCGCCGGGGCCTT 652
AV605490BovineEST     GCTGGCGGCACTGATGTACACGGACACGGTGCAGACCTTCGTCATTCTCGCCGGGGCCTT 397
                      ************************************************************


AV208941BovineSGLT2   CGTCCTCATGGGTTACGCCTTCCACGAGGTGGGCGGGTATTCGGGGCTTTTCGACAAATA 712
AV605490BovineEST     CGTCCTCATGGGTTACGCCTTCCACGAGGTGGGCGGGTATTCGGGGCTTTTCGACAAATA 457
                      ************************************************************
```

```
AV208941BovineSGLT2   CTTGCGGGCAGTGACGTCCCTGACGGTATCCGAGGATCCGGCCGTGGGCAACATCTCCAG 772
AV605490BovineEST     CTTGCGGGCAGTGACGTCCCTGACGGTATCCGAGGATCCGGCCGTGGGCAACATCTCCAG 517
                      ************************************************************

AV208941BovineSGLT2   CTCCTGCTAT-CGACCCCGGCCGGACTCCTACCACCTGCTCCGGGACCCTGTGACGGGGG 831
AV605490BovineEST     CTCCTGCTATTCGACCCCGGCCGGACTCCTACCACT----------------------- 553
                      ********** ************************

AV208941BovineSGLT2   ACCTGCCATGGCCCGCGCTGCTTCTGGGGCTTACTATCGTGTCCAGCTGGTACTGGTGCA 891
AV605490BovineEST     ------------------------------------------------------------

AV208941BovineSGLT2   GCGACCAGGTTATAGTGCAGCGCTGCCTGGCTGGGAAAAACCTCACCCACATCAAGGCGG 951
AV605490BovineEST     ------------------------------------------------------------

AV208941BovineSGLT2   GCTGCATCCTGTGCGGCTACTTGAAGCTGATGCCCATGTTCCTCATGGTCATGCCTGGAA 1011
AV605490BovineEST     ------------------------------------------------------------

AV208941BovineSGLT2   TGATCAGCCGCGTTCTTTACCCGGACGAAGTGGCGTGCGTGGTGCCCGAGGTGTGTAAGC 1071
AV605490BovineEST     ------------------------------------------------------------

AV208941BovineSGLT2   GCGTGTGCGGCACCGAGGTGGGCTGCTCCAATATCGCCTACCCGCGGCTCGTCGTGAAGC 1131
AV605490BovineEST     ------------------------------------------------------------

AV208941BovineSGLT2   TCATGCCCAATGGTCTGCGCGGACTCATGCTGGCGGTCATGCTGGCGGCGCTCATGTCCT 1191
AV605490BovineEST     ------------------------------------------------------------

AV208941BovineSGLT2   CGCTGGCCTCCATCTTCAACAGCAGCAGCACACTCTTCACCATGGACATCTACACGCGCC 1251
AV605490BovineEST     ------------------------------------------------------------

AV208941BovineSGLT2   TGCGGCCCCGCGCGGGCGACCGCGAGCTGCTGCTAGTAGGACGGCTCTGGGTGGTGTTCA 1311
AV605490BovineEST     ------------------------------------------------------------

AV208941BovineSGLT2   TCGTGGCCGTGTCGGTGGCCTGGCTGCCCGTGGTGCAGGCGGCGCAGGGCGGGCAGCTCT 1371
AV605490BovineEST     ------------------------------------------------------------

AV208941BovineSGLT2   TCGATTACATCCAGTCGGTCTCCAGCTACCTGGCGCCGCCGGTGTCGGCCGTCTTCGTGT 1431
AV605490BovineEST     ------------------------------------------------------------

AV208941BovineSGLT2   TGGCGCTCTTCGTGCCCCGCGTCAACGAGAAGGGCGCCTTCTGGGGACTGATCGGGGGCC 1491
AV605490BovineEST     ------------------------------------------------------------


AV208941BovineSGLT2   TGCTGATGGGCCTGGCACGCCTGGTTCCCGAGTTCTCCTTCGGCTCCGGCAGCTGCGTGC 1551
AV605490BovineEST     ------------------------------------------------------------

AV208941BovineSGLT2   GCCCCTCCGGGTGCCCGGCTCTCCTCTGCCGCGTCCACTACCTCTACTTCGCCATCCTGC 1611
AV605490BovineEST     ------------------------------------------------------------

AV208941BovineSGLT2   TCTTCGTCTGCTCCGGCCTCCTCACCCTCGTGGTCTCACTGTGCACACCGCCCATTCCGC 1671
AV605490BovineEST     ------------------------------------------------------------
```

```
AV208941BovineSGLT2   GCAAGCACCTCTACCGCCTGGTTTTCAGTCTCCGGCACAGCAAGGAAGAGAGGGAGGACC 1731
AV605490BovineEST     ------------------------------------------------------------

AV208941BovineSGLT2   TGGATGCTGAGGAGCTAGAAGGTCCAACCGCAGCCCCCGTGCAGAACGGGCGCCCTGAGC 1791
AV605490BovineEST     ------------------------------------------------------------

AV208941BovineSGLT2   ACGCAGTGGAGATGGAGGCGCCCCCGCCCCCAAGGCCAGGCCTGTTGCGGCAGTGCCTGC 1851
AV605490BovineEST     ------------------------------------------------------------

AV208941BovineSGLT2   TCTGGTTCTGTGGCGTGAGCAGGGGTGGGGTGGGCAGCCCCCAACGCCCTACCCAGGAGG 1911
AV605490BovineEST     ------------------------------------------------------------

AV208941BovineSGLT2   AGACGACTGCTGCAGCCAGGCGGCTGGAGGACATCAGTGAGGACCCACGCTGGGCCCGCG 1971
AV605490BovineEST     ------------------------------------------------------------

AV208941BovineSGLT2   TGGTCAACCTCAACGCCCTGCTCATGATGGCCGTGGCCACATTCCTCTGGGGCTTTTATG 2031
AV605490BovineEST     ------------------------------------------------------------

AV208941BovineSGLT2   CCTGAGGCCCACTGCATTGGACACCCTGAGCCACAGCCTTAGATGAGTGGGGGTGGGGAG 2091
AV605490BovineEST     ------------------------------------------------------------

AV208941BovineSGLT2   CCAGCGGCGGTGAGAAGGGCCTGGGGCCAGAGAGTAGAGGGGAGGCCCCGGGACCCCTAC 2151
AV605490BovineEST     ------------------------------------------------------------

AV208941BovineSGLT2   TCTCTGCCTTGTTTCTGCCTGGGACCCAGTCCATAGCCACACCCTGTGAGGCCTTGGCCA 2211
AV605490BovineEST     ------------------------------------------------------------

AV208941BovineSGLT2   GCTGGCCACTGTAGTTCCCCTAAGAACAAATAAAGCTGCCTTGCCTAGTCAAAAAAAAAA 2271
AV605490BovineEST     ------------------------------------------------------------

AV208941BovineSGLT2   AAAA 2275
AV605490BovineEST     ----
```

The sequences highlighted in red were primers designed according to the bovine EST sequence, while those highlighted in yellow are primers for the real SGLT2 gene.

Appendix V

List of publications

Paper

To, C.H., Kong, C.W., **Chan, C.Y.**, Shahidullah, M. and Do, C.W. (2002). The mechanism of aqueous humour formation. *Clin Exp Optom*; **85**(6): 335-49.

Conference abstracts

1. Law C.S., **Chan C.Y.**, Candia O.A., To C.H. (2005). Fluid Transport Across Porcine Ciliary Body Epithelium. ARVO, Florida.

2. **Chan, C.Y.**, Guggenheim, J.A. and To, C.H. (2004). mRNA expression of glucose transporters in the bovine ciliary body/ epithelium (CBE). ARVO, Florida.

3. **Chan, C.Y.**, Guggenheim, J.A. and To, C.H. (2004). Glucose transport kinetics in the bovine ciliary epithelium. *Ophthal Physiol Opt*, 24 (2); p. 3. (British Congress of Optometry and Vision Science (BCOVS) 2003, Birmingham).

4. **Chan, C.Y.**, To, C.Y., Zamudio, A.C. and Candia, O.A. (2003). Measurement of aqueous humor formation rate using a modified Ussing-type chamber by capillary method. ARVO, Florida.

5. **Chan, C.Y.** and To, C.H. (2003). Glucose transport kinetics in the bovine ciliary epithelium. SERI-ARVO, Singapore.

6. **Chan, C.Y.** and To, C.H. (2002). Glucose Transport in the Bovine Ciliary Body Epithelium (CBE). ARVO, Florida.

References

Abdel-Latif, A.A. (1997). *Biochemistry of the eye.* London: Chapman & Hall Medical.

Abe, H., Kawakit, Y., Hodate, K. and Saito, M. (2001). Postnatal development of glucose transporter proteins in bovine skeletal muscle and adipose tissue. *J Vet Med Sci*; **63**(10): 1071-5.

Abel, E.D. (2004). Glucose transport in the heart. *Front Biosci*; **9**: 201-15.

Abel, E.D., Peroni, O., Kim, J.K., Kim, Y.B., Boss, O. *et al.* (2001). Adipose-selective targeting of the GLUT4 gene impairs insulin action in muscle and liver. *Nature*; **409**(6821): 729-33.

Adler, A.J. and Southwick, R.E. (1992). Distribution of glucose and lactate in the interphotoreceptor matrix. *Ophthalmic Res*; **24**(4): 243-52.

Adorante, J.S. and Cala, P.M. (1995). Mechanisms of regulatory volume decrease in nonpigmented human ciliary epithelial cells. *Am J Physiol*; **268**(3 Pt 1): C721-31.

Ahmed, N., Battah, S., Karachalias, N., Babaei-Jadidi, R., Horanyi, M. *et al.* (2003). Increased formation of methylglyoxal and protein glycation, oxidation and nitrosation in triosephosphate isomerase deficiency. *Biochim Biophys Acta*; **1639**(2): 121-32.

Aiello, L.P. (1997). Vascular endothelial growth factor. 20th-century mechanisms, 21st-century therapies. *Invest Ophthalmol Vis Sci*; **38**(9): 1647-52.

Aizu, Y., Katayama, H., Takahama, S., Hu, J., Nakagawa, H. *et al.* (2003). Topical instillation of ciliary neurotrophic factor inhibits retinal degeneration in streptozotocin-induced diabetic rats. *Neuroreport*; **14**(16): 2067-71.

Alard, P., Lantz, O., Sebagh, M., Calvo, C.F., Weill, D. *et al.* (1993). A versatile ELISA-PCR assay for mRNA quantitation from a few cells. *Biotechniques*; **15**(4): 730-7.

Alberts, B., Johnson, A., Lewis, J., Raff, M., Roberts, K. *et al.* (2002). Manipulation proteins, DNA and RNA. In: *Molecular Biology of the Cell* (Eds, Alberts, B., Johnson, A., Lewis, J. *et al*). New York: Garland Science, pp. 469-546.

Alcalde, A.I., Barcina, Y., Larralde, J. and Ilundain, A. (1986). Role of calcium in the phloretin effects on sugar transport in rat small intestine. *Rev Esp Fisiol*; **42**(1): 23-8.

Altomare, E., Vendemiale, G., Grattagliano, I., Angelini, P., Micelli-Ferrari, T. *et al.* (1995). Human diabetic cataract: role of lipid peroxidation. *Diabete Metab*; **21**(3): 173-9.

Alvarado, F. (1978). Resolution by graphical methods of the equations for allosteric competitive inhibition and activation in Michaelian enzyme and transport systems. Application to the competitive inhibition of glucose transport in brain by phlorizin and phloretin. *J Physiol (Paris)*; **74**(7): 633-9.

Alvarado, F. and Crane, R.K. (1964). Studies on the Mechanism of Intestinal Absorption of Sugars. Vii.Phenylglycoside Transport and Its Possible Relationship to Phlorizin Inhibition of the Active Transport of Sugars by the Small Intestine. *Biochim Biophys Acta*; **93**: 116-35.

American Diabetes Association (1998). Economic consequences of diabetes mellitus in the U.S. in 1997. *Diabetes Care*; **21**(2): 296-309.

Ames, A., 3rd (1992). Energy requirements of CNS cells as related to their function and to their vulnerability to ischemia: a commentary based on studies on retina. *Can J Physiol Pharmacol*; **70**(Suppl): S158-64.

Amos, A.F., McCarty, D.J. and Zimmet, P. (1997). The rising global burden of diabetes and its complications: estimates and projections to the year 2010. *Diabet Med*; **14**(Suppl 5): S1-85.

Antonetti, D.A., Barber, A.J., Khin, S., Lieth, E., Tarbell, J.M. *et al.* (1998). Vascular permeability in experimental diabetes is associated with reduced endothelial occludin content: vascular endothelial growth factor decreases occludin in retinal endothelial cells. Penn State Retina Research Group. *Diabetes*; **47**(12): 1953-9.

Archer, D.B. (1999). Bowman Lecture 1998. Diabetic retinopathy: some cellular, molecular and therapeutic considerations. *Eye*; **13**(Pt 4): 497-523.

Arguillere, P., Patey, A. and Hirsch, M. (1986). Quantitative analysis of tight junctions during ciliary epithelium development. *Exp Eye Res*; **42**(3): 239-48.

Asano, T., Takata, K., Katagiri, H., Ishihara, H., Inukai, K. *et al.* (1993). The role of N-glycosylation in the targeting and stability of GLUT1 glucose transporter. *FEBS Lett*; **324**(3): 258-61.

Astrup, A. and Finer, N. (2000). Redefining type 2 diabetes: 'diabesity' or 'obesity dependent diabetes mellitus'? *Obes Rev*; **1**(2): 57-9.

Augustin, R., Carayannopoulos, M.O., Dowd, L.O., Phay, J.E., Moley, J.F. *et al.* (2004). Identification and characterization of human glucose transporter-like protein-9 (GLUT9): alternative splicing alters trafficking. *J Biol Chem*; **279**(16): 16229-36.

Augustin, R., Pocar, P., Navarrete-Santos, A., Wrenzycki, C., Gandolfi, F. *et al.* (2001). Glucose transporter expression is developmentally regulated in in vitro derived bovine preimplantation embryos. *Mol Reprod Dev*; **60**(3): 370-6.

Avery, L. (1998). Diabetes mellitus types 1 and 2: an overview. *Nurs Stand*; **13**(8): 35-8.

Bachelard, H.S. (1971). Specificity and kinetic properties of monosaccharide uptake into guinea pig cerebral cortex in vitro. *J Neurochem*; **18**(2): 213-22.

Badr, G.A., Tang, J., Ismail-Beigi, F. and Kern, T.S. (2000). Diabetes downregulates GLUT1 expression in the retina and its microvessels but not in the cerebral cortex or its microvessels. *Diabetes*; **49**(6): 1016-21.

Badr, G.A., Zhang, J.Z., Tang, J., Kern, T.S. and Ismail-Beigi, F. (1999). Glut1 and glut3 expression, but not capillary density, is increased by cobalt chloride in rat cerebrum and retina. *Brain Res Mol Brain Res*; **64**(1): 24-33.

Baldwin, S.A. (1993). Mammalian passive glucose transporters: members of an ubiquitous family of active and passive transport proteins. *Biochim Biophys Acta*; **1154**(1): 17-49.

Baly, D.L. and Horuk, R. (1988). The biology and biochemistry of the glucose transporter. *Biochim Biophys Acta*; **947**(3): 571-90.

Ban, Y. and Rizzolo, L.J. (1997). A culture model of development reveals multiple properties of RPE tight junctions. *Mol Vis*; **3**: 18.

Ban, Y. and Rizzolo, L.J. (2000). Regulation of glucose transporters during development of the retinal pigment epithelium. *Brain Res Dev Brain Res*; **121**(1): 89-95.

Bandyopadhyay, G., Sajan, M.P., Kanoh, Y., Standaert, M.L., Burke, T.R., Jr. *et al.* (2000). Glucose activates mitogen-activated protein kinase (extracellular signal-regulated kinase) through proline-rich tyrosine kinase-2 and the Glut1 glucose transporter. *J Biol Chem*; **275**(52): 40817-26.

Barber, A.J., Lieth, E., Khin, S.A., Antonetti, D.A., Buchanan, A.G. *et al.* (1998). Neural apoptosis in the retina during experimental and human diabetes. Early onset and effect of insulin. *J Clin Invest*; **102**(4): 783-91.

Bayer, E.A., Ben-Hur, H. and Wilchek, M. (1987). Enzyme-based detection of glycoproteins on blot transfers using avidin-biotin technology. *Anal Biochem*; **161**(1): 123-31.

Bazzoni, G. and Dejana, E. (2004). Endothelial cell-to-cell junctions: molecular organization and role in vascular homeostasis. *Physiol Rev*; **84**(3): 869-901.

Bell, G.I., Burant, C.F., Takeda, J. and Gould, G.W. (1993). Structure and function of mammalian facilitative sugar transporters. *J Biol Chem*; **268**(26): 19161-4.

Bell, G.I., Kayano, T., Buse, J.B., Burant, C.F., Takeda, J. *et al.* (1990). Molecular biology of mammalian glucose transporters. *Diabetes Care*; **13**(3): 198-208.

Bennett, M.V., Barrio, L.C., Bargiello, T.A., Spray, D.C., Hertzberg, E. *et al.* (1991). Gap junctions: new tools, new answers, new questions. *Neuron*; **6**(3): 305-20.

Benson, D.A., Boguski, M.S., Lipman, D.J., Ostell, J., Ouellette, B.F. *et al.* (1999). GenBank. *Nucleic Acids Res*; **27**(1): 12-7.

Berger, J., Biswas, C., Vicario, P.P., Strout, H.V., Saperstein, R. *et al.* (1989). Decreased expression of the insulin-responsive glucose transporter in diabetes and fasting. *Nature*; **340**(6228): 70-2.

Bergersen, L., Johannsson, E., Veruki, M.L., Nagelhus, E.A., Halestrap, A. *et al.* (1999). Cellular and subcellular expression of monocarboxylate transporters in the pigment epithelium and retina of the rat. *Neuroscience*; **90**(1): 319-31.

Berry, G.T., Mallee, J.J., Kwon, H.M., Rim, J.S., Mulla, W.R. *et al.* (1995). The human osmoregulatory Na+/myo-inositol cotransporter gene (SLC5A3): molecular cloning and localization to chromosome 21. *Genomics*; **25**(2): 507-13.

Betz, A.L., Drewes, L.R. and Gilboe, D.D. (1975). Inhibition of glucose transport into brain by phlorizin, phloretin and glucose analogues. *Biochim Biophys Acta*; **406**(4): 505-15.

Beyer-Mears, A., Mistry, K., Diecke, F.P. and Cruz, E. (1996). Zopolrestat prevention of proteinuria, albuminuria and cataractogenesis in diabetes mellitus. *Pharmacology*; **52**(5): 292-302.

Bildin, V.N., Iserovich, P., Fischbarg, J. and Reinach, P.S. (2001). Differential expression of Na:K:2Cl cotransporter, glucose transporter 1, and aquaporin 1 in freshly isolated and cultured bovine corneal tissues. *Exp Biol Med (Maywood)*; **226**(10): 919-26.

Bill, A. (1986). The blood-aqueous barrier. *Trans Ophthalmol Soc U K*; **105**(Pt 2): 149-55.

Bill, A., Tornquist, P. and Alm, A. (1980). Permeability of the intraocular blood vessels. *Trans Ophthalmol Soc U K*; **100**(3): 332-6.

Birnbaum, M.J. (1989). Identification of a novel gene encoding an insulin-responsive glucose transporter protein. *Cell*; **57**(2): 305-15.

Birnbaum, M.J. (1992). The insulin-sensitive glucose transporter. *Int Rev Cytol*; **137**: 239-97.

Bloch, R. (1973). Inhibition of glucose transport in the human erythrocyte by cytochalasin B. *Biochemistry*; **12**(23): 4799-801.

Bluemink, J.G. (1971). Cytokinesis and cytochalasin-induced furrow regression in the first-cleavage zygote of Xenopus laevis. *Z Zellforsch Mikrosk Anat*; **121**(1): 102-26.

Boado, R.J. and Pardridge, W.M. (1990). The brain-type glucose transporter mRNA is specifically expressed at the blood-brain barrier. *Biochem Biophys Res Commun*; **166**(1): 174-9.

Boado, R.J. and Pardridge, W.M. (1993). Glucose deprivation causes posttranscriptional enhancement of brain capillary endothelial glucose transporter gene expression via GLUT1 mRNA stabilization. *J Neurochem*; **60**(6): 2290-6.

Boado, R.J. and Pardridge, W.M. (2002). Glucose deprivation and hypoxia increase the expression of the GLUT1 glucose transporter via a specific mRNA cis-acting regulatory element. *J Neurochem*; **80**(3): 552-4.

Boileau, P., Mrejen, C., Girard, J. and Hauguel-de Mouzon, S. (1995). Overexpression of GLUT3 placental glucose transporter in diabetic rats. *J Clin Invest*; **96**(1): 309-17.

Bonnefont-Rousselot, D., Bastard, J.P., Jaudon, M.C. and Delattre, J. (2000). Consequences of the diabetic status on the oxidant/antioxidant balance. *Diabetes Metab*; **26**(3): 163-76.

Bosch, R.R., Janssen, S.W., Span, P.N., Olthaar, A., van Emst-de Vries, S.E. *et al.* (2003). Exploring levels of hexosamine biosynthesis pathway intermediates and protein kinase C isoforms in muscle and fat tissue of Zucker Diabetic Fatty rats. *Endocrine*; **20**(3): 247-52.

Bowler, J.M., Peart, D., Purves, R.D., Carre, D.A., Macknight, A.D. *et al.* (1996). Electron probe X-ray microanalysis of rabbit ciliary epithelium. *Exp Eye Res*; **62**(2): 131-9.

Brekkan, E., Lundqvist, A. and Lundahl, P. (1996). Immobilized membrane vesicle or proteoliposome affinity chromatography. Frontal analysis of interactions of cytochalasin B and D-glucose with the human red cell glucose transporter. *Biochemistry*; **35**(37): 12141-5.

Breslauer, K.J., Frank, R., Blocker, H. and Marky, L.A. (1986). Predicting DNA duplex stability from the base sequence. *Proc Natl Acad Sci U S A*; **83**(11): 3746-50.

Brown, G.K. (2000). Glucose transporters: structure, function and consequences of deficiency. *J Inherit Metab Dis*; **23**(3): 237-46.

Brownlee, M. (1995). Advanced protein glycosylation in diabetes and aging. *Annu Rev Med*; **46**: 223-34.

Brownlee, M. (2001). Biochemistry and molecular cell biology of diabetic complications. *Nature*; **414**(6865): 813-20.

Bruch, R.C. and White, H.B., 3rd (1982). Compositional and structural heterogeneity of avidin glycopeptides. *Biochemistry*; **21**(21): 5334-41.

Bryant, N.J., Govers, R. and James, D.E. (2002). Regulated transport of the glucose transporter GLUT4. *Nat Rev Mol Cell Biol*; **3**(4): 267-77.

Burant, C.F. and Davidson, N.O. (1994). GLUT3 glucose transporter isoform in rat testis: localization, effect of diabetes mellitus, and comparison to human testis. *Am J Physiol*; **267**(6 Pt 2): R1488-95.

Burant, C.F., Sivitz, W.I., Fukumoto, H., Kayano, T., Nagamatsu, S. *et al.* (1991). Mammalian glucose transporters: structure and molecular regulation. *Recent Prog Horm Res*; **47**: 349-87; discussion 387-8.

Burant, C.F., Takeda, J., Brot-Laroche, E., Bell, G.I. and Davidson, N.O. (1992). Fructose transporter in human spermatozoa and small intestine is GLUT5. *J Biol Chem*; **267**(21): 14523-6.

Burg, M.B. (1995). Molecular basis of osmotic regulation. *Am J Physiol*; **268**(6 Pt 2): F983-96.

Burns, E.L. and Price, E.M. (1993). Random mutagenesis of the sheep Na,K-ATPase alpha-1 subunit generates a novel T797N mutation that results in a ouabain-resistant enzyme. *J Biol Chem*; **268**(34): 25632-5.

Busik, J.V., Olson, L.K., Grant, M.B. and Henry, D.N. (2002). Glucose-induced activation of glucose uptake in cells from the inner and outer blood-retinal barrier. *Invest Ophthalmol Vis Sci*; **43**(7): 2356-63.

Candia, O.A., Zamudio, A.C., Polikoff, L.A. and Alvarez, L.J. (2002). Distribution of acetylcholine-sensitive currents around the rabbit crystalline lens. *Exp Eye Res*; **74**(6): 769-76.

Cao, X. and Phillis, J.W. (1995). The free radical scavenger, alpha-lipoic acid, protects against cerebral ischemia-reperfusion injury in gerbils. *Free Radic Res*; **23**(4): 365-70.

Caprioli, J. (1992). The ciliary epithelia and aqueous humor. In: *Adler's Physiology of the Eye: Clinical Application* (Eds, Hart, W.M. and Alder, F.H.). St. Louis: Mosby Year Book, pp. 228-247.

Carayannopoulos, M.O., Chi, M.M., Cui, Y., Pingsterhaus, J.M., McKnight, R.A. *et al.* (2000). GLUT8 is a glucose transporter responsible for insulin-stimulated glucose uptake in the blastocyst. *Proc Natl Acad Sci U S A*; **97**(13): 7313-8.

Carre, D.A., Tang, C.S., Krupin, T. and Civan, M.M. (1992). Effect of bicarbonate on intracellular potential of rabbit ciliary epithelium. *Curr Eye Res*; **11**(7): 609-24.

Carruthers, A. (1990). Facilitated diffusion of glucose. *Physiol Rev*; **70**(4): 1135-76.

Castello, A., Rodriguez-Manzaneque, J.C., Camps, M., Perez-Castillo, A., Testar, X. *et al.* (1994). Perinatal hypothyroidism impairs the normal transition of GLUT4 and GLUT1 glucose transporters from fetal to neonatal levels in heart and brown adipose tissue. Evidence for tissue-specific regulation of GLUT4 expression by thyroid hormone. *J Biol Chem*; **269**(8): 5905-12.

Castro, M., Caprile, T., Astuya, A., Millan, C., Reinicke, K. *et al.* (2001). High-affinity sodium-vitamin C co-transporters (SVCT) expression in embryonic mouse neurons. *J Neurochem*; **78**(4): 815-23.

Chakrabarti, S., Cukiernik, M., Hileeto, D., Evans, T. and Chen, S. (2000). Role of vasoactive factors in the pathogenesis of early changes in diabetic retinopathy. *Diabetes Metab Res Rev*; **16**(6): 393-407.

Chan, V. (1992). Extraction of nucleic acids from clinical samples and cultured cells. In: *Diagnostic Molecular Pathology. A Practical Approach.* (Eds, Herrington, C. and Mcgee, J.D.). Oxford: Oxford University Press, pp. 1-23.

Charron, M.J. and Kahn, B.B. (1990). Divergent molecular mechanisms for insulin-resistant glucose transport in muscle and adipose cells in vivo. *J Biol Chem*; **265**(14): 7994-8000.

Chellan, P. and Nagaraj, R.H. (1999). Protein crosslinking by the Maillard reaction: dicarbonyl-derived imidazolium crosslinks in aging and diabetes. *Arch Biochem Biophys*; **368**(1): 98-104.

Chin, E., Zamah, A.M., Landau, D., Gronbcek, H., Flyvbjerg, A. *et al.* (1997). Changes in facilitative glucose transporter messenger ribonucleic acid levels in the diabetic rat kidney. *Endocrinology*; **138**(3): 1267-75.

Choeiri, C., Staines, W. and Messier, C. (2002). Immunohistochemical localization and quantification of glucose transporters in the mouse brain. *Neuroscience*; **111**(1): 19-34.

Chomczynski, P. and Sacchi, N. (1987). Single-step method of RNA isolation by acid guanidinium thiocyanate-phenol-chloroform extraction. *Anal Biochem*; **162**(1): 156-9.

Chou, Q., Russell, M., Birch, D.E., Raymond, J. and Bloch, W. (1992). Prevention of pre-PCR mis-priming and primer dimerization improves low-copy-number amplifications. *Nucleic Acids Res*; **20**(7): 1717-23.

Chu, T.C. and Candia, O.A. (1987a). Electrically silent Na+ and Cl- fluxes across the rabbit ciliary epithelium. *Invest Ophthalmol Vis Sci*; **28**(3): 445-50.

Chu, T.C. and Candia, O.A. (1988). Active transport of ascorbate across the isolated rabbit ciliary epithelium. *Invest Ophthalmol Vis Sci*; **29**(4): 594-9.

Chu, T.C., Candia, O.A. and Podos, S.M. (1987b). Electrical parameters of the isolated monkey ciliary epithelium and effects of pharmacological agents. *Invest Ophthalmol Vis Sci*; **28**(10): 1644-8.

Chylack, L.T., Jr. and Cheng, H.M. (1978). Sugar metabolism in the crystalline lens. *Surv Ophthalmol*; **23**(1): 26-37.

Ciulla, T.A., Amador, A.G. and Zinman, B. (2003). Diabetic retinopathy and diabetic macular edema: pathophysiology, screening, and novel therapies. *Diabetes Care*; **26**(9): 2653-64.

Ciulla, T.A., Harris, A., Latkany, P., Piper, H.C., Arend, O. *et al.* (2002). Ocular perfusion abnormalities in diabetes. *Acta Ophthalmol Scand*; **80**(5): 468-77.

Civan, M.M., Coca-Prados, M. and Peterson-Yantorno, K. (1996). Regulatory volume increase of human non-pigmented ciliary epithelial cells. *Exp Eye Res*; **62**(6): 627-40.

Clarke, P., Gray, A., Legood, R., Briggs, A. and Holman, R. (2003). The impact of diabetes-related complications on healthcare costs: results from the United Kingdom Prospective Diabetes Study (UKPDS Study No. 65). *Diabet Med*; **20**(6): 442-50.

Clow, K.A., Rodnick, K.J., MacCormack, T.J. and Driedzic, W.R. (2004). The regulation and importance of glucose uptake in the isolated Atlantic cod heart: rate-limiting steps and effects of hypoxia. *J Exp Biol*; **207**(Pt 11): 1865-74.

Coady, M.J., Wallendorff, B., Gagnon, D.G. and Lapointe, J.Y. (2002). Identification of a novel Na+/myo-inositol cotransporter. *J Biol Chem*; **277**(38): 35219-24.

Coca-Prados, M., Anguita, J., Chalfant, M.L. and Civan, M.M. (1995). PKC-sensitive Cl-channels associated with ciliary epithelial homologue of pICln. *Am J Physiol*; **268**(3 Pt 1): C572-9.

Coca-Prados, M., Ghosh, S., Gilula, N.B. and Kumar, N.M. (1992). Expression and cellular distribution of the alpha 1 gap junction gene product in the ocular pigmented ciliary epithelium. *Curr Eye Res*; **11**(2): 113-22.

Cole, D. (1966). Aqueous humour formation. *Doc Ophthalmol*; **21**: 116-238.

Cole, D.F. (1984). Ocular fluids. In: *The eye* (Ed, Davson, H.). New York and London: Academic Press, Inc.

Collins, T. and Cybulsky, M.I. (2001). NF-kappaB: pivotal mediator or innocent bystander in atherogenesis? *J Clin Invest*; **107**(3): 255-64.

Cornford, E.M., Hyman, S., Cornford, M.E. and Clare-Salzler, M. (1995). Down-regulation of blood-brain glucose transport in the hyperglycemic nonobese diabetic mouse. *Neurochem Res*; **20**(7): 869-73.

Cox, K.H., DeLeon, D.V., Angerer, L.M. and Angerer, R.C. (1984). Detection of mrnas in sea urchin embryos by in situ hybridization using asymmetric RNA probes. *Dev Biol*; **101**(2): 485-502.

Cramer, S.C., Pardridge, W.M., Hirayama, B.A. and Wright, E.M. (1992). Colocalization of GLUT2 glucose transporter, sodium/glucose cotransporter, and gamma-glutamyl transpeptidase in rat kidney with double-peroxidase immunocytochemistry. *Diabetes*; **41**(6): 766-70.

Craven, P.A., Studer, R.K. and DeRubertis, F.R. (1994). Impaired nitric oxide-dependent cyclic guanosine monophosphate generation in glomeruli from diabetic rats. Evidence for protein kinase C-mediated suppression of the cholinergic response. *J Clin Invest*; **93**(1): 311-20.

Crone, C. (1965). Facilitated transfer of glucose from blood into brain tissue. *J Physiol*; **181**(1): 103-13.

Crook, R.B., Takahashi, K., Mead, A., Dunn, J.J. and Sears, M.L. (2000). The role of NaKCl cotransport in blood-to-aqueous chloride fluxes across rabbit ciliary epithelium. *Invest Ophthalmol Vis Sci*; **41**(9): 2574-83.

Crosson, C.E. and Pautler, E.L. (1982). Glucose transport across isolated bovine pigment epithelium. *Exp Eye Res*; **35**(4): 371-7.

Cruzado, J.M., Lloberas, N., Torras, J., Riera, M., Fillat, C. *et al.* (2004). Regression of advanced diabetic nephropathy by hepatocyte growth factor gene therapy in rats. *Diabetes*; **53**(4): 1119-27.

Cunha-Vaz, J. (1979). The blood-ocular barriers. *Surv Ophthalmol*; **23**(5): 279-96.

Darbre, P. (1999). RNA anaylsis by Northern blotting. In: *Basic Molecular Biology* (Ed, Darbre, P.). Chichester: John Wiley & Sons Ltd., pp. 119-123.

Das, U.N. (1999). GLUT-4, tumor necrosis factor, essential fatty acids and daf-genes and their role in insulin resistance and non-insulin dependent diabetes mellitus. *Prostaglandins Leukot Essent Fatty Acids*; **60**(1): 13-20.

Davidson, N.O., Hausman, A.M., Ifkovits, C.A., Buse, J.B., Gould, G.W. *et al.* (1992). Human intestinal glucose transporter expression and localization of GLUT5. *Am J Physiol*; **262**(3 Pt 1): C795-800.

Davson, H. (1990). *Physiology of the eye.* London: Macmillan Press.

Dawson, P.A., Mychaleckyj, J.C., Fossey, S.C., Mihic, S.J., Craddock, A.L. *et al.* (2001). Sequence and functional analysis of GLUT10: a glucose transporter in the Type 2 diabetes-linked region of chromosome 20q12-13.1. *Mol Genet Metab*; **74**(1-2): 186-99.

De Martin, R., Hoeth, M., Hofer-Warbinek, R. and Schmid, J.A. (2000). The transcription factor NF-kappa B and the regulation of vascular cell function. *Arterioscler Thromb Vasc Biol*; **20**(11): E83-8.

De Vivo, D.C., Trifiletti, R.R., Jacobson, R.I., Ronen, G.M., Behmand, R.A. *et al.* (1991). Defective glucose transport across the blood-brain barrier as a cause of persistent hypoglycorrhachia, seizures, and developmental delay. *N Engl J Med*; **325**(10): 703-9.

Derham, B.K. and Harding, J.J. (1999). Alpha-crystallin as a molecular chaperone. *Prog Retin Eye Res*; **18**(4): 463-509.

Dernouchamps, J.P. and Heremans, J.F. (1975). Molecular sieve effect of the blood-aqueous barrier. *Exp Eye Res*; **21**(3): 289-97.

Despopoulos, A. (1966). Glucose transport in hamster intestine: inhibition by glucosides. *Am J Physiol*; **211**(6): 1329-33.

Di Benedetto, A., Aragona, P., Romano, G., Romeo, G., Di Cesare, E. *et al.* (1999). Age and metabolic control influence lens opacity in type I, insulin-dependent diabetic patients. *J Diabetes Complications*; **13**(3): 159-62.

Diabetes UK (2004).Diabetes in the UK 2004. [WWW]. <URL: http://www.diabetes.org.uk/infocentre/reports/in_the_UK_2004.doc> [Accessed 28 October 2004].

Diamond, J.M. (1974). Tight and leaky junctions of epithelia: a perspective on kisses in the dark. *Fed Proc*; **33**(11): 2220-4.

Diez-Sampedro, A., Eskandari, S., Wright, E.M. and Hirayama, B.A. (2001). Na+-to-sugar stoichiometry of SGLT3. *Am J Physiol Renal Physiol*; **280**(2): F278-82.

Diez-Sampedro, A., Hirayama, B.A., Osswald, C., Gorboulev, V., Baumgarten, K. *et al.* (2003). A glucose sensor hiding in a family of transporters. *Proc Natl Acad Sci U S A*; **100**(20): 11753-8.

DiMattio, J. (1984a). In vivo entry of glucose analogs into lens and cornea of the rat. *Invest Ophthalmol Vis Sci*; **25**(2): 160-5.

DiMattio, J. and Streitman, J. (1986). Facilitated glucose transport across the retinal pigment epithelium of the bullfrog (Rana catesbeiana). *Exp Eye Res*; **43**(1): 15-28.

DiMattio, J. and Zadunaisky, J.A. (1981). Glucose transport into the ocular compartments of the rat. *Exp Eye Res*; **32**(5): 517-32.

DiMattio, J. and Zadunaisky, J.A. (1982). Glucose transport across ocular barriers of the spiny dogfish, Squalus acanthias. *J Exp Zool*; **219**(2): 197-203.

DiMattio, J. and Zadunaisky, J.A. (1983). Reduced ocular glucose transport and increased non-electrolyte permeability in rats with retinal degeneration (RCS). *Exp Eye Res*; **37**(3): 217-23.

DiMattio, J., Zadunaisky, J.A. and Altszuler, N. (1984b). Onset of changes in glucose transport across ocular barriers in streptozotocin-induced diabetes. *Invest Ophthalmol Vis Sci*; **25**(7): 820-6.

Dimitrakoudis, D., Ramlal, T., Rastogi, S., Vranic, M. and Klip, A. (1992). Glycaemia regulates the glucose transporter number in the plasma membrane of rat skeletal muscle. *Biochem J*; **284 (Pt 2)**: 341-8.

Dimond, R.L. and Loomis, W.F. (1976). Structure and function of beta-blucosidases in Dictyostelium discoideum. *J Biol Chem*; **251**(9): 2680-7.

Do, C.W. and To, C.H. (2000). Chloride secretion by bovine ciliary epithelium: a model of aqueous humor formation. *Invest Ophthalmol Vis Sci*; **41**(7): 1853-60.

Doege, H., Bocianski, A., Joost, H.G. and Schurmann, A. (2000b). Activity and genomic organization of human glucose transporter 9 (GLUT9), a novel member of the family of sugar-transport facilitators predominantly expressed in brain and leucocytes. *Biochem J*; **350**(Pt 3): 771-6.

Doege, H., Bocianski, A., Scheepers, A., Axer, H., Eckel, J. *et al.* (2001). Characterization of human glucose transporter (GLUT) 11 (encoded by SLC2A11), a novel sugar-transport facilitator specifically expressed in heart and skeletal muscle. *Biochem J*; **359**(Pt 2): 443-9.

Doege, H., Schurmann, A., Bahrenberg, G., Brauers, A. and Joost, H.G. (2000a). GLUT8, a novel member of the sugar transport facilitator family with glucose transport activity. *J Biol Chem*; **275**(21): 16275-80.

Doege, H., Schurmann, A., Ohnimus, H., Monser, V., Holman, G.D. *et al.* (1998). Serine-294 and threonine-295 in the exofacial loop domain between helices 7 and 8 of glucose transporters (GLUT) are involved in the conformational alterations during the transport process. *Biochem J*; **329**(Pt 2): 289-93.

Doi, K., Sawada, F., Toda, G., Yamachika, S., Seto, S. *et al.* (2001). Alteration of antioxidants during the progression of heart disease in streptozotocin-induced diabetic rats. *Free Radic Res*; **34**(3): 251-61.

Doi, S., Gemou-Engesaeth, V., Kay, A.B. and Corrigan, C.J. (1994). Polymerase chain reaction quantification of cytokine messenger RNA expression in peripheral blood mononuclear cells of patients with acute exacerbations of asthma: effect of glucocorticoid therapy. *Clin Exp Allergy*; **24**(9): 854-67.

Dollery, C.T., Henkind, P. and Orme, M.L. (1971). Assimilation of D and L I-C-14 glucose into the retina, brain and other tissues. *Diabetes*; **20**(8): 519-21.

Dominguez, C., Ruiz, E., Gussinye, M. and Carrascosa, A. (1998). Oxidative stress at onset and in early stages of type 1 diabetes in children and adolescents. *Diabetes Care*; **21**(10): 1736-42.

Donma, O., Yorulmaz, E., Pekel, H. and Suyugul, N. (2002). Blood and lens lipid peroxidation and antioxidant status in normal individuals, senile and diabetic cataractous patients. *Curr Eye Res*; **25**(1): 9-16.

Dresel, P.E. and Knickle, L. (1987). Cytochalasin-B and phloretin depress contraction and relaxation of aortic smooth muscle. *Eur J Pharmacol*; **144**(2): 153-7.

Drewes, L.R., Horton, R.W., Betz, A.L. and Gilboe, D.D. (1977). Cytochalasin B inhibition of brain glucose transport and the influence of blood components on inhibitor concentration. *Biochim Biophys Acta*; **471**(3): 477-86.

Du, Y., Miller, C.M. and Kern, T.S. (2003). Hyperglycemia increases mitochondrial superoxide in retina and retinal cells. *Free Radic Biol Med*; **35**(11): 1491-9.

Duhaiman, A.S. (1995). Glycation of human lens proteins from diabetic and (nondiabetic) senile cataract patients. *Glycoconj J*; **12**(5): 618-21.

Dunn, J.J., Lytle, C. and Crook, R.B. (2001). Immunolocalization of the Na-K-Cl cotransporter in bovine ciliary epithelium. *Invest Ophthalmol Vis Sci*; **42**(2): 343-53.

Dunn, M.J. (1994). Detection of proteins on blots using the avidin-biotin system. *Methods Mol Biol*; **32**: 227-32.

Dwyer, D.S. (2001). Model of the 3-D structure of the GLUT3 glucose transporter and molecular dynamics simulation of glucose transport. *Proteins*; **42**(4): 531-41.

Dwyer, K.J. and Pardridge, W.M. (1993). Developmental modulation of blood-brain barrier and choroid plexus GLUT1 glucose transporter messenger ribonucleic acid and immunoreactive protein in rabbits. *Endocrinology*; **132**(2): 558-65.

Ebeling, P., Bourey, R., Koranyi, L., Tuominen, J.A., Groop, L.C. *et al.* (1993). Mechanism of enhanced insulin sensitivity in athletes. Increased blood flow, muscle glucose transport protein (GLUT-4) concentration, and glycogen synthase activity. *J Clin Invest*; **92**(4): 1623-31.

Edelman, J.L., Sachs, G. and Adorante, J.S. (1994). Ion transport asymmetry and functional coupling in bovine pigmented and nonpigmented ciliary epithelial cells. *Am J Physiol*; **266**(5 Pt 1): C1210-21.

Eichhorn, M., Bermbach, G., Dermietzel, R. and Lutjen-Drecoll, E. (1993a). Characterization of bovine ciliary pigmented epithelial cells in monolayer culture: an ultrastructural, enzyme histochemical and immunohistochemical study. *Graefes Arch Clin Exp Ophthalmol*; **231**(1): 21-8.

Eichhorn, M. and Lutjen-Drecoll, E. (1993b). Distribution of endothelin-like immunoreactivity in the human ciliary epithelium. *Curr Eye Res*; **12**(8): 753-7.

Eladari, D., Chambrey, R., Pezy, F., Podevin, R.A., Paillard, M. *et al.* (2002). pH dependence of Na+/myo-inositol cotransporters in rat thick limb cells. *Kidney Int*; **62**(6): 2144-51.

Elbrink, J. and Bihler, I. (1972). Characteristics of the membrane transport of sugars in the lens of the eye. *Biochim Biophys Acta*; **282**(1): 337-51.

Elena, P.P., Fredj-Reygrobellet, D., Moulin, G. and Lapalus, P. (1984). Pharmacological characteristics of beta-adrenergic-sensitive adenylate cyclase in non pigmented and in pigmented cells of bovine ciliary process. *Curr Eye Res*; **3**(12): 1383-9.

Ennis, S.R., Johnson, J.E. and Pautler, E.L. (1982). In situ kinetics of glucose transport across the blood-retinal barrier in normal rats and rats with streptozocin-induced diabetes. *Invest Ophthalmol Vis Sci*; **23**(4): 447-56.

Evans, J.L. and Goldfine, I.D. (2000). Alpha-lipoic acid: a multifunctional antioxidant that improves insulin sensitivity in patients with type 2 diabetes. *Diabetes Technol Ther*; **2**(3): 401-13.

Fernandes, R., Suzuki, K. and Kumagai, A.K. (2003). Inner blood-retinal barrier GLUT1 in long-term diabetic rats: an immunogold electron microscopic study. *Invest Ophthalmol Vis Sci*; **44**(7): 3150-4.

Fernandez-Vigo, J., Castro, J. and Macarro, A. (1997). Diabetic iris neovascularization. Natural history and treatment. *Acta Ophthalmol Scand*; **75**(1): 89-93.

Ferraris, R.P. (2001). Dietary and developmental regulation of intestinal sugar transport. *Biochem J*; **360**(Pt 2): 265-76.

Feugeas, J.P., Neel, D., Pavia, A.A., Laham, A., Goussault, Y. *et al.* (1990). Glycosylation of the human erythrocyte glucose transporter is essential for glucose transport activity. *Biochim Biophys Acta*; **1030**(1): 60-4.

Fischbarg, J., Kuang, K.Y., Vera, J.C., Arant, S., Silverstein, S.C. *et al.* (1990). Glucose transporters serve as water channels. *Proc Natl Acad Sci U S A*; **87**(8): 3244-7.

Flier, J.S., Mueckler, M.M., Usher, P. and Lodish, H.F. (1987). Elevated levels of glucose transport and transporter messenger RNA are induced by ras or src oncogenes. *Science*; **235**(4795): 1492-5.

Flugel, C., Lutjen-Drecoll, E., Zadunaisk, J.A. and Wiederholt, M. (1989). Regional differences in the morphology and enzyme distribution of the spiny dogfish (Squalus acanthias) ciliary epithelium. *Exp Eye Res*; **49**(6): 1097-114.

Forbes, J.M., Yee, L.T., Thallas, V., Lassila, M., Candido, R. *et al.* (2004). Advanced glycation end product interventions reduce diabetes-accelerated atherosclerosis. *Diabetes*; **53**(7): 1813-23.

Frank, R.N. (2004). Diabetic retinopathy. *N Engl J Med*; **350**(1): 48-58.

Franke, S., Dawczynski, J., Strobel, J., Niwa, T., Stahl, P. *et al.* (2003). Increased levels of advanced glycation end products in human cataractous lenses. *J Cataract Refract Surg*; **29**(5): 998-1004.

Freddo, T.F. (1984). Intercellular junctions of the iris epithelia in Macaca mulatta. *Invest Ophthalmol Vis Sci*; **25**(9): 1094-104.

Fromter, E. and Diamond, J. (1972). Route of passive ion permeation in epithelia. *Nat New Biol*; **235**(53): 9-13.

Fuhrmann, G.F., Dernedde, S. and Frenking, G. (1992). Phloretin keto-enol tautomerism and inhibition of glucose transport in human erythrocytes (including effects of phloretin on anion transport). *Biochim Biophys Acta*; **1110**(1): 105-11.

Fukumoto, H., Kayano, T., Buse, J.B., Edwards, Y., Pilch, P.F. *et al.* (1989). Cloning and characterization of the major insulin-responsive glucose transporter expressed in human skeletal muscle and other insulin-responsive tissues. *J Biol Chem*; **264**(14): 7776-9.

Fukumoto, H., Seino, S., Imura, H., Seino, Y., Eddy, R.L. *et al.* (1988b). Sequence, tissue distribution, and chromosomal localization of mRNA encoding a human glucose transporter-like protein. *Proc Natl Acad Sci U S A*; **85**(15): 5434-8.

Gall, J.G. and Pardue, M.L. (1969). Formation and detection of RNA-DNA hybrid molecules in cytological preparations. *Proc Natl Acad Sci U S A*; **63**(2): 378-83.

Galuk, D. (1991). Diabetes mellitus. Types I and II. *Adv Clin Care*; **6**(2): 5-7.

Garadi, R. and Lou, M.F. (1989). Aldose reductase in early streptozotocin-induced diabetic rat lens. *Invest Ophthalmol Vis Sci*; **30**(11): 2370-5.

Garner, B., Davies, M.J. and Truscott, R.J. (2000). Formation of hydroxyl radicals in the human lens is related to the severity of nuclear cataract. *Exp Eye Res*; **70**(1): 81-8.

Garvey, W.T., Hueckstead, T.P. and Birnbaum, M.J. (1989). Pretranslational suppression of an insulin-responsive glucose transporter in rats with diabetes mellitus. *Science*; **245**(4913): 60-3.

Garvey, W.T., Maianu, L., Hancock, J.A., Golichowski, A.M. and Baron, A. (1992). Gene expression of GLUT4 in skeletal muscle from insulin-resistant patients with obesity, IGT, GDM, and NIDDM. *Diabetes*; **41**(4): 465-75.

Garvey, W.T., Maianu, L., Hueckstead, T.P., Birnbaum, M.J., Molina, J.M. *et al.* (1991). Pretranslational suppression of a glucose transporter protein causes insulin resistance in adipocytes from patients with non-insulin-dependent diabetes mellitus and obesity. *J Clin Invest*; **87**(3): 1072-81.

Gaynes, B.I. and Watkins, J.B., 3rd (1989). Comparison of glucose, sorbitol and fructose accumulation in lens and liver of diabetic and insulin-treated rats and mice. *Comp Biochem Physiol B*; **92**(4): 685-90.

Gerhart, D.Z., Leino, R.L., Taylor, W.E., Borson, N.D. and Drewes, L.R. (1994). GLUT1 and GLUT3 gene expression in gerbil brain following brief ischemia: an in situ hybridization study. *Brain Res Mol Brain Res*; **25**(3-4): 313-22.

Gherzi, R., Melioli, G., De Luca, M., D'Agostino, A., Guastella, M. *et al.* (1991). High expression levels of the "erythroid/brain" type glucose transporter (GLUT1) in the basal cells of human eye conjunctiva and oral mucosa reconstituted in culture. *Exp Cell Res*; **195**(1): 230-6.

Ghosh, S., Hernando, N., Martin-Alonso, J.M., Martin-Vasallo, P. and Coca-Prados, M. (1991). Expression of multiple Na+,K(+)-ATPase genes reveals a gradient of isoforms along the nonpigmented ciliary epithelium: functional implications in aqueous humor secretion. *J Cell Physiol*; **149**(2): 184-94.

Giambernardi, T.A., Rodeck, U. and Klebe, R.J. (1998). Bovine serum albumin reverses inhibition of RT-PCR by melanin. *Biotechniques*; **25**(4): 564-6.

Gillis, M.K. and Chylack, L.T., Jr. (1982). Depletion of sorbitol and fructose from young and older rat lenses. *Exp Eye Res*; **35**(2): 183-90.

Giovannini, A., Amato, G.P., Mariotti, C. and Ripa, E. (1999). Diabetic maculopathy induced by vitreo-macular traction: evaluation by optical coherence tomography (OCT). *Doc Ophthalmol*; **97**(3-4): 361-6.

Glasser, A. and Kaufman, P. (2003). Accommodation and presbyopia. In: *Alder's Physiology of the Eye* (Eds, Kaufman, P. and Alm, A.). St. Louis: Mosby, pp. 197-233.

Godwin, M., Muirhead, M., Huynh, J., Helt, B. and Grimmer, J. (1999). Prevalence of gestational diabetes mellitus among Swampy Cree women in Moose Factory, James Bay. *Cmaj*; **160**(9): 1299-302.

Goldman, R.D. (1972). The effects of cytochalasin B on the microfilaments of baby hamster kidney (BHK-21) cells. *J Cell Biol*; **52**(2): 246-54.

Gong, X., Wang, X., Han, J., Niesman, I., Huang, Q. *et al.* (2001). Development of cataractous macrophthalmia in mice expressing an active MEK1 in the lens. *Invest Ophthalmol Vis Sci*; **42**(3): 539-48.

Gonzalez, R.G., Barnett, P., Aguayo, J., Cheng, H.M. and Chylack, L.T., Jr. (1984). Direct measurement of polyol pathway activity in the ocular lens. *Diabetes*; **33**(2): 196-9.

Gorovits, N., Cui, L., Busik, J.V., Ranalletta, M., Hauguel de-Mouzon, S. *et al.* (2003). Regulation of hepatic GLUT8 expression in normal and diabetic models. *Endocrinology*; **144**(5): 1703-11.

Gosmanov, A.R., Schneider, E.G. and Thomason, D.B. (2003). NKCC activity restores muscle water during hyperosmotic challenge independent of insulin, ERK, and p38 MAPK. *Am J Physiol Regul Integr Comp Physiol*; **284**(3): R655-65.

Gottschalk, I., Lundqvist, A., Zeng, C.M., Hagglund, C.L., Zuo, S.S. *et al.* (2000). Conversion between two cytochalasin B-binding states of the human GLUT1 glucose transporter. *Eur J Biochem*; **267**(23): 6875-82.

Gould, G.W., Brant, A.M., Kahn, B.B., Shepherd, P.R., McCoid, S.C. *et al.* (1992). Expression of the brain-type glucose transporter is restricted to brain and neuronal cells in mice. *Diabetologia*; **35**(4): 304-9.

Gould, G.W. and Holman, G.D. (1993). The glucose transporter family: structure, function and tissue-specific expression. *Biochem J*; **295**(Pt 2): 329-41.

Gould, G.W., Thomas, H.M., Jess, T.J. and Bell, G.I. (1991). Expression of human glucose transporters in Xenopus oocytes: kinetic characterization and substrate specificities of the erythrocyte, liver, and brain isoforms. *Biochemistry*; **30**(21): 5139-45.

Gray, S., Feinberg, M.W., Hull, S., Kuo, C.T., Watanabe, M. *et al.* (2002). The Kruppel-like factor KLF15 regulates the insulin-sensitive glucose transporter GLUT4. *J Biol Chem*; **277**(37): 34322-8.

Green, K., Bountra, C., Georgiou, P. and House, C.R. (1985). An electrophysiologic study of rabbit ciliary epithelium. *Invest Ophthalmol Vis Sci*; **26**(3): 371-81.

Green, N.M. (1990). Avidin and streptavidin. *Methods Enzymol*; **184**: 51-67.

Gribble, F.M., Williams, L., Simpson, A.K. and Reimann, F. (2003). A novel glucose-sensing mechanism contributing to glucagon-like peptide-1 secretion from the GLUTag cell line. *Diabetes*; **52**(5): 1147-54.

Gruetter, R., Novotny, E.J., Boulware, S.D., Rothman, D.L., Mason, G.F. *et al.* (1992). Direct measurement of brain glucose concentrations in humans by 13C NMR spectroscopy. *Proc Natl Acad Sci U S A*; **89**(3): 1109-12.

Gu, K., Cowie, C.C. and Harris, M.I. (1998). Mortality in adults with and without diabetes in a national cohort of the U.S. population, 1971-1993. *Diabetes Care*; **21**(7): 1138-45.

Guillemain, G., Loizeau, M., Pincon-Raymond, M., Girard, J. and Leturque, A. (2000). The large intracytoplasmic loop of the glucose transporter GLUT2 is involved in glucose signaling in hepatic cells. *J Cell Sci*; **113**(Pt 5): 841-7.

Ha, H. and Kim, K.H. (1999). Pathogenesis of diabetic nephropathy: the role of oxidative stress and protein kinase C. *Diabetes Res Clin Pract*; **45**(2-3): 147-51.

Hager, K., Hazama, A., Kwon, H.M., Loo, D.D., Handler, J.S. *et al.* (1995). Kinetics and specificity of the renal Na+/myo-inositol cotransporter expressed in Xenopus oocytes. *J Membr Biol*; **143**(2): 103-13.

Hahn, T., Barth, S., Weiss, U., Mosgoeller, W. and Desoye, G. (1998). Sustained hyperglycemia in vitro down-regulates the GLUT1 glucose transport system of cultured human term placental trophoblast: a mechanism to protect fetal development? *Faseb J*; **12**(12): 1221-31.

Hahn, T., Hartmann, M., Blaschitz, A., Skofitsch, G., Graf, R. *et al.* (1995). Localisation of the high affinity facilitative glucose transporter protein GLUT 1 in the placenta of human, marmoset monkey (Callithrix jacchus) and rat at different developmental stages. *Cell Tissue Res*; **280**(1): 49-57.

Haitoglou, C.S., Tsilibary, E.C., Brownlee, M. and Charonis, A.S. (1992). Altered cellular interactions between endothelial cells and nonenzymatically glucosylated laminin/type IV collagen. *J Biol Chem*; **267**(18): 12404-7.

Hajduch, E., Litherland, G.J., Turban, S., Brot-Laroche, E. and Hundal, H.S. (2003). Insulin regulates the expression of the GLUT5 transporter in L6 skeletal muscle cells. *FEBS Lett*; **549**(1-3): 77-82.

Hale, P.N. and Maurice, D.M. (1969). Sugar transport across the corneal endothelium. *Exp Eye Res*; **8**(2): 205-15.

Hales, C.N. and Barker, D.J. (1992). Type 2 (non-insulin-dependent) diabetes mellitus: the thrifty phenotype hypothesis. *Diabetologia*; **35**(7): 595-601.

Hales, C.N., Desai, M., Ozanne, S.E. and Crowther, N.J. (1996). Fishing in the stream of diabetes: from measuring insulin to the control of fetal organogenesis. *Biochem Soc Trans*; **24**(2): 341-50.

Halton, D.M., Taylor, N.F. and Lopes, D.P. (1980). The uptake of 3-deoxy-3-fluoro-D-glucose by synaptosomes from rat brain cortex. *J Neurosci Res*; **5**(3): 241-52.

Hammes, H.P. (2003). Pathophysiological mechanisms of diabetic angiopathy. *J Diabetes Complications*; **17**(2 Suppl): 16-9.

Hammes, H.P., Lin, J., Wagner, P., Feng, Y., Vom Hagen, F. *et al.* (2004). Angiopoietin-2 causes pericyte dropout in the normal retina: evidence for involvement in diabetic retinopathy. *Diabetes*; **53**(4): 1104-10.

Hammes, H.P., Martin, S., Federlin, K., Geisen, K. and Brownlee, M. (1991). Aminoguanidine treatment inhibits the development of experimental diabetic retinopathy. *Proc Natl Acad Sci U S A*; **88**(24): 11555-8.

Hansen, O. (1984). Interaction of cardiac glycosides with (Na+ + K+)-activated ATPase. A biochemical link to digitalis-induced inotropy. *Pharmacol Rev*; **36**(3): 143-63.

Hara, K., Lutjen-Drecoll, E., Prestele, H. and Rohen, J.W. (1977). Structural differences between regions of the ciliary body in primates. *Invest Ophthalmol Vis Sci*; **16**(10): 912-24.

Harding, J.J. (1999). Can cataract be prevented? *Eye*; **13**(Pt 3b): 454-6.

Harding, J.J. (2001). Can drugs or micronutrients prevent cataract? *Drugs Aging*; **18**(7): 473-86.

Hardy, S.P., Goodfellow, H.R., Valverde, M.A., Gill, D.R., Sepulveda, V. *et al.* (1995). Protein kinase C-mediated phosphorylation of the human multidrug resistance P-glycoprotein regulates cell volume-activated chloride channels. *Embo J*; **14**(1): 68-75.

Harik, S.I., Gravina, S.A. and Kalaria, R.N. (1988). Glucose transporter of the blood-brain barrier and brain in chronic hyperglycemia. *J Neurochem*; **51**(6): 1930-4.

Harik, S.I., Kalaria, R.N., Whitney, P.M., Andersson, L., Lundahl, P. *et al.* (1990). Glucose transporters are abundant in cells with "occluding" junctions at the blood-eye barriers. *Proc Natl Acad Sci U S A*; **87**(11): 4261-4.

Harper, D.R., Kit, M.L. and Kangro, H.O. (1990). Protein blotting: ten years on. *J Virol Methods*; **30**(1): 25-39.

Harrison, P.R., Conkie, D., Affara, N. and Paul, J. (1974). In situ localization of globin messenger RNA formation. I. During mouse fetal liver development. *J Cell Biol*; **63**(2 Pt 1): 402-13.

Haspel, H.C., Wilk, E.W., Birnbaum, M.J., Cushman, S.W. and Rosen, O.M. (1986). Glucose deprivation and hexose transporter polypeptides of murine fibroblasts. *J Biol Chem*; **261**(15): 6778-89.

Hediger, M.A., Coady, M.J., Ikeda, T.S. and Wright, E.M. (1987). Expression cloning and cDNA sequencing of the Na+/glucose co-transporter. *Nature*; **330**(6146): 379-81.

Hediger, M.A., Turk, E. and Wright, E.M. (1989). Homology of the human intestinal Na+/glucose and Escherichia coli Na+/proline cotransporters. *Proc Natl Acad Sci U S A*; **86**(15): 5748-52.

Hegde, K.R., Henein, M.G. and Varma, S.D. (2003). Establishment of mouse as an animal model for study of diabetic cataracts: biochemical studies. *Diabetes Obes Metab*; **5**(2): 113-9.

Heidland, A., Sebekova, K. and Schinzel, R. (2001). Advanced glycation end products and the progressive course of renal disease. *Am J Kidney Dis*; **38**(4 Suppl 1): S100-6.

Heinrich, D., Metz, J., Raviola, E. and Forssmann, W.G. (1976). Ultrastructure of perfusion-fixed fetal capillaries in the human placenta. *Cell Tissue Res*; **172**(2): 157-69.

Helbig, H., Korbmacher, C., Wohlfarth, J., Berweck, S., Kuhner, D. *et al.* (1989). Electrogenic Na+-ascorbate cotransport in cultured bovine pigmented ciliary epithelial cells. *Am J Physiol*; **256**(1 Pt 1): C44-9.

Hellwig, B. and Joost, H.G. (1991). Differentiation of erythrocyte-(GLUT1), liver-(GLUT2), and adipocyte-type (GLUT4) glucose transporters by binding of the inhibitory ligands cytochalasin B, forskolin, dipyridamole, and isobutylmethylxanthine. *Mol Pharmacol*; **40**(3): 383-9.

Hiraki, Y., Rosen, O.M. and Birnbaum, M.J. (1988). Growth factors rapidly induce expression of the glucose transporter gene. *J Biol Chem*; **263**(27): 13655-62.

Hirayama, B.A., Loo, D.D. and Wright, E.M. (1997). Cation effects on protein conformation and transport in the Na+/glucose cotransporter. *J Biol Chem*; **272**(4): 2110-5.

Hirayama, B.A., Lostao, M.P., Panayotova-Heiermann, M., Loo, D.D., Turk, E. *et al.* (1996). Kinetic and specificity differences between rat, human, and rabbit Na+-glucose cotransporters (SGLT-1). *Am J Physiol*; **270**(6 Pt 1): G919-26.

Hirsch, M., Bellon, B., Hartmann, C.H., Keller, N. and Druet, P. (1980). Localization of autologous antiperoxidase antibodies in the anterior uvea of the rabbit eye. *Exp Eye Res*; **30**(3): 253-60.

Hirsch, M., Montcourrier, P., Arguillere, P. and Keller, N. (1985). The structure of tight junctions in the ciliary epithelium. *Curr Eye Res*; **4**(4): 493-501.

Hirsh, A.J., Yao, S.Y., Young, J.D. and Cheeseman, C.I. (1997). Inhibition of glucose absorption in the rat jejunum: a novel action of alpha-D-glucosidase inhibitors. *Gastroenterology*; **113**(1): 205-11.

Hocquette, J.F., Bornes, F., Balage, M., Ferre, P., Grizard, J. *et al.* (1995). Glucose-transporter (GLUT4) protein content in oxidative and glycolytic skeletal muscles from calf and goat. *Biochem J*; **305 (Pt 2)**: 465-70.

Hodson, S.A. and Wigham, C.G. (1987). Paracellular ionic and transcellular water diffusions across rabbit corneal endothelium. *J Physiol*; **385**: 89-96.

Holland, M.G. and Gipson, C.C. (1970). Chloride ion transport in the isolated ciliary body. *Invest Ophthalmol*; **9**(1): 20-9.

Horibe, Y., Hosoya, K., Kim, K.J. and Lee, V.H. (1997). Kinetic evidence for Na(+)-glucose co-transport in the pigmented rabbit conjunctiva. *Curr Eye Res*; **16**(10): 1050-5.

Horikoshi, Y., Sasaki, A., Taguchi, N., Maeda, M., Tsukagoshi, H. *et al.* (2003). Human GLUT5 immunolabeling is useful for evaluating microglial status in neuropathological study using paraffin sections. *Acta Neuropathol (Berl)*; **105**(2): 157-62.

Hornnes, P.J. (1985). On the decrease of glucose tolerance in pregnancy. A review. *Diabete Metab*; **11**(5): 310-5.

Hosoya, K., Kompella, U.B., Kim, K.J. and Lee, V.H. (1996). Contribution of Na(+)-glucose cotransport to the short-circuit current in the pigmented rabbit conjunctiva. *Curr Eye Res*; **15**(4): 447-51.

Hosoya, K., Tomi, M., Ohtsuki, S., Takanaga, H., Ueda, M. *et al.* (2001). Conditionally immortalized retinal capillary endothelial cell lines (TR-iBRB) expressing differentiated endothelial cell functions derived from a transgenic rat. *Exp Eye Res*; **72**(2): 163-72.

Hotta, N. (1997). New concepts and insights on pathogenesis and treatment of diabetic complications: polyol pathway and its inhibition. *Nagoya J Med Sci*; **60**(3-4): 89-100.

Hresko, R.C., Kruse, M., Strube, M. and Mueckler, M. (1994). Topology of the Glut 1 glucose transporter deduced from glycosylation scanning mutagenesis. *J Biol Chem*; **269**(32): 20482-8.

Hsu, S.C. and Molday, R.S. (1991). Glycolytic enzymes and a GLUT-1 glucose transporter in the outer segments of rod and cone photoreceptor cells. *J Biol Chem*; **266**(32): 21745-52.

Hsu, S.C. and Molday, R.S. (1994). Glucose metabolism in photoreceptor outer segments. Its role in phototransduction and in NADPH-requiring reactions. *J Biol Chem*; **269**(27): 17954-9.

Hudspeth, A.J. and Yee, A.G. (1973). The intercellular junctional complexes of retinal pigment epithelia. *Invest Ophthalmol*; **12**(5): 354-65.

Huijberts, M.S., Wolffenbuttel, B.H., Boudier, H.A., Crijns, F.R., Kruseman, A.C. *et al.* (1993). Aminoguanidine treatment increases elasticity and decreases fluid filtration of large arteries from diabetic rats. *J Clin Invest*; **92**(3): 1407-11.

Hundal, H.S., Ahmed, A., Guma, A., Mitsumoto, Y., Marette, A. *et al.* (1992). Biochemical and immunocytochemical localization of the 'GLUT5 glucose transporter' in human skeletal muscle. *Biochem J*; **286**(Pt 2): 339-43.

Ibberson, M., Uldry, M. and Thorens, B. (2000). GLUTX1, a novel mammalian glucose transporter expressed in the central nervous system and insulin-sensitive tissues. *J Biol Chem*; **275**(7): 4607-12.

Igarashi, T., Miyake, K., Kato, K., Watanabe, A., Ishizaki, M. *et al.* (2003). Lentivirus-mediated expression of angiostatin efficiently inhibits neovascularization in a murine proliferative retinopathy model. *Gene Ther*; **10**(3): 219-26.

Iizuka, S., Kishida, K., Tsuboi, S., Emi, K. and Manabe, R. (1984). Electrical characteristics of the isolated dog ciliary body. *Curr Eye Res*; **3**(3): 417-21.

Ikeda, T. (2000). Diabetic maculopathy. *Acta Ophthalmol Scand*; **78**(5): 605-6.

Illsley, N.P. (2000). Glucose transporters in the human placenta. *Placenta*; **21**(1): 14-22.

Imam, A., Drushella, M.M. and Taylor, C.R. (1986). A novel immunoperoxidase procedure of using human monoclonal antibodies for the detection of cellular antigens in tissue sections. *J Immunol Methods*; **86**(1): 17-20.

Inoguchi, T., Sonta, T., Tsubouchi, H., Etoh, T., Kakimoto, M. *et al.* (2003). Protein kinase C-dependent increase in reactive oxygen species (ROS) production in vascular tissues of diabetes: role of vascular NAD(P)H oxidase. *J Am Soc Nephrol*; **14**(8 Suppl 3): S227-32.

Inukai, K., Asano, T., Katagiri, H., Anai, M., Funaki, M. *et al.* (1994). Replacement of both tryptophan residues at 388 and 412 completely abolished cytochalasin B photolabelling of the GLUT1 glucose transporter. *Biochem J*; **302**(Pt 2): 355-61.

Ishida, K., Yamashita, H., Katagiri, H. and Oka, Y. (1995). Regulation of glucose transporter 1 (GLUT1) gene expression by epidermal growth factor in bovine corneal endothelial cells. *Jpn J Ophthalmol*; **39**(3): 225-32.

Jacob, T.J. and Civan, M.M. (1996). Role of ion channels in aqueous humor formation. *Am J Physiol*; **271**(3 Pt 1): C703-20.

Jacobs, D.B. (1993). Insulin activates its receptor tyrosine kinase and potentiates movement of glucose transporters in bovine lens. *Invest Ophthalmol Vis Sci*; **34 (Suppl)**: 1372.

James, D.E., Strube, M. and Mueckler, M. (1989). Molecular cloning and characterization of an insulin-regulatable glucose transporter. *Nature*; **338**(6210): 83-7.

Jansson, T., Wennergren, M. and Illsley, N.P. (1993). Glucose transporter protein expression in human placenta throughout gestation and in intrauterine growth retardation. *J Clin Endocrinol Metab*; **77**(6): 1554-62.

Jennings, M.L. and Solomon, A.K. (1976). Interaction between phloretin and the red blood cell membrane. *J Gen Physiol*; **67**(4): 381-97.

Jervis, E.L., Johnson, F.R., Sheff, M.F. and Smyth, D.H. (1956). The effect of phlorhizin on intestinal absorption and intestinal phosphatase. *J Physiol*; **134**(3): 675-88.

Ji, H.J., Zhang, Q.Q. and Leung, B.S. (1990). Survey of oncogene and growth factor/receptor gene expression in cancer cells by intron-differential RNA/PCR. *Biochem Biophys Res Commun*; **170**(2): 569-75.

Jindal, S.K., Ishii, E., Letarte, M., Vera, S., Teerds, K.J. *et al.* (1995). Regulation of transforming growth factor alpha gene expression in an ovarian surface epithelial cell line derived from a human carcinoma. *Biol Reprod*; **52**(5): 1027-37.

Johnson, L.W. and Smith, C.H. (1985). Glucose transport across the basal plasma membrane of human placental syncytiotrophoblast. *Biochim Biophys Acta*; **815**(1): 44-50.

Joost, H.G., Bell, G.I., Best, J.D., Birnbaum, M.J., Charron, M.J. *et al.* (2002). Nomenclature of the GLUT/SLC2A family of sugar/polyol transport facilitators. *Am J Physiol Endocrinol Metab*; **282**(4): E974-6.

Joost, H.G. and Thorens, B. (2001). The extended GLUT-family of sugar/polyol transport facilitators: nomenclature, sequence characteristics, and potential function of its novel members (review). *Mol Membr Biol*; **18**(4): 247-56.

Jung, H. (2002). The sodium/substrate symporter family: structural and functional features. *FEBS Lett*; **529**(1): 73-7.

Kador, P.F., Akagi, Y. and Kinoshita, J.H. (1985). Diabetic cataracts in animal models: prevention and reversibility with aldose reductase inhibitors. *Diabet Med*; **2**(3): 194-6.

Kahlenberg, A., Urman, B. and Dolansky, D. (1971). Preferential uptake of D-glucose by isolated human erythrocyte membranes. *Biochemistry*; **10**(16): 3154-62.

Kahn, B.B., Rosen, A.S., Bak, J.F., Andersen, P.H., Damsbo, P. *et al.* (1992). Expression of GLUT1 and GLUT4 glucose transporters in skeletal muscle of humans with insulin-dependent diabetes mellitus: regulatory effects of metabolic factors. *J Clin Endocrinol Metab*; **74**(5): 1101-9.

Kalaria, R.N., Gravina, S.A., Schmidley, J.W., Perry, G. and Harik, S.I. (1988). The glucose transporter of the human brain and blood-brain barrier. *Ann Neurol*; **24**(6): 757-64.

Kamei, Y., Tsutsumi, O., Yamakawa, A., Oka, Y., Taketani, Y. *et al.* (1999). Maternal epidermal growth factor deficiency causes fetal hypoglycemia and intrauterine growth retardation in mice: possible involvement of placental glucose transporter GLUT3 expression. *Endocrinology*; **140**(9): 4236-43.

Kanai, Y., Lee, W.S., You, G., Brown, D. and Hediger, M.A. (1994). The human kidney low affinity Na+/glucose cotransporter SGLT2. Delineation of the major renal reabsorptive mechanism for D-glucose. *J Clin Invest*; **93**(1): 397-404.

Kane, S., Seatter, M.J. and Gould, G.W. (1997). Functional studies of human GLUT5: effect of pH on substrate selection and an analysis of substrate interactions. *Biochem Biophys Res Commun*; **238**(2): 503-5.

Kaneto, H., Xu, G., Song, K.H., Suzuma, K., Bonner-Weir, S. *et al.* (2001). Activation of the hexosamine pathway leads to deterioration of pancreatic beta-cell function through the induction of oxidative stress. *J Biol Chem*; **276**(33): 31099-104.

Kanzaki, M., Nagasawa, M., Kojima, I., Sato, C., Naruse, K. *et al.* (1999). Molecular identification of a eukaryotic, stretch-activated nonselective cation channel. *Science*; **285**(5429): 882-6.

Kasahara, M. and Hinkle, P.C. (1977). Reconstitution and purification of the D-glucose transporter from human erythrocytes. *J Biol Chem*; **252**(20): 7384-90.

Kato, H., Takita, J., Miyazaki, T., Nakajima, M., Fukai, Y. *et al.* (2002). Glut-1 glucose transporter expression in esophageal squamous cell carcinoma is associated with tumor aggressiveness. *Anticancer Res*; **22**(5): 2635-9.

Kaulen, P., Kahle, G., Keller, K. and Wollensak, J. (1991). Autoradiographic mapping of the glucose transporter with cytochalasin B in the mammalian eye. *Invest Ophthalmol Vis Sci*; **32**(6): 1903-11.

Kawahara, K. and Matsuzaki, K. (1993). A stretch-activated cation channel in the apical membrane of A6 cells. *Jpn J Physiol*; **43**(6): 817-32.

Kayano, T., Burant, C.F., Fukumoto, H., Gould, G.W., Fan, Y.S. *et al.* (1990). Human facilitative glucose transporters. Isolation, functional characterization, and gene localization of cDNAs encoding an isoform (GLUT5) expressed in small intestine, kidney, muscle, and adipose tissue and an unusual glucose transporter pseudogene-like sequence (GLUT6). *J Biol Chem*; **265**(22): 13276-82.

Kayano, T., Fukumoto, H., Eddy, R.L., Fan, Y.S., Byers, M.G. *et al.* (1988). Evidence for a family of human glucose transporter-like proteins. Sequence and gene localization of a protein expressed in fetal skeletal muscle and other tissues. *J Biol Chem*; **263**(30): 15245-8.

Kelly, D.J., Zhang, Y., Hepper, C., Gow, R.M., Jaworski, K. *et al.* (2003). Protein kinase C beta inhibition attenuates the progression of experimental diabetic nephropathy in the presence of continued hypertension. *Diabetes*; **52**(2): 512-8.

Khan, Z.A. and Chakrabarti, S. (2003). Growth factors in proliferative diabetic retinopathy. *Exp Diabesity Res*; **4**(4): 287-301.

Khayat, Z.A., McCall, A.L. and Klip, A. (1998). Unique mechanism of GLUT3 glucose transporter regulation by prolonged energy demand: increased protein half-life. *Biochem J*; **333**(Pt 3): 713-8.

Kim, Y., Tamura, T., Iwashita, S., Tokuyama, K. and Suzuki, M. (1994). Effect of high-fat diet on gene expression of GLUT4 and insulin receptor in soleus muscle. *Biochem Biophys Res Commun*; **202**(1): 519-26.

Kinoshita, J.H., Futterman, S., Satoh, K. and Merola, L.O. (1963). Factors Affecting the Formation of Sugar Alcohols in Ocular Lens. *Biochim Biophys Acta*; **74**: 340-50.

Kishida, K., Sasabe, T., Iizuka, S., Manabe, R. and Otori, T. (1982). Sodium and chloride transport across the isolated rabbit ciliary body. *Curr Eye Res*; **2**(3): 149-52.

Kistler, J., Lin, J.S., Bond, J., Green, C., Eckert, R. *et al.* (1999). Connexins in the lens: are they to blame in diabetic cataractogenesis? *Novartis Found Symp*; **219**: 97-108; discussion 108-12.

Kitagawa, T., Masumi, A. and Akamatsu, Y. (1991). Transforming growth factor-beta 1 stimulates glucose uptake and the expression of glucose transporter mRNA in quiescent Swiss mouse 3T3 cells. *J Biol Chem*; **266**(27): 18066-71.

Kitamura, M. (1999). Gene therapy for diabetic nephropathy. *Perit Dial Int*; **19 Suppl 2**: S238-41.

Klepper, J., Vera, J.C. and De Vivo, D.C. (1998). Deficient transport of dehydroascorbic acid in the glucose transporter protein syndrome. *Ann Neurol*; **44**(2): 286-7.

Klepper, J., Wang, D., Fischbarg, J., Vera, J.C., Jarjour, I.T. *et al.* (1999). Defective glucose transport across brain tissue barriers: a newly recognized neurological syndrome. *Neurochem Res*; **24**(4): 587-94.

Knecht, D.A. and Dimond, R.L. (1984). Visualization of antigenic proteins on Western blots. *Anal Biochem*; **136**(1): 180-4.

Knott, R.M., Robertson, M. and Forrester, J.V. (1993). Regulation of glucose transporter (GLUT 3) and aldose reductase mRNA inbovine retinal endothelial cells and retinal pericytes in high glucose and high galactose culture. *Diabetologia*; **36**(9): 808-12.

Knott, R.M., Robertson, M., Muckersie, E. and Forrester, J.V. (1996). Regulation of glucose transporters (GLUT-1 and GLUT-3) in human retinal endothelial cells. *Biochem J*; **318**(Pt 1): 313-7.

Kobayashi, M., Nikami, H., Morimatsu, M. and Saito, M. (1996). Expression and localization of insulin-regulatable glucose transporter (GLUT4) in rat brain. *Neurosci Lett*; **213**(2): 103-6.

Koefoed-Johnsen, V. and Ussing, H.H. (1958). The nature of the frog skin potential. *Acta Physiol Scand*; **42**(3-4): 298-308.

Koepsell, H., Fritzsch, G., Korn, K. and Madrala, A. (1990). Two substrate sites in the renal Na(+)-D-glucose cotransporter studied by model analysis of phlorizin binding and D-glucose transport measurements. *J Membr Biol*; **114**(2): 113-32.

Köhler, G. and Milstein, C. (1975). Continuous cultures of fused cells secreting antibody of predefined specificity. *Nature*; **256**(5517): 495-7.

Kowluru, R.A. (2003a). Effect of reinstitution of good glycemic control on retinal oxidative stress and nitrative stress in diabetic rats. *Diabetes*; **52**(3): 818-23.

Kowluru, R.A. and Koppolu, P. (2002). Diabetes-induced activation of caspase-3 in retina: effect of antioxidant therapy. *Free Radic Res*; **36**(9): 993-9.

Kowluru, R.A., Koppolu, P., Chakrabarti, S. and Chen, S. (2003b). Diabetes-induced activation of nuclear transcriptional factor in the retina, and its inhibition by antioxidants. *Free Radic Res*; **37**(11): 1169-80.

Koya, D., Haneda, M., Nakagawa, H., Isshiki, K., Sato, H. *et al.* (2000). Amelioration of accelerated diabetic mesangial expansion by treatment with a PKC beta inhibitor in diabetic db/db mice, a rodent model for type 2 diabetes. *Faseb J*; **14**(3): 439-47.

Koya, D., Jirousek, M.R., Lin, Y.W., Ishii, H., Kuboki, K. *et al.* (1997). Characterization of protein kinase C beta isoform activation on the gene expression of transforming growth factor-beta, extracellular matrix components, and prostanoids in the glomeruli of diabetic rats. *J Clin Invest*; **100**(1): 115-26.

Koya, D. and King, G.L. (1998). Protein kinase C activation and the development of diabetic complications. *Diabetes*; **47**(6): 859-66.

Kozart, D.M. (1968). Light and electron microscopic study of regional morphologic differences in the processes of the ciliary body in the rabbit. *Invest Ophthalmol*; **7**(1): 15-33.

Krebs, H.A. (1972). The Pasteur effect and the relations between respiration and fermentation. *Essays Biochem*; **8**: 1-34.

Krishan, A. (1972). Cytochalasin-B: time-lapse cinematographic studies on its effects on cytokinesis. *J Cell Biol*; **54**(3): 657-64.

Krupin, T. and Civan, M.M. (1995). Physiologic basis of aqueous humor formation. In: *The Glaucomas* (Eds, Ritch, R., Shields, M.B. and Krupin, T.). St. Louis: CV Mosby, pp. 251-280.

Krupin, T. and Civan, M.M. (1996). Physiologic basis of aqueous humor formation. In: *The Glaucomas* (Eds, Ritch, R., Shields, M.B. and Krupin, T.). St. Louis: CV Mosby.

Krupin, T., Reinach, P.S., Candia, O.A. and Podos, S.M. (1984). Transepithelial electrical measurements on the isolated rabbit iris-ciliary body. *Exp Eye Res*; **38**(2): 115-23.

Krupka, R.M. (1985). Asymmetrical binding of phloretin to the glucose transport system of human erythrocytes. *J Membr Biol*; **83**(1-2): 71-80.

Kuang, H., Zou, W., Liu, D., Shi, R., Cheng, L. *et al.* (2003). The potential role of IGF-I receptor mRNA in rats with diabetic retinopathy. *Chin Med J (Engl)*; **116**(3): 478-80.

Kuboki, K., Jiang, Z.Y., Takahara, N., Ha, S.W., Igarashi, M. *et al.* (2000). Regulation of endothelial constitutive nitric oxide synthase gene expression in endothelial cells and in vivo : a specific vascular action of insulin. *Circulation*; **101**(6): 676-81.

Kumagai, A.K., Glasgow, B.J. and Pardridge, W.M. (1994). GLUT1 glucose transporter expression in the diabetic and nondiabetic human eye. *Invest Ophthalmol Vis Sci*; **35**(6): 2887-94.

Kumagai, A.K., Vinores, S.A. and Pardridge, W.M. (1996). Pathological upregulation of inner blood-retinal barrier Glut1 glucose transporter expression in diabetes mellitus. *Brain Res*; **706**(2): 313-7.

Kurien, B.T. and Scofield, R.H. (2003). Protein blotting: a review. *J Immunol Methods*; **274**(1-2): 1-15.

Kuriyama, H., Sasaki, K. and Fukuda, M. (1983). Studies on diabetic cataract in rats induced by streptozotocin. II. Biochemical examinations of rat lenses in relation to cataract stages. *Ophthalmic Res*; **15**(4): 191-7.

Kwon, H.M., Yamauchi, A., Uchida, S., Preston, A.S., Garcia-Perez, A. *et al.* (1992). Cloning of the cDNa for a Na+/myo-inositol cotransporter, a hypertonicity stress protein. *J Biol Chem*; **267**(9): 6297-301.

Kyselova, Z., Stefek, M. and Bauer, V. (2004). Pharmacological prevention of diabetic cataract. *J Diabetes Complications*; **18**(2): 129-40.

Laemmli, U.K. (1970). Cleavage of structural proteins during the assembly of the head of bacteriophage T4. *Nature*; **227**(259): 680-5.

Lang, F., Busch, G.L., Ritter, M., Volkl, H., Waldegger, S. *et al.* (1998). Functional significance of cell volume regulatory mechanisms. *Physiol Rev*; **78**(1): 247-306.

Laris, P.C. and Henius, G.V. (1982). Influence of glucose on Ehrlich cell volume, ion transport, and membrane potential. *Am J Physiol*; **242**(5): C326-32.

Larkin, P.D. and Park, W.D. (1999). Transcript accumulation and utilization of alternate and non-consensus splice sites in rice granule-bound starch synthase are temperature-sensitive and controlled by a single-nucleotide polymorphism. *Plant Mol Biol*; **40**(4): 719-27.

Leach, L. and Firth, J.A. (1992). Fine structure of the paracellular junctions of terminal villous capillaries in the perfused human placenta. *Cell Tissue Res*; **268**(3): 447-52.

Lebovitz, H.E. (2001). Insulin resistance: definition and consequences. *Exp Clin Endocrinol Diabetes*; **109**(Suppl 2): S135-48.

Lee, A.Y. and Chung, S.S. (1999). Contributions of polyol pathway to oxidative stress in diabetic cataract. *Faseb J*; **13**(1): 23-30.

Lee, W.H. and Bondy, C.A. (1993). Ischemic injury induces brain glucose transporter gene expression. *Endocrinology*; **133**(6): 2540-4.

Lee, W.J., Peterson, D.R., Sukowski, E.J. and Hawkins, R.A. (1997). Glucose transport by isolated plasma membranes of the bovine blood-brain barrier. *Am J Physiol*; **272**(5 Pt 1): C1552-7.

Lee, W.S., Kanai, Y., Wells, R.G. and Hediger, M.A. (1994). The high affinity Na+/glucose cotransporter. Re-evaluation of function and distribution of expression. *J Biol Chem*; **269**(16): 12032-9.

Leong, M.M., Milstein, C. and Pannell, R. (1986). Luminescent detection method for immunodot, Western, and Southern blots. *J Histochem Cytochem*; **34**(12): 1645-50.

Leske, M.C., Chylack, L.T., Jr. and Wu, S.Y. (1991). The Lens Opacities Case-Control Study. Risk factors for cataract. *Arch Ophthalmol*; **109**(2): 244-51.

Leung, D.W., Loo, D.D., Hirayama, B.A., Zeuthen, T. and Wright, E.M. (2000b). Urea transport by cotransporters. *J Physiol*; **528**(Pt 2): 251-7.

Leung, G.M. and Lam, K.S. (2000a). Diabetic complications and their implications on health care in Asia. *Hong Kong Med J*; **6**(1): 61-8.

Lewis, B.S. and Harding, J.J. (1990). The effects of aminoguanidine on the glycation (non-enzymic glycosylation) of lens proteins. *Exp Eye Res*; **50**(5): 463-7.

Lewis, S.A. (1996). Epithelial electrophysiology. In: *Epithelial Transport: A Guid to Methods and Experimental Analysis* (Eds, Wills, N.K., Reuss, L. and Lewis, S.A.). London: Chapman & Hall, pp. 93-117.

Li, H., Myeroff, L., Smiraglia, D., Romero, M.F., Pretlow, T.P. *et al.* (2003). SLC5A8, a sodium transporter, is a tumor suppressor gene silenced by methylation in human colon aberrant crypt foci and cancers. *Proc Natl Acad Sci U S A*; **100**(14): 8412-7.

Li, Q., Manolescu, A., Ritzel, M., Yao, S., Slugoski, M. *et al.* (2004). Cloning and functional characterization of the human GLUT7 isoform SLC2A7 from the small intestine. *Am J Physiol Gastrointest Liver Physiol*; **287**(1): G236-42.

Li, W., Chan, L.S., Khatami, M. and Rockey, J.H. (1985). Characterization of glucose transport by bovine retinal capillary pericytes in culture. *Exp Eye Res*; **41**(2): 191-9.

Lin, J. (1997). Pathophysiology of cataracts: copper ion and peroxidation in diabetics. *Jpn J Ophthalmol*; **41**(3): 130-7.

Lin, S., Santi, D.V. and Spudich, J.A. (1974b). Biochemical studies on the mode of action of cytochalasin B. Preparation of (3H)cytochalasin B and studies on its binding of cells. *J Biol Chem*; **249**(7): 2268-74.

Lin, S. and Spudich, J.A. (1974a). Biochemical studies on the mode of action of cytochalasin B. Cytochalasin B binding to red cell membrane in relation to glucose transport. *J Biol Chem*; **249**(18): 5778-83.

Lingrel, J.B. and Kuntzweiler, T. (1994). Na+,K(+)-ATPase. *J Biol Chem*; **269**(31): 19659-62.

Lisinski, I., Schurmann, A., Joost, H.G., Cushman, S.W. and Al-Hasani, H. (2001). Targeting of GLUT6 (formerly GLUT9) and GLUT8 in rat adipose cells. *Biochem J*; **358**(Pt 2): 517-22.

Liu, P., Leffler, B.J., Weeks, L.K., Chen, G., Bouchard, C.M. *et al.* (2004). Sphingomyelinase activates GLUT4 translocation via a cholesterol-dependent mechanism. *Am J Physiol Cell Physiol*; **286**(2): C317-29.

Lodish, H., Berk, A., Matsudaira, P., Kaiser, C., Krieger, M. *et al.* (2003). Chemical foundations. In: *Molecular Cell Biology* (Eds, Lodish, H., Berk, A., Matsudaira, P. *et al*). New York: W.H.Freeman and Company, pp. 29-54.

Loike, J.D., Cao, L., Kuang, K., Vera, J.C., Silverstein, S.C. *et al.* (1993). Role of facilitative glucose transporters in diffusional water permeability through J774 cells. *J Gen Physiol*; **102**(5): 897-906.

Lonnroth, P. (1991). Regulation of insulin action at the cellular level. *J Intern Med Suppl*; **735**: 23-9.

Loo, D.D., Hirayama, B.A., Gallardo, E.M., Lam, J.T., Turk, E. *et al.* (1998). Conformational changes couple Na+ and glucose transport. *Proc Natl Acad Sci U S A*; **95**(13): 7789-94.

Loo, D.D., Zeuthen, T., Chandy, G. and Wright, E.M. (1996). Cotransport of water by the Na+/glucose cotransporter. *Proc Natl Acad Sci U S A*; **93**(23): 13367-70.

Lostao, M.P., Hirayama, B.A., Panayotova-Heiermann, M., Sampogna, S.L., Bok, D. *et al.* (1995). Arginine-427 in the Na+/glucose cotransporter (SGLT1) is involved in trafficking to the plasma membrane. *FEBS Lett*; **377**(2): 181-4.

Lu, M., Perez, V.L., Ma, N., Miyamoto, K., Peng, H.B. *et al.* (1999). VEGF increases retinal vascular ICAM-1 expression in vivo. *Invest Ophthalmol Vis Sci*; **40**(8): 1808-12.

Lucas, V.A. and Duncan, G. (1983). Specificity of glucose transport inhibitors in the frog lens. *Exp Eye Res*; **37**(2): 175-82.

Lutz, A.J. and Pardridge, W.M. (1993). Insulin therapy normalizes GLUT1 glucose transporter mRNA but not immunoreactive transporter protein in streptozocin-diabetic rats. *Metabolism*; **42**(8): 939-44.

Macheda, M.L., Williams, E.D., Best, J.D., Wlodek, M.E. and Rogers, S. (2003). Expression and localisation of GLUT1 and GLUT12 glucose transporters in the pregnant and lactating rat mammary gland. *Cell Tissue Res*; **311**(1): 91-7.

Mackenzie, B., Loo, D.D., Panayotova-Heiermann, M. and Wright, E.M. (1996). Biophysical characteristics of the pig kidney Na+/glucose cotransporter SGLT2 reveal a common mechanism for SGLT1 and SGLT2. *J Biol Chem*; **271**(51): 32678-83.

Mackenzie, B., Loo, D.D. and Wright, E.M. (1998). Relationships between Na+/glucose cotransporter (SGLT1) currents and fluxes. *J Membr Biol*; **162**(2): 101-6.

Mackenzie, B., Panayotova-Heiermann, M., Loo, D.D., Lever, J.E. and Wright, E.M. (1994). SAAT1 is a low affinity Na+/glucose cotransporter and not an amino acid transporter. A reinterpretation. *J Biol Chem*; **269**(36): 22488-91.

Maher, F., Vannucci, S.J. and Simpson, I.A. (1994). Glucose transporter proteins in brain. *Faseb J*; **8**(13): 1003-11.

Mahraoui, L., Rodolosse, A., Barbat, A., Dussaulx, E., Zweibaum, A. *et al.* (1994). Presence and differential expression of SGLT1, GLUT1, GLUT2, GLUT3 and GLUT5 hexose-transporter mRNAs in Caco-2 cell clones in relation to cell growth and glucose consumption. *Biochem J*; **298**(3 Pt 3): 629-33.

Malathi, P. and Crane, R.K. (1969). Phlorizin hydrolase: a beta-glucosidase of hamster intestinal brush border membrane. *Biochim Biophys Acta*; **173**(2): 245-56.

Mamchaoui, K., Makhloufi, Y. and Saumon, G. (2002). Glucose transporter gene expression in freshly isolated and cultured rat pneumocytes. *Acta Physiol Scand*; **175**(1): 19-24.

Mandarino, L.J., Finlayson, J. and Hassell, J.R. (1994). High glucose downregulates glucose transport activity in retinal capillary pericytes but not endothelial cells. *Invest Ophthalmol Vis Sci*; **35**(3): 964-72.

Mantych, G.J., Hageman, G.S. and Devaskar, S.U. (1993b). Characterization of glucose transporter isoforms in the adult and developing human eye. *Endocrinology*; **133**(2): 600-7.

Mantych, G.J., James, D.E. and Devaskar, S.U. (1993a). Jejunal/kidney glucose transporter isoform (Glut-5) is expressed in the human blood-brain barrier. *Endocrinology*; **132**(1): 35-40.

Marcus, R.G., England, R., Nguyen, K., Charron, M.J., Briggs, J.P. *et al.* (1994). Altered renal expression of the insulin-responsive glucose transporter GLUT4 in experimental diabetes mellitus. *Am J Physiol*; **267**(5 Pt 2): F816-24.

Martin, M.G., Turk, E., Lostao, M.P., Kerner, C. and Wright, E.M. (1996). Defects in Na+/glucose cotransporter (SGLT1) trafficking and function cause glucose-galactose malabsorption. *Nat Genet*; **12**(2): 216-20.

Masters, B.A., Werner, H., Roberts, C.T., Jr., LeRoith, D. and Raizada, M.K. (1991). Developmental regulation of insulin-like growth factor-I-stimulated glucose transporter in rat brain astrocytes. *Endocrinology*; **128**(5): 2548-57.

Masterson, E. and Chader, G.J. (1981). Characterization of glucose transport by cultured chick pigmented epithelium. *Exp Eye Res*; **32**(3): 279-89.

Matsui, H., Murakami, M., Wynns, G.C., Conroy, C.W., Mead, A. *et al.* (1996). Membrane carbonic anhydrase (IV) and ciliary epithelium. Carbonic anhydrase activity is present in the basolateral membranes of the non-pigmented ciliary epithelium of rabbit eyes. *Exp Eye Res*; **62**(4): 409-17.

Matsuura, T., Tamura, T., Chinen, Y. and Ohta, T. (2002). A novel mutation (N32K) of GLUT2 gene in a Japanese patient with Fanconi-Bickel syndrome. *Clin Genet*; **62**(3): 255-6.

McCartney, M.D. and Cantu-Crouch, D. (1992). Rabbit corneal epithelial wound repair: tight junction reformation. *Curr Eye Res*; **11**(1): 15-24.

McVie-Wylie, A.J., Lamson, D.R. and Chen, Y.T. (2001). Molecular cloning of a novel member of the GLUT family of transporters, SLC2a10 (GLUT10), localized on chromosome 20q13.1: a candidate gene for NIDDM susceptibility. *Genomics*; **72**(1): 113-7.

Meinild, A., Klaerke, D.A., Loo, D.D., Wright, E.M. and Zeuthen, T. (1998). The human Na+-glucose cotransporter is a molecular water pump. *J Physiol*; **508**(Pt 1): 15-21.

Meinild, A.K., Hirayama, B.A., Wright, E.M. and Loo, D.D. (2002). Fluorescence studies of ligand-induced conformational changes of the Na(+)/glucose cotransporter. *Biochemistry*; **41**(4): 1250-8.

Melnik, E., Latorre, R., Hall, J.E. and Tosteson, D.C. (1977). Phloretin-induced changes in ion transport across lipid bilayer membranes. *J Gen Physiol*; **69**(2): 243-57.

Merriman-Smith, B.R., Krushinsky, A., Kistler, J. and Donaldson, P.J. (2003). Expression patterns for glucose transporters GLUT1 and GLUT3 in the normal rat lens and in models of diabetic cataract. *Invest Ophthalmol Vis Sci*; **44**(8): 3458-66.

Merriman-Smith, R., Donaldson, P. and Kistler, J. (1999). Differential expression of facilitative glucose transporters GLUT1 and GLUT3 in the lens. *Invest Ophthalmol Vis Sci*; **40**(13): 3224-30.

Metz, J., Aoki, A. and Forssmann, W.G. (1978). Studies on the ultrastructure and permeability of the hemotrichorial placenta. I. Intercellular junctions of layer I and tracer administration into the maternal compartment. *Cell Tissue Res*; **192**(3): 391-407.

Miceli, M.V., Newsome, D.A. and Schriver, G.W. (1990). Glucose uptake, hexose monophosphate shunt activity, and oxygen consumption in cultured human retinal pigment epithelial cells. *Invest Ophthalmol Vis Sci*; **31**(2): 277-83.

Michelle Furtado, L., Poon, V. and Klip, A. (2003). GLUT4 activation: thoughts on possible mechanisms. *Acta Physiol Scand*; **178**(4): 287-96.

Miller, J.H., Mullin, J.M., McAvoy, E. and Kleinzeller, A. (1992). Polarity of transport of 2-deoxy-D-glucose and D-glucose by cultured renal epithelia (LLC-PK1). *Biochim Biophys Acta*; **1110**(2): 209-17.

Miller, S. and Steinberg, R.H. (1976). Transport of taurine, L-methionine and 3-o-methyl-D-glucose across frog retinal pigment epithelium. *Exp Eye Res*; **23**(2): 177-89.

Miller, W.R., Hulme, M.J., Bartlett, J.M., MacCallum, J. and Dixon, J.M. (1997). Changes in messenger RNA expression of protein kinase A regulatory subunit ialpha in breast cancer patients treated with tamoxifen. *Clin Cancer Res*; **3**(12 Pt 1): 2399-404.

Misra, A., Vikram, N.K. and Kumar, A. (2004). Diabetic maculopathy and lipid-lowering therapy. *Eye*; **18**(1): 107-8.

Miura, S., Tsunoda, N., Ikeda, S., Kai, Y., Ono, M. *et al.* (2003). Regulatory sequence elements of mouse GLUT4 gene expression in adipose tissues. *Biochem Biophys Res Commun*; **312**(2): 277-84.

Miyamoto, K., Khosrof, S., Bursell, S.E., Rohan, R., Murata, T. *et al.* (1999). Prevention of leukostasis and vascular leakage in streptozotocin-induced diabetic retinopathy via intercellular adhesion molecule-1 inhibition. *Proc Natl Acad Sci U S A*; **96**(19): 10836-41.

Miyamoto, K., Tatsumi, S., Morimoto, A., Minami, H., Yamamoto, H. *et al.* (1994). Characterization of the rabbit intestinal fructose transporter (GLUT5). *Biochem J*; **303**(Pt 3): 877-83.

Mobasheri, A., Neama, G., Bell, S., Richardson, S. and Carter, S.D. (2002). Human articular chondrocytes express three facilitative glucose transporter isoforms: GLUT1, GLUT3 and GLUT9. *Cell Biol Int*; **26**(3): 297-300.

Mooradian, A.D. and Morin, A.M. (1991). Brain uptake of glucose in diabetes mellitus: the role of glucose transporters. *Am J Med Sci*; **301**(3): 173-7.

Morgello, S., Uson, R.R., Schwartz, E.J. and Haber, R.S. (1995). The human blood-brain barrier glucose transporter (GLUT1) is a glucose transporter of gray matter astrocytes. *Glia*; **14**(1): 43-54.

Morimura, H., Shimada, S., Otori, Y., Saishin, Y., Yamauchi, A. *et al.* (1997). The differential osmoregulation and localization of taurine transporter mRNA and Na+/myo-inositol cotransporter mRNA in rat eyes. *Brain Res Mol Brain Res*; **44**(2): 245-52.

Morrison, J.C. and Freddo, T.F. (1996). Anatomy, microcirculation, and ultrastructure of the ciliary body. In: *The Glaucomas* (Eds, Ritch, R., Shields, M.B. and Krupin, T.). St. Louis: CV Mosby, pp. 125-138.

Mueckler, M. (1994a). Facilitative glucose transporters. *Eur J Biochem*; **219**(3): 713-25.

Mueckler, M., Caruso, C., Baldwin, S.A., Panico, M., Blench, I. *et al.* (1985). Sequence and structure of a human glucose transporter. *Science*; **229**(4717): 941-5.

Mueckler, M., Weng, W. and Kruse, M. (1994b). Glutamine 161 of Glut1 glucose transporter is critical for transport activity and exofacial ligand binding. *J Biol Chem*; **269**(32): 20533-8.

Mueller, R. and Young, I. (2001). DNA technology and applications. In: *Emery's Elements of Medical Genetics* (Eds, Mueller, R. and Young, I.). Edinburgh: Elsevier Science Limited, pp. 55-79.

Mullarkey, C.J., Edelstein, D. and Brownlee, M. (1990). Free radical generation by early glycation products: a mechanism for accelerated atherogenesis in diabetes. *Biochem Biophys Res Commun*; **173**(3): 932-9.

Muller, L.M. and Kennedy, J.A. (1996). Quantification of rat pre-pro-thyrotropin releasing hormone (TRH) mRNA by reverse transcription-polymerase chain reaction using external and internal standardisation. *J Neurosci Methods*; **68**(2): 269-74.

Muther, T.F. and Friedland, B.R. (1980). Autoradiographic localization of carbonic anhydrase in the rabbit ciliary body. *J Histochem Cytochem*; **28**(10): 1119-24.

Nagamatsu, S., Kornhauser, J.M., Burant, C.F., Seino, S., Mayo, K.E. *et al.* (1992). Glucose transporter expression in brain. cDNA sequence of mouse GLUT3, the brain facilitative glucose transporter isoform, and identification of sites of expression by in situ hybridization. *J Biol Chem*; **267**(1): 467-72.

Nagamatsu, S., Sawa, H., Kamada, K., Nakamichi, Y., Yoshimoto, K. *et al.* (1993). Neuron-specific glucose transporter (NSGT): CNS distribution of GLUT3 rat glucose transporter (RGT3) in rat central neurons. *FEBS Lett*; **334**(3): 289-95.

Nagaraj, R.H., Kern, T.S., Sell, D.R., Fogarty, J., Engerman, R.L. *et al.* (1996). Evidence of a glycemic threshold for the formation of pentosidine in diabetic dog lens but not in collagen. *Diabetes*; **45**(5): 587-94.

Nagata, K., Hori, N., Sato, K., Ohta, K., Tanaka, H. *et al.* (1999). Cloning and functional expression of an SGLT-1-like protein from the Xenopus laevis intestine. *Am J Physiol*; **276**(5 Pt 1): G1251-9.

Nakamura, S., Makita, Z., Ishikawa, S., Yasumura, K., Fujii, W. *et al.* (1997). Progression of nephropathy in spontaneous diabetic rats is prevented by OPB-9195, a novel inhibitor of advanced glycation. *Diabetes*; **46**(5): 895-9.

Nelson, J.A. and Falk, R.E. (1993). Phloridzin and phloretin inhibition of 2-deoxy-D-glucose uptake by tumor cells in vitro and in vivo. *Anticancer Res*; **13**(6A): 2293-9.

Nielsen, N.V. and Vinding, T. (1984). The prevalence of cataract in insulin-dependent and non-insulin-dependent-diabetes mellitus. *Acta Ophthalmol (Copenh)*; **62**(4): 595-602.

Nishikawa, T., Edelstein, D., Du, X.L., Yamagishi, S., Matsumura, T. *et al.* (2000). Normalizing mitochondrial superoxide production blocks three pathways of hyperglycaemic damage. *Nature*; **404**(6779): 787-90.

Nishio, Y., Kashiwagi, A., Taki, H., Shinozaki, K., Maeno, Y. *et al.* (1998). Altered activities of transcription factors and their related gene expression in cardiac tissues of diabetic rats. *Diabetes*; **47**(8): 1318-25.

Nishizaki, T., Kammesheidt, A., Sumikawa, K., Asada, T. and Okada, Y. (1995). A sodium- and energy-dependent glucose transporter with similarities to SGLT1-2 is expressed in bovine cortical vessels. *Neurosci Res*; **22**(1): 13-22.

Nishizaki, T. and Matsuoka, T. (1998). Low glucose enhances Na+/glucose transport in bovine brain artery endothelial cells. *Stroke*; **29**(4): 844-9.

Nixon, A.J., Brower-Toland, B.D. and Sandell, L.J. (1999). Primary nucleotide structure of predominant and alternate splice forms of equine insulin-like growth factor I and their gene expression patterns in tissues. *Am J Vet Res*; **60**(10): 1234-41.

Nonaka, A., Kiryu, J., Tsujikawa, A., Yamashiro, K., Miyamoto, K. *et al.* (2000). PKC-beta inhibitor (LY333531) attenuates leukocyte entrapment in retinal microcirculation of diabetic rats. *Invest Ophthalmol Vis Sci*; **41**(9): 2702-6.

Noske, W., Stamm, C.C. and Hirsch, M. (1994). Tight junctions of the human ciliary epithelium: regional morphology and implications on transepithelial resistance. *Exp Eye Res*; **59**(2): 141-9.

Novelli, M., De Tata, V., Bombara, M., Bergamini, E. and Masiello, P. (2000). Age-dependent reduction in GLUT-2 levels is correlated with the impairment of the insulin secretory response in isolated islets of Sprague-Dawley rats. *Exp Gerontol*; **35**(5): 641-51.

Oates, P.J. (2002). Polyol pathway and diabetic peripheral neuropathy. *Int Rev Neurobiol*; **50**: 325-92.

Obrosova, I., Cao, X., Greene, D.A. and Stevens, M.J. (1998). Diabetes-induced changes in lens antioxidant status, glucose utilization and energy metabolism: effect of DL-alpha-lipoic acid. *Diabetologia*; **41**(12): 1442-50.

Oh, J., Krupin, T., Tang, L.Q., Sveen, J. and Lahlum, R.A. (1994). Dye coupling of rabbit ciliary epithelial cells in vitro. *Invest Ophthalmol Vis Sci*; **35**(5): 2509-14.

Ohneda, M., Johnson, J.H., Inman, L.R., Chen, L., Suzuki, K. *et al.* (1993). GLUT2 expression and function in beta-cells of GK rats with NIDDM. Dissociation between reductions in glucose transport and glucose-stimulated insulin secretion. *Diabetes*; **42**(7): 1065-72.

Ohtsubo, M., Noguchi, S., Takeda, K., Morohashi, M. and Kawamura, M. (1990). Site-directed mutagenesis of Asp-376, the catalytic phosphorylation site, and Lys-507, the putative ATP-binding site, of the alpha-subunit of Torpedo californica Na+/K(+)-ATPase. *Biochim Biophys Acta*; **1021**(2): 157-60.

Okisaka, S. and Kuwabara, T. (1974). Selective destruction of the pigmented epithelium in the ciliary body of the eye. *Science*; **184**(143): 1298-9.

Oku, A., Ueta, K., Arakawa, K., Kano-Ishihara, T., Matsumoto, M. *et al.* (2000). Antihyperglycemic effect of T-1095 via inhibition of renal Na+-glucose cotransporters in streptozotocin-induced diabetic rats. *Biol Pharm Bull*; **23**(12): 1434-7.

Omer, S., Lomthaisong, K. and Bicknell, A.B. (2002). Identification of two alternate splice variants of a novel serine protease expressed in steroidogenic tissues. *Endocr Res*; **28**(4): 339-48.

Ono, Y., Aoki, S., Ohnishi, K., Yasuda, T., Kawano, K. *et al.* (1998). Increased serum levels of advanced glycation end-products and diabetic complications. *Diabetes Res Clin Pract*; **41**(2): 131-7.

Orci, L., Ravazzola, M., Baetens, D., Inman, L., Amherdt, M. *et al.* (1990). Evidence that down-regulation of beta-cell glucose transporters in non-insulin-dependent diabetes may be the cause of diabetic hyperglycemia. *Proc Natl Acad Sci U S A*; **87**(24): 9953-7.

Orci, L., Thorens, B., Ravazzola, M. and Lodish, H.F. (1989). Localization of the pancreatic beta cell glucose transporter to specific plasma membrane domains. *Science*; **245**(4915): 295-7.

Oulianova, N. and Berteloot, A. (1996). Sugar transport heterogeneity in the kidney: two independent transporters or different transport modes through an oligomeric Protein? 1. Glucose transport studies. *J Membr Biol*; **153**(3): 181-94.

Oulianova, N., Falk, S. and Berteloot, A. (2001). Two-step mechanism of phlorizin binding to the SGLT1 protein in the kidney. *J Membr Biol*; **179**(3): 223-42.

Panayotova-Heiermann, M., Eskandari, S., Turk, E., Zampighi, G.A. and Wright, E.M. (1997). Five transmembrane helices form the sugar pathway through the Na+/glucose cotransporter. *J Biol Chem*; **272**(33): 20324-7.

Panayotova-Heiermann, M., Loo, D.D. and Wright, E.M. (1995). Kinetics of steady-state currents and charge movements associated with the rat Na+/glucose cotransporter. *J Biol Chem*; **270**(45): 27099-105.

Panayotova-Heiermann, M. and Wright, E.M. (2001). Mapping the urea channel through the rabbit Na(+)-glucose cotransporter SGLT1. *J Physiol*; **535**(Pt 2): 419-25.

Pappenheimer, J.R. and Setchell, B.P. (1973). Cerebral glucose transport and oxygen consumption in sheep and rabbits. *J Physiol*; **233**(3): 529-51.

Pardridge, W.M., Boado, R.J. and Farrell, C.R. (1990b). Brain-type glucose transporter (GLUT-1) is selectively localized to the blood-brain barrier. Studies with quantitative western blotting and in situ hybridization. *J Biol Chem*; **265**(29): 18035-40.

Parent, L., Supplisson, S., Loo, D.D. and Wright, E.M. (1992). Electrogenic properties of the cloned Na+/glucose cotransporter: I. Voltage-clamp studies. *J Membr Biol*; **125**(1): 49-62.

Pascuzzo, G.J., Johnson, J.E. and Pautler, E.L. (1980). Glucose transport in isolated mammalian pigment epithelum. *Exp Eye Res*; **30**(1): 53-8.

Payne, J., Maher, F., Simpson, I., Mattice, L. and Davies, P. (1997). Glucose transporter Glut 5 expression in microglial cells. *Glia*; **21**(3): 327-31.

Pedemonte, C.H. and Kaplan, J.H. (1990). Chemical modification as an approach to elucidation of sodium pump structure-function relations. *Am J Physiol*; **258**(1 Pt 1): C1-23.

Pedersen, O., Bak, J.F., Andersen, P.H., Lund, S., Moller, D.E. *et al.* (1990). Evidence against altered expression of GLUT1 or GLUT4 in skeletal muscle of patients with obesity or NIDDM. *Diabetes*; **39**(7): 865-70.

Pedersen, O., Kahn, C.R., Flier, J.S. and Kahn, B.B. (1991). High fat feeding causes insulin resistance and a marked decrease in the expression of glucose transporters (Glut 4) in fat cells of rats. *Endocrinology*; **129**(2): 771-7.

Pederson, J.E. (1982). Fluid permeability of monkey ciliary epithelium in vivo. *Invest Ophthalmol Vis Sci*; **23**(2): 176-80.

Phay, J.E., Hussain, H.B. and Moley, J.F. (2000). Cloning and expression analysis of a novel member of the facilitative glucose transporter family, SLC2A9 (GLUT9). *Genomics*; **66**(2): 217-20.

Phillips, S.L., DeRubertis, F.R. and Craven, P.A. (1999). Regulation of the laminin C1 promoter in cultured mesangial cells. *Diabetes*; **48**(10): 2083-9.

Pino, R.M. and Thouron, C.L. (1983). Vascular permeability in the rat eye to endogenous albumin and immunoglobulin G (IgG) examined by immunohistochemical methods. *J Histochem Cytochem*; **31**(3): 411-6.

Piroli, G.G., Grillo, C.A., Hoskin, E.K., Znamensky, V., Katz, E.B. *et al.* (2002). Peripheral glucose administration stimulates the translocation of GLUT8 glucose transporter to the endoplasmic reticulum in the rat hippocampus. *J Comp Neurol*; **452**(2): 103-14.

Pokupec, R., Kalauz, M., Turk, N. and Turk, Z. (2003). Advanced glycation endproducts in human diabetic and non-diabetic cataractous lenses. *Graefes Arch Clin Exp Ophthalmol*; **241**(5): 378-84.

Postic, C., Burcelin, R., Rencurel, F., Pegorier, J.P., Loizeau, M. *et al.* (1993). Evidence for a transient inhibitory effect of insulin on GLUT2 expression in the liver: studies in vivo and in vitro. *Biochem J*; **293**((Pt 1)): 119-24.

Poulaki, V., Joussen, A.M., Mitsiades, N., Mitsiades, C.S., Iliaki, E.F. *et al.* (2004). Insulin-like growth factor-I plays a pathogenetic role in diabetic retinopathy. *Am J Pathol*; **165**(2): 457-69.

Poulsen, P., Vaag, A.A., Kyvik, K.O., Moller Jensen, D. and Beck-Nielsen, H. (1997). Low birth weight is associated with NIDDM in discordant monozygotic and dizygotic twin pairs. *Diabetologia*; **40**(4): 439-46.

Raichle, M.E., Larson, K.B., Phelps, M.E., Grubb, R.L., Jr., welch, M.J. *et al.* (1975). In vivo measurement of brain glucose transport and metabolism employing glucose- -11C. *Am J Physiol*; **228**(6): 1936-48.

Rajah, T.T., Olson, A.L. and Grammas, P. (2001). Differential glucose uptake in retina- and brain-derived endothelial cells. *Microvasc Res*; **62**(3): 236-42.

Rajakumar, R.A., Thamotharan, S., Menon, R.K. and Devaskar, S.U. (1998). Sp1 and Sp3 regulate transcriptional activity of the facilitative glucose transporter isoform-3 gene in mammalian neuroblasts and trophoblasts. *J Biol Chem*; **273**(42): 27474-83.

Rao, P., Cozar-Castellano, I., Roccisana, J., Vasavada, R.C. and Garcia-Ocana, A. (2004). Hepatocyte growth factor gene therapy for islet transplantation. *Expert Opin Biol Ther*; **4**(4): 507-18.

Raval, P. (1994). Qualitative and quantitative determination of mRNA. *J Pharmacol Toxicol Methods*; **32**(3): 125-7.

Ravelli, A.C., van der Meulen, J.H., Michels, R.P., Osmond, C., Barker, D.J. *et al.* (1998). Glucose tolerance in adults after prenatal exposure to famine. *Lancet*; **351**(9097): 173-7.

Raviola, G. (1971). The fine structure of the ciliary zonule and ciliary epithelium. With special regard to the organization and insertion of the zonular fibrils. *Invest Ophthalmol*; **10**(11): 851-69.

Raviola, G. (1977). The structural basis of the blood-ocular barriers. *Exp Eye Res*; **25**(Suppl): 27-63.

Raviola, G. and Raviola, E. (1978). Intercellular junctions in the ciliary epithelium. *Invest Ophthalmol Vis Sci*; **17**(10): 958-81.

Rayner, D.V., Thomas, M.E. and Trayhurn, P. (1994). Glucose transporters (GLUTs 1-4) and their mRNAs in regions of the rat brain: insulin-sensitive transporter expression in the cerebellum. *Can J Physiol Pharmacol*; **72**(5): 476-9.

Reese, T.S. and Karnovsky, M.J. (1967). Fine structural localization of a blood-brain barrier to exogenous peroxidase. *J Cell Biol*; **34**(1): 207-17.

Reichenbach, A. (1989). Attempt to classify glial cells by means of their process specialization using the rabbit retinal Muller cell as an example of cytotopographic specialization of glial cells. *Glia*; **2**(4): 250-9.

Renard, E. (2002). Implantable closed-loop glucose-sensing and insulin delivery: the future for insulin pump therapy. *Curr Opin Pharmacol*; **2**(6): 708-16.

Reusch, J.E., Sussman, K.E. and Draznin, B. (1993). Inverse relationship between GLUT-4 phosphorylation and its intrinsic activity. *J Biol Chem*; **268**(5): 3348-51.

Richter, M., Guscetti, F. and Spiess, B. (2002). Aldose reductase activity and glucose-related opacities in incubated lenses from dogs and cats. *Am J Vet Res*; **63**(11): 1591-7.

Riley, M.V. and Kishida, K. (1986). ATPases of ciliary epithelium: cellular and subcellular distribution and probable role in secretion of aqueous humor. *Exp Eye Res*; **42**(6): 559-68.

Rink, T.J. (1984). Aspects of the regulation of cell volume. *J Physiol (Paris)*; **79**(6): 388-94.

Risek, B. and Gilula, N.B. (1991). Spatiotemporal expression of three gap junction gene products involved in fetomaternal communication during rat pregnancy. *Development*; **113**(1): 165-81.

Ristow, M. (2004). Neurodegenerative disorders associated with diabetes mellitus. *J Mol Med*; **82**(8): 510-29.

Rizzolo, L.J. (1997). Polarity and the development of the outer blood-retinal barrier. *Histol Histopathol*; **12**(4): 1057-67.

Robinson, K.A., Weinstein, M.L., Lindenmayer, G.E. and Buse, M.G. (1995). Effects of diabetes and hyperglycemia on the hexosamine synthesis pathway in rat muscle and liver. *Diabetes*; **44**(12): 1438-46.

Robinson, S. and Kessling, A. (1992). Diabetes secondary to genetic disorders. *Baillieres Clin Endocrinol Metab*; **6**(4): 867-98.

Roeder, L.M., Tildon, J.T. and Williams, I.B. (1985). Transport of 2-deoxy-D-glucose by dissociated brain cells. *Brain Res*; **345**(2): 298-305.

Rogers, S., Chandler, J.D., Clarke, A.L., Petrou, S. and Best, J.D. (2003b). Glucose transporter GLUT12-functional characterization in Xenopus laevis oocytes. *Biochem Biophys Res Commun*; **308**(3): 422-6.

Rogers, S., Docherty, S.E., Slavin, J.L., Henderson, M.A. and Best, J.D. (2003a). Differential expression of GLUT12 in breast cancer and normal breast tissue. *Cancer Lett*; **193**(2): 225-33.

Rogers, S., Macheda, M.L., Docherty, S.E., Carty, M.D., Henderson, M.A. *et al.* (2002). Identification of a novel glucose transporter-like protein-GLUT-12. *Am J Physiol Endocrinol Metab*; **282**(3): E733-8.

Roll, P., Massacrier, A., Pereira, S., Robaglia-Schlupp, A., Cau, P. *et al.* (2002). New human sodium/glucose cotransporter gene (KST1): identification, characterization, and mutation analysis in ICCA (infantile convulsions and choreoathetosis) and BFIC (benign familial infantile convulsions) families. *Gene*; **285**(1-2): 141-8.

Rollins, B.J., Morrison, E.D., Usher, P. and Flier, J.S. (1988). Platelet-derived growth factor regulates glucose transporter expression. *J Biol Chem*; **263**(32): 16523-6.

Rosenberg, I.M. (1996). Tracking the target proteins. In: *Protein Analysis and Purification* (Ed, Rosenberg, I.M.). Boston: Birkhauser, pp. 19-31.

Rosenberg, I.M. (1996). Transfer and detection of proteins on membrane supports. In: *Protein Analysis and Purification* (Ed, Rosenberg, I.M.). Boston: Birkhauser, pp. 153-182.

Rotimi, C., Daniel, H., Zhou, J., Obisesan, A., Chen, G. *et al.* (2003). Prevalence and determinants of diabetic retinopathy and cataracts in West African type 2 diabetes patients. *Ethn Dis*; **13**(2 Suppl 2): S110-7.

Royer, C., Lachuer, J., Crouzoulon, G., Roux, J., Peyronnet, J. *et al.* (2000). Effects of gestational hypoxia on mRNA levels of Glut3 and Glut4 transporters, hypoxia inducible factor-1 and thyroid hormone receptors in developing rat brain. *Brain Res*; **856**(1-2): 119-28.

Rudich, A., Konrad, D., Torok, D., Ben-Romano, R., Huang, C. *et al.* (2003). Indinavir uncovers different contributions of GLUT4 and GLUT1 towards glucose uptake in muscle and fat cells and tissues. *Diabetologia*; **46**(5): 649-58.

Sabbatini, A.R., Werner, P.A., Guha, C., Paddock, G.V. and Galbraith, R.M. (1993). The vitamin D-binding protein gene: quantitation of amplified nucleic acids by ELISA. *Biotechniques*; **15**(4): 706-13.

Saiki, R.K., Gelfand, D.H., Stoffel, S., Scharf, S.J., Higuchi, R. *et al.* (1988). Primer-directed enzymatic amplification of DNA with a thermostable DNA polymerase. *Science*; **239**(4839): 487-91.

Saiki, R.K., Scharf, S., Faloona, F., Mullis, K.B., Horn, G.T. *et al.* (1985). Enzymatic amplification of beta-globin genomic sequences and restriction site analysis for diagnosis of sickle cell anemia. *Science*; **230**(4732): 1350-4.

Sankar, R., Thamotharan, S., Shin, D., Moley, K.H. and Devaskar, S.U. (2002). Insulin-responsive glucose transporters-GLUT8 and GLUT4 are expressed in the developing mammalian brain. *Brain Res Mol Brain Res*; **107**(2): 157-65.

Santer, R., Schneppenheim, R., Dombrowski, A., Gotze, H., Steinmann, B. *et al.* (1997). Mutations in GLUT2, the gene for the liver-type glucose transporter, in patients with Fanconi-Bickel syndrome. *Nat Genet*; **17**(3): 324-6.

Sasaki, T., Minoshima, S., Shiohama, A., Shintani, A., Shimizu, A. *et al.* (2001). Molecular cloning of a member of the facilitative glucose transporter gene family GLUT11 (SLC2A11) and identification of transcription variants. *Biochem Biophys Res Commun*; **289**(5): 1218-24.

Sato, M. and Mueckler, M. (1999). A conserved amino acid motif (R-X-G-R-R) in the Glut1 glucose transporter is an important determinant of membrane topology. *J Biol Chem*; **274**(35): 24721-5.

Schalin-Jantti, C., Yki-Jarvinen, H., Koranyi, L., Bourey, R., Lindstrom, J. *et al.* (1994). Effect of insulin on GLUT-4 mRNA and protein concentrations in skeletal muscle of patients with NIDDM and their first-degree relatives. *Diabetologia*; **37**(4): 401-7.

Schalkwijk, C.G., Posthuma, N., ten Brink, H.J., ter Wee, P.M. and Teerlink, T. (1999). Induction of 1,2-dicarbonyl compounds, intermediates in the formation of advanced glycation end-products, during heat-sterilization of glucose-based peritoneal dialysis fluids. *Perit Dial Int*; **19**(4): 325-33.

Schleicher, E.D. and Weigert, C. (2000). Role of the hexosamine biosynthetic pathway in diabetic nephropathy. *Kidney Int Suppl*; **77**: S13-8.

Schlingemann, R.O., Hofman, P., Klooster, J., Blaauwgeers, H.G., Van der Gaag, R. *et al.* (1998). Ciliary muscle capillaries have blood-tissue barrier characteristics. *Exp Eye Res*; **66**(6): 747-54.

Schultheis, P.J. and Lingrel, J.B. (1993). Substitution of transmembrane residues with hydrogen-bonding potential in the alpha subunit of Na,K-ATPase reveals alterations in ouabain sensitivity. *Biochemistry*; **32**(2): 544-50.

Schultz, R.O., Peters, M.A., Sobocinski, K., Nassif, K. and Schultz, K.J. (1983). Diabetic keratopathy as a manifestation of peripheral neuropathy. *Am J Ophthalmol*; **96**(3): 368-71.

Schurmann, A., Doege, H., Ohnimus, H., Monser, V., Buchs, A. *et al.* (1997). Role of conserved arginine and glutamate residues on the cytosolic surface of glucose transporters for transporter function. *Biochemistry*; **36**(42): 12897-902.

Sebag, J. (1996). Diabetic vitreopathy. *Ophthalmology*; **103**(2): 205-6.

Sensi, M., Pricci, F., Pugliese, G., De Rossi, M.G., Petrucci, A.F. *et al.* (1995). Role of advanced glycation end-products (AGE) in late diabetic complications. *Diabetes Res Clin Pract*; **28**(1): 9-17.

Setter, S.M., Campbell, R.K. and Cahoon, C.J. (2003). Biochemical pathways for microvascular complications of diabetes mellitus. *Ann Pharmacother*; **37**(12): 1858-66.

Seyfang, A. and Duszenko, M. (1991). Specificity of glucose transport in Trypanosoma brucei. Effective inhibition by phloretin and cytochalasin B. *Eur J Biochem*; **202**(1): 191-6.

Seyoum, B., Mengistu, Z., Berhanu, P., Abdulkadir, J., Feleke, Y. *et al.* (2001). Retinopathy in patients of Tikur Anbessa Hospital diabetic clinic. *Ethiop Med J*; **39**(2): 123-31.

Sharma, R. and Ehinger, B. (2002). Development and structure of the retina. In: *Adler's Physiology of the Eye* (Eds, Alm, A. and Ehinger, B.). St. Louis: Mosby, Inc., pp. 319-347.

Shepherd, E.J., Helliwell, P.A., Lister, N., Mace, O.J., Morgan, E.L. *et al.* (2004). Stress and glucocorticoid inhibit apical GLUT2-trafficking and intestinal glucose absorption in rat small intestine. *J Physiol.*

Shepherd, P.R., Gibbs, E.M., Wesslau, C., Gould, G.W. and Kahn, B.B. (1992). Human small intestine facilitative fructose/glucose transporter (GLUT5) is also present in insulin-responsive tissues and brain. Investigation of biochemical characteristics and translocation. *Diabetes*; **41**(10): 1360-5.

Shepherd, P.R. and Kahn, B.B. (1999). Glucose transporters and insulin action--implications for insulin resistance and diabetes mellitus. *N Engl J Med*; **341**(4): 248-57.

Shetty, M., Ismail-Beigi, N., Loeb, J.N. and Ismail-Beigi, F. (1993). Induction of GLUT1 mRNA in response to inhibition of oxidative phosphorylation. *Am J Physiol*; **265**(5 Pt 1): C1224-9.

Shimizu, H., Riley, M.V. and Cole, D.F. (1967). The isolation of whole cells from the ciliary epithelium together with some observations on the metabolism of the two cell types. *Exp Eye Res*; **6**(2): 141-51.

Shin, B.C., Suzuki, T., Tanaka, S., Kuraoka, A., Shibata, Y. *et al.* (1996). Connexin 43 and the glucose transporter, GLUT1, in the ciliary body of the rat. *Histochem Cell Biol*; **106**(2): 209-14.

Silverman, M. (1976). Glucose transport in the kidney. *Biochim Biophys Acta*; **457**(3-4): 303-51.

Silverman, M. (1991). Structure and function of hexose transporters. *Annu Rev Biochem*; **60**: 757-94.

Simpson, I.A., Chundu, K.R., Davies-Hill, T., Honer, W.G. and Davies, P. (1994). Decreased concentrations of GLUT1 and GLUT3 glucose transporters in the brains of patients with Alzheimer's disease. *Ann Neurol*; **35**(5): 546-51.

Sivitz, W.I., DeSautel, S.L., Kayano, T., Bell, G.I. and Pessin, J.E. (1989). Regulation of glucose transporter messenger RNA in insulin-deficient states. *Nature*; **340**(6228): 72-4.

Smogorzewski, M., Galfayan, V. and Massry, S.G. (1998). High glucose concentration causes a rise in [Ca2+]i of cardiac myocytes. *Kidney Int*; **53**(5): 1237-43.

Snoeck, A., Remacle, C., Reusens, B. and Hoet, J.J. (1990). Effect of a low protein diet during pregnancy on the fetal rat endocrine pancreas. *Biol Neonate*; **57**(2): 107-18.

Sokoloff, L. (1973). Metabolism of ketone bodies by the brain. *Annu Rev Med*; **24**: 271-80.

Sone, H., Deo, B.K. and Kumagai, A.K. (2000). Enhancement of glucose transport by vascular endothelial growth factor in retinal endothelial cells. *Invest Ophthalmol Vis Sci*; **41**(7): 1876-84.

Spray, D.C. and Bennett, M.V. (1985). Physiology and pharmacology of gap junctions. *Annu Rev Physiol*; **47**: 281-303.

Stanga, P.E., Boyd, S.R. and Hamilton, A.M. (1999). Ocular manifestations of diabetes mellitus. *Curr Opin Ophthalmol*; **10**(6): 483-9.

Steane, S.E., Mylott, D. and White, M.K. (1998). Regulation of a heterologous glucose transporter promoter in chicken embryo fibroblasts. *Biochem Biophys Res Commun*; **252**(2): 318-23.

Stewart, P.A., Hayakawa, K. and Farrell, C.L. (1994). Quantitation of blood-brain barrier ultrastructure. *Microsc Res Tech*; **27**(6): 516-27.

Stitt, A.W. (2001). Advanced glycation: an important pathological event in diabetic and age related ocular disease. *Br J Ophthalmol*; **85**(6): 746-53.

Stitt, A.W., Anderson, H.R., Gardiner, T.A., McIntyre, I. and Archer, D.B. (1994). The combined effects of diabetes and ionising radiation on the rat retina: an ultrastructural study. *Curr Eye Res*; **13**(1): 79-86.

Stitt, A.W., Moore, J.E., Sharkey, J.A., Murphy, G., Simpson, D.A. *et al.* (1998). Advanced glycation end products in vitreous: Structural and functional implications for diabetic vitreopathy. *Invest Ophthalmol Vis Sci*; **39**(13): 2517-23.

Stoesser, G., Tuli, M.A., Lopez, R. and Sterk, P. (1999). The EMBL Nucleotide Sequence Database. *Nucleic Acids Res*; **27**(1): 18-24.

Stramm, L.E. and Pautler, E.L. (1982). Transport of 3-O-methylglucose in isolated rat retinal pigment epithelial cells. *Exp Eye Res*; **35**(2): 91-7.

Strange, K. (1992). Regulation of solute and water balance and cell volume in the central nervous system. *J Am Soc Nephrol*; **3**(1): 12-27.

Studer, R.K., Craven, P.A. and DeRubertis, F.R. (1993). Role for protein kinase C in the mediation of increased fibronectin accumulation by mesangial cells grown in high-glucose medium. *Diabetes*; **42**(1): 118-26.

Stumpel, F., Burcelin, R., Jungermann, K. and Thorens, B. (2001). Normal kinetics of intestinal glucose absorption in the absence of GLUT2: evidence for a transport pathway requiring glucose phosphorylation and transfer into the endoplasmic reticulum. *Proc Natl Acad Sci U S A*; **98**(20): 11330-5.

Suryanarayana, P., Kumar, P.A., Saraswat, M., Petrash, J.M. and Reddy, G.B. (2004). Inhibition of aldose reductase by tannoid principles of Emblica officinalis: implications for the prevention of sugar cataract. *Mol Vis*; **10**: 148-54.

Suzen, S. and Buyukbingol, E. (2003). Recent studies of aldose reductase enzyme inhibition for diabetic complications. *Curr Med Chem*; **10**(15): 1329-52.

Suzuki, Y.J., Forman, H.J. and Sevanian, A. (1997). Oxidants as stimulators of signal transduction. *Free Radic Biol Med*; **22**(1-2): 269-85.

Swamy-Mruthinti, S., Green, K. and Abraham, E.C. (1996). Inhibition of cataracts in moderately diabetic rats by aminoguanidine. *Exp Eye Res*; **62**(5): 505-10.

Swamy-Mruthinti, S., Shaw, S.M., Zhao, H.R., Green, K. and Abraham, E.C. (1999). Evidence of a glycemic threshold for the development of cataracts in diabetic rats. *Curr Eye Res*; **18**(6): 423-9.

Tabatabai, N.M., Blumenthal, S.S., Lewand, D.L. and Petering, D.H. (2001). Differential regulation of mouse kidney sodium-dependent transporters mRNA by cadmium. *Toxicol Appl Pharmacol*; **177**(3): 163-73.

Takagi, H., Tanihara, H., Seino, Y. and Yoshimura, N. (1994). Characterization of glucose transporter in cultured human retinal pigment epithelial cells: gene expression and effect of growth factors. *Invest Ophthalmol Vis Sci*; **35**(1): 170-7.

Takahashi, H., Kaminski, A.E. and Zieske, J.D. (1996). Glucose transporter 1 expression is enhanced during corneal epithelial wound repair. *Exp Eye Res*; **63**(6): 649-59.

Takahashi, H., Ohara, K., Ohmura, T., Takahashi, R. and Zieske, J.D. (2000). Glucose transporter 1 expression in corneal wound repair under high serum glucose level. *Jpn J Ophthalmol*; **44**(5): 470-4.

Takata, K. (1996). Glucose transporters in the transepithelial transport of glucose. *J Electron Microsc (Tokyo)*; **45**(4): 275-84.

Takata, K., Hirano, H. and Kasahara, M. (1997). Transport of glucose across the blood-tissue barriers. *Int Rev Cytol*; **172**: 1-53.

Takata, K., Kasahara, M., Oka, Y. and Hirano, H. (1993). Mammalian sugar transporters: Their localization and link to cellular fucntions. *Acta Histochem Cytochem*; (26): 165-178.

Takata, K., Kasahara, T., Kasahara, M., Ezaki, O. and Hirano, H. (1990). Erythrocyte/HepG2-type glucose transporter is concentrated in cells of blood-tissue barriers. *Biochem Biophys Res Commun*; **173**(1): 67-73.

Takata, K., Kasahara, T., Kasahara, M., Ezaki, O. and Hirano, H. (1991). Ultracytochemical localization of the erythrocyte/HepG2-type glucose transporter (GLUT1) in the ciliary body and iris of the rat eye. *Invest Ophthalmol Vis Sci*; **32**(5): 1659-66.

Takata, K., Kasahara, T., Kasahara, M., Ezaki, O. and Hirano, H. (1992). Localization of erythrocyte/HepG2-type glucose transporter (GLUT1) in human placental villi. *Cell Tissue Res*; **267**(3): 407-12.

Takata, K., Kasahara, T., Kasahara, M., Ezaki, O. and Hirano, H. (1994). Immunolocalization of glucose transporter GLUT1 in the rat placental barrier: possible role of GLUT1 and the gap junction in the transport of glucose across the placental barrier. *Cell Tissue Res*; **276**(3): 411-8.

Tamori, Y., Hashiramoto, M., Clark, A.E., Mori, H., Muraoka, A. *et al.* (1994). Substitution at Pro385 of GLUT1 perturbs the glucose transport function by reducing conformational flexibility. *J Biol Chem*; **269**(4): 2982-6.

Tanaka, S., Avigad, G., Brodsky, B. and Eikenberry, E.F. (1988). Glycation induces expansion of the molecular packing of collagen. *J Mol Biol*; **203**(2): 495-505.

Tang, J., Mohr, S., Du, Y.D. and Kern, T.S. (2003). Non-uniform distribution of lesions and biochemical abnormalities within the retina of diabetic humans. *Curr Eye Res*; **27**(1): 7-13.

The Diabetes Control and Complications Trial Research Group (1993). The effect of intensive treatment of diabetes on the development and progression of long-term complications in insulin-dependent diabetes mellitus. *N Engl J Med*; **329**(14): 977-86.

Thies, R.S. and Mandel, L.J. (1985). Role of glucose in corneal metabolism. *Am J Physiol*; **249**(5 Pt 1): C409-16.

Thompson, J.D., Brodsky, I. and Yunis, J.J. (1992). Molecular quantification of residual disease in chronic myelogenous leukemia after bone marrow transplantation. *Blood*; **79**(6): 1629-35.

Thorens, B. (1992). Molecular and cellular physiology of GLUT-2, a high-Km facilitated diffusion glucose transporter. *Int Rev Cytol*; **137**: 209-38.

Thorens, B., Sarkar, H.K., Kaback, H.R. and Lodish, H.F. (1988). Cloning and functional expression in bacteria of a novel glucose transporter present in liver, intestine, kidney, and beta-pancreatic islet cells. *Cell*; **55**(2): 281-90.

To, C.H., Cheung, K.K., Chiu, S.H., Lai, H.M. and Lung, K.S. (1998c). The saturation characteristics of glucose transport in bovine retinal pigment epithelium. *Yan Ke Xue Bao*; **14**(3): 126-9.

To, C.H. and Do, C.W. (1998d). Ion transport mechanisms in the formation of aqueous humor. *HK J Ophthalmol*; **2**(1): 35-42.

To, C.H., Do, C.W., Zamudio, A.C. and Candia, O.A. (2001). Model of ionic transport for bovine ciliary epithelium: effects of acetazolamide and HCO. *Am J Physiol Cell Physiol*; **280**(6): C1521-30.

To, C.H. and Hodson, S.A. (1998b). The glucose transport in retinal pigment epithelium is via passive facilitated diffusion. *Comp Biochem Physiol A Mol Integr Physiol*; **121**(4): 441-4.

To, C.H., Mok, K.H., Do, C.W., Lee, K.L. and Millodot, M. (1998a). Chloride and sodium transport across bovine ciliary body/epithelium (CBE). *Curr Eye Res*; **17**(9): 896-902.

Tolentino, M.J. and Adamis, A.P. (1998). Angiogenic factors in the development of diabetic iris neovascularization and retinopathy. *Int Ophthalmol Clin*; **38**(1): 77-94.

Towbin, H., Staehelin, T. and Gordon, J. (1979). Electrophoretic transfer of proteins from polyacrylamide gels to nitrocellulose sheets: procedure and some applications. *Proc Natl Acad Sci U S A*; **76**(9): 4350-4.

Tsang, R., Ao, Z. and Cheeseman, C. (1994). Influence of vascular and luminal hexoses on rat intestinal basolateral glucose transport. *Can J Physiol Pharmacol*; **72**(4): 317-26.

Tseng, C.H. (2004). Mortality and causes of death in a national sample of diabetic patients in Taiwan. *Diabetes Care*; **27**(7): 1605-9.

Tserentsoodol, N., Shin, B.C., Suzuki, T. and Takata, K. (1998). Colocalization of tight junction proteins, occludin and ZO-1, and glucose transporter GLUT1 in cells of the blood-ocular barrier in the mouse eye. *Histochem Cell Biol*; **110**(6): 543-51.

Tsujihara, K., Hongu, M., Saito, K., Inamasu, M., Arakawa, K. *et al.* (1996). Na(+)-glucose cotransporter inhibitors as antidiabetics. I. Synthesis and pharmacological

properties of 4'-dehydroxyphlorizin derivatives based on a new concept. *Chem Pharm Bull (Tokyo)*; **44**(6): 1174-80.

Tsukaguchi, H., Tokui, T., Mackenzie, B., Berger, U.V., Chen, X.Z. *et al.* (1999). A family of mammalian Na+-dependent L-ascorbic acid transporters. *Nature*; **399**(6731): 70-5.

Tsukamoto, H., Mishima, H.K., Kurokawa, T., Kiuchi, Y., Sato, E. *et al.* (1995). Isoforms of glucose transporter in the iris-ciliary body. *Jpn J Ophthalmol*; **39**(3): 242-7.

Turczynski, B., Michalska-Malecka, K., Slowinska, L., Szczesny, S. and Romaniuk, W. (2003). Correlations between the severity of retinopathy in diabetic patients and whole blood and plasma viscosity. *Clin Hemorheol Microcirc*; **29**(2): 129-37.

Turk, E., Kim, O., le Coutre, J., Whitelegge, J.P., Eskandari, S. *et al.* (2000). Molecular characterization of Vibrio parahaemolyticus vSGLT: a model for sodium-coupled sugar cotransporters. *J Biol Chem*; **275**(33): 25711-6.

Turk, E. and Wright, E.M. (1997). Membrane topology motifs in the SGLT cotransporter family. *J Membr Biol*; **159**(1): 1-20.

Turk, E., Zabel, B., Mundlos, S., Dyer, J. and Wright, E.M. (1991). Glucose/galactose malabsorption caused by a defect in the Na+/glucose cotransporter. *Nature*; **350**(6316): 354-6.

Turner, R.J. and Moran, A. (1982a). Further studies of proximal tubular brush border membrane D-glucose transport heterogeneity. *J Membr Biol*; **70**(1): 37-45.

Turner, R.J. and Moran, A. (1982b). Heterogeneity of sodium-dependent D-glucose transport sites along the proximal tubule: evidence from vesicle studies. *Am J Physiol*; **242**(4): F406-14.

Turner, R.J. and Silverman, M. (1978). Sugar uptake into brush border vesicles from dog kidney. II. Kinetics. *Biochim Biophys Acta*; **511**(3): 470-86.

Uemura, S., Matsushita, H., Li, W., Glassford, A.J., Asagami, T. *et al.* (2001). Diabetes mellitus enhances vascular matrix metalloproteinase activity: role of oxidative stress. *Circ Res*; **88**(12): 1291-8.

Uldry, M., Ibberson, M., Horisberger, J.D., Chatton, J.Y., Riederer, B.M. *et al.* (2001). Identification of a mammalian H(+)-myo-inositol symporter expressed predominantly in the brain. *Embo J*; **20**(16): 4467-77.

Uldry, M. and Thorens, B. (2004). The SLC2 family of facilitated hexose and polyol transporters. *Pflugers Arch*; **447**(5): 480-9.

Unger, R.H. (1991). Diabetic hyperglycemia: link to impaired glucose transport in pancreatic beta cells. *Science*; **251**(4998): 1200-5.

Ussing, H.H. and Zerahn, K. (1951). Active transport of sodium as the source of electric current in the short-circuited isolated frog skin. *Acta Physiol Scand*; **23**(2-3): 110-27.

Vachereau, A. (1989). Luminescent immunodetection of western-blotted proteins from coomassie-stained polyacrylamide gel. *Anal Biochem*; **179**(1): 206-8.

Valera, A., Solanes, G., Fernandez-Alvarez, J., Pujol, A., Ferrer, J. *et al.* (1994). Expression of GLUT-2 antisense RNA in beta cells of transgenic mice leads to diabetes. *J Biol Chem*; **269**(46): 28543-6.

Van den Enden, M.K., Nyengaard, J.R., Ostrow, E., Burgan, J.H. and Williamson, J.R. (1995). Elevated glucose levels increase retinal glycolysis and sorbitol pathway metabolism. Implications for diabetic retinopathy. *Invest Ophthalmol Vis Sci*; **36**(8): 1675-85.

van den Heuvel, L.P., Assink, K., Willemsen, M. and Monnens, L. (2002). Autosomal recessive renal glucosuria attributable to a mutation in the sodium glucose cotransporter (SGLT2). *Hum Genet*; **111**(6): 544-7.

van Heyningen, R. (1959). Formation of polyols by the lens of the rat with 'sugar' cataract. *Nature*; **468**: 194-195.

Vannucci, S.J., Gibbs, E.M. and Simpson, I.A. (1997). Glucose utilization and glucose transporter proteins GLUT-1 and GLUT-3 in brains of diabetic (db/db) mice. *Am J Physiol*; **272**(2 Pt 1): E267-74.

Vannucci, S.J., Reinhart, R., Maher, F., Bondy, C.A., Lee, W.H. *et al.* (1998a). Alterations in GLUT1 and GLUT3 glucose transporter gene expression following unilateral hypoxia-ischemia in the immature rat brain. *Brain Res Dev Brain Res*; **107**(2): 255-64.

Varma, S.D. and Kinoshita, J.H. (1974). The absence of cataracts in mice with congenital hyperglycemia. *Exp Eye Res*; **19**(6): 577-82.

Vaxillaire, M., Pueyo, M.E., Clement, K., Fiet, J., Timsit, J. *et al.* (1999). Insulin secretion and insulin sensitivity in diabetic and non-diabetic subjects with hepatic nuclear factor-1alpha (maturity-onset diabetes of the young-3) mutations. *Eur J Endocrinol*; **141**(6): 609-18.

Vegge, T. (1971). An epithelial blood-aqueous barrier to horseradish peroxidase in the ciliary processes of the vervet monkey (Cercopithecus aethiops). *Z Zellforsch Mikrosk Anat*; **114**(3): 309-20.

Veyhl, M., Spangenberg, J., Puschel, B., Poppe, R., Dekel, C. *et al.* (1993). Cloning of a membrane-associated protein which modifies activity and properties of the Na(+)-D-glucose cotransporter. *J Biol Chem*; **268**(33): 25041-53.

Vilchis, C. and Salceda, R. (1996). Characterization of [2-3H]deoxy-D-glucose uptake in retina and retinal pigment epithelium of normal and diabetic rats. *Neurochem Int*; **28**(2): 213-9.

Vinores, S.A., Campochiaro, P.A., Williams, E.H., May, E.E., Green, W.R. *et al.* (1988). Aldose reductase expression in human diabetic retina and retinal pigment epithelium. *Diabetes*; **37**(12): 1658-64.

Waeber, G., Thompson, N., Haefliger, J.A. and Nicod, P. (1994). Characterization of the murine high Km glucose transporter GLUT2 gene and its transcriptional regulation by glucose in a differentiated insulin-secreting cell line. *J Biol Chem*; **269**(43): 26912-9.

Wagstaff, P., Kang, H.Y., Mylott, D., Robbins, P.J. and White, M.K. (1995). Characterization of the avian GLUT1 glucose transporter: differential regulation of GLUT1 and GLUT3 in chicken embryo fibroblasts. *Mol Biol Cell*; **6**(11): 1575-89.

Walle, T. and Walle, U.K. (2003). The beta-D-glucoside and sodium-dependent glucose transporter 1 (SGLT1)-inhibitor phloridzin is transported by both SGLT1 and multidrug resistance-associated proteins 1/2. *Drug Metab Dispos*; **31**(11): 1288-91.

Wandel, S., Buchs, A., Schurmann, A., Summers, S.A., Powers, A.C. *et al.* (1996). Glucose transport activity and ligand binding (cytochalasin B, IAPS-forskolin) of chimeric constructs of GLUT2 and GLUT4 expressed in COS-7-cells. *Biochim Biophys Acta*; **1284**(1): 56-62.

Watanabe, T., Matsushima, S., Okazaki, M., Nagamatsu, S., Hirosawa, K. *et al.* (1996). Localization and ontogeny of GLUT3 expression in the rat retina. *Brain Res Dev Brain Res*; **94**(1): 60-6.

Watanabe, T., Mio, Y., Hoshino, F.B., Nagamatsu, S., Hirosawa, K. *et al.* (1994). GLUT2 expression in the rat retina: localization at the apical ends of Muller cells. *Brain Res*; **655**(1-2): 128-34.

Watson, P.J. (2003). Exocrine pancreatic insufficiency as an end stage of pancreatitis in four dogs. *J Small Anim Pract*; **44**(7): 306-12.

Wehner, F. and Tinel, H. (1998). Role of Na+ conductance, Na(+)-H+ exchange, and Na(+)-K(+)-2Cl- symport in the regulatory volume increase of rat hepatocytes. *J Physiol*; **506 (Pt 1)**: 127-42.

Welten, A.G., Schalkwijk, C.G., ter Wee, P.M., Meijer, S., van den Born, J. *et al.* (2003). Single exposure of mesothelial cells to glucose degradation products (GDPs) yields early advanced glycation end-products (AGEs) and a proinflammatory response. *Perit Dial Int*; **23**(3): 213-21.

Wessells, N.K., Spooner, B.S., Ash, J.F., Bradley, M.O., Luduena, M.A. *et al.* (1971). Microfilaments in cellular and developmental processes. *Science*; **171**(967): 135-43.

Wetzel, R.K. and Sweadner, K.J. (2001). Immunocytochemical localization of NaK-ATPase isoforms in the rat and mouse ocular ciliary epithelium. *Invest Ophthalmol Vis Sci*; **42**(3): 763-9.

Wheeler, T.J. and Hauck, M.A. (1985). Reconstitution of the glucose transporter from bovine heart. *Biochim Biophys Acta*; **818**(2): 171-82.

Wiederholt, M. and Zadunaisky, J.A. (1987). Effects of ouabain and furosemide on transepithelial electrical parameters of the isolated shark ciliary epithelium. *Invest Ophthalmol Vis Sci*; **28**(8): 1353-6.

Wilfinger, W.W., Mackey, K. and Chomczynski, P. (1997). Effect of pH and ionic strength on the spectrophotometric assessment of nucleic acid purity. *Biotechniques*; **22**(3): 474-6, 478-81.

Williams, B., Gallacher, B., Patel, H. and Orme, C. (1997). Glucose-induced protein kinase C activation regulates vascular permeability factor mRNA expression and peptide production by human vascular smooth muscle cells in vitro. *Diabetes*; **46**(9): 1497-503.

Witkovsky, P. and Yang, C.Y. (1982). Transport and phosphorylation of 2-deoxy-D-glucose by amphibian retina. Effects of light and darkness. *J Gen Physiol*; **80**(2): 173-90.

Wood, I.S. and Trayhurn, P. (2003). Glucose transporters (GLUT and SGLT): expanded families of sugar transport proteins. *Br J Nutr*; **89**(1): 3-9.

Wright, E.M. (2001). Renal Na(+)-glucose cotransporters. *Am J Physiol Renal Physiol*; **280**(1): F10-8.

Wright, E.M., Martin, M.G. and Turk, E. (2003). Intestinal absorption in health and disease--sugars. *Best Pract Res Clin Gastroenterol*; **17**(6): 943-56.

Wright, E.M. and Turk, E. (2004). The sodium/glucose cotransport family SLC5. *Pflugers Arch*; **447**(5): 510-8.

Wu, R., Flammer, J. and Haefliger, I. (2003). Transepithelial short circuit currents in human and porcine isolated ciliary bodies: effect of acetazolamide and epinephrine. *Klin Monatsbl Augenheilkd*; **220**(3): 156-60.

Wu, X. and Freeze, H.H. (2002). GLUT14, a duplicon of GLUT3, is specifically expressed in testis as alternative splice forms. *Genomics*; **80**(6): 553-7.

Wu, X., Li, W., Sharma, V., Godzik, A. and Freeze, H.H. (2002). Cloning and characterization of glucose transporter 11, a novel sugar transporter that is alternatively spliced in various tissues. *Mol Genet Metab*; **76**(1): 37-45.

Xia, P., Inoguchi, T., Kern, T.S., Engerman, R.L., Oates, P.J. *et al.* (1994). Characterization of the mechanism for the chronic activation of diacylglycerol-protein kinase C pathway in diabetes and hypergalactosemia. *Diabetes*; **43**(9): 1122-9.

Yajnik, C.S., Shelgikar, K.M., Sahasrabudhe, R.A., Naik, S.S., Pai, V.R. *et al.* (1990). The spectrum of pancreatic exocrine and endocrine (beta-cell) function in tropical calcific pancreatitis. *Diabetologia*; **33**(7): 417-21.

Yantorno, R.E., Coca-Prados, M., Krupin, T. and Civan, M.M. (1989). Volume regulation of cultured, transformed, non-pigmented epithelial cells from human ciliary body. *Exp Eye Res*; **49**(3): 423-37.

Yu, S. and Ding, W.G. (1998). The 45 kDa form of glucose transporter 1 (GLUT1) is localized in oligodendrocyte and astrocyte but not in microglia in the rat brain. *Brain Res*; **797**(1): 65-72.

Zadunaisky, J.A. and Degnan, K.J. (1976). Passage of sugars and urea across the isolated retina pigment epithelium of the frog. *Exp Eye Res*; **23**(2): 191-6.

Zampighi, G.A., Kreman, M., Boorer, K.J., Loo, D.D., Bezanilla, F. *et al.* (1995). A method for determining the unitary functional capacity of cloned channels and transporters expressed in Xenopus laevis oocytes. *J Membr Biol*; **148**(1): 65-78.

Zeller, W.P., Goto, M., Parker, J., Cava, J.R., Gottschalk, M.E. *et al.* (1994). Glucose transporters (GLUT1, 2, & 4) in fat, muscle and liver in a rat model of endotoxic shock. *Biochem Biophys Res Commun*; **198**(3): 923-7.

Zeng, X.X., Ng, Y.K. and Ling, E.A. (2000). Neuronal and microglial response in the retina of streptozotocin-induced diabetic rats. *Vis Neurosci*; **17**(3): 463-71.

Zern, M.A. and Kresina, T.F. (1997). Hepatic drug delivery and gene therapy. *Hepatology*; **25**(2): 484-91.

Zhang, J.Z., Gao, L., Widness, M., Xi, X. and Kern, T.S. (2003). Captopril inhibits glucose accumulation in retinal cells in diabetes. *Invest Ophthalmol Vis Sci*; **44**(9): 4001-5.

Zhang, J.Z. and Ismail-Beigi, F. (1998). Activation of Glut1 glucose transporter in human erythrocytes. *Arch Biochem Biophys*; **356**(1): 86-92.

Zhao, F.Q., Glimm, D.R. and Kennelly, J.J. (1993). Distribution of mammalian facilitative glucose transporter messenger RNA in bovine tissues. *Int J Biochem*; **25**(12): 1897-903.

Zhou, J. and Bondy, C.A. (1993). Placental glucose transporter gene expression and metabolism in the rat. *J Clin Invest*; **91**(3): 845-52.

Zieman, S. and Kass, D. (2004). Advanced glycation end product cross-linking: pathophysiologic role and therapeutic target in cardiovascular disease. *Congest Heart Fail*; **10**(3): 144-9; quiz 150-1.

Zisman, A., Peroni, O.D., Abel, E.D., Michael, M.D., Mauvais-Jarvis, F. *et al.* (2000). Targeted disruption of the glucose transporter 4 selectively in muscle causes insulin resistance and glucose intolerance. *Nat Med*; **6**(8): 924-8.

Zraika, S., Dunlop, M., Proietto, J. and Andrikopoulos, S. (2002). The hexosamine biosynthesis pathway regulates insulin secretion via protein glycosylation in mouse islets. *Arch Biochem Biophys*; **405**(2): 275-9.